

Olav Andreas Aarstad

## Alginate sequencing

Block distribution in alginates and its impact on  
macroscopic properties

Thesis for the degree of Philosophiae Doctor

Trondheim, January 2013

Norwegian University of Science and Technology  
Faculty of Natural Sciences and Technology  
Department of Biotechnology



**NTNU – Trondheim**  
Norwegian University of  
Science and Technology

**NTNU**

Norwegian University of Science and Technology

Thesis for the degree of Philosophiae Doctor

Faculty of Natural Sciences and Technology  
Department of Biotechnology

© Olav Andreas Aarstad

ISBN 978-82-471-4144-1 (printed ver.)  
ISBN 978-82-471-4145-8 (electronic ver.)  
ISSN 1503-8181

Doctoral theses at NTNU, 2013:26

Printed by NTNU-trykk

## **Acknowledgement**

I wish to express my gratitude to my supervisor Prof. Gudmund Skjåk-Bræk for excellent guidance and for giving me the opportunity to do this work. His expertise in the alginate research field, as well as his immense general knowledge is very much appreciated, and his kindness, generosity and patient encouragement should serve as an example to follow.

Wenche Iren Strand is thanked for her indispensable technical assistance and for her warm and caring personality. I would also like to thank Anne Tøndervik and Håvard Sletta who both played a crucial role in the project, providing epimerases and lyases.

Simon Ballance is thanked for introducing me to HPAEC-PAD, for good collaboration and many nice fishing trips.

My office mates, Kåre Andre Kristiansen and Finn Aachmann are thanked for pleasant conversations and fruitful discussions.

I am grateful to Kate Bowman and Øystein Arlov for their proofreading of my manuscript.

All my colleagues at the department are thanked for creating an amiable atmosphere without a trace of the fierce competition that I have heard is common in some scientific communities.

Last but not least, I wish to thank my friends and family for their care and support.

## **Preface**

This thesis is submitted in partial fulfillment of the requirements for the academic title Philosophiae Doctor at the Norwegian University of Science and Technology (NTNU). The work was carried out at the Norwegian Biopolymer Laboratory (NOBIPOL), Department of Biotechnology, NTNU, Trondheim, under supervision of Professor dr.techn. Gudmund Skjåk-Bræk. The work was financed through an individual doctoral fellowship by NTNU as a part of joint research project with The Norwegian Research Council entitled “Polysaccharide engineering”. The thesis consists of a general introduction, aims of the study and a summary of five scientific papers given in the appendix.

### **Contributions to other publications not included in this thesis:**

Heggset, E. B, Sikorski P., **Aarstad, O. A.**, Eijsink V. G. H. and Vårum, K. M. (2011). Directionality in degradation of a chitosan oligomer substrate by Chitinase A and B from *Serratia marcescens*. Manuscript

Gimmestad, M., Ertesvåg, H., Heggset, T. M. B., **Aarstad, O. A.**, Svanem, B. I. G, Valla, S. (2009) Characterization of Three New *Azotobacter vinelandii* Alginate Lyases, One of Which Is Involved in Cyst Germination. *J. bacteriol.* **191**, 4845-4853.

## Summary

Alginate is a family of linear copolymers found in brown algae and some bacteria. It consists of 1→4 linked β-D-mannuronic acid (M) and α-L-guluronic acid (G) organized in homopolymeric regions of G-residues (G-blocks), M-residues (M-blocks) and alternating residues (MG-blocks). The relative amount of the monomers and their distribution is highly variable and dependent on species, type of tissue, season and life cycle. Moreover, the distribution of the three blocktypes cannot be predicted from the monomer ratio by statistical methods. Alginate has several promising biomedical applications in cell immobilization, immunoisolation and as a bioscaffold due to its ability to form temperature independent hydrogels in the presence of calcium ions under mild conditions. The gel properties are dependent on monomer composition and distribution, and the gel strength is correlated to the average G-block length ( $N_{G>1}$ ) as determined by NMR spectroscopy. However, MG-blocks also have a role in determining macroscopic properties, such as syneresis and stress-strain profiles, and some commercially available alginates rich in MG-blocks exhibit atypical gel behaviour.

The goals of the present work were therefore to investigate alginate fine structure i.e. the distribution of monomers in the alginate chain, and to study structure-function relationships in alginate gels. This involved the use of specific alginate degrading enzymes (alginate lyases) and the construction and characterization of a new alginate lyase with high specificity towards G-G linkages. These enzymes were characterized in terms of substrate specificity, minimum substrate and end products prior to their application in the block distribution analysis.

Lyase-degraded alginate samples contained a mixture of oligomers with different chain lengths and composition which had to be analysed further in order to determine the block distribution. A method for separation and quantification of alginate oligomers using high performance anion-exchange chromatography with pulsed amperometric detection (HPAEC-PAD) was therefore developed. Moreover, alginate oligomers with known chain length and composition are needed as standards to identify alginate oligomers of different compositions and chain lengths in complex mixtures. An oligomer library was made, consisting of homologous series of M-, G- and MG-oligomers, with and without the 4-5 unsaturated non-reducing end which result from lyase degradation. The possibility of producing almost monodisperse oligomers by the use of semi preparative HPAEC PAD has also been explored.

Chain length distribution of the three block types in alginates purified from brown seaweed was determined using the methodology mentioned above, together with NMR analysis and size exclusion chromatography with multi angle laser light scattering detection (SEC-MALLS). The observed distribution of chains lengths was broader than that which could be anticipated from NMR frequencies and statistical calculations. The most surprising finding was the presence of a fraction of extremely long G-blocks with a degree of polymerization (DP) of more than 100 in all three alginates analysed, regardless of large differences in composition and average G-block length as calculated from NMR. A fraction of very long M-blocks was also found in all samples whereas the MG-blocks were considerably shorter. Intrigued by the finding of extremely long G-blocks in algal alginate, we decided to analyse the G-block distribution in engineered alginates together with a study of gel properties of the resulting material. Epimerization of Poly-M with the mannuronan C-5 epimerases AlgE6, AlgE64 and EM1 resulted in polymers comprised of homopolymeric blocks of M and G, with a similar distribution of G-blocks, mainly from DP 20-50. The structural features that distinguish the *in vitro* epimerized alginates from the algal alginate of the same composition are the broader block distributions and the lack of extremely long G-blocks in the former. Calcium gels made from Poly-M epimerized with AlgE6 were found to be more compressible and exhibited higher syneresis and rupture strength, but a lower rigidity (Youngs modulus) than gels made from *Laminaria hyperborea* alginate with the same content of guluronic acid. When extremely long G-blocks isolated from the brown algae *L. hyperborea* were added to the *in vitro* epimerized alginate, a marked decrease in syneresis was observed and the gel became more rigid and brittle, demonstrating that there are functional features of alginate gels which cannot be explained solely on the basis of triad frequencies obtained from NMR.

## Sammendrag

Alginat er en samlebetegnelse for en familie av uforgrenede kopolymerer som finnes i brunalger og enkelte bakterier. Alginat består av 1→4 bundet β-D-mannuronsyre (M) og α-L-guluronsyre (G) og monomerene er fordelt som G-blokker, M-blokker og MG-blokker. Forholdet mellom monomerene og deres fordeling i kjeden er sterkt avhengig av hvilken organisme som alginatet er utvunnet fra. Vevstype, sesong og del i livssyklus har også betydning. I tillegg kan ikke fordelingen av de tre blokktypene beregnes ved hjelp av statistiske metoder ut fra forholdet mellom monomerene. På grunn av sin evne til å danne hydrogeler i nærvær av kalsium under milde betingelser, uavhengig av temperatur, har alginat flere lovende biomedisinske anvendelser innenfor immobilisering av celler, som immunbarriere og som biologisk matrise for regenerering av vev. Geleegenskapene er avhengige av andelen av de to monomerene, samt deres fordeling og gelstyrken er korrelert til gjennomsnittlig G-block lengde ( $N_{G>1}$ ) bestemt ved NMR spektroskopi. MG-blokker har imidlertid også betydning for gelens makroskopiske egenskaper som synerese og kraft-deformasjons profiler, og noen kommersielt tilgjengelige alginater med høyt innhold av disse alternerende blokkene har avvikende gelingsegenskaper.

Formålet med dette arbeidet var derfor å studere finstrukturen i alginater, det vil si fordelingen av monomerene i kjeden, samt å studere struktur-funksjon sammenhengene for alginatgeler. Dette innebar bruk av spesifikke alginatnedbrytende enzymer (alginat lyaser) samt utvikling og karakterisering av en ny alginat lyase med høy spesifisitet for G-G bindinger. Disse enzymene ble karakterisert med hensyn på substratspesifisitet, minste substrat og endeprodukter før de ble anvendt til å bestemme blokkfordelingen i alginater. Alginater nedbrutt med lyaser inneholder en blanding av oligomerer med ulik sammensetning og kjedelengde som må analyseres videre for å kunne bestemme blokkfordelingen.

En metode for separasjon og kvantifisering av alginatoligomerer ved hjelp av høypresisjon anionbytter-kromatografi med pulsamperimetriisk deteksjon (HPAEC-PAD) ble derfor utviklet. I tillegg kreves det at man har standarder av alginatoligomerer med kjent kjedelengde og sammensetning tilgjengelig for å kunne identifisere alginatoligomerer i komplekse blandinger. Et oligomerbibliotek ble derfor laget, bestående av homologe serier av M-, G- og MG- oligomerer med og uten den 4-5 umettede ikkereduserende enden som dannes under lyasenedbrytningen. Muligheten for å produsere tilnærmet monodisperse oligomerer ved hjelp av semipreparativ HPAEC PAD har også blitt undersøkt.

Kjedelengdefordelingen for hver av de tre blokktypene ble bestemt i tre utvalgte alginater fra brunalger ved å bruke metodikken nevnt ovenfor og i tillegg NMR analyse og eksklusjonskromatografi med multi-vinkel lysspredningsdeteksjon (SEC-MALLS).

Den observerte kjedelengdefordelingen var bredere enn hva man forventet ut fra NMR frekvenser og statistiske beregninger. Mest overraskende var funnet av en fraksjon ekstremt lange G blokker med kjedelengde på over 100 i alle alginatprøvene, uavhengig av store forskjeller i sammensetning og gjennomsnittlig G-blokk lengde beregnet fra NMR.

En fraksjon av svært lange M-blokker ble også påvist mens MG-blokkene var betydelig kortere.

Fascinert over funnet av de ekstremt lange G-blokkene i alginat fra brunalger, bestemte vi oss for å analysere blokkfordelingen i skreddersydde alginater og for å studere gelegenskapene til disse alginatene. Epimerisering av Poly-M med mannuronan C-5 epimerasene AlgE6, AlgE64 og EM1 resulterte i polymerer som består av M- og G-blokker der fordelingen av G-blokker var lik, hovedsaklig med kjedelengder mellom 20 og 50. Det som skiller de *in vitro* epimeriserte alginatene fra alginater fra brunalger med liknende sammensetning er den bredere blokkfordelingen og fraværet av ekstremt lange G-blokker.

Kalsiumgeler laget av Poly-M epimerisert med AlgE6 hadde høyere synerese og kunne deformeres mer enn geler laget av alginat fra *Laminaria hyperborea* med lik sammensetning. De hadde også høyere bruddstyrke, men var mindre rigide (lavere Youngs modulus). Ved tilsats av ekstremt lange G-blokker isolert fra *L. hyperborea* ble det observert en tydelig nedgang i synerese og gelen ble sterkere og mindre elastisk. Studien viser at det finnes funksjonelle egenskaper ved alginategeler som ikke kan forklares utelukkende ut fra triadefrekvenser bestemt ved NMR analyse.



## List of papers

1. Ballance, S., Holtan, S., **Aarstad, O. A.**, Sikorski, P., Skjåk-Bræk, G. and Christensen, B.E. (2005) Application of high-performance anion-exchange chromatography with pulsed amperometric detection and statistical analysis to study oligosaccharide distributions- a complementary method to investigate the structure and some properties of alginates. *J. Chrom.A* **1093**, 59-68.
2. Ballance, S., **Aarstad, O. A.**, Aachmann, F. L., Skjåk-Bræk, G. and Christensen, B. E. (2009) Preparation of high purity monodisperse oligosaccharides derived from mannuronan by size-exclusion chromatography followed by high-performance anion exchange chromatography with pulsed amperometric detection. *Carbohydr. res.* **344**, 255-259.
3. Tøndervik, A., Klinkenberg, G., **Aarstad, O. A.**, Drabløs, F., Ertesvåg, H., Ellingsen, T., Skjåk-Bræk, G., Valla, S. and Sletta, H. (2010) Isolation of mutant alginate lyases with cleavage specificity for di-guluronic acid linkages. *J. Biol. Chem.* **285**, 35284-35292.
4. **Aarstad, O. A.**, Tøndervik, A., Sletta, H. and Skjåk-Bræk, G. (2012) Alginate Sequencing: An Analysis of Block Distribution in Alginates Using Specific Alginate Degrading Enzymes. *Biomacromolecules* **13**, 106-116.
5. **Aarstad, O. A.**, Strand, B. L., Klepp-Andersen, L. M and Skjåk-Bræk, G. An analysis of G-block distributions and their impact on gel properties of *in vitro* epimerized mannuronan. Manuscript

## Symbols and abbreviations

$\alpha$	Degree of scission
$\Delta$	4-deoxy-L-erythro-hex-4-enopyranosyluronate
$\overline{DP}_n$	Number average degree of polymerization
E	Youngs modulus
G	$\alpha$ -L-guluronic acid
GDL	Glucono delta-lactone
HPAEC-PAD	High-performance anion-exchange chromatography with pulsed amperometric detection
ITC	isothermal titration calorimetry
M	$\beta$ -D-mannuronic acid
$\overline{M}_n$	Number average molecular mass
$\overline{M}_w$	Weight average molecular mass
MRF	Molar response factor
$[\eta]$	Intrinsic viscosity
$N_{G>1}$	Average G-block length>1
$N_{M>1}$	Average M-block length>1
NMR	Nuclear magnetic resonance spectroscopy
RI	Refractive Index
RF	Response factor
SEC	Size exclusion chromatography
SEC-MALLS	Size exclusion chromatography with multi-angle laser light scattering
TOF-MS	Time of flight-mass spectrometry
TSP	3-(trimethylsilyl)-propionic-2,2,3,3-d <sub>4</sub> acid
TTHA	Triethylenetetraamine- hexaacetate

## Table of contents

Acknowledgements .....	i
Preface .....	ii
Summary .....	iii
Sammendrag .....	v
List of papers .....	vii
Symbols and abbreviations .....	viii
Table of contents .....	ix
1 INTRODUCTION .....	1
1.1 Alginate .....	1
1.1.1 Source and biological function .....	1
1.1.2 Chemical structure .....	1
1.1.2.1 Composition and sequence .....	3
1.1.2.2 Conformation .....	3
1.1.2.3 Molecular weight .....	4
1.1.3 Physical properties .....	4
1.1.3.1 Solubility .....	5
1.1.3.2 Viscosity and chain extension .....	5
1.1.3.3 Stability .....	6
1.1.3.4 Ion binding .....	8
1.1.4 Alginate gels .....	10
1.1.4.1 Gel properties .....	10
1.1.4.2 Syneresis .....	11
1.1.4.3 Mechanical strength and elasticity .....	11
1.1.5 Analysis of alginate .....	13
1.1.5.1 Chemical characterization .....	16
1.1.5.2 NMR .....	16
1.1.5.3 SEC .....	18
1.1.5.4 HPLC .....	18
1.1.5.5 SEC-MALLS .....	19
1.1.6 Biosynthesis .....	19
1.1.7 Applications .....	21
1.1.7.1 Biomedical and pharmaceutical applications .....	22
1.2 Mannuronan C-5 epimerases .....	24
1.2.1 Reaction mechanism .....	24
1.2.2 Structure and mode of action of AlgE epimerases .....	26
1.2.3 Biotechnical Applications of C-5 epimerases .....	29
1.3 Alginate Lyases .....	30
1.3.1 Sources and biological function .....	30
1.3.2 Substrate specificity .....	30
1.3.3 Biotechnical applications of alginate lyases .....	31
2 AIMS .....	33
3 SUMMARY OF PAPERS .....	34
3.1 Paper I .....	34
3.1.1 Preparation of oligomer standards .....	34
3.1.2 HPAEC analysis of partially acid hydrolysed Poly-M, Poly-MG and G-blocks .....	35

3.1.3	Oligomer distributions in M-, G- and MG-hydrolysates.....	36
3.1.4	Simulation of the depolymerisation of Poly-MG.....	37
3.2	Paper II.....	38
3.2.1	Pre-purification of M-oligomers by SEC.....	38
3.2.2	isolation of M oligomers by semipreparative HPAEC-PAD.....	39
3.3	Paper III.....	40
3.3.1	Construction and characterization of lyase mutants.....	40
3.3.2	Reasons for the increased specificity towards G-G linkages.....	41
3.4	Paper IV.....	43
3.4.1	Characterization of lyases.....	44
3.4.2	Block distribution in alginates from <i>Macrocystis pyrifera</i> , <i>Durvillea potatorum</i> and <i>Laminaria hyperborea</i> .....	45
3.5	Paper V.....	50
3.5.1	Epimerization of mannuronan by the mannuronan C-5 epimerases AlgE6, AlgE64 and EM1.....	50
3.5.2	Analysis of gels made from AlgE6 epimerized mannuronan and the effect of long G-blocks.....	52
4	CONCLUDING REMARKS.....	55
5	REFERENCES.....	57

# 1 INTRODUCTION

## 1.1 Alginate

### 1.1.1 Source and biological function

Alginate is a collective term used for linear, 1→4 linked copolymers of β-D-mannuronic acid (M) and α-L-guluronic acid (G). It is mainly found in marine brown algae (*Phaeophyceae*) where it is located in the intercellular matrix as a gel containing Na<sup>+</sup>, Mg<sup>2+</sup>, Ca<sup>2+</sup>, Sr<sup>2+</sup> or Ba<sup>2+</sup> ions. Comprising up to 40% of the dry plant weight [1], alginate is considered to be its principal skeletal material [2]. The relative amount of the two monomers, as well as their arrangement, is highly dependent on the source, which gives rise to a great diversity of alginate structures. In brown algae, the composition depends both on the age of the plant and the type of tissue [3]. The G/M ratio in all types of algal tissue increases with age and the rigid and strong holdfasts and stipes contains more G than the flexible leaves.

A closely related polysaccharide, in which the mannuronic acid residues are O-2 and O-3 acetylated to varying degrees [4], is found in cyst forming soil bacteria such as *Azotobacter vinelandii* and *Azotobacter chroococcum* [5, 6]. It is a prerequisite in the formation of a metabolically dormant cyst which protects the bacterium during periods of drought or lack of nutrients [7]. Bacterial alginates are also produced by several members of the *Pseudomonas* genera family [8]. It was first isolated from a mucoid phenotype *Pseudomonas aeruginosa* strain obtained from the sputum of a cystic fibrosis patient [9]. The secreted alginate forms a biofilm that promotes colonization of the pulmonary tract, protects against host immune system and increases the resistance to antibiotics [10].

Infection of this opportunistic pathogen is very common in patients suffering from cystic fibrosis and usually results in severe deterioration of lung function. There has therefore been considerable interest in the study of alginate biofilms in this context. [11-13].

### 1.1.2 Chemical structure

Alginate was first reported by E.C.C. Stanford in 1881[14]. The present description of the polysaccharide, as a family of block-copolymers with correct identification of the building blocks, conformation and type of glycosidic linkage (Figure 1.1), was however not achieved until the early 1970s.

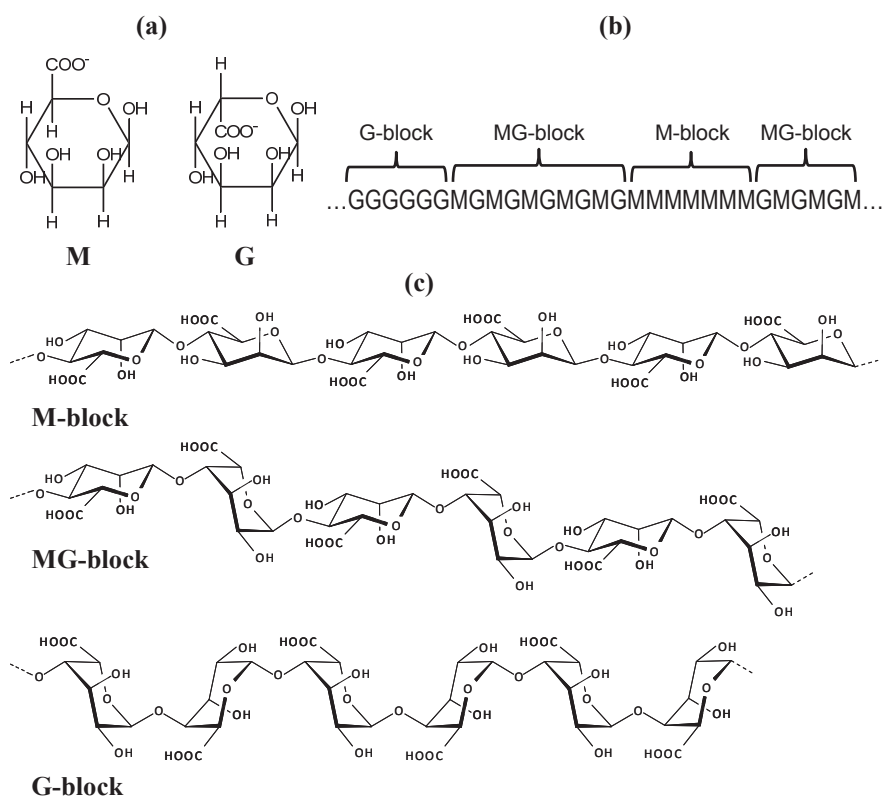


**Figure 1.1 Alginate Chemical structure.**

a) Haworth formulas of  $\beta$ -D-mannuronic acid (M) and  $\alpha$ -L-guluronic acid. b) Block composition in alginates. c) Conformation of alginate blocks with M and G in chair conformation  ${}^4C_1$  and  ${}^1C_4$  respectively.

The first step towards structural elucidation of alginate was taken in 1926, when the monomers in alginate were found to be uronic acids [15],[16]. Chemical methods combined with measurements of optical rotation provided evidence that alginate consists of  $\beta$ -D-mannuronic acid. [17-20]. From fiber diffraction studies, the monomers were proposed to be 1 $\rightarrow$ 4 linked [21]. This was later confirmed by Hirst et al [22] who observed that sodium alginate could be methylated only in O-2 and O-3 positions. In 1955, Fischer and Dorfel made the important discovery that both  $\beta$ -D-mannuronic acid and  $\alpha$ -L-guluronic acid are present in hydrolysates of alginic acid. In their study, monomers were separated as lactones by paper chromatography and the identity of L-guluronic acid was confirmed by comparison to a synthesized standard [23].

### 1.1.2.1 Composition and sequence

The first evidence for alginate being a copolymer was provided when both  $\beta$ -D-mannuronic acid and L-guluronic acid were found in the same fragments of partially hydrolysed alginate [24, 25]. The copolymeric nature of alginate was further investigated by Haug and Smidsrød. Alginate was fractionated by precipitation with magnesium and calcium ions, heterogeneous acid hydrolysis, followed by quantification of  $\beta$ -D-mannuronic acid and  $\alpha$ -L-guluronic acid. In a series of papers it was concluded that alginate is a true block copolymer with homopolymeric regions of each block type (G-blocks, M-blocks and MG-blocks) [26-29]. Computer simulations of composition and distribution of alginate have been developed using either a Monte Carlo approach or a stepwise polymerization from a primer. [30-32]. The conclusion from these studies was that in contrast to many copolymeric polysaccharides alginate does not have a repeating unit nor is the ordering of G and M units random (Bernoulli) distribution. Experimental data was best described by second order Markovian statistics. This model is also referred to as the penultimate model in the polymerization of synthetic copolymers, where the last two units in a growing chain influence the rate of addition of the next unit. The penultimate model seemed to be realistic since it was widely believed at the time that different sugar residues in complex carbohydrates were added to the polymer by means of nucleotide sugar and glycosyltransferases. The discovery that mannuronic acid residues within a polymer can be converted into guluronic acid residues by the action of a family of isoenzymes with C-5 epimerase activity implies that the alginate sequence is better described by a cooperative polymer modification process. Such models have been developed by Plate et al [33] and Gonzalez and Kehr [34].

### 1.1.2.2 Conformation

X-ray fibre diffraction studies [35-37] have shown that the chair conformations are  ${}^4C_1$  for  $\beta$ -D-mannuronic acid and  ${}^1C_4$  for  $\alpha$ -L-guluronic acid. Statistical mechanical calculations supported the latter by asserting that the relative extension of the different block types estimated from light scattering analyses and viscometry could only be explained if  $\alpha$ -L-guluronic acid is in the  ${}^1C_4$  conformation [38].

Alginate therefore contains all types of glycosidic linkages: diequatorial (M-M), equatorial-axial (M-G), axial-equatorial (G-M) and diaxial (G-G). As a result of this, mannuronate chains have a flat ribbon-like structure with a dimer length of 10.4 Å and intra-chain hydrogen bonds between the ring oxygen and the 3-OH group on the subsequent unit,

whereas guluronate has a more buckled shape. The dimer length is 8.7 Å with hydrogen bonds between the carboxyl group and the 2-OH group on the prior residues and 3-OH group of the subsequent residue. Alternating (M-G)<sub>n</sub> chains have hydrogen bonds between the carboxyl group on the mannuronate and the 2-OH group on the preceding guluronate residue.

### 1.1.2.3 Molecular weight

Like polysaccharides in general, alginates are polydisperse with respect to molecular weight. The molecular mass of an alginate is therefore an average of the whole distribution of molecular masses. The most commonly used are number, weight and z-averages, defined as:

$$\overline{M}_n = \frac{\sum_i n_i M_i}{\sum_i n_i} = \frac{\sum_i c_i}{\sum_i \frac{c_i}{M_i}} \quad (1-1)$$

$$\overline{M}_w = \frac{\sum_i n_i M_i^2}{\sum_i n_i M_i} = \frac{\sum_i c_i M_i}{\sum_i c_i} \quad (1-2)$$

$$\overline{M}_z = \frac{\sum_i n_i M_i^3}{\sum_i n_i M_i^2} = \frac{\sum_i c_i M_i^2}{\sum_i c_i M_i} \quad (1-3)$$

where  $c_i$  is the weight concentration (g/l),  $n_i$  is the molar concentration and  $M_i$  is the molecular weight.

There are many experimental methods for determination of molecular weights and it is therefore very important to know which kind of average is obtained from different methods.

Another useful parameter is the polydispersity index, defined as  $P.i = \overline{M}_w / \overline{M}_n$ , which is a measure of the heterogeneity with respect to molecular weight.  $P.i = 1$  for a monodisperse sample and 2 for a randomly degraded (kuhn distributed) polymer.

Most commercially available alginates have a weight average between  $10^5$  and  $10^6$  Da, but low molecular weight samples can easily be prepared by acid hydrolysis.  $P.i$  is usually close to 2 but industrial producers sometimes blend different alginates in order to obtain desired physical properties so these may have a higher  $P.i$ .

### 1.1.3 Physical properties

Alginate shares the general properties of polysaccharides, such as their ability to retain water and alter viscosity of solutions due to their macromolecular character. As a polyelectrolyte, alginates are more influenced by ionic strength and pH than neutral polysaccharides. The



combination of polymeric behaviour, ion-binding properties and the influence of monomeric composition, opens up the possibility for tailoring alginate and fine tuning local conditions.

### 1.1.3.1 Solubility

Monovalent salts of alginates are generally soluble in water due to the large entropy contribution from the dissociation of counterions. This drive is reduced with increasing ionic strength of the solvent and it is therefore recommended to dissolve alginates in pure water prior to addition of salts [39]. Presence of divalent metal ions that bind strongly to the polymer will also reduce the solubility [40].

The pH of the solvent is important, as the undissociated alginic acid is insoluble in water. [41]. The pKa values of  $\beta$ -D-mannuronic acid (M) and  $\alpha$ -L-guluronic acid are 3.38 and 3.65 respectively [42] and a rapid decrease in pH below 3 will cause precipitation of alginic acid, whereas a controlled pH reduction from a slowly hydrolyzing acid like GDL (D-glucono- $\delta$ -lactone) results in the formation of an acidic gel [43, 44].

The solubility of homopolymeric blocks increases in the order G-blocks < M-blocks < MG-blocks [43, 45]. Solubility is therefore not solely dependent on pKa values but is a complex function of polymer concentration, molecular weight and sequence.

A sample of a high molecular weight alginate with an alternating structure ( $F_G = 0.47$ ,  $F_{GG} = 0.0$ ) was found to be soluble over the whole pH range after 30 minutes of equilibration [46]. The solubility of MG-blocks has been attributed to higher flexibility and geometric restrictions that prevents formation of intermolecular hydrogen bonds. It should be noted that this sample eventually formed an acidic gel after several days.

### 1.1.3.2 Viscosity and chain extension

In aqueous solution, alginate has a very extended random coil conformation with partially free drainage due to both electrostatic repulsion and inherent chain stiffness [41, 47]. As a consequence of the extended shape, alginate yields highly viscous solutions. The viscosity is dependent on concentration, molecular weight and factors that influence the chain extension, such as pH, ionic strength and cation type.

The intrinsic viscosity,  $[\eta]$  is defined as 
$$[\eta] \equiv \lim_{c \rightarrow 0} \lim_{\dot{\gamma} \rightarrow 0} \left( \frac{\eta_{sp}}{c} \right) = v_h \cdot v \quad (1-4)$$

where  $c$  is the weigh concentration,  $\dot{\gamma}$  is the shear rate,  $\eta_{sp}$  is the specific viscosity,  $v_h$  is the specific hydrodynamic volume and  $v$  is the Einstein-Simha viscosity factor characteristic for the polymer at given conditions.

It has been shown that the intrinsic viscosity is proportional to the inverse square root of the ionic strength ( $[\eta] \propto 1/\sqrt{I}$ ) and that the intrinsic viscosity of an acid-soluble alginate fraction, rich in alternating sequences, is independent of pH between 4.6 and 10, but decreases continuously between 4.6 and 2.0 [48]. The intrinsic viscosity is related to molecular weight through the Mark-Houwink-Sakurada (MHS) equation:

$$[\eta] = k \cdot \overline{M}_w^a \quad (1-5)$$

where  $k$  and  $a$  are constants related to the conformation of a given polymer under specified conditions.

When  $a$  and  $k$  are determined by light scattering experiments, the molecular weight can be determined by simply measuring the efflux times through a capillary viscometer. Moreover, the 'a' parameter provides information about the conformation of the polymer since  $a = 0$  for compact spheres, 0.5-0.8 for flexible coils, 0.8-1.8 for stiff coils and 1.8 for stiff rods.

There has been some controversy regarding the values of  $k$  and  $a$  for alginates of different composition, as the literature is not clear-cut. This may be due to the lack of well-defined samples and in particular the presence of aggregates, differences in instrumental setups and data processing.

The relative extension of the three types of blocks (in 0.1M NaCl) has been found to increase in the order  $MG < MM < GG$  based on light scattering data, viscometry and theoretical considerations [38]. This is in contradiction with a more recent study where poly-M, Poly-MG ( $F_G=0.47$ ) and *in vitro* epimerised high-G alginate ( $F_G>0.9$ ) studied by SEC-MALLS-online Viscometry (SMV) were found to obey essentially the same  $[\eta]$ -Mw and  $R_g$ -Mw relations whereas periodate oxidized alginates had a lower  $a$  value as expected. [49]. On a local scale however, polyalternating sequences may behave differently from the other sequences as M-G and G-M gives rise to kinks, which change the local directionality.

### 1.1.3.3 Stability

The glycosidic linkages in alginates are susceptible to degradation by acid hydrolysis [50], enzymatic or base catalyzed  $\beta$ -elimination [51] and oxidative-reductive depolymerization (ORD) by free radicals [52, 53]. In the manufacturing process and for most industrial

purposes, depolymerization is unfavourable. Both pH and temperature must therefore be considered during the extraction procedure and in specific applications.

Acid hydrolysis is an important tool in the study of sequence and composition in polysaccharides. The difference in degradation rates between various glycosidic linkages makes it possible to isolate and analyse fractions enriched in specific sequences. Most side reactions can be avoided compared to oxidative-reductive degradation and information is not lost as in the  $\beta$ -elimination reaction where C-5 epimers results in the same 4-5 unsaturated non-reducing end. The acid catalyzed hydrolysis of glycosidic bonds is an  $S_N1$  reaction that proceeds in 3 steps [54]:

1. Formation of the conjugate acid by a rapid equilibrium controlled protonation of the glycosidic oxygen.
2. A slow, rate determining unimolecular heterolysis of the conjugate acid resulting in a cyclic carbonium-oxonium ion, supposedly in a half chair conformation and a new non-reducing end.
3. The carbonium ion reacts rapidly with water to give  $H^+$  and a new reducing end.

The rate of hydrolysis of alginates is in contrast to neutral polysaccharides and not proportional to the proton activity [50]. At low pH (<2), alginates are hydrolysed at a slower rate than neutral polysaccharides due to an inductive effect of the carboxyl group which lowers the concentration of the conjugate acid and the subsequent electron transfer step. The opposite is the case in the pH region where the carboxyl group is partially ionized and the negative charge will cause the proton concentration near the chain to be higher than in the bulk of the solution. The main contribution to a higher hydrolysis rate is intramolecular hydrolysis catalyzed by the undissociated carboxyl group on the glycan acting directly as a proton donor.

The hydrolysis rate of the glycosidic bonds in alginate are equal at low pH, but shows different pH dependency and decreases in the order  $k_{G-M} > k_{M-M} > k_{M-G} > k_{G-G}$  between pH 2 and 4.5 [55-57].

The ratio between  $k_{G-M}$  and  $k_{M-M}$  varies between 12.8 and 6.7 in the pH region 2.8 - 4.5 [56]. This has been utilized to produce strictly alternating oligomer fractions from Poly-MG ( $F_G=0.47$ ) where more than 90% of the even numbered oligomers have M on the non-reducing and G on the reducing end [57].

Alginate is stable in the pH-region 5-10 (in the absence of oxygen and reducing agents) but is degraded by a  $\beta$ -elimination reaction under strongly alkaline conditions.

This happens through removal of the H-5 hydrogen by nucleophilic attack followed by elimination of the C-4 bond to give a new reducing end and a 4-5 unsaturated (4-deoxy-L-*erythro*-hex-4-enopyranosyluronate) non-reducing end. The reaction rate depends on the electron attracting effect of the C-6 group and the nature of the leaving group. Alginate is therefore more resistant to  $\beta$ -elimination than neutral polysaccharides, and particularly, esterified uronic acids. The fact that the degradation rate also increases with ionic strength, in the presence of basic anions like phosphate and carbonate and cations forming ion pairs with the carboxyl groups, shows that  $\beta$ -elimination is a general base catalyzed reaction [51].

Polyphenols located in the physodes of brown algae typically constitutes less than 1% of the dry matter, but nevertheless may cause severe degradation in the presence of molecular oxygen through the formation of peroxides followed by the formation of free radicals. Most of the polyphenols can be avoided by a cross-linking reaction with formaldehyde prior to alginate extraction, converting it into an insoluble resin. Bleaching with  $\text{NaClO}_2$  or chromatography on polyamide/activated carbon may be performed in special cases where a low concentration of polyphenols is crucial [58].

#### **1.1.3.4 Ion binding.**

The ion binding characteristics of alginate is important since it to a large extent governs the solution behaviour of the polymer. Moreover, the binding of divalent cations is responsible for the formation of an ionically cross-linked gel with the physical properties dependent on the type and amount of ions present during gelation.

From numerous studies on the ion-equilibrium between pairs of divalent cations, it has been established that the binding of divalent ions is selective and increases with an increasing proportion of guluronic acid. The selectivity coefficient,  $k_{\text{Ca/Mg}}$  is about 20 times higher for G-blocks than for M-blocks, showing that the interaction is not purely electrostatic [59]. The affinity of alkaline earth metals to G-blocks increases in the order  $\text{Mg}^{2+} < \text{Ca}^{2+} < \text{Sr}^{2+} < \text{Ba}^{2+}$  [40] whereas M- and MG-blocks shows little or no preference to the different ions. Calcium ions bind to G-blocks in a cooperative process [60], which is the molecular basis for the formation of a polymer network described by the “egg-box” model [61] depicted in Figure 1.2 In this model, junctions are formed when calcium ions are coordinated between pairs of consecutive G-residues from opposing chains. The average number of chain segments

participating in a junction may in principle be found by determining the stoichiometry of guluronic acid and cooperatively bound calcium as this ratio is 1:4 for a dimer and 1:2 for an infinite sheet. From such measurements it was proposed that the junction zones consist of dimers [62]. Later SAXS studies suggests that further lateral association occurs at increasing fractional  $\text{Ca}^{2+}$  saturation [63].

The minimum number of consecutive G units required to form stable junctions ( $\text{LG}_{\text{min}}$ ) has been investigated by  $\text{Ca}^{2+}$  activity measurements in solutions of oligo- and polyguluronates [64] and by studying the size and composition of alginate leaching from alginate gels [65].  $\text{LG}_{\text{min}}$  is in the range of 8-20 for  $\text{Ca}^{2+}$  but only 3 for the higher binding affinity ion  $\text{Sr}^{2+}$ . The availability of an alginate with a strictly polyalternating sequence has made it possible to study the role of MG sequences in calcium alginate gels. MG/MG junctions were directly demonstrated by Donati *et al.* [66] who made a weak hydrogel from this material. In the same work, the existence of mixed MG/GG junctions was also confirmed.

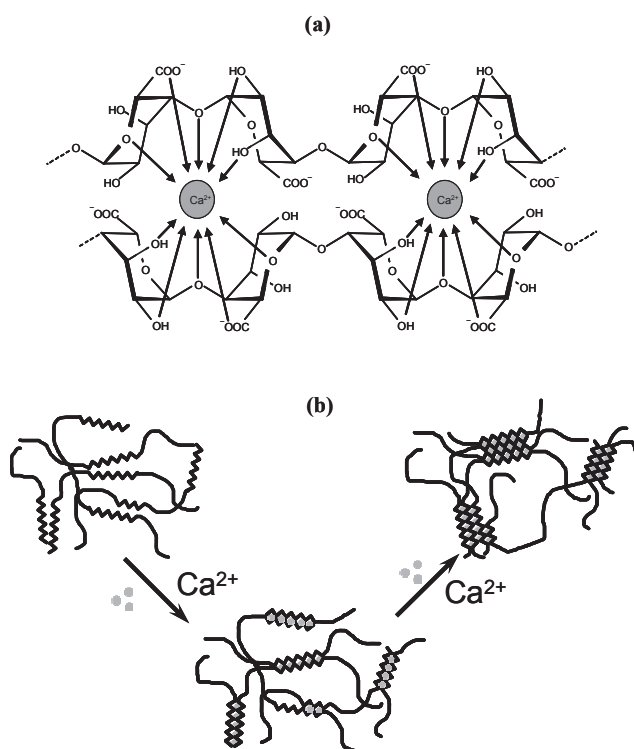


**Figure 1.2 The egg-box model**

Formation of junction zones in alginate caused by chelation of  $\text{Ca}^{2+}$  ions.

a) Coordination of  $\text{Ca}^{2+}$  between adjacent dimers. b) Lateral association of alginate chains

#### **1.1.4 Alginate gels**

Alginate gels may be prepared by either internal gelation or by the diffusion method [39], the difference being how the gelling ions are introduced.

Internal gelation takes place when calcium ions are released from within the system. This is usually done by mixing a solution of alginate with particles of  $\text{CaCO}_3$ . Lowering of pH with a slowly hydrolyzing lactone, such as GDL, will release calcium ions and a homogeneous gel is formed [67]. The gelling kinetics can be controlled by addition of calcium sequestrants like phosphate, EDTA or citrate, or by adjusting the  $\text{CaCO}_3$  particle size.

In the diffusion method, calcium (or other divalent ions) diffuses into an alginate solution (or pulp containing alginate) from an outer reservoir. Alginate diffuses from the center towards an inwardly moving gelling zone, resulting in an alginate concentration gradient, which increases towards the gel surface. The degree of heterogeneity can be controlled by selection of the appropriate alginate and gelling conditions. Maximum heterogeneity is obtained with a low molecular weight alginate in a solution containing a low concentration of gelling ions and in the absence of non-gelling ions [68].

##### **1.1.4.1 Gel properties**

Although many of the factors that control the properties of alginate gels are well understood, it is a formidable task to construct a quantitative model, which based on information on weight distribution, composition and sequence, predicts macroscopic behaviour such as syneresis, Young's modulus and deformation at rupture. In addition to being theoretically challenging, the main obstacle has been the lack of homogeneous and completely characterized model systems, and also the ability to systematically change one factor affecting gel properties while keeping the other constant. Rheological data applied in model development should also be interpreted with care since alginate gels exhibit hysteresis due to the slow dissociation of junctions that must take place in order to reorganize the network into a more thermodynamically stable state [69]. The physical properties of the gel are therefore not only dependent on molecular weight and composition, but also on the conditions when it is formed, and there are no clear cut criteria to decide if or when equilibrium is reached.

Although alginate gels are cold setting and gelling takes place independent of temperature when the concentration of free  $\text{Ca}^{2+}$  exceeds a certain threshold, the kinetics will be temperature and calcium dependent, thus affecting the macroscopic properties [70].

#### 1.1.4.2 Syneresis

Volume reduction in gels with the concomitant release of water is referred to as syneresis,

$$\text{defined as: } S = ((W_0 - W) / W_0) \times 100 \quad (1-6)$$

where  $W_0$  and  $W$  is the initial and final weight.

SAXS studies suggests that growth of junction zones are the primary driving force for syneresis [71]. Syneresis therefore provides information about equilibrium properties of the gel in terms of how fast and how much the junction zones are reorganized. In general, syneresis increases with increasing  $\text{Ca}^{2+}$  concentration, gelling time and  $M_w$  up to a certain level [72]. A high degree of syneresis has been attributed to the amount of alternating sequences (MG-blocks) through a "zipping" mechanism between secondary MG/MG junctions, leading to a partial network collapse under calcium-saturated conditions [73].

However recently unpublished results show somewhat surprisingly a high degree of syneresis also in gels made of in vitro epimerized mannuronan almost devoid of MG-blocks. A model of syneresis in alginate gels must therefore somehow incorporate the chain length distribution of the different blocks.

#### 1.1.4.3 Mechanical strength and elasticity

The relationship between chemical and physical properties has been studied for both gels and capsules made by the diffusion method [72, 74-76] and internally set gels [71, 77]. Apart from differences in gelling kinetics and a concentration gradient in the former, the properties are qualitatively affected in the same direction by changes in composition, molecular weight or ionic environment. The mechanical strength of a gel is frequently evaluated as the Youngs modulus ( $E$ ), defined as

$$E = (F/A) / (\Delta l/l) \quad (1-7)$$

where  $F$  is the force needed to compress a material with contact surface  $A$  to a fraction  $\Delta l$  of the total length.

It is dependent on the number, stability and length of cross links as well as the length and flexibility of the elastic segments between junction zones [78].

Since G-blocks constitute the primary junction zones in calcium-alginate gels, the rigidity has been found to increase with the fraction of guluronic acid and average G-block length [69, 79] as expected. The presence of divalent ions with higher affinity towards G-blocks will also result in a stronger gel [75] as the strength and number of stable crosslinks increases [80]. Furthermore, the average number of junction zones in each chain, and hence the molecular weight is of importance and the modulus increases with increasing molecular weight up to

about  $2.4 \cdot 10^5$  Da, independent of alginate concentration [72]. Syneresis has to be considered when the rigidity is compared between different alginate gels since

$$E = k \cdot C_{\text{Alg.}}^2 \quad [72] \quad (1-8)$$

Rubber elasticity theory has been applied on synthetic polymer networks to calculate deformation properties. The theory describes networks in terms of point-like cross links between flexible coils where energy is stored as reduced entropy upon deformation.[81] Although some predictions also holds for alginate gels, such as the Modulus- $M_w$  dependency, a low ratio between loss and storage moduli and low frequency dependency (in the range  $0.01$  to  $50\text{s}^{-1}$ ), a complete description of stress-strain curves for alginate gels is not obtained [70]. Since an alginate network consists of junction zones rather than points and the length of elastic chains between junctions are too short to be considered as flexible coils, the main assumptions in rubber elasticity theory are not valid. It has been found that the temperature dependence on modulus in alginate gels is negative and the elasticity is therefore enthalpy-driven [70, 82].

Large deformation behaviour in terms of rupture strength and deformation at rupture is relevant for many of the applications where an alginate hydrogel function is used as a scaffold e.g in bone tissue engineering. Alginate gels, like many other biopolymers, show strain-hardening behaviour, which has been attributed to the deformation of junction zones [83]. Fracture of alginate gels can be described as a cascade process where the junction carrying the highest stress yields first and the released energy accelerates the breakage of neighbouring junctions. Rupture strength is therefore not only affected by the number and length of crosslinks, but is also dependent on how stresses are dispersed through the gel. High modulus gels with a high G content are in general more brittle than Low-modulus gels with a high M content due to a higher number of network chains in the latter. Enrichment of alternating sequences in alginates with a low G-content by epimerization with the mannuronan C-5 epimerase Alge4, leads to an further increase in rupture strength and deformation at rupture [84]. The MG/MG junctions were proposed to act as weak reels embedded in the network that dissipates applied stress by sliding over one another.



### **1.1.5 Analysis of alginate**

Alginate and alginate-based materials have been studied by a wide range of techniques, which may be classified either based on physical principle or by the kind of information that can be obtained. It should be noted that most of this applies for characterization of oligo- and polysaccharides in general, with the exception of approaches that take advantage of specific alginate degrading enzymes or ion binding characteristics of alginate.

A brief summary is given in tables 1.1 and 1.2, and some methods will be discussed in more detail in following chapters.

**Table 1.1 Methods for chemical characterization of alginate.**

Method	Sample preparation	Information	Comments	Ref
Spectro-photometry	Degradation in sulphuric acid and formation of coloured products by reaction with a number of aromatic nitrogen heterocycles and phenols.	-Amount of uronic acids. -M/G ratio.	Chemical interference from neutral sugars and low selectivity towards different uronic acids. Incomplete reactions. Standards needed for calibration.	[85-88]
UV-Spectro-photometry of alginates degraded by alginate lyases	Degradation with M- and G- specific lyases	-Amount of uronic acids -M/G ratio	Suited for rapid, automated screening of a large number of samples.	[89, 90]
HPLC-UV/RI/fluorescence detector	Complete acid hydrolysis and derivatization if necessary, followed by separation on anion exchange columns.	-Amount of uronic acids. -M/G ratio.	Derivatization depends on detection methods. More sensitive and reproducible than colorimetric batch methods.	[91-93]
NMR	Partial acid hydrolysis (DPn ~ 30-50)	-M/G ratio. -Sequence parameters in terms of triad frequencies. -Acetylation pattern. -Linkage position. -Monomer conformation. -Anomeric ratio.	Can also be used to study alginate- ion interactions and chemically modified/ grafted alginates.	[56, 94-98]
IR and NIR	Not needed.	-2 and 3 O-Acetyl groups in bacterial alginates. -Amount of uronic acids (M/G ratio).	Alginate concentration may be measured directly in dried seaweed powder.	[99, 100]
HPLC	Partial acid hydrolysis or degradation by alginate lyases.	Separation and quantification of oligomers in hydrolysates/lysates.		[101]
SEC			Preparative technique.	[102-104]
HPAEC-PAD				[57, 103, 105]
CE			4 -Aminobenzonitrile or labeled with chromophors such as 4-ABN or APTS through reductive amination.	[103, 106, 107]
ESI-MS MALDI-TOF-MS			Detection of oligomers in hydrolysates /lysates	Semi-quantitative method.
SEC-MALLS- (viscometry)	Not needed.	-Molecular weight distribution. -Radius of gyration ( $R_G$ ). -Polydispersity index (PI). $R_G$ - $M_w$ and $[\eta]$ - $M_w$ relationships. -Persistence length ( $q$ ).		[49]

**Abbreviations:** (HPLC) high performance liquid chromatography; (UV) ultra violet; (RI) refractive index; (NMR) nuclear magnetic resonance; (IR) infrared; (NIR) near infrared; (SEC) size exclusion chromatography; (HPAEC-PAD) high performance anion exchange chromatography- pulsed amperometric detection; (CE) capillary electrophoresis; (4-ABN) 4-Aminobenzonitrile; (APTS) aminopyrenetrisulfonate; (ESI-MS) electrospray ionization-mass spectrometry; (MALDI-TOF-MS) matrix assisted laser desorption ionization-time of flight-mass spectrometry; (MALLS) multiple angle laser light scattering.

**Table 1.2 Methods for physical characterization of alginate and alginate based materials.**

Method	Sample preparation	Information	Comments	Ref
MALLS (static)	Not needed	- Second virial coefficient ( $A_2$ ), as a measure of deviation from ideal solution. - $R_G$	Even small amounts of aggregates will influence on the results	[49, 109, 110]
Analytical ultracentrifugation	Not needed	Diffusion coefficient, $M_w$ , $A_2$	Of historical interest, but not widely used anymore	[111]
Viscometry	Not needed	Intrinsic viscosity $[\eta]$	$M_w$ can be calculated through the MHS equation	[41, 112]
CD	Not needed.	- Conformational changes (formation of junction zones), ion binding. - Diadic composition ( $F_G, F_M, F_{MG}$ ).	Not used for routine analysis of alginates.	[62, 66, 113]
SAXS	Alginate hydrogels	-Number of chains participating in junction zones	Cross sectional radius of gyration of junctions.	[63, 71, 114]
XPS	Alginate hydrogels	Surface contamination	Elemental composition of surface (1-10nm)	[115, 116]
Fiber X-ray diffraction	Extrusion of alginate solution and fiber stretching	-Monomer conformation and size. -Coordination of gelling ions		[35, 37, 117]
AFM	Depends on operating mode. Binding to activated surface by carbodiimide chemistry or reductive amination.	-Forces involved in single molecular pair binding events. - Morphology of alginate complexes/microgels	Has potential to provide sequence information from individual alginate chains	[118-121]
Dynamic oscillation	Not needed	Gelling kinetics from time dependence of storage and loss modulus ( $G'$ and $G''$ )	Provides a working definition of a gel ( $G' > G''$ ).	[82, 121, 122]
Creep compliance measurements	Alginate hydrogels	Stress-strain profiles. -Youngs modulus		[74, 77]
TEM / SEM	Alginate gels/ fibers	Pore size, microstructure	Sample preparation may be a complex and painstaking procedure	[123, 124]
CLSM	Fluorescence labeled alginate hydrogels	Visualization of alginate concentration gradient in microcapsules		[125]
X-ray fluorescence spectroscopy	see ref.126	Calcium distribution in alginate gels		[126]
ITC	Alginate oligomer with well defined chain-length and composition	Binding affinity ( $K_a$ ) $\Delta H$ , $\Delta S$ , $\Delta G$	Has been used to study the binding of R-modules in mannuronan C-5 epimerases	[127]

**Abbreviations:** (CD) circular dichroism; (SAXS) Small-angle X-ray scattering; (XPS) X-ray photoelectron spectroscopy; (AFM) atomic force microscopy; (TEM) transmission electron microscopy; (SEM) scanning electron microscopy; (CLSM) confocal laser scanning microscopy; (ITC) isothermal titration calorimetry.

#### **1.1.5.1 Chemical characterization**

Chemical characterization includes information about the amount and ratio of uronic acids, the configuration and position of glycosidic linkages, and the distribution of monomers in the polymer chains. The degree and pattern of O-2 and O-3 acetylation in bacterial alginates is also of importance. Alginates used for medical applications also have to be analysed for pyrogenic contaminants.

Chemical methods have been very useful for the determination of M/G ratio and total content of uronic acids (see [88] for a comprehensive overview). Although fast and simple spectrophotometric measurements facilitate routine analysis, these methods do not discriminate well between the uronic acids and neutral sugars also cause interference. This can be overcome by separation of the hydrolysis products prior to analysis [86], but correction factors are still needed since partial degradation of monomers takes place during hydrolysis and guluronic acid is less stable than mannuronic acid.

#### **1.1.5.2 NMR**

Much more information about alginate sequences and composition became available after the introduction of high-resolution  $^1\text{H}$  and  $^{13}\text{C}$  nuclear magnetic resonance spectroscopy (NMR) [94-96]. The magnetic field strength experienced by the nuclei and hence the transition energy between spin states, will depend on its chemical environment. Differences in chemical shifts makes it possible to determine the average fraction of M and G ( $F_G$  and  $F_M$ ) in the polymer chain, as well as the fraction of the four diads ( $F_{GG}$ ,  $F_{GM}$ ,  $F_{MG}$  and  $F_{MM}$ ) and eight triads ( $F_{GGG}$ ,  $F_{GGM}$ ,  $F_{MGG}$ ,  $F_{GMG}$ ,  $F_{MGM}$ ,  $F_{GMM}$ ,  $F_{MMG}$  and  $F_{MMM}$ ). An example of a  $^1\text{H}$ -NMR spectra is given in Figure 1.3.

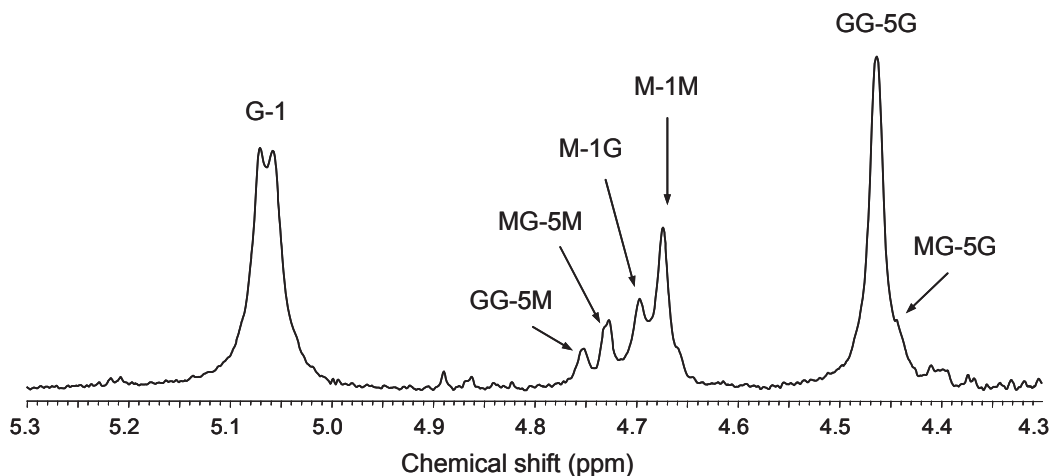


**Figure 1.3**  $^1\text{H-NMR}$  (300 MHz) spectrum of *Laminaria Hyperborea* alginate. Characteristic signals in the anomeric region are indicated in the figure

The molar fractions can be calculated from the integration of the characteristic signals in the anomeric region according to the following relations:

$$F_G = I_G / I_{\text{total}} \quad (1-9)$$

$$F_M = I_M / I_{\text{total}} \quad (1-10)$$

$$F_{MM} + F_{MG} = F_M \quad (1-11)$$

$$F_{GG} + F_{GM} = F_G \quad (1-12)$$

$$F_{MM} + F_{MG} + F_{GG} + F_{GM} = 1 \quad (1-13)$$

The average G- and M-block length can be calculated from equation 1-14 and 1-15.

$$N_{G>1} = (F_G - F_{MGM}) / F_{GGM} \quad (1-14)$$

$$N_{M>1} = (F_M - F_{GMG}) / F_{MMG} \quad (1-15)$$

Substituents like O-2 and O-3 acetyl groups on M-units in bacterial alginates will also cause a chemical shift and the corresponding signals can be used to calculate the degree of acetylation [98]. Additional information that can be extracted from NMR experiments includes monomer conformation, position and orientation of the glycosidic linkage, the anomeric ratio, and the number average degree of polymerization ( $\overline{DP}_n$ ) of partially degraded alginates [56, 103, 128, 129].

Although NMR is a powerful method, the sequence frequencies obtained represent an average of the whole population of sequences present in a heterogeneous alginate sample. For a more detailed description, a fractionation step prior to NMR is needed. This can be done by heterogeneous acid hydrolysis or selective precipitation with divalent metal ions, but for a complete analysis of the block distribution, alginate has to be degraded with specific alginate lyases followed by separation and analysis of degradation products.

#### **1.1.5.3 SEC**

Size exclusion chromatography (SEC) on Biogel or Superdex materials with RI or UV detection is frequently used to separate alginate oligomers based on differences in hydrodynamic volume [97, 104]. The efficiency is usually lower than for anion exchange HPLC methods but a plate number of more than 20000 can still be achieved. Although SEC chromatograms may contain useful information on their own, the method is mainly used to isolate oligomers for various applications or further analysis by NMR, HPLC or MS methods [101],[104, 130].

#### **1.1.5.4 HPLC**

High performance anion exchange chromatography (HPLC) methods have been used to separate and quantify mannuronic and guluronic acid after complete acid hydrolysis [91, 92]. The high resolution makes these methods suited for analysis of oligomer distribution in acid hydrolysates [57, 103] and lyase digested samples [101, 129] where oligomers with the same chain-length, but different composition can be separated.

High performance anion exchange chromatography with pulsed amperometric detection (HPAEC-PAD) has become an important technique for mono and oligosaccharide analysis since its invention in the 1980s. (See [131] for a review). A highly alkaline mobile phase (10-100mM NaOH) is used in contrast to traditional mobile phases such as Na<sub>2</sub>SO<sub>4</sub>, phosphate buffers or NaNO<sub>3</sub>. At high pH, the small differences in acidity of hydroxyl groups in carbohydrates (typical pK<sub>a</sub> values between 12 and 13) are utilized to achieve a higher resolution than cannot be obtained at lower pH and several columns (CarboPac series) have been developed for this purpose [132].

The packing material is a non-porous polymeric resin with MicroBeads carrying the anion-exchange functional groups electrostatically attached to larger cation-exchange resin particles.

Although the loading capacity is lower than for porous packing materials, the non-porous resins ensure minimized band broadening and superior separation. The detection principle based on pulsed amperometry (PAD) is also a novel one, which offers several advantages compared to RI and UV detectors; the detection is very sensitive (in the pmol range), highly selective for carbohydrates using the appropriate potential form and requires no sample preparation or post column derivatization. Moreover it allows the use of gradient mobile phases. [133]

In a PAD detector, the analyte is electrocatalytically oxidized on a gold surface and the measured oxidation current is proportional to concentration. A reductive or oxidative potential has to be applied between each current measurement in order to avoid electrode poisoning by oxidation products. It is important to note that the oxidation current depends on the diffusion of analyte onto the gold surface as well as the oxidation kinetics. The detector response is therefore dependent on both the hydrodynamic volume of the oligomer, sterical factors and the monosaccharide type. For a quantitative analysis of a mixture of alginate oligomers, standards are needed to determine the detector-response factors for G- and M-oligomers as a function of chain length [57, 103].

#### **1.1.5.5 SEC-MALLS**

Size exclusion chromatography with online multiple angle laser light scattering detection combined with RI detection is used to analyse the weight distribution in polymeric samples. The molecular weight and radius of gyration can be calculated through the Rayleigh-Gans-Debye equation for each slice of the SEC chromatogram. This method is more direct and reliable than universal calibration SEC methods and covers the whole molecular weight range from  $10^4$  to more than  $10^6$  Dalton. Other detectors can also be attached [134]. A viscometry detector will provide a  $[\eta]$ - $M_w$  relationship and hence the  $k$  and  $a$  parameters in the MHS equation [49]. These data are also used in the Bohdanecký model [135] for the estimation of persistence length ( $q$ ), a measure for the chain extension.

#### **1.1.6 Biosynthesis**

Biosynthesis of alginate was first studied in the brown algae *Fucus gardneri* by Lin and Hassid [136] who discovered activity from hexokinase, fosfomannomutase, D-mannose-1-phosphate guanyltransferase, guanosine diphosphate-D-mannose dehydrogenase and D-mannuronic acid transferase in a cell free extract. Evidence for epimerization on the polymer level was also first found in brown algae [137]. The preparation of enzymes from marine

algae is however difficult as anionic polysaccharides and phenols released during the extraction procedure form strong complexes with proteins, causing loss of activity [138]. Complex eukaryotic systems are also very challenging to study in terms of protein overexpression and genetic manipulation.

Most of the present knowledge about alginate biosynthesis (Figure 1.4) and the enzymes involved therefore comes from studies of the bacteria *P. aeruginosa* and *A. vinelandii* [139]. The gene cluster for alginate production in *A. vinelandii* is organized in a similar way as in *P. aeruginosa* [140]. The intracellular activity of the key enzymes appears to be very low, indicating that the enzymes are organized in a complex (metabolon) to facilitate efficient coupling of enzymatic reactions [141].

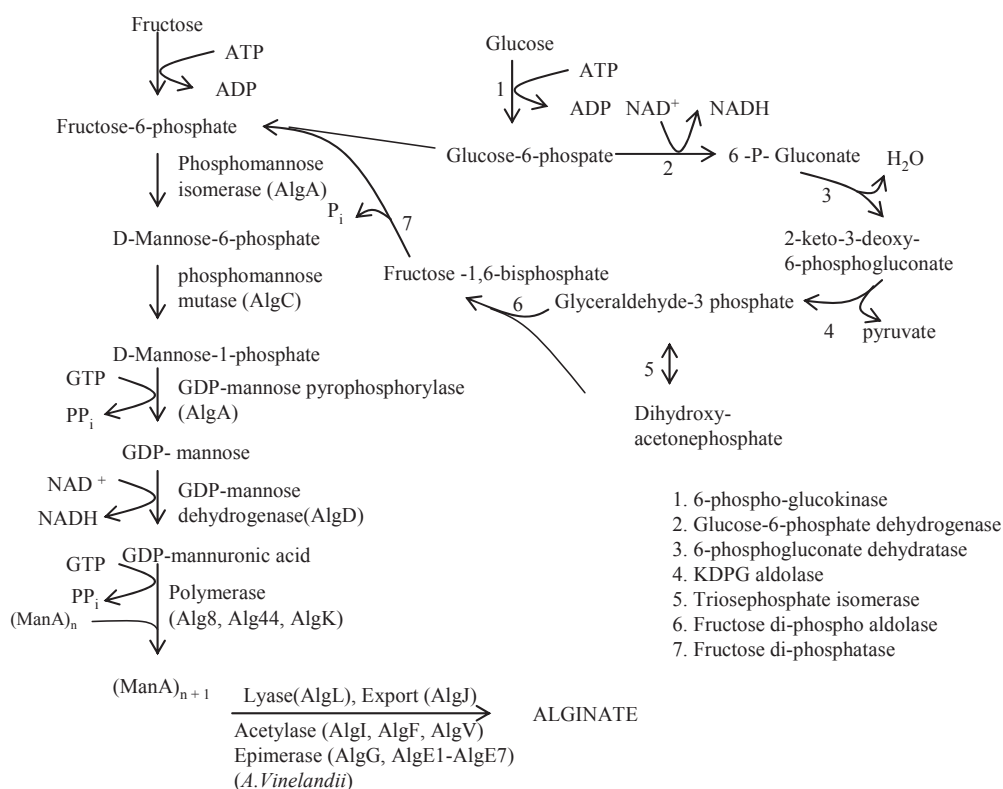


**Figure 1.4 Biosynthesis of alginate in *Azotobacter vinelandii*.**  
The Entner-Duodoroff pathway is shown in step 1-7.

*A. vinelandii* can synthesize alginate from a range of mono- and disaccharides such as fructose, glycerol, gluconate, lactose, mannitol, mannose, sorbitol and sucrose [142]. Hexose precursors are catalysed by the Entner-Doudoroff pathway and enter alginate biosynthesis as fructose-6-phosphate from the intermediate glyceraldehyde-3-phosphate [143]. Following the



cytosolic reactions, mannuronic acid residues from GDP-ManA are added to the non-reducing end of a growing mannuronan chain by an enzyme complex in the cytoplasmic membrane [143, 144]. The mannuronic acid residues in bacterial alginates are partly O-3 and/or O-3 acetylated in contrast to alginates produced by marine algae. Acetylation takes place on the polymer level in the periplasmic space by the action of AlgI, AlgV and AlgF [145, 146]. The degree of acetylation in alginates from several strains of *A. vinelandii* and *Pseudomonas* species has been reported to be in the range 4-57 % [4] and will influence solution and gelling properties [147] as well as the distribution and amount of G-residues since acetylated M-units are not a substrate for mannuronan C-5 epimerases [148].

The periplasmic epimerase AlgG is found both in *A. vinelandii* and *P. aeruginosa* and introduces single guluronic acid units through C-5 epimerization. Its presence but not its activity is necessary for polymer formation [149]. The reason for this is probably that AlgG is a part of a protein complex and protects the newly formed mannuronan chain against degradation by the periplasmic lyase AlgL [150]. The putative biological role of AlgL is to prevent accumulation of alginate in the periplasmic space, which occasionally fail to become exported out of the cell. [151]. It also has a role in controlling chain length and detachment of biofilm to allow colonization [141].

The main difference between alginates from *Pseudomonas* species and *A. vinelandii* is that only the latter contains G-blocks [98] due to the action of a family of secreted mannuronan C-5 epimerases [152]. The epimerization reaction and the enzymes involved will be discussed later.

### **1.1.7 Applications**

Most of the present applications of alginate are based on either its rheological properties i.e. water binding, viscosity and shear thinning, or the unique gelling characteristics allowing temperature independent gelling under physiological conditions. Commercially available alginates are extracted from algae with an annual production estimated to about 38,000 tonnes [153]. Bacterial alginates however have a potential in biomedical applications where compositional homogeneity is important, and it may be possible to produce “tailor-made” alginates with 0-80% guluronic acid in vivo by expressing epimerase genes from a plasmid in an alginate producing bacterium [154].

Industrial applications of alginates include its use as a thickener in water soluble textile printing paste, glazing of paper, creaming of latex and as a water binding agent in the

production of ceramics [155]. Alginates are also widely used in the food industry where alginic acid,  $\text{Ca}^{2+}$ -,  $\text{Na}^+$ -,  $\text{NH}_4^+$ - and  $\text{K}^+$  alginates as well as propylene glycol alginate (PGA) are currently permitted as food additives within Europe. It is used as thickener and stabilizer in sauces emulsions, beverages and ice cream. The gelling properties are exploited in the restructuring of foods. This can be achieved either by internal setting or the diffusion setting method. Typical examples are pet foods, fruit jellies, dairy products, onion rings and pimento strips in olives [155].

#### **1.1.7.1 Biomedical and pharmaceutical applications**

In recent years there has been extensive research on many promising biomedical applications. A significant pharmaceutical use of alginate is in the treatment of esophageal reflux. An alginate solution containing sodium bicarbonate will form a buoyant acid gel with entrapped  $\text{CO}_2$  when it comes in contact with the gastric juice that serves as a mechanical barrier against reflux of the stomach content into the oesophagus [155, 156].

Alginates with a high content of mannuronic acid (96-100%) have been found to induce production of TNF, IL-1 and IL-6 in monocytes, probably due to a non-specific interaction of  $\beta(1\rightarrow4)$  linked uronic acid polymers [157]. This has caused a growing interest in the biological activity of the molecule itself [158] and chemically modified /grafted alginates as it is possible that immunostimulating /cell signaling and heparin/ heparansulfate mimicking properties will be utilized in future applications.

Alginate is also used in woven and gauze dressings in the form of calcium alginate fibers, which form an adherent biofilm that absorbs exudate and provides a moist environment for wound healing. The immune stimulating effect of alginates with a high M-content may also be utilized in this context for the treatment of chronic wounds.

Since alginate is non-toxic, biodegradable and has attractive and readily adjustable rheological properties, there have been numerous studies on alginates as a matrix in drug delivery systems [159, 160]. Acid labile, gastric irritating or insoluble drugs can be incorporated into alginate beads, microcapsules or tablets for delayed and diffusion controlled release. Therapeutic proteins with a short biological half-life may be administered locally in a slow and predictable manner by injecting alginate microcapsules loaded with the relevant protein. Recently, alginate capsules have also been utilized as a means of controlled release of  $\text{Mn}^{2+}$  ions in manganese-enhanced magnetic resonance imaging (Mn-MRI) [161].

Work on novel medical applications has been spurred on by the discovery that low molecular weight guluronic acid oligomers are able to disrupt intermolecular interactions in mucosal

systems through electrostatic competitive inhibition, causing the gel matrix to weaken [162]. The synergetic effect between mucous and macromolecules associated with chronic inflammation is anticipated to be reduced by the same mechanism [163]. A specified composition of guluronic acid oligomers for improved mucociliary clearance in CF patients infected with *P. aeruginosa* is currently undergoing clinical trials [164]. Similar formulations aiming at overcoming multidrug resistance in bacteria [165] and combating biofilms [166] have been patented.

Alginate hydrogels has become the most common matrix for immobilization of living cells because of the mild gelling conditions [167]. Gel beads are formed when a suspension of cells in 1-4% alginate solution is dripped into a gelling bath containing 20-100 mM of divalent cations such as  $\text{Ca}^{2+}$ ,  $\text{Ba}^{2+}$  and  $\text{Sr}^{2+}$  and gel spheres, with diameters ranging from a few microns to 5mm, can be made by a simple device. [158]. Immobilized cells have a range of applications such as in the industrial production of ethanol and organic acids in bioreactors with immobilized yeast cells [168-170], as artificial seeds in the form of encapsulated plant embryos [171] and production of penicillin and monoclonal antibodies from immobilized fungi [172] and hybridoma cells [173].

Much of the work on cell immobilization has been directed towards immunoisolation of transplanted cells. The purpose is to prevent the most potent cytokines from penetrating into the capsule while allowing nutrients, signalling substances and therapeutic substances produced by the cells to diffuse through the capsule membrane. Insulin producing Islets of Langerhans, for the treatment of type 1 diabetes, is the most studied system [158], but a range of cells may in principle be suited for cell therapy, including hepatocytes [174] and endostatin producing cells for the treatment of brain tumours [175]. Immunoisolation puts extraordinary demands on the capsule in terms of pore size and distribution, biocompatibility, response to deformation and long term stability in the presence of non-gelling ions. Although much progress has been made, the “ideal” capsule for a given application is yet to be manufactured.

In the related field of tissue engineering, alginate hydrogels are used as scaffolds as a substitute for the extracellular matrix (ECM) [176]. Alginate is not a bioadhesive polymer, but can be grafted with ligands that are recognized by cell receptors. The peptide sequence RGD (Arg-Gly-Asp) found in many ECM proteins is recognized by integrins, a family of transmembrane proteins involved in signal transduction and attachment to the ECM. Grafting of RGD to alginate through carbodiimide chemistry enables myoblasts to adhere, proliferate

and show signs of differentiation [177]. Another example of cell-matrix interactions is the binding of galactose-modified alginate to asialoglycoprotein receptors on hepatocytes [178].

## 1.2 Mannuronan C-5 epimerases

The conversion of  $\beta$ -D-mannuronic acid into  $\alpha$ -L-guluronic acid is catalyzed by a family of mannuronan C-5 epimerase isoenzymes and constitutes the final step in alginate biosynthesis. This reaction occurs at the polymer level with the only known analogue being the epimerization of D-glucuronic acid into L-iduronic acid in heparin/heparin sulphate and dermatan sulphate [179]. Mannuronan-C5 epimerase activity was first detected in *A. vinelandii* [180] and has later been reported in several brown algae [138, 181] and *Pseudomonas* sp. [182-184].

The mannuronan C-5 epimerase AlgE2 from *A. vinelandii* was the first to be purified and characterized using affinity chromatography on an alginate grafted sepharose gel followed by gel electrophoresis [185]. A synthetic oligonucleotide probe based on its N-terminal sequence was used to screen the *A. vinelandii* genome, and the hybridizing DNA was subcloned into *E. coli* [186]. Later studies have shown that the *A. vinelandii* genome encodes a family of seven extracellular homologous epimerases (AlgE1-AlgE7) [152, 187] in addition to the periplasmic epimerase AlgG, which resembles the epimerase found in *P. aeruginosa* [140]. A library of mutant epimerases, based on AlgE1-AlgE6 genes, has recently been constructed by site-directed mutagenesis and error prone PCR [90, 188].

Epimerases from algae are much less studied, as it has not yet been possible to purify or clone any of the enzymes involved in the biosynthetic pathway of alginate. However, several cDNAs with homology to AlgG have been isolated from *Laminaria Digitata* [181], and a sequence analysis indicates that this encodes at least 21 mannuronan C-5 epimerases. The large number of epimerases involved in alginate biosynthesis in *A. vinelandii* and probably also in brown algae emphasizes the importance of controlling alginate sequence in order to meet physiological requirements.

### 1.2.1 Reaction mechanism

A three-step reaction mechanism for C-5 epimerization has been proposed (Figure 1.5) and is motivated by alkaline- and lyase-catalyzed  $\beta$ -elimination reactions of uronic acids and their methylesters [189]. More recently, an X-ray crystallography study of the catalytic A-module of AlgE4, which supports the general mechanism, has been published [190].

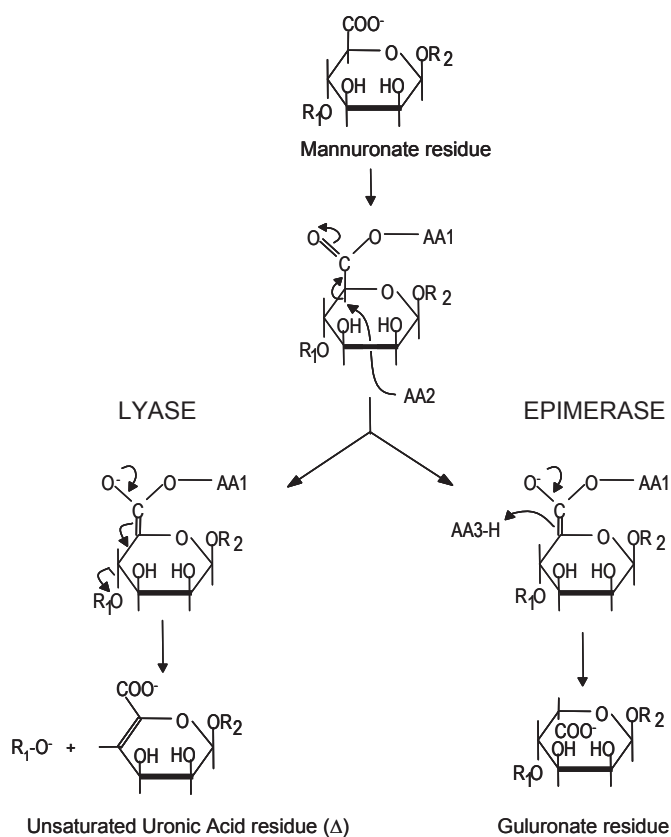


**Figure 1.5 Unified reaction mechanism for mannuronan C-5 epimerases and lyases**

AA1-3 refers to the amino acids involved in the stabilization of the enolate ion(AA1), abstraction of the proton at C-5 (AA2), and proton donation from the opposite side of the sugar plane (AA3).

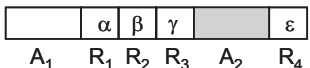
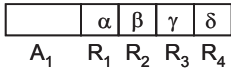
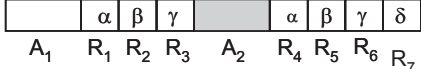
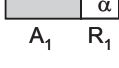
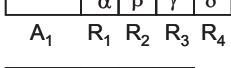
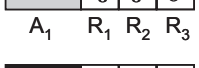
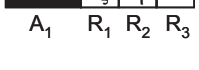
The first step involves neutralization of the carboxyl group by formation of a salt bridge with the positively charged amino acid side chain AA-1. A resonance stabilized enolate intermediate is then formed by a base-catalyzed abstraction of the C-5 proton, where deprotonated Tyr<sup>149</sup> (via Arg<sup>195</sup>) may act as the proton acceptor AA-2 [190]. In the final step, three outcomes are possible depending on where the proton is donated:

- i) C-5 epimerization by protonation on the opposite side of the sugar ring by AA-3 (His<sup>154</sup>).
- ii) Reversible protonation by AA-1 or solvent to yield mannuronic acid.
- iii)  $\beta$ -elimination by donation of the proton to the O-4 leaving group catalyzed by the alginate lyases, resulting in a new reducing end and a 4-deoxy-L-*erythro*-hex-4-enopyranosyluronate non-reducing end.

The release of 5-H during epimerization, which has been confirmed by NMR spectroscopy [191], also forms the basis of a convenient epimerase activity assay, using 5-<sup>3</sup>H-mannuronan as the substrate [192]. Mannuronan C-5 epimerization is considered to be irreversible in contrast to epimerization of D-glucuronic acid into L-iduronic acid in glycosaminoglycans [179, 193]. The finding that a minor amount of tritium was incorporated in M-units when mannuronan was incubated with the C-5 epimerase AlgE4 in tritiated water has been explained by a reversible second step [194].

### 1.2.2 Structure and mode of action of AlgE epimerases

The mannuronan C-5 epimerases AlgE1-AlgE7 from *A. vinelandii* have all been produced recombinantly in *E. coli* and are by far the most studied. These enzymes are modular, being composed of 1 or 2 catalytic A-modules (385 amino acids) and one to seven regulatory R-modules (153 amino acids). A high degree of homology within the modules strongly suggests a common origin and an evolutionary pathway of the algE genes through gene fusion, duplication and conversion has been proposed [152]. The modular structure and molecular weights of AlgE1-7 are shown in Figure 1.6.

	Module structure	[kDa]	Enzymatic activity
AlgE1	 <p>A<sub>1</sub>   α   β   γ   A<sub>2</sub>   ε   R<sub>4</sub></p>	147,2	GG- and MG-epimerase
AlgE2	 <p>A<sub>1</sub>   α   β   γ   δ   R<sub>4</sub></p>	103,1	GG-epimerase
AlgE3	 <p>A<sub>1</sub>   α   β   γ   A<sub>2</sub>   α   β   γ   δ   R<sub>4</sub>   R<sub>5</sub>   R<sub>6</sub>   R<sub>7</sub></p>	191,0	GG- and MG-epimerase
AlgE4	 <p>A<sub>1</sub>   α   R<sub>1</sub></p>	57,7	MG-epimerase
AlgE5	 <p>A<sub>1</sub>   α   β   γ   δ   R<sub>4</sub></p>	103,7	GG-epimerase
AlgE6	 <p>A<sub>1</sub>   ε   ε   ε   R<sub>1</sub>   R<sub>2</sub>   R<sub>3</sub></p>	90,2	GG-epimerase
AlgE7	 <p>A<sub>1</sub>   ξ   η   δ   R<sub>1</sub>   R<sub>2</sub>   R<sub>3</sub></p>	90,4	GG-epimerase and lyase

**Figure 1.6 Modular structure, molecular weight and products of the extracellular Mannuronan C-5 epimerases AlgE1-7 from *A. vinelandii*.**

Each epimerase is composed of different numbers of A modules (385 amino acids) and R modules (153 amino acids). Closely related R modules are indicated by identical greek letters.

Crystallization of the native enzymes has not been successful, but the crystal structure of the A-module from AlgE4 has recently been elucidated, showing a right handed parallel  $\beta$ -helix structure with an amphipathic  $\alpha$ -helix on the N-terminal end [190].

The R-module from AlgE4 has been assigned a right handed parallel  $\beta$ -roll structure from NMR studies [195]. The structure of the two modules are shown in Figure 1.7.

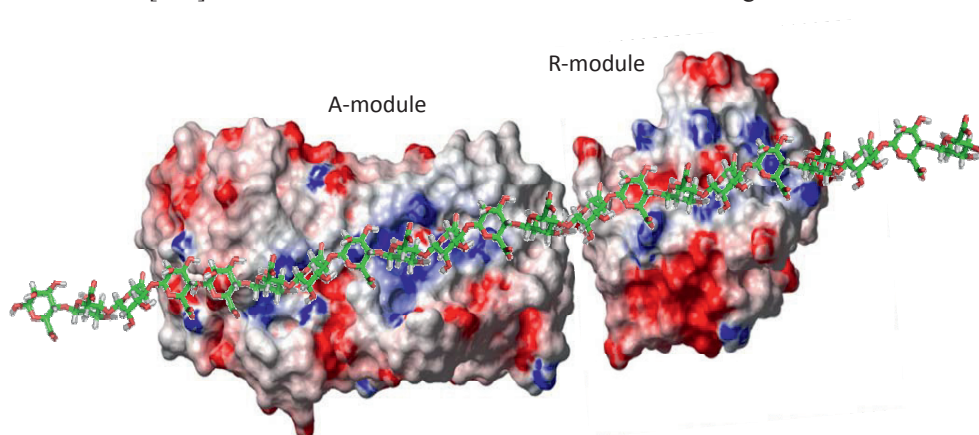


**Figure 1.7 Structure of the A- and R-module of AlgE4 with the electrostatic surface potential.**

The structure of the A-module was solved by X-ray crystallography [190] while the R-module was solved by NMR [195]. The modules oriented to illustrate tentative structure of AlgE4 with poly-M. The program PDB 2PQR, version 1.5 [196], was used to prepare the structures for electrostatic potential distribution calculations, performed with the programs APBS [197]. Visualization of the potential plotted on the solvent accessible surface was made with the program PyMOL, version 0.99 [198]. Red and blue denote regions of negative (i.e. less than -3 kT/e) and positive (i.e. more than 3 kT/e) potential on the surface, respectively. Structural models were visualized with PyMOL version 0.99.

In contrast to the calcium-independent periplasmic epimerase AlgG, all of the secreted AlgE epimerases require  $\text{Ca}^{2+}$  for activity [199, 200]. The R-modules contain 4-6 repeats of a nine amino acid long  $\text{Ca}^{2+}$  binding motif [152, 186], whereas 6  $\text{Ca}^{2+}$  binding sites have been identified in the crystal structure of the A-module from AlgE4 [190]. Even though the R-module is not catalytically active on its own, it reduces the  $\text{Ca}^{2+}$  concentration needed for full activity and increases the reaction rate [200].

Each epimerase gives rise to a distinct epimerization pattern i.e. distribution of guluronic acid residues. Moreover, the substrate specificity and  $\text{Ca}^{2+}$  concentration required for full activity is different [201]. This clearly facilitates the production of a large variety of alginates with different compositions and sequences, which are adjusted to specific environmental conditions and developmental stages. The epimerization patterns of the different epimerases have been investigated in a number of studies using Poly-M ( $F_G=0.0$ ) and Poly-MG,

( $F_G=0.47$ ) as substrates. AlgE1 and AlgE3 both consist of two A-modules and are capable of making both G-blocks and MG-blocks [201, 202] while AlgE2, AlgE5 and AlgE6 make mostly short, medium and long G-blocks respectively [104, 186, 187, 202, 203]. AlgE7 is a bifunctional epimerase and lyase with both reactions probably taking place at the same active site [204]. AlgE4 is the only epimerase, which introduces strictly alternating sequences [152, 194]. This capability to produce polyalternating alginate ( $F_G=0.47$ ) or to enrich alginates with alternating sequences has been used to study the role of alternating structures in solution and alginate gels [46, 66, 77, 84].

The mode of action of the epimerases is reflected in the resulting chain length distribution of G-blocks or MG-blocks introduced. Enzymes acting on polymeric substrates may dissociate after each reaction (multi-chain mechanism) or continue along the polymer until it reaches the end of the chain (single-chain mechanism). Behaviour along these extremes is referred to as processivity:  $P = 1/(1-p)$  (1-15)

where  $P$  is the number of reaction for each enzyme-substrate encounter and  $p$  is the probability for association after each reaction.

Some of the enzymes involved in DNA and RNA modification and replication

e.g. DNA polymerase III provides the most familiar example of processivity, although this mode of action may be widespread also amongst polysaccharide-modifying enzymes.

Processivity has been reported for chitinases [205] and is suggested to be involved in the assembly of heparin/heparansulfate in GAGs [206]. A processive enzyme must be able to recognize and bind substrate residues surrounding the catalytic site. This requirement is met by all of the AlgE epimerases, and even the smallest enzyme AlgE4, comprised of one A and one R module, can accommodate more than 10 sugar residues in its binding site [190, 195].

The mode of action and subsite properties of AlgE4, AlgE1 and AlgE6 have been studied using methodologies involving time-resolved NMR, specific alginate lyases, chromatographic techniques and MS [104, 106, 207].

The minimum substrate which AlgE4 required for activity was found to be a mannuronic acid hexamer (M6) where the third residue from the non-reducing end was epimerized, while AlgE1 and AlgE6 epimerized the fourth residue of M8 and M7, respectively. Alternating sequences are also a substrate for the latter and acting on Poly-MG ( $F_G=0.47$ ), AlgE1 forms long G-blocks ( $DP>50$ ) while AlgE6 produces a broader range of shorter G-blocks [104].

Even though the distribution of G-residues is far from random, it is difficult to unequivocally decide whether this is a result of a processive mode of action or a preference toward specific



sequences at the end of a G- or MG-block (preferred attack mechanism). The slightly higher initial reaction rate of AlgE1 and AlgE6 on a substrate already containing G-blocks, together with sigmoidal epimerization curves for poly-M and poly-MG, supports a preferred attack mechanism [104]. Processivity and preferred attack are however not mutually exclusive, and the observed G-block distribution may be modelled by a combination of the two mechanisms. AlgE4 does not seem to have a higher affinity for single G-residues flanked by stretches of M-residues, and a degree of processivity around 10 has been estimated, based on an analysis of partially epimerized Poly-MG degraded by a G-lyase [106].

### **1.2.3 Biotechnical Applications of C-5 epimerases**

Apart from being important tools in the study of structure-function relationships in alginate materials, the AlgE epimerases and epimerase mutants constructed from algE genes have interesting potential applications. Commercially produced alginate has so far been extracted from brown algae, where composition and sequence will vary with type of tissue, species and season. The product is therefore a mixture of sub-populations of alginates, and treatment with AlgE epimerases can provide a more homogeneous alginate with less batch to batch variations suitable for biomedical applications [154]. *In vitro* epimerization would also enhance the mechanical properties of alginate gels and capsules [77, 79, 208] and could contribute to the increasing demand for strong gelling alginates. Alginates with compositions and sequences suited for specific applications may also be tailor-made by applying the epimerases, either together or in succession on mannuronan produced from epimerase deficient mutants [79]. Since acetylated or grafted mannuronic acid units are not substrates for the AlgE enzymes [98], alginate materials with selective modification of M-residues and novel properties can be made by performing the required reaction on mannuronan, followed by epimerization of the unsubstituted residues. This has been exploited to produce biologically active galactose-substituted alginates and flexible periodate-oxidized alginates, where both were able to form stable gels [209, 210]. A reverse approach where polysaccharides containing mannose are converted into substrates for the epimerases through TEMPO-mediated C-6 oxidation, followed by epimerization has also been studied [211].

### 1.3 Alginate Lyases

Alginate lyases catalyse the degradation of alginate by cleaving glycosidic bonds by a  $\beta$ -elimination mechanism [189]. The two first steps in the reaction i.e. neutralization of the carboxyl group and subsequent proton abstraction at C-5 are shared with the epimerase reaction (Figure 1.6), but diverge from the latter in the final step as the proton is donated to the O-4 leaving group, resulting in a new reducing end and a 4-deoxy-L-*erythro*-hex-4-enopyranosyluronate non-reducing end.

#### 1.3.1 Sources and biological function

The occurrence of alginate lyases is widespread and have been found in marine molluscs [212] and bacteria which use alginate as a carbon and energy source by non-enzymatic rearrangement of the 4-deoxy-L-*erythro*-hex-4-enopyranosyluronate monomer into 4-deoxy-L-*erythro*-5-hexoseulose which is reduced to 2-keto-3-deoxy-D-gluconic acid and funnelled into the Entner-Doudoroff pathway [213, 214]. Alginate lyases are also expressed by marine algae [215], alginate producing *Azotobacter* species [216] and mucous *P.aeruginosa* strains [217] which do not metabolize alginate. A few bacteriophages specific for *Azotobacter* and *Pseudomonad* species carry lyases that are used to penetrate the cyst or biofilm surrounding the bacteria [218]. See [219] for a comprehensive list of enzyme sources and characteristics. The soil bacteria *A. vinelandii* and *A. Chroococcum* encode both periplasmic and putative extracellular lyases [216, 220, 221].

They clearly have a role in the degradation of the cyst coat during germination, but are also expressed during cyst formation. The periplasmic lyase AlgL in *P. aeruginosa* is involved in cell detachment from the alginate biofilm produced by the bacteria, allowing colonization of new sites [222]. Other proposed biological functions of the periplasmic lyases are to control the chain length of the newly synthesized alginate as mentioned earlier, as well as providing primers for the mannuronic acid polymerase.

#### 1.3.2 Substrate specificity

The classification of alginate lyases is somewhat ambiguous, as almost all described lyases cleave more than one of the four possible glycosidic linkages, although with different rates. In addition, some lyases also degrade acetylated alginates. Nevertheless, alginate lyases are classified as G-lyases (EC 4.2.2.11) or M-lyases (EC.4.2.2.3) based on which substrate they display the highest activity. Early studies on lyase specificity have been complicated by the lack of homopolymeric substrate, and in some cases crude enzyme preparations containing

more than one lyase. Progress in molecular biology yielding pure enzymes combined with the availability of mannuronan (FG=0.0) and strictly alternating poly-MG (FG=0.47) has resolved many of these difficulties.

Most of the lyases studied are classified as M-lyases [219], some of which also degrade acetylated M-blocks [220, 223]. Alginate lyases, which solely cleave one type of glycosidic bonds are rare, the only known examples being the M-M specific lyase AlxM isolated from the marine bacterium ATCC 433367 [224, 225] and the *K. pneumoniae* mutant AlyA5 which has a strong preference for G-G linkages [226].

The majority of alginate lyases are endo-acting enzymes, attacking a recognized sequence in the polymer chain, but a few cases of exo-activity have been reported [227, 228]. The reason for this is not clear, but a highly processive alginate exolyase with monomers as their main product may be favourable for organisms, which feed on algae.

End products and substrate binding sites of a few alginate lyases have been studied using alginate fragments enriched in G-, M- or MG- blocks and in some cases monodisperse oligomers of varying compositions as substrate [101, 129, 221, 229-231]. The products ranged from dimers to pentamers except for a G-lyase from *E. Chloacae* where a heptamer was the optimal substrate. The conclusion from these studies was that the substrate binding sites can accommodate 5-6 residues and the catalytic site is located between residue 2 and 3 from the non reducing end.

Not much work has been done on product inhibition of lyases. Kinetic studies on a M-lyase from *H.tuberculata* indicated reversible but strong end product inhibition which were explained by the binding of degradation products from M-blocks, rendering the enzyme inactive towards M-G bonds [232]. End product inhibition may also be observed for the G-lyase AlyA1 from *K. Pneumoniae*. [Anne Tøndervik, personal communication]

### **1.3.3 Biotechnical applications of alginate lyases**

Although alginate lyases are not produced for commercial applications, they are used in both basic and applied research. A possible large-scale application is in the production of biofuel from algae, although it is questionable whether this is appropriate as alginate has numerous other high-cost industrial applications.

Alginate lyases form the basis of a convenient assay of alginate concentration where the absorbance at 230 nm of the resulting  $\Delta$  residue is measured [89]. A robotic screening assay of epimerase activity has also been developed, applying the G-lyase AlyA from

*K. pneumoniae* [90] where the measured absorbance is proportional to the content of G-blocks as confirmed by NMR.

An important application of alginate in basic research is in the fine-structure study of alginate. The problem with block-structure elucidation becomes much more manageable when the polymer is degraded into shorter homopolymeric fragments which can be separated and analysed by NMR and MS techniques. A combination of lyases with high specificities followed by separation of degradation products and NMR analysis has been used to analyse the chain length distribution of the three block types in different alginates (paper3).

Detailed studies of the properties of the mannuronan C-5 epimerases AlgE1, AlgE4 and AlgE6 have also been carried out using the same methodology [104, 106].

Alginate oligomers have been reported to induce a range of biological responses including enhanced germination and root elongation in plants [233], growth of bifidobacteria [234] and induction of cytokine production in RAW264.7 cells [130]. Alginate lyases can be used to prepare oligomers with well-defined sequences [102], which may be suited for these purposes.

The ability of alginate lyases to weaken or dissolve alginate gels and composite materials containing alginate has some applications, as in the production of protoplast from algae [235, 236]. It also provides a gentle procedure for dissolving gel capsules with embedded cells without the use of  $\text{Ca}^{2+}$  chelators which may have toxic effects.

In medicine, alginate lyases may be used for the treatment of chronic mucoid *P. aeruginosa* infections in the lungs of cystic fibrosis patients since degradation of the alginate biofilm produced by the bacteria causes it to become more susceptible to antibiotic therapy [237].

Typically high concentrations of  $\text{Zn}^{2+}$  and  $\text{Ca}^{2+}$  in CF sputum may have an inhibitory effect on some lyases [238], and activity on acetylated alginate is needed. However, both the Aly1-III lyase from *Sphingomonas sp.* and a lyase from the marine bacterium ATCC 433367 were shown to degrade *P. aeruginosa* alginate [223, 239].

## 2 AIMS

The main objective of this thesis was to study the fine structure in alginates i.e. the chain-length distribution of the different block types. This was motivated by previous work, showing correlation between sequence parameters obtained from NMR and properties of alginate gels, such as the Young's modulus, creep compliance, rupture strength, swelling and syneresis. Knowledge about the distribution of blocks, rather than the averaged values obtained from NMR would hopefully facilitate a better understanding of the factors affecting the macroscopic behaviour of the system.

### The specific aims were to:

- 1) Establish methods for separation and quantification of alginate oligomers with different compositions.
- 2) Produce oligomers with well-defined compositions and chain lengths to be used as standards. These oligomers may also have other potential applications in immunology, polysaccharide sequencing by AFM and as modulators of rheological properties of mucus.
- 3) Characterize the alginate lyases used in this sequencing approach in terms of activity, substrate specificity and end products.
- 4) Construct and study a novel alginate lyase with high specificity towards cleavage of  $\alpha(1\rightarrow4)$  linked G-units.
- 5) Determine the chain-length distribution of M-blocks, G-blocks and MG-blocks in alginates from different brown algae, as well as *in vitro* epimerized mannuronan by applying the methodology listed above
- 6) Investigate the possibly different roles of intermediate and long G blocks in alginate gels.

As a spin-off from the aims above, the methodology developed were to be applied in the study of mode of action and substrate binding properties of mannuronan-C-5 epimerase mutants with novel properties.

## 3 SUMMARY OF PAPERS

### 3.1 Paper I

#### **Application of high-performance anion-exchange chromatography with pulsed amperometric detection and statistical analysis to study oligosaccharide distributions- a complementary method to investigate the structure and some properties of alginates**

Information about the distribution of oligosaccharides is essential for the elucidation of metabolism, structure and function of complex carbohydrates. High performance anion exchange chromatography with pulsed amperometric detection (HPAEC-PAD) has become an important technique in this respect, and has been applied to separate and quantify oligomers in hydrolysates from a number of polysaccharides including dextrane [240], hyaluronic acid [241], starch [242], pectin [243] and mannuronan [103].

In paper 1 we have used HPAEC-PAD to determine the amount and distribution of oligomers in acid hydrolysates of G-blocks ( $F_G = 0.95$ ) and Poly-MG ( $F_G = 0.47$ ). The same analysis performed on a hydrolysate of Poly-M ( $F_G = 0.0$ ) is also presented here, but is not included in paper 1 as it has been published elsewhere [103]. The observed number and weight distributions were compared with the corresponding Kuhn equations which predict the distribution of oligomers from a randomly degraded polymer. A Monte Carlo simulation of the degradation of Poly-MG was also performed in order to find the distribution of M-M linkages and the ratio between the two acid hydrolysis rate constants,  $K_{M-G}$  and  $K_{G-M}$ , which best accounts for the experimentally determined oligomer distributions.

#### **3.1.1 Preparation of oligomer standards**

The detector response for a PAD detector is dependent on the oligomer chain-length (DP) and composition. The reason for this is that diffusion of analyte onto the gold surface where it is oxidized is the rate determining step, and the diffusion coefficient is inversely proportional to the hydrodynamic volume. Moreover, the oxidation rate strongly depends on the class of compound, and to a smaller extent on stereochemistry and side groups.

In addition to their use in peak assignment, pure oligomers standards are therefore also needed to calibrate the molar response of PAD as a function of DP.

Acid hydrolysates of Poly-M, Poly-MG and G blocks were prepared by a two-step hydrolysis at 95 °C in order to avoid precipitation and thereby a heterogeneous degradation.

The resulting oligomer mixtures were fractionated on Superdex 30 size exclusion columns yielding G-, M- and MG-oligomer standards with a DP ranging from 2 to 15.

### 3.1.2 HPAEC analysis of partially acid hydrolysed Poly-M, Poly-MG and G-blocks

CarboPac PA100 or 200 columns are the natural choices for separation of neutral oligosaccharides. Negatively charged polyelectrolytes will however bind strongly to these anion-exchange resins, causing unnecessary long retention times or a need for high concentrations of eluent. The older IonPac AS4A column with lower charge density and a low operating pressure (600-700 psi) was therefore chosen. Oligomers and acid hydrolysates were analysed with the same amounts of added 1→4)- $\alpha$ -D-digalacturonic acid as internal standard in order to determine relative molar response factors defined as;

$$\text{MRF}_{\text{rel}} = (A_x/A_{\text{i.s.}})(m_{\text{i.s.}}/m_x) \quad (3-1)$$

where  $m$  is the sum of moles for each chain-length in the sample,  $A$  is the integrated area of peak(s) from HPAEC–PAD assigned to each chain-length and i.s. denotes the internal standard.

Chromatograms of the three hydrolysates (Figure 3.1) shows that a high resolution separation was obtained in all cases, and oligomers with DP>30 could be separated. It is seen from the figure that M-oligomers are more strongly retained than G-oligomers with the same DP. To which degree this is caused by steric factors and local flexibility, or by differences in pKa values of the hydroxyl groups remains an open question. The structure is however certainly of importance as the MG-oligomers have retention times comparable with M-oligomers. From inspection of the chromatograms it was also found that the reducing end has more influence on retention time than a unit inside the chain, as the even numbered -MG oligomers elutes before the -GM oligomers with the same DP.

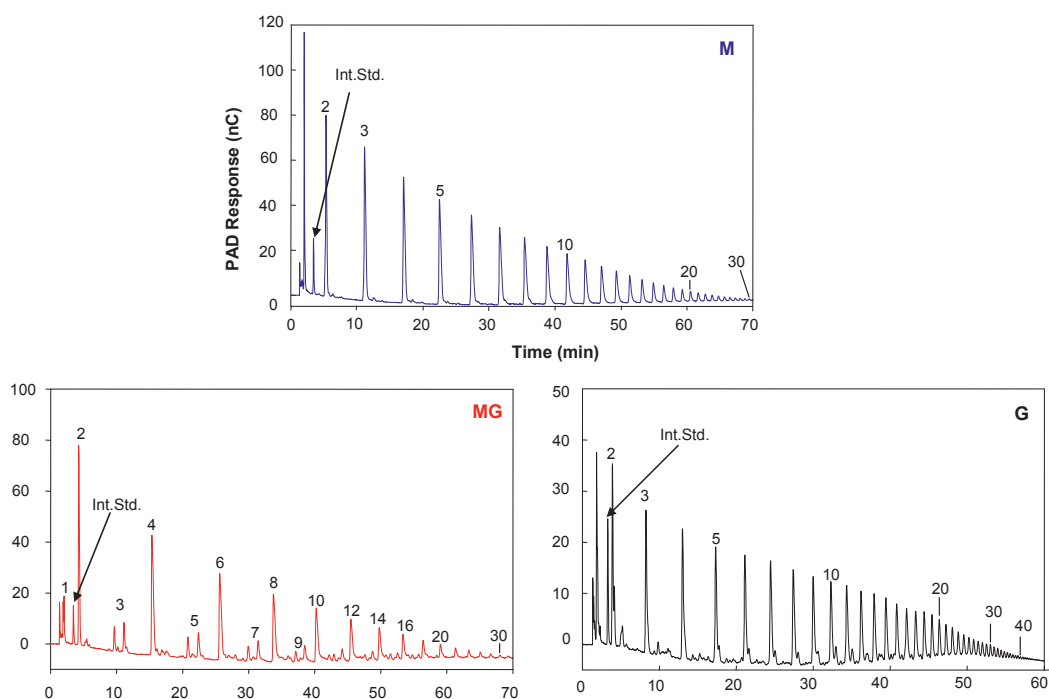


**Figure 3.1 Hydrolysates of Poly-M, Poly-MG and G-blocks analysed by HPAEC-PAD.**  
 The samples were separated on an ionPac AS4A (4 x 250 mm) column at a flow rate of 1.0 ml/min using a linear gradient of 8.75 mM/min sodium acetate in 100mM NaOH.

### 3.1.3 Oligomer distributions in M-, G- and MG-hydrolysates

The relative response factors of each series of oligomers were plotted as a function of DP from 2-15 and fitted to a first order logarithmic function. A decrease in  $MRF_{Rel}$  as a function of chain length was observed as expected. Moreover, the G-oligomers have a markedly lower  $MRF_{Rel}$  than the corresponding M- and MG- oligomers and the cause for this is currently not known.

Calculated and extrapolated  $MRF_{Rel}$  values were used to calculate the number and weight distributions in each hydrolysate. The distributions were compared with Kuhn distributions with the same number average chain length as determined by NMR analysis of the respective hydrolysates (Figure 3.2).



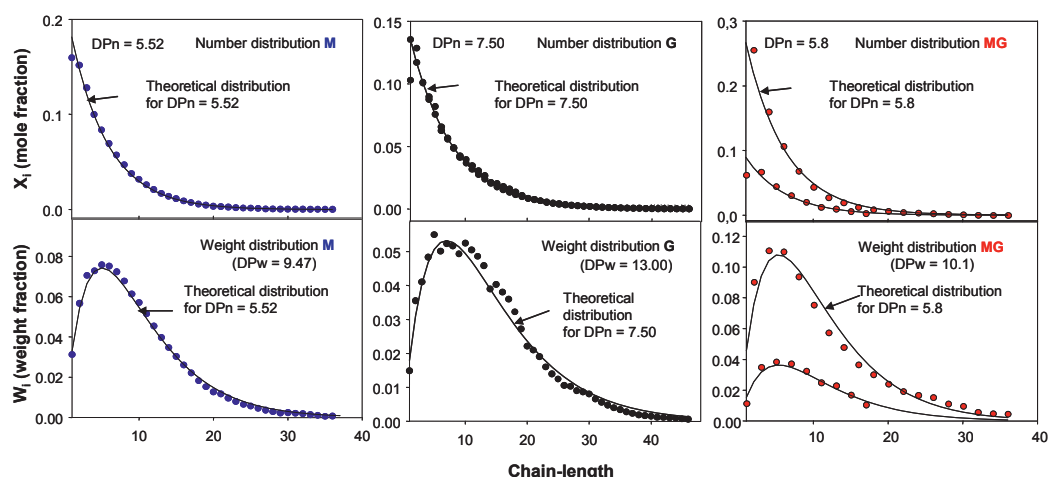


**Figure 3.2** Number and weight distribution of oligomers in hydrolysates of Poly-M, Poly-MG and G-blocks together with the Kuhn distribution that best describes the data in terms of a least squares fit.

The calculated oligomer distribution in the M-hydrolysate fits very well to the Kuhn distribution, indicating a homogeneous and random degradation. The G-oligomers also follow a Kuhn distribution, although with some discrepancy. This can be due to uncertainties in the analysis, but may well reflect the compositional inhomogeneity ( $F_M = 0.05$ ) and a polydispersity index of the starting material other than 2.

The MG-hydrolysate was best described by two Kuhn distributions, one for the even numbered and one for the odd numbered oligomers. The reason for this is that G-M linkages are hydrolysed faster than M-G linkages. Odd numbered oligomers resulting from hydrolysis of one G-M and one M-G linkage are therefore less abundant than even numbered oligomers generated from hydrolysis of two G-M linkages.

### 3.1.4 Simulation of the depolymerisation of Poly-MG

Depolymerization of poly-MG was simulated using a Monte Carlo model with an ensemble of 10,000 chains, a  $DP_n$  of 2400 and sequence parameters  $F_{GG} = 0.0$ ,  $F_G = 0.47$  and  $F_{MM} = 0.06$  was carried out by random selection of chains followed by random selection of linkage. The M-G, G-M, and M-M linkages were hydrolyzed with probability  $p_{MG}$ ,  $p_{GM}$  and  $p_{MM}$  respectively. The best agreement with the observed distribution was obtained with a hydrolysis rate ratio between GM and MG of  $K_{GM} / K_{MG} = 8.3 \pm 1$ , an average M-block length of 3.4, and an average MG-block length of 38. The study shows that HPAEC-PAD can be used to separate and quantify homologous alginate oligomers and is a useful tool in fine structure studies of alginates.

## 3.2 Paper II

### **Preparation of high purity monodisperse oligosaccharides derived from mannuronan by size-exclusion chromatography followed by high-performance anion exchange chromatography with pulsed amperometric detection.**

Monodisperse alginate oligomers with uniform composition are useful as standards for the analysis of complex mixtures of alginate oligomers, and have been applied in the study of the substrate specificity and mode of action of mannuronan C-5 epimerases and alginate lyases [97, 104, 106]. They also have potential applications as substrates in a range of experiments, such as in the study of biologically active epitopes and in ITC and AFM studies of molecular interactions. Other applications may include grafting on biomaterials and tuning of rheological properties of alginate gels.

In paper 2 we wanted to evaluate a new method for the production of alginate oligomers with very high purity. Pellicular resin ion exchange columns provides high resolution, but at the expense of a very low loading capacity. Using SEC as a pre-purification step, we show that the yield of oligosaccharides can be substantially increased.

#### **3.2.1 Pre-purification of M-oligomers by SEC**

HPAEC-PAD analysis of M-oligomers separated by SEC in a previous study [103] and in paper 1 revealed an unidentified peak eluting in front of each oligomer. Since these peaks were not present in chromatograms of M-hydrolysates, it was suspected that a reaction happened at the reducing end during removal of ammonium acetate (the SEC mobile phase) by freeze drying. Ammonium was therefore removed prior to freeze drying by passing pooled oligomer fractions through a column of 20-50 mesh AG-50W-X8 cation-exchange resin, and this treatment avoided the formation of the unidentified compound as confirmed by HPAEC-PAD. The derivative was identified in an M dimer fraction with the side peak present as 1-deoxy-1-immino-D-mannuronic acid at the reducing end residue from  $^{13}\text{C}$  HSQC- NMR, 2D IP-COSY-NMR and ESI-Q-TOF-MS analysis. The acid-catalyzed formation of imines occurs during freeze drying in ammonium acetate as the pH drops from 6.9 to about 5 and is promoted by the removal of water.

### 3.2.2 Isolation of M oligomers by semipreparative HPAEC-PAD

Oligomer fractions of DP 5, 10 and 15 were further purified on a semipreparative Ion Pac AS4A (9x250mm) column and fractions were automatically collected, desalted on an AG-50W-X8 cation-exchange column and freeze-dried. Acetic acid was added to the sample vials before collection in order to neutralize the fractions, and no signs of  $\beta$ -elimination were observed when the samples were re-analyzed on the analytical column. Chromatograms from semipreparative and analytical separations are compared in Figure 3.3.

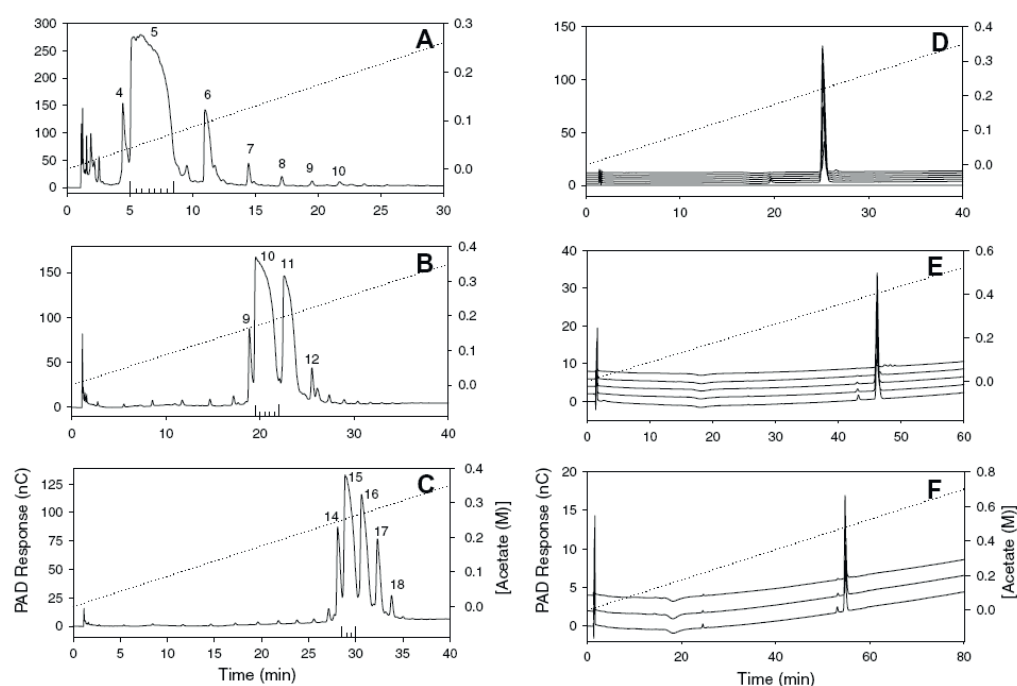


**Figure 3.3** Semi-preparative HPAEC-PAD chromatograms (A–C) of M-oligosaccharides recovered from SEC and treated with AG-50W-X8 cation-exchange resin. The nominal DP was 5 (A), 10 (B) and 15 (C) from a total injection mass of 0.5, 0.25 and 0.1 mg, respectively. Collected fractions are indicated in the chromatograms. Analytical HPAEC-PAD chromatography (D–F) of the collected and desalted fractions. The dotted line is the acetate gradient.

The purity of the recovered oligomers were greater than 96% in all cases, with a yield per run of 480  $\mu$ g, 185  $\mu$ g and 48  $\mu$ g for M5, M10 and M15 respectively.

We conclude that pre-purification on SEC, followed by semipreparative HPAEC can be used to isolate milligram quantities of almost monodisperse alginate oligomers for special purposes.

### 3.3 Paper III

#### Isolation of Mutant Alginate Lyases with Cleavage Specificity for Di-guluronic Acid Linkages.

Specific alginate lyases are invaluable tools for sequence analysis of alginate. Moreover, the separation and analysis of lyase-degraded alginates is at present the only method which can provide more detailed information on block distribution than the averages calculated from CD and NMR spectra. In order to analyse the distribution of the three block types in alginates, it is necessary to use four lyases with the following cleavage specificities:

- a) M-M and G-M / M-G
- b) G-G and G-M / M-G
- c) M-M
- d) G-G

Degradation of alginates with lyases displaying specificities a) and b) will preserve only G- and M-blocks respectively, while the combination of lyases with specificities c) and d) leaves only the MG-blocks intact. Lyases with specificities a), b) and c) have been described previously [97, 224, 244]. In this paper we report the construction of a *Klebsiella pneumoniae* PL7 family lyase AlyA mutant with increased specificity towards cleavage of G-G linkages.

#### 3.3.1 Construction and characterization of lyase mutants

A library of lyase mutants was constructed from the *alyA* gene in *K. pneumoniae* using error prone PCR mutagenesis. Two *E. coli* strains were used as cloning hosts for the native and mutant lyase genes which were ligated into an expression vector containing the regulatory *Pm/Xy/S* promoter system. A robotic screen was developed in which the soluble protein products from each colony of the *E. coli* library were transferred to 384-well microplates containing either a buffered solution of G-blocks ( $F_G = 0.95$ ) or Poly-MG ( $F_G = 0.47$ ). Lyase activity was monitored as increase in absorbance at 230 nm.

After high throughput screening of 6720 lyase mutants, eight enzyme variants with strongly increased preference for G-G linkages were chosen for further characterization. The activity on G-blocks was generally much reduced compared with the wild type AlyA. The mutant with the highest activity towards G-blocks, denoted AlyA5, was compared with AlyA, and HPAEC-PAD chromatograms of Poly-MG and G-blocks incubated with these lyases shown in Figure 3.4 confirm the large differences in specific activity.

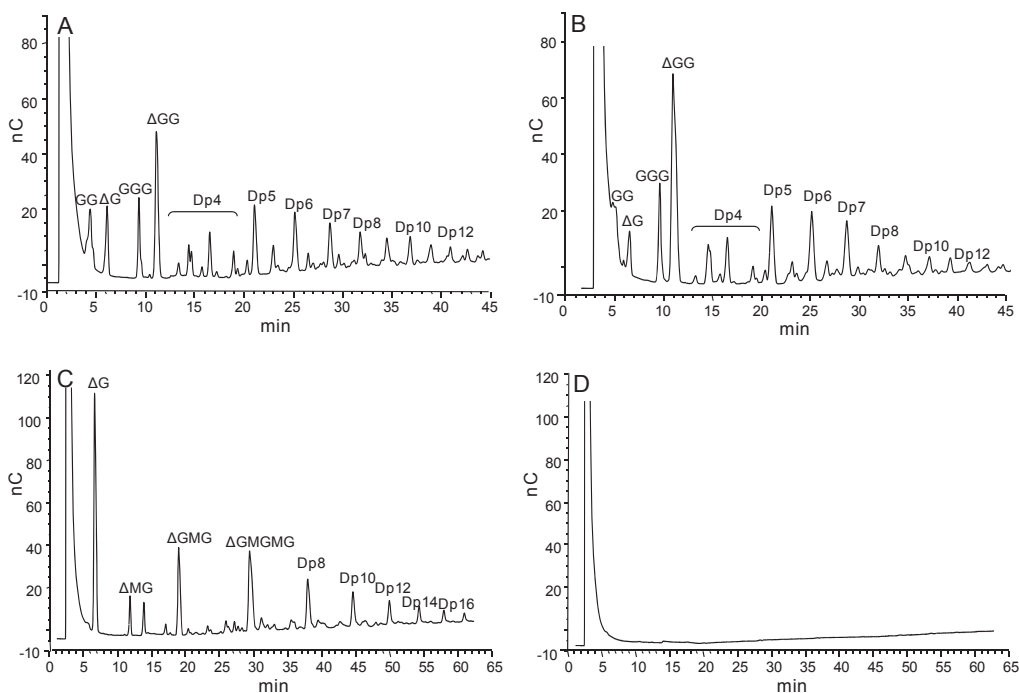


**Figure 3.4 HPAEC-PAD analysis of G-blocks and poly-MG degraded by AlyA wild type (A and C) and AlyA5 (B and D)**

Degradation was performed in 50 mM Tris with 0.2 M NaCl and 1 mM CaCl<sub>2</sub> and was allowed to proceed until A<sub>230</sub>=2 in the G-block samples. The corresponding polyMG degradation reactions were stopped at the same time points. The saturated dimer and trimer (GG and GGG) originate from the reducing end of the G-blocks.

Lyases have different requirements for ionic strength and type of cations for optimal activity. Initial studies showed that AlyA activity is optimal in a 50 mM Tris buffer at pH 7.5 with 0.2 M NaCl and 1 mM Ca<sup>2+</sup>, using alginate from the brown algae *Laminaria hyperborea* as a substrate. However, this alginate contains all three block types, and it seemed possible that the activity requirements are not the same for the different substructures in the substrate. AlyA activity on G-blocks was unaffected by the concentration of Ca<sup>2+</sup> (0-2 mM) while AlyA5 activity was stimulated by increasing levels of Ca<sup>2+</sup>. Interestingly, the activities of both AlyA and AlyA5 on Poly-MG was strongly stimulated by Ca<sup>2+</sup>, and in the case of AlyA5 there was almost no detectable activity in the absence of Ca<sup>2+</sup>.

### 3.3.2 Reasons for the increased specificity towards G-G linkages

Sequence alignment between AlyA and the PL7 family lyase A1-II from *Sphingomonas* sp. A1, for which the three-dimensional structure has been determined, was used as a basis for an analysis of protein-substrate interactions. It was concluded that the altered specificity of the

mutants may be caused by an increased affinity for M-units in the subsites +2 and possibly +4 which leads to non-productive binding of poly-MG. A weaker binding of G-units in +2 could also explain why the mutants display lower activity on G-blocks than the wild type lyase.

### 3.4 Paper IV

#### Alginate Sequencing: An Analysis of Block Distribution in Alginates Using Specific Alginate Degrading Enzymes

The properties of alginate gels are determined by the relative amount and distribution of the M and G monomers. Models that correlate macroscopic behaviour of alginate gels to their composition have so far been based on sequence parameters obtained from NMR. As some alginates with similar sequence parameters exhibit clear differences in gelling properties, there is a need for more detailed knowledge about alginate sequences to gain understanding of rheological properties on a molecular basis.

In paper 4 we have developed a method for the determination of the chain-length distribution of each of the three block types in alginate by applying the tools developed in our three previous papers, following a strategy outlined in Figure 3.5.

A block distribution analysis was performed on three brown seaweed alginates from *Macrocystis pyrifera*, *Durvillea potatorum* and *Laminaria hyperborea* with large differences in sequence parameters ( $F_G = 0.32-0.67$ ) as an initial validation of the method.

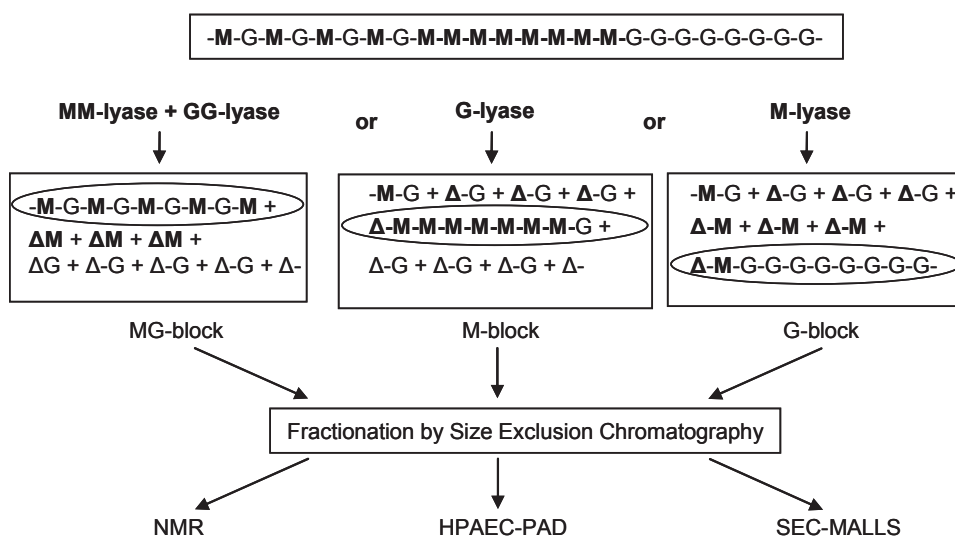


**Figure 3.5 Schematic presentation of a strategy for alginate sequencing**

Alginate is degraded by alginate lyases with appropriate specificities, leaving the blocks of interest intact. Fractionation by size exclusion chromatography followed by analysis of composition and chain-length of the fragments yields information on block-distribution.

Guluronic acid, Mannuronic Acid and 4-deoxy-L-erythro-hex-4-ene-pyranosyluronate are abbreviated G, M and  $\Delta$ .

### 3.4.1 Characterization of alginate lyases

Much of this work was focused on the optimization of degradation conditions.

It was therefore essential to acquire detailed information about the lyases applied in this study in terms of activity, substrate specificity, products and the minimal substrate needed for activity. In addition, a preliminary study was done on possible end product inhibition (unpublished data). Although end product inhibition has been reported for the M-lyase from *H. tuberculata* [232], none of the lyases used in this study showed a notable decrease in activity when lyase degradation products of defined length and composition were added to their substrates.

Lyase specificity was quantified as relative activity towards Poly-M ( $F_G = 0.0$ ), Poly-MG ( $F_G = 0.46$ ) and G-blocks ( $F_G = 0.95$ ), and the activity of the different lyases on these substrates was measured as the increase in absorbance at 230 nm (Figure 3.6).

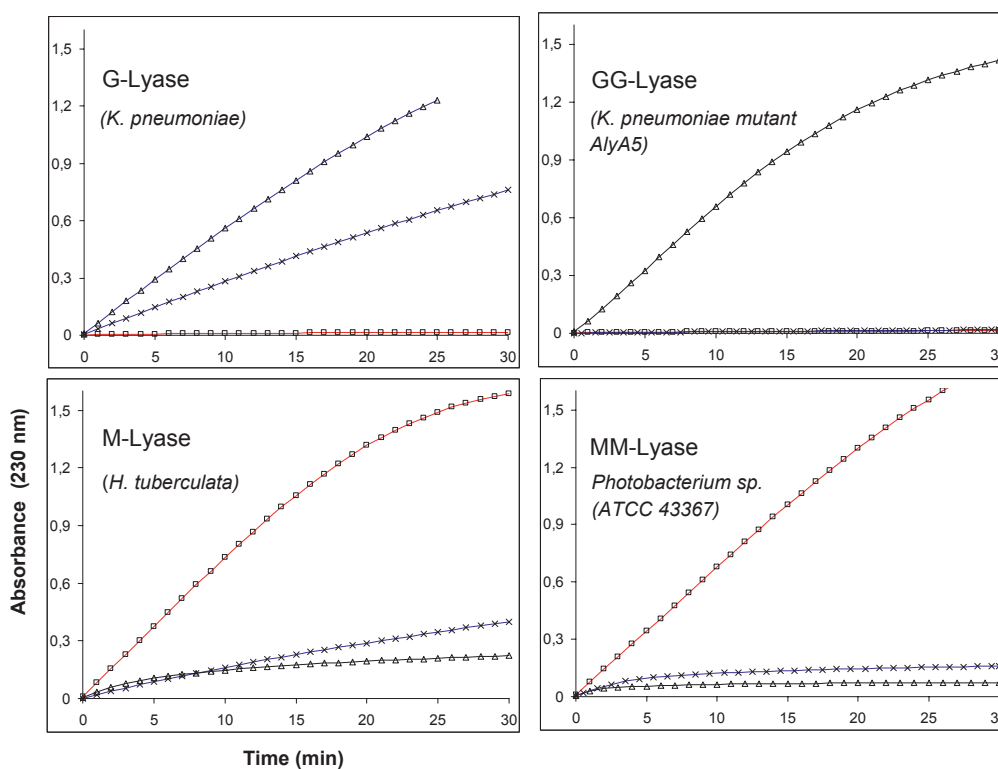


**Figure 3.6 Specificity of the alginate lyases used in this study**

Lyase activity on poly-M ( $\square$ ), Poly-MG ( $\times$ ) and G-blocks ( $\Delta$ ) monitored as an increase in absorbance at 230 nm. The degradation was performed in 200 mM ammonium acetate with 50 mM NaCl, and in addition 1 mM  $\text{CaCl}_2$  in the case of AlyA5. Origin of lyases: M-lyase from *H. tuberculata*, G-lyase (AlyA) from *K. pneumoniae*, GG-lyase (AlyA5) constructed from AlyA and MM-lyase from *Photobacterium* sp. (ATCC 43367).



Lyase endproducts were analysed by HPAEC-PAD after incubating the lyases with their optimal substrate. Both the *H. tuberculata* M-lyase and the MM- specific lyase from *Photobacterium* sp.(ATCC 43367) degraded PolyM into dimers and trimers. The G-lyase AlyA from *K. pneumoniae* and the GG- specific mutant AlyA5 degraded G-blocks into dimers and trimers, but oligomers with chain length 4-6 were also seen in the chromatograms. This may be caused by differences in subsites, but is also due to the presence of 5% M units in the substrate which cannot be degraded by the G-lyases.

Unsaturated  $\Delta$ M-,  $\Delta$ G-, and  $\Delta$ MG-oligomer from a library made in connection with this paper were also tried as substrates. The minimum substrate for the M- and MM-lyase was found to be a M tetramer, although a very slow degradation of the M trimer was observed if a large amount of enzyme was used. The G- and GG-lyase requires a G-hexamer to support activity. All enzymes seemed to prefer the glycosidic linkage between the third and fourth residue from the non-reducing end in a hexamer.

Regarding the analysis of MG-block distribution, it is important to avoid significant G-M cleavage, and at the same time choose conditions that will degrade all M- and G-blocks with DP>6. Optimal conditions were found by incubating the GG- and MM-lyase with their respective substrates, using PolyMG as a negative control.

Optimization is less critical in the analysis of G- and M-block distribution since the cleavage of G-G and M-M bonds by M- and G-lyase respectively is very slow.

#### **3.4.2 Block distribution in alginates from *Macrocystis pyrifera*, *Durvillea potatorum* and *Laminaria hyperborea*.**

Alginates from the brown seaweeds *Macrocystis pyrifera*, *Durvillea potatorum* and *Laminaria hyperborea* were degraded by alginate lyases according to figure 3.5. The resulting mixtures of unsaturated oligomers were fractionated on SEC columns, and an example is given in Figure 3.7.

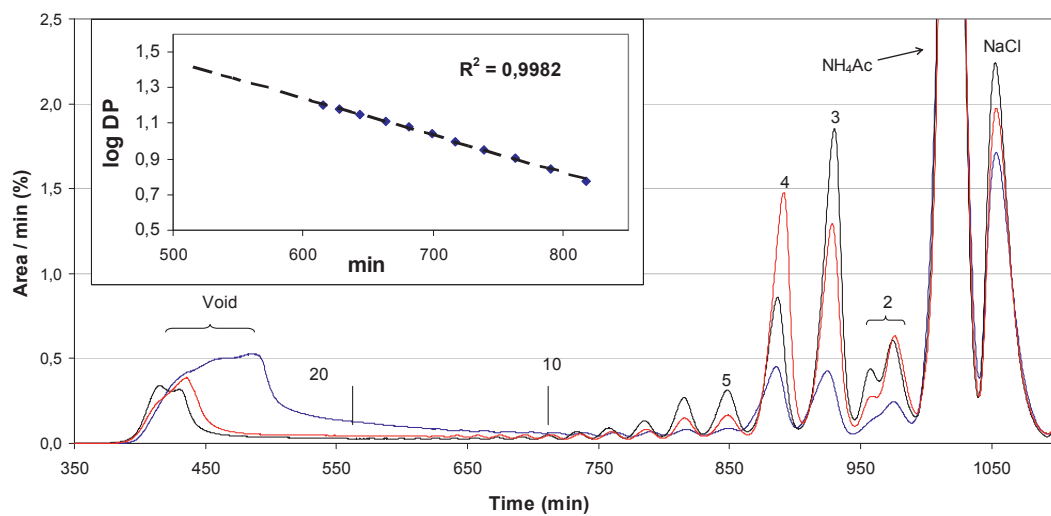


**Figure 3.7** Overlaid SEC chromatograms of alginates from *M. pyrifer*, *D. potatorum* and *L. hyperborea* degraded with M-lyase.

A plot of Log (DP) as a function of retention time (inserted) was used to estimate DP in the unresolved region of the chromatogram. The lysates were separated on three Superdex 30 columns serially connected using 0.1 M  $\text{NH}_4\text{Ac}$  as mobile phase and a flow rate of 0.8 ml/min.

Chain-length assignment and calculation of the weightfraction of each chain length was based on SEC chromatograms. A regression line from a plot of the logarithm of chain length as a function of elution time was used to find integration limits for unresolved peaks up to DP 30. The distributions of oligomers in the degraded alginate samples are shown in Figure 3.8.

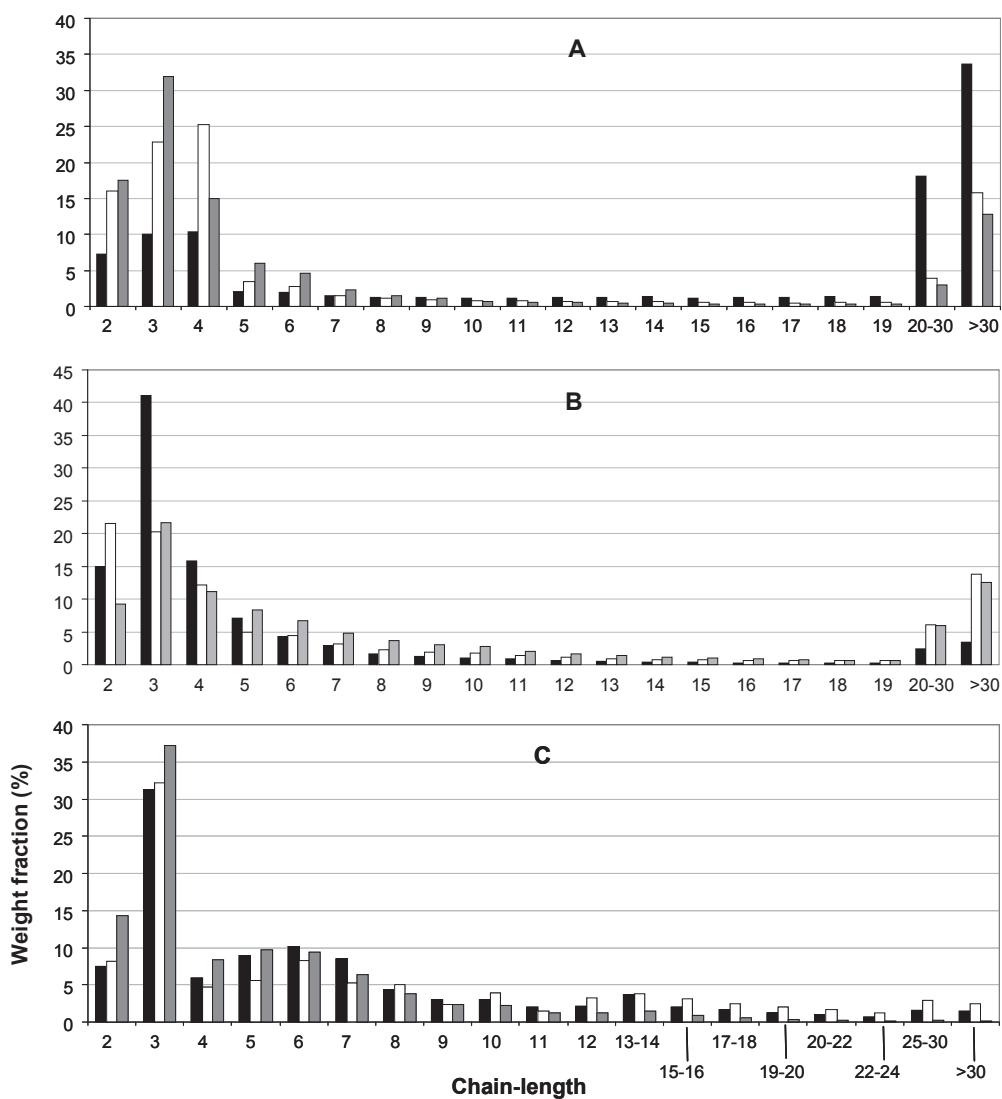


**Figure 3.8** Weight distribution of oligomers in alginates from *D. potatorum* (■) *M. pyriferia* (□), and *L. hyperborea* (■) degraded by (A) M-lyase, (B) G-lyase, and (C) MM- GG-lyase calculated from SEC chromatograms.

It is important to underline that the oligomer distributions in figure 3.8 do not represent the actual block distribution as most of the oligomers with DP<6 are compositionally heterogeneous degradation products. Moreover, the composition near the ends will depend on the degradation pattern of the particular lyase. Fractions of DP 2-7 from each SEC separation were therefore collected, analysed by  $^1\text{H-NMR}$ , and compared with HPAEC-PAD chromatograms of the degraded samples in order to identify some of the short oligomers of

irregular sequence. Taken together with an analysis of the end signals in the  $^1\text{H-NMR}$  spectra it was concluded that the actual M- and G-block lengths are 1-3 units shorter than the corresponding oligomer whereas the actual MG-block lengths are 2-3 units shorter.

The void parts of the SEC chromatograms were also collected and analysed in terms of compositional purity and  $\text{DP}_n$  by NMR (Figure 3.9) and SEC-MALLS.

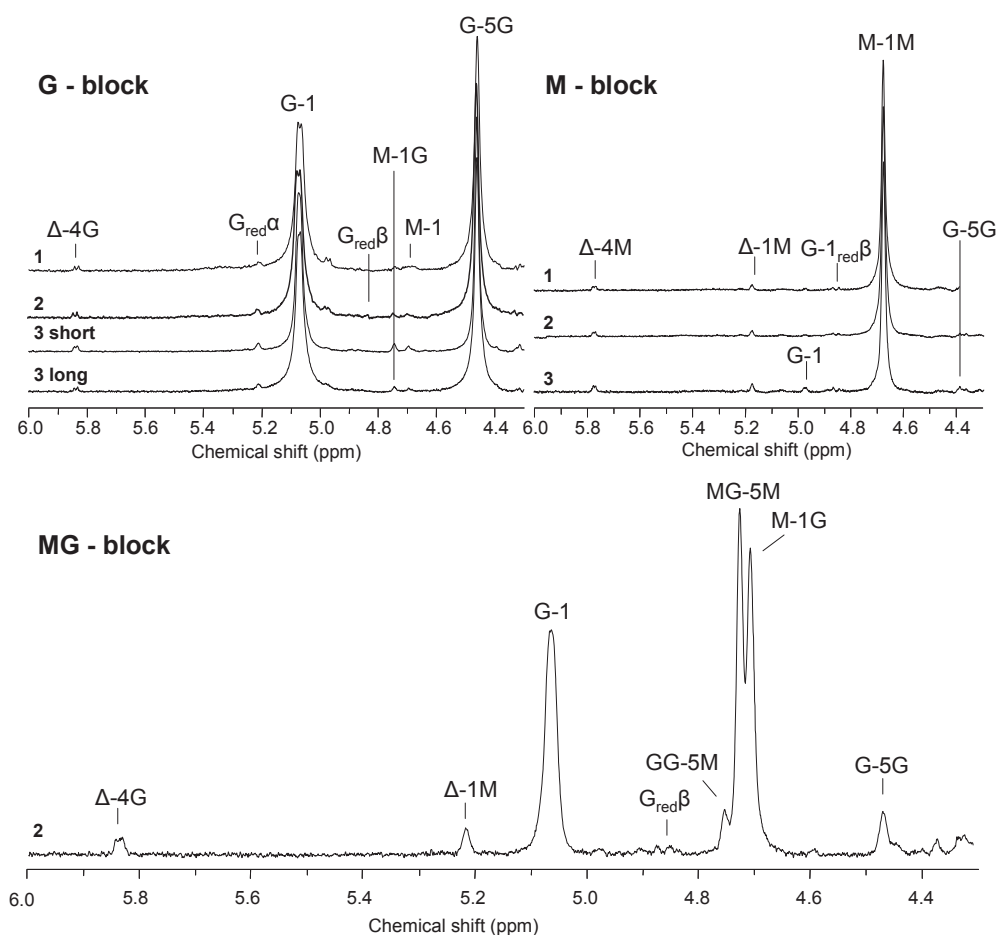


**Figure 3.9**  $^1\text{H-NMR}$  (400 MHz) spectra of void fractions from SEC separations of *D. potatorum* (1), *M. pyriferu* (2) and *L. hyperborea* (3)\* degraded by (A) M-lyase, (B) G-lyase and (C) MM- and GG-lyase.

\* The void of *L. hyperborea* degraded by M-lyase were collected in two fractions, 3a and 3b, in order of elution.

The results are summarized in table 3.1. The high purity of all void fractions indicates that the alginate has been sufficiently degraded by the lyases. There is however no clear-cut way to

assure that no unwanted degradation has occurred due to a lack of absolute specificity, and the possibility of underestimating the MG-block length can therefore not be excluded.

**Table 3.1 SEC-MALLS and <sup>1</sup>H-NMR analysis of the void fractions in figure 7.**

Alginate	Lyase	Block	Purity (%)	DP <sub>n</sub> <sup>1)</sup>	DP <sub>n</sub> <sup>2)</sup>
<i>D. potatorum</i>	G	M	≥99	91	94
<i>M. pyrifera</i>	G	M	≥99	90	96
<i>L. hyperborea</i>	G	M	≥99	-	54
<i>D. potatorum</i>	M	G	≥98	163	273
<i>M. pyrifera</i>	M	G	≥98	132	105
<i>L. hyperborea</i> a	M	G	≥98	120	117
<i>L. hyperborea</i> b	M	G	≥97	61	70
<i>M. pyrifera</i>	MM+GG	MG	≥93	-	39

1) SEC-MALLS

2) <sup>1</sup>H-NMR

All alginates, irrespective of the proportion of guluronic acid, were found to contain a significant fraction of extremely long homogenous G-blocks, causing the distribution of G-blocks to differ markedly from second-order Markovian statistics. The same alginates also contained a fraction of very long M-blocks, whereas the MG-blocks were considerably shorter.

It is not clear if the longest G-blocks have a specific role in alginate gels.

Since the binding of calcium between G-blocks is a cooperative process, the formation of junctions between long G-blocks is thermodynamically favoured. Furthermore, the initiation of this zipper process is faster when there is no need for complete overlap between two G-blocks in order to form a stable junction. We suggest that these alginates form gels which can be looked upon as a composite material where almost fully epimerised molecules form dimers that act as reinforcement bars. This primary framework is surrounded by a heterogeneous population of alginates composed of shorter G-blocks and flexible alternating elements, which form a continuous network at a later stage.

### 3.5 Paper V

#### **An analysis of G-block distributions and their impact on gel properties of *in vitro* epimerized mannuronan.**

Because most commercially available alginates from brown algae are extracted from the whole plant, the product is a heterogeneous mixture of sub-populations of alginates. This complicates the study of structure-function relationships in alginate gels, and it is desirable to produce a more homogeneous alginate for this purpose.

In paper 5 we have treated mannuronan with three mannuronan C-5 epimerases to obtain homogeneous alginates. The G-block distribution was analysed by SEC, NMR and SEC-MALLS and compared with an alginate from *L. hyperborea* stipe. Calcium saturated alginate gels made from *L. hyperborea* alginate and two AlgE6 epimerized alginates were characterized in terms of syneresis, Young's modulus, rupture strength and fractional deformation at rupture. A gel of AlgE6 epimerized alginate with added G-blocks isolated from *L. hyperborea* alginate was also made in order to study the influence of extremely long G-blocks on gel properties.

#### **3.5.1 Epimerization of mannuronan by the mannuronan C-5 epimerases AlgE6, AlgE64 and EM1**

G-block forming mannuronan C-5 epimerases with high activity have potential in upgrading alginates with weak gelling properties. Two such enzymes have been constructed very recently; the EM1 epimerase selected from screening of a mutant library based on algE1-*algE6* genes from *A. vinelandii* [90] and the hybrid epimerase AlgE64 comprised of an A-module from AlgE6 and a R-module from AlgE4 [245]. Their catalytic properties were compared with the native AlgE6 epimerase through a HPAEC-PAD and NMR analysis of the development of G-blocks in mannuronan incubated with the different enzymes as a function of the degree of epimerization. The NMR analysis confirmed that the enzymes are G-block forming epimerases yielding alginates with an average G-block length ( $N_{G>1}$ ) slightly higher than in *L. hyperborea* alginate with similar G-content. It was not possible to quantify each oligomer in HPAEC-PAD chromatograms of epimerized alginates degraded with M-lyase, however the formation and elongation of G-blocks can be studied qualitatively. A similar evolution of G-blocks was observed for the three epimerases. The formation of G-blocks with DP>15 even at 4% epimerization indicates processivity or a preferred attack mechanism. The block length increases with degree of epimerization but seems to approach a limit between DP 50 and 60 in samples with  $F_G$  between 0.6 and 0.8 whereas *L. hyperborea* alginate ( $F_G=0.67$ ) contains a

fraction of considerably longer G-blocks. This is shown in Figure 3.10 where SEC chromatograms of a M-lyase digest of *L. hyperborea* alginate and the highest epimerized samples from each epimerization series are compared.

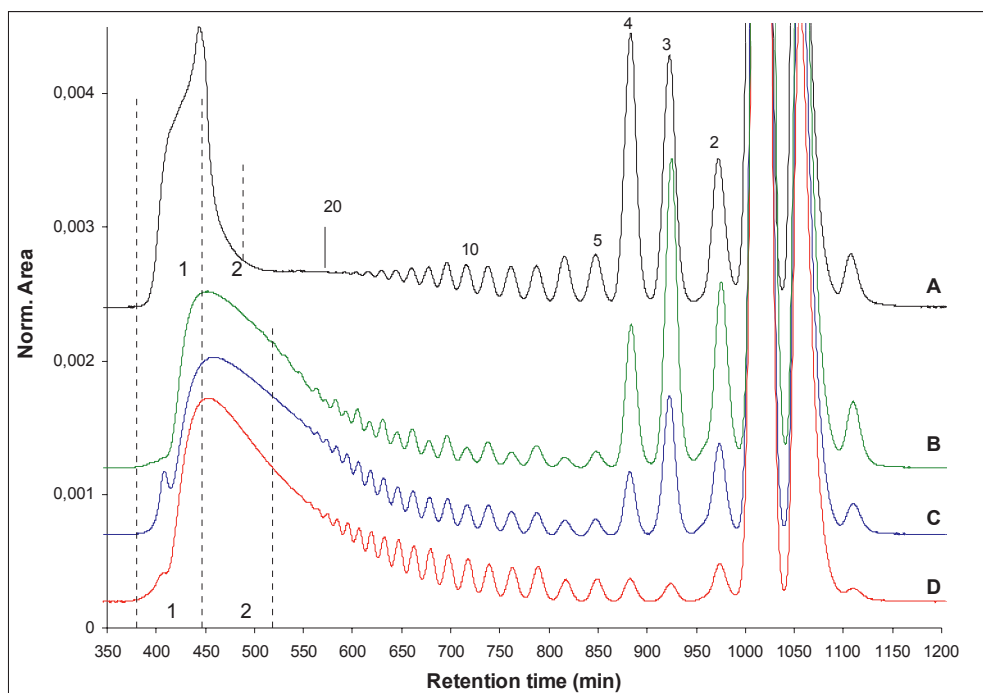


**Figure 3.10** SEC chromatograms showing the G block distributions in alginates from (A) *L. hyperborea*, and mannuronan epimerized with; (B), AlgE6,  $F_G = 0.68$  (C) EM1,  $F_G = 0.77$  and (D) AlgE64,  $F_G = 0.84$ . The alginates (50mg, 10mg/ml) were degraded with M-lyase (0.016U/mg) for 24 hours at 30 °C and separated on three Superdex 30 columns serially connected using 0.1M  $\text{NH}_4\text{Ac}$  as mobile phase and a flow rate of 0.8 ml/min. All chromatograms were baseline corrected and normalized in order to adjust for differences in injection volumes. Collected void fractions are indicated with dotted lines.

It is seen from the figure that *L. hyperborea* contains a fraction of long G-blocks not present in the epimerized samples, and the distribution is also narrower. This is confirmed by NMR and SEC-MALLS analysis of the void fractions (Table 3.2).

The G-block distribution in epimerized samples are very similar, despite differences in G content up to 16%. Furthermore, time-resolved  $^{13}\text{C}$ -NMR studies have shown that AlgE64 initially forms longer G-blocks than EM1 and AlgE6 (a rapid increase in  $F_{\text{GGM}}$  compared to  $F_{\text{MGM}}$  and  $F_{\text{GMG}}$ ) [245]. Similar distributions, regardless of differences in degree of epimerization and catalytic properties can be explained by the epimerases lacking the ability to epimerize single or a few M-units between intermediate long G-blocks at a significant rate.

**Table 3.2. Chain length and purity of G-blocks in alginate from *L. hyperborea* stipe and *in vitro* epimerized mannuronan.**

Sample	F <sub>G</sub>	Fraction	F <sub>G</sub>	DP <sub>n</sub> <sup>a)</sup>	DP <sub>n</sub> <sup>b)</sup>
<i>L. Hyperborea</i>	0,67	void 1	0,98	110	137
		void 2	0,97	70	60
mannuronan +AlgE64	0,88	void 1	0,96	46	66
		void 2	0,95	33	27
mannuronan +EM1	0,77	void 1	0,94	48	78
		void 2	0,93	32	25
mannuronan +AlgE6	0,68	void 1	0,96	48	62
		void 2	0,94	35	26

a) Calculated from <sup>1</sup>H-NMR

b) Calculated from SEC-MALLS

### 3.5.2 Analysis of gels made from AlgE6 epimerized mannuronan and the effect of long G-blocks

The gels compared in this study were made from *L. hyperborea* alginate (F<sub>G</sub> = 0.67) and mannuronan epimerized with AlgE6 (F<sub>G</sub> = 0.51 and 0.68). In order to study the impact of long G-blocks on gel properties, a gel was also made from a solution of Poly-M epimerized with AlgE6 (F<sub>G</sub> = 0.51) where extremely long G-blocks (DP>100) isolated from *L. hyperborea* were added as to give a total F<sub>G</sub> = 0.67. The syneresis, Youngs modulus, fractional compression at rupture and rupture strength were measured in calcium saturated gels, and the results are shown in Figure 3.11 (A-D).

The high syneresis in gels made from AlgE6 epimerized mannuronan compared to *L. hyperborea* alginate is surprising. Alternating sequences are considered to be the structural element mainly responsible for syneresis[66, 246], but the NMR spectra of AlgE6 epimerized mannuronan show that these samples are almost devoid of MG-blocks. However, by adding long G-blocks to the AlgE6 (F<sub>G</sub> = 0,51) sample, syneresis decreased to a level comparable with *L. hyperborea* alginate. Reorganization of the ionic gel network upon increasing calcium levels therefore seems to be crucially dependent on the length of junction zones.



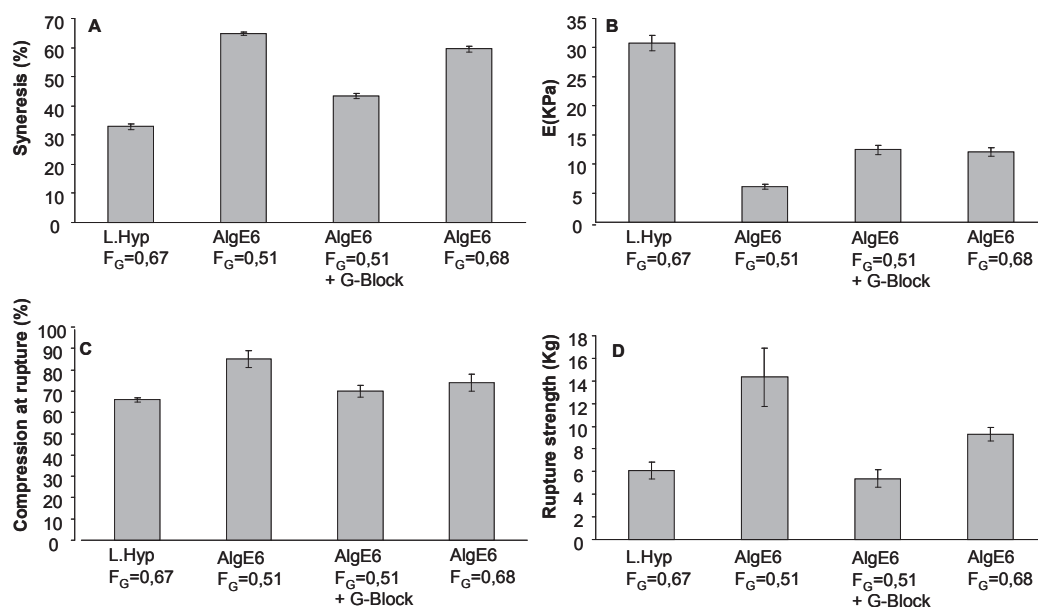


**Figure 3.11 Characterization of alginate gels**

(A) Syneresis, (B) Young's modulus, (C) compression at rupture and (D) rupture strength.

Gels were made from 1% solutions of alginate from *L. hyperborea* stipe, AlgE6 epimerized mannanuronan ( $F_G = 0.51$  and  $0.67$ ) and AlgE6 epimerized mannanuronan ( $F_G = 0.51$ ) with long G-blocks added to give a final  $F_G = 0.67$ . All gels were immersed in a solution of 50 mM  $\text{CaCl}_2$  and 200mM NaCl for 24 hours prior to measurements. Values are means of 12 gels  $\pm$  StDev for A and B, and means of 4 gels for C and D.

Another atypical feature of the gels made from epimerized mannanuronan was their low Young's moduli (Figure 3.11 B) relative to the high content of G. Despite a higher  $N_{G>1}$  than *L. hyperborea* alginate, the Young's modulus was reduced by a factor of 2.5 and 5 for gels made from epimerized material with  $F_G = 0.68$  and  $0.51$ , respectively. To our knowledge, this is the first example of an alginate where the positive relationship between rigidity and  $N_{G>1}$  is not obeyed. Since the epimerized alginates also have a higher  $M_w$  than *L. hyperborea* alginate, the number of loose ends cannot explain this discrepancy, and it seems like the effect is solely attributed to the lack of long G-blocks. This is at present the strongest support for our reinforcement bar hypothesis.

Compressibility at rupture and rupture strength of the gels made from epimerized mannanuronan were higher than what could be expected from NMR sequence parameters, and also higher than for algal alginates rich in MG sequences.

Addition of long G-blocks resulted in a more brittle gel, again approaching the properties of the gel from *L. hyperborea* alginate. The difference in compressibility between gels from *L. hyperborea* alginate and *in vitro* epimerized mannanuronan gels were at its most extreme when

the gels were calcium depleted, and the latter could be compressed into a thin semi-transparent film without rupture (data not included in the paper).

The presence of the extremely long G-blocks found in natural alginates, which cannot be identified from compositional data using NMR, might explain an old mystery as to why alginates with the same apparent composition and diad frequencies display different functional properties. Even though it is not presently possible to assign an explicit role to these G-blocks in Ca-alginate gels, our data shows that they can be utilized to decouple the connection between syneresis and Young's modulus in AlgE6 epimerized mannuronan.

#### 4 CONCLUDING REMARKS

In alginate as in polysaccharides in general, the physical properties are governed by the distribution of the different monomers in the polymer chain. The work presented aims at extending the knowledge on alginate fine structure and thereby contribute to a better understanding of structure-function relationships. The results from the sequence analysis were further applied to study the impact of G-block length on the macroscopic properties of alginate gels.

A method for the determination of chain-length distributions of G-blocks, M-blocks and MG-blocks in alginates was developed. This involved the characterization and application of specific alginate lyases, one of which was constructed for this specific purpose, and also construction of an oligomer library. Combined with chromatographic methods, SEC-MALLS and NMR, it was shown that:

- HPAEC-PAD is a powerful tool for the analysis of alginate oligomers of varying composition. It is a quantitative method, provided that standards are available for detector calibration, and can be used to study the catalytic properties of alginate lyases in detail by applying homopolymeric alginates and alginate oligomers with known chain length and sequence as substrates.  
It is at present not possible to identify every oligomer in the complex mixtures that results from lyase-degradation, but differences in chromatograms of lysates is readily seen. Thus HPAEC-PAD provides a fingerprint of each alginate.
- The block distribution in alginates can be determined by the methodology. When applied on three brown seaweed alginates, a fraction of extremely long G-blocks with  $DP_n > 100$  were found, irrespective of a varying content of guluronic acid. Long M-blocks ( $DP_n \geq 90$ ) were also present in all samples, whereas the MG-block length was shorter ( $DP_n \leq 40$ ). The actual block-length in seaweed alginates is therefore considerably higher than what is estimated from NMR data, and is not satisfactorily predicted from second order markovian statistics.
- An analysis of G-block distribution in mannuron epimerized with the mannuronan C-5 epimerases AlgE6, AlgE64 and EM1 revealed that none of these enzymes were able to

form the long G-blocks which are observed in algal alginates. Even at high degrees of epimerization, the maximum G-block length did not exceed 60 units. The condensation of intermediate long G-blocks separated by a single or a few M-residues is therefore a very slow process.

Given the compositional heterogeneity of alginates extracted from brown seaweed, a study on structure-function relationships in alginate gels was performed on polymannuronan epimerized by AlgE6 *in vitro*, which results in a more homogeneous alginate. Compared to algal alginate from *L. hyperborea* with the same composition, calcium saturated gels made from the epimerized material displayed the following characteristics:

- Strong increase in syneresis
- Low Youngs modulus
- High compressibility before rupture
- High rupture strength

None of these properties have previously been observed for high-G alginates devoid of MG-blocks. Addition of long G-blocks isolated from *L. hyperborea* to epimerized alginate resulted in more brittle gels with reduced syneresis and higher Youngs modulus.

The study shows that there are macroscopic properties of alginate gels made from *in vitro* epimerized mannuronan which cannot be explained from the sequence parameters determined by NMR. Furthermore, there are functional roles for G-blocks in alginate gels which G-blocks with a DP between 50 and 60 are unable to fill.

## 5 REFERENCES

1. Black, W.A.P., *Seasonal variation in weight and chemical composition of the common British Laminariaceae*. J. Mar. Biol. Assoc. U. K., 1950. **29**: p. 45-72.
2. Painter, T.J., *Algal polysaccharides*. Polysaccharides, 1983. **2**: p. 195-285.
3. Haug, A., B. Larsen, and O. Smidsrød, *Uronic Acid Sequence in Alginate from Different Sources*. Carbohydrate Research, 1974. **32**(2): p. 217-225.
4. Skjåk-Bræk, G., H. Grasdalen, and B. Larsen, *Monomer Sequence and Acetylation Pattern in Some Bacterial Alginates*. Carbohydrate Research, 1986. **154**: p. 239-250.
5. Gorin, P.A.J. and J.F.T. Spencer, *Exocellular alginic acid from Azotobacter vinelandii*. Can. J. Chem., 1966. **44**(9): p. 993-8.
6. Cote, G.L. and L.H. Krull, *Characterization of the exocellular polysaccharides from Azotobacter chroococcum*. Carbohydr. Res., 1988. **181**: p. 143-52.
7. Sadoff, H.L., *Encystment and germination in Azotobacter vinelandii*. Bacteriol. Rev., 1975. **39**(4): p. 516-39.
8. Govan, J.R., J.A. Fyfe, and T.R. Jarman, *Isolation of alginate-producing mutants of Pseudomonas fluorescens, Pseudomonas putida and Pseudomonas mendocina*. Journal of General Microbiology, 1981. **125**(1): p. 217-20.
9. Linker, A. and R.S. Jones, *Polysaccharide resembling alginic acid from a Pseudomonas microorganism*. Nature (London, U. K.), 1964. **204**: p. 187-8.
10. Boyd, A. and A.M. Chakrabarty, *Pseudomonas aeruginosa biofilms: role of the alginate exopolysaccharide*. J. Ind. Microbiol., 1995. **15**(3): p. 162-8.
11. Qiu, D., V.M. Eisinger, D.W. Rowen, and H.D. Yu, *Regulated proteolysis control mucoid conversion in Pseudomonas aeruginosa*. Proc. Natl. Acad. Sci. U. S. A., 2007. **104**(19): p. 8107-8112.
12. Alkawash, M.A., J.S. Soothill, and N.L. Schiller, *Alginate lyase enhances antibiotic killing of mucoid Pseudomonas aeruginosa in biofilms*. Apmis, 2006. **114**(2): p. 131-138.
13. Ramsey, D.M. and D.J. Wozniak, *Understanding the control of Pseudomonas aeruginosa alginate synthesis and the prospects for management of chronic infections in cystic fibrosis*. Mol. Microbiol., 2005. **56**(2): p. 309-322.
14. Stanford, E.C.C., Journal of the chemical Society, 1881. **44**.
15. Atsuki, K. and Y. Tomoda, *Studies on seaweeds of Japan. I. The chemical constituents of Laminaria*. J. Soc. Chem. Ind. Japan, 1926. **29**: p. 509-17.
16. Schmidt, E. and F. Vocke, *Polyglucuronic acids. I*. Ber. Dtsch. Chem. Ges. B, 1926. **59B**: p. 1585-8.

17. Miwa, T., *Alginic acid*. Nippon Kagaku Kaishi (1921-47), 1930. **51**: p. 738-45.
18. Nelson, W.L. and L.H. Cretcher, *Isolation and identification of d-mannuronic acid lactone from the Macrocystis pyrifera*. J. Am. Chem. Soc., 1930. **52**: p. 2130-2.
19. Bird, G.M. and P. Haas, *Nature of the cell wall constituents of Laminaria spp. Mannuronic acid*. Biochem. J., 1931. **25**: p. 403-11.
20. Nelson, W.L. and L.H. Cretcher, *Properties of d-mannuronic acid lactone*. J. Am. Chem. Soc., 1932. **54**: p. 3409-12.
21. Kringstad, H. and G. Lunde, *Alginic acid. II. X-ray investigation of spun threads of alginic acid*. Kolloid-Z., 1938. **83**: p. 202-3.
22. Hirst, E.L., J.K.N. Jones, and W.O. Jones, *Structure of alginic acid. I*. J. Chem. Soc., 1939: p. 1880-5.
23. Fischer, F.G. and H. Dorfel, *The polyuronic acids of brown algae*. Hoppe-Seyler's Z. Physiol. Chem., 1955. **302**: p. 186-203.
24. Hirst, E.L. and D.A. Rees, *The structure of alginic acid. V. Isolation and unambiguous characterization of some hydrolysis products of the methylated polysaccharide*. J. Chem. Soc., 1965(Feb.): p. 1182-7.
25. Vincent, D.I., *Oligosaccharides from alginic acid*. Chem. Ind. (London, U. K.), 1960: p. 1109-10.
26. Haug, A. and O. Smidsrød, *Fractionation of alginates by precipitation with calcium and magnesium ions*. Acta Chemica Scandinavica, 1965. **19**: p. 1221-1226.
27. Haug, A. and B. Larsen. *Studies on the composition and properties of alginates*. in *Proc. Int. Seaweed Symp., 4th 1961*. 1964. London: Pergamon Press.
28. Haug, A., B. Larsen, and O. Smidsrød, *A study of the constitution of alginic acid by partial acid hydrolysis*. Acta Chemica Scandinavica, 1966. **20**: p. 183-190.
29. Haug, A., B. Larsen, and O. Smidsrød, *Studies of the sequence of uronic acid residues in alginic acid*. Acta Chemica Scandinavica, 1967. **21**: p. 691-704.
30. Painter, T., O. Smidsrød, B. Larsen, and A. Haug, *A Computer Study of Changes in Composition-Distribution Occurring during Random Depolymerisation of a Binary Linear Heteropolysaccharide*. Acta Chemica Scandinavica, 1968. **22**(5): p. 1637-&.
31. Larsen, B., T. Painter, A. Haug, and O. Smidsrød, *A statistical description of the alginate molecule in terms of a penultimate-unit copolymer*. Acta Chemica Scandinavica, 1969. **23**: p. 355-370.
32. Smidsrød, O. and S.G. Whittington, *Monte Carlo Investigation of Chemical Inhomogeneity in Copolymers*. Macromolecules, 1969. **2**(1): p. 42-&.

33. Plate, N.A., A.D. Litmanovich, O.V. Noa, A.L. Toom, and N.B. Vasil'ev, *Effect of neighboring groups in macromolecular reactions. Distribution of units*. J. Polym. Sci., Polym. Chem. Ed., 1974. **12**(10): p. 2165-85.
34. Gonzalez, J.J. and K.W. Kehr, *Distribution of reacted sequences in homopolymers*. Macromolecules, 1978. **11**(5): p. 996-1000.
35. Atkins, E.D.T., W. Mackie, and E.E. Smolko, *Crystalline structures of alginic acids*. Nature (London), 1970. **225**(5233): p. 626-8.
36. Atkins, E.D.T., I.A. Nieduszynski, W. Mackie, K.D. Parker, and E.E. Smolko, *Structural components of alginic acid. I. Crystalline structure of poly- $\beta$ -D-mannuronic acid. Results of x-ray diffraction and polarized infrared studies*. Biopolymers, 1973. **12**(8): p. 1865-78.
37. Atkins, E.D.T., I.A. Nieduszynski, W. Mackie, K.D. Parker, and E.E. Smolko, *Structural components of alginic acid. II. Crystalline structure of poly  $\alpha$ -L-guluronic acid. Results of x-ray diffraction and polarized infrared studies*. Biopolymers, 1973. **12**(8): p. 1879-87.
38. Smidsrød, O., *Relative Extension of Alginates Having Different Chemical Composition*. Carbohydrate Research, 1973. **27**(1): p. 107-118.
39. Moe, S., K. Draget, G. Skjåk-Bræk, and O. Smidsrød, *Alginates.*, in *Food Polysaccharides and Their Applications.*, A.M. Stephen, Editor. 1995, Marcel Dekker Inc.: New York, Basel, Hong Kong. p. 245-286.
40. Haug, A. and O. Smidsrød, *The effect of divalent metals on the properties of alginate solutions. II. Comparison of different metal ions*. Acta Chemica Scandinavica, 1965. **19**: p. 341-351.
41. Smidsrød, O., *Solution Properties of Alginate*. Carbohydrate Research, 1970. **13**(3): p. 359-&.
42. Haug, A., *Report No 30 Norwegian Institute of seaweed research*. 1964.
43. Haug, A. and B. Larsen, *The solubility of alginate at low pH*. Acta Chemica Scandinavica, 1963. **17**: p. 1653-1662.
44. Draget, K.I., G. Skjåk-Bræk, and O. Smidsrød, *Alginic acid gels: the effect of alginate chemical composition and molecular weight*. Carbohydrate Polymers, 1994. **25**: p. 31-38.
45. Haug, A., Myklesta.S, B. Larsen, and O. Smidsrød, *Correlation between Chemical Structure and Physical Properties of Alginates*. Acta Chemica Scandinavica, 1967. **21**(3): p. 768-&.
46. Dentini, M., G. Rinaldi, D. Risica, A. Barbetta, and G. Skjåk-Bræk, *Comparative studies on solution characteristics of mannuronan epimerized by C-5 epimerases*. Carbohydrate Polymers, 2005. **59**: p. 489-499.

47. Smidsrød, O. and A. Haug, *A light scattering study of alginate*. Acta Chemica Scandinavica, 1968. **22**: p. 797-810.
48. Smidsrød, O., *Solution properties of alginate*. Carbohydrate Research, 1970. **13**: p. 359-372.
49. Vold, I.M.N., K.A. Kristiansen, and B.E. Christensen, *A study of the chain stiffness and extension of alginates, in vitro epimerized alginates, and periodate-oxidized alginates using size-exclusion chromatography combined with light scattering and viscosity detectors*. Biomacromolecules, 2006. **7**: p. 2136-2146.
50. Smidsrød, O., A. Haug, and B. Larsen, *The influence of pH on the rate of hydrolysis of acidic polysaccharides*. Acta Chemica Scandinavica, 1966. **20**: p. 1026-1034.
51. Haug, A., B. Larsen, and O. Smidsrød, *Alkaline degradation of alginate*. Acta Chemica Scandinavica, 1967. **21**: p. 2859-2870.
52. Smidsrød, O., A. Haug, and B. Larsen, *Oxidative-reductive depolymerization: a note on the comparison of degradation rates of different polymers by viscosity measurements*. Carbohydrate Research, 1967. **5**: p. 482-485.
53. Smidsrød, O., A. Haug, and B. Larsen, *The influence of reducing substances on the rate of degradation of alginates*. Acta Chemica Scandinavica, 1963. **17**: p. 1473-1474.
54. Edward, J.T., *Stability of glycosides to acid hydrolysis*. Chem. Ind. (London, U. K.), 1955: p. 1102-4.
55. Smidsrød, O., B. Larsen, T. Painter, and A. Haug, *The role of intramolecular autocatalysis in the acid hydrolysis of polysaccharides containing 1,4-linked hexuronic acid*. Acta Chemica Scandinavica, 1969. **23**: p. 1573-1580.
56. Holtan, S., Q.J. Zhang, W.I. Strand, and G. Skjak-Braek, *Characterization of the hydrolysis mechanism of polyalternating alginate in weak acid and assignment of the resulting MG-oligosaccharides by NMR spectroscopy and ESI-mass spectrometry*. Biomacromolecules, 2006. **7**(7): p. 2108-2121.
57. Ballance, S., S. Holtan, O.A. Aarstad, P. Sikorski, G. Skjak-Braek, and B.E. Christensen, *Application of high-performance anion-exchange chromatography with pulsed amperometric detection and statistical analysis to study oligosaccharide distributions - a complementary method to investigate the structure and some properties of alginates*. J. Chromatogr., A, 2005. **1093**(1-2): p. 59-68.
58. Skjåk-Braek, G., E. Murano, and S. Paoletti, *Alginate as Immobilization Material .2. Determination of Polyphenol Contaminants by Fluorescence Spectroscopy, and Evaluation of Methods for Their Removal*. Biotechnology and Bioengineering, 1989. **33**(1): p. 90-94.
59. Smidsrød, O. and A. Haug, *Dependence upon uronic acid composition of some ion-exchange properties of alginates*. Acta Chemica Scandinavica, 1968. **22**: p. 1989-1997.



60. Smidsrød, O. and A. Haug, *Dependence upon the gel-sol state of ion-exchange properties of alginate*. Acta Chemica Scandinavica, 1972. **26**: p. 2063-2074.
61. Grant, G.T., E.R. Morris, D.A. Rees, P.J.C. Smith, and D. Thom, *Biological interactions between polysaccharides and divalent cations. Egg-box model*. FEBS (Fed. Eur. Biochem. Soc.) Lett., 1973. **32**(1): p. 195-8.
62. Morris, E.R., D.A. Rees, D. Thom, and J. Boyd, *Chiroptical and stoichiometric evidence of a specific, primary dimerization process in alginate gelation*. Carbohydr. Res., 1978. **66**: p. 145-54.
63. Stokke, B.T., K.I. Draget, O. Smidsrød, Y. Yuguchi, H. Urakawa, and K. Kajiwara, *Small-angle x-ray scattering and rheological characterization of alginate gels. 1. Calcium alginate gels*. Macromolecules, 2000. **33**(5): p. 1853-1863.
64. Kohn, R. and B. Larsen, *Preparation of water-soluble polyuronic acids and their calcium salts, and the determination of calcium ion activity in relation to the degree of polymerization*. Acta Chemica Scandinavica, 1972. **26**: p. 2455-2468.
65. Stokke, B.T., O. Smidsrød, F. Zanetti, W. Strand, and G. Skjåk-Bræk, *Distribution of uronate residues in alginate chains in relation to alginate gelling properties - 2: Enrichment of  $\beta$ -D-mannuronic acid and depletion of  $\alpha$ -L-guluronic acid in sol fraction*. Carbohydrate Polymers, 1993. **21**: p. 39-46.
66. Donati, I., S. Holtan, Y.A. Mørch, M. Borgogna, M. Dentini, and G. Skjåk-Bræk, *New Hypothesis on the Role of Alternating Sequences in Calcium-Alginate Gels*. Biomacromolecules, 2005. **6**(2): p. 1031-1040.
67. Draget, K.I., K. Østgaard, and O. Smidsrød, *Homogeneous alginate gels: A technical approach*. Carbohydrate Polymers, 1991. **14**: p. 159-178.
68. Skjåk-Bræk, G., H. Grasdalen, and O. Smidsrød, *Inhomogeneous polysaccharide ionic gels*. Carbohydrate Polymers, 1989. **10**: p. 31-54.
69. Smidsrød, O., *Molecular basis for some physical properties of alginates in the gel state*. Faraday Discuss. Chem. Soc., 1974. **57**: p. 263-74.
70. Andresen, I. and O. Smidsrød, *Temperature dependence of the elastic properties of alginate gels*. Carbohydrate Research, 1977. **58**: p. 271-279.
71. Draget, K.I., O. Gaserød, I. Aune, P.O. Andersen, B. Storbakken, B.T. Stokke, and O. Smidsrød, *Effects of molecular weight and elastic segment flexibility on syneresis in Ca-alginate gels*. Food Hydrocolloids, 2001. **15**(4-6): p. 485-490.
72. Martinsen, A., G. Skjåk-Bræk, and O. Smidsrød, *Alginate as Immobilization Material .1. Correlation between Chemical and Physical-Properties of Alginate Gel Beads*. Biotechnology and Bioengineering, 1989. **33**(1): p. 79-89.
73. Mørch, Y.A., I. Donati, B.L. Strand, and G. Skjk-Brk, *Molecular Engineering as an Approach to Design New Functional Properties of Alginate*. Biomacromolecules, 2007. **8**(9): p. 2809-2814.

74. Smidsrød, O., A. Haug, and B. Lian, *Properties of Poly(1,4-Hexuronates) in Gel State .1. Evaluation of a Method for Determination of Stiffness*. Acta Chemica Scandinavica, 1972. **26**(1): p. 71-&.
75. Smidsrød, O., *Properties of Poly(1,4-Hexuronates) in Gel State .2. Comparison of Gels of Different Chemical Composition*. Acta Chemica Scandinavica, 1972. **26**(1): p. 79-&.
76. Strand, B.L., Y.A. Mørch, K.R. Syvertsen, T. Espevik, and G. Skjåk-Bræk, *Microcapsules made by enzymatically tailored alginate*. Journal of Biomedical Materials Research, 2003. **64**(3): p. 540-550.
77. Mørch, Y.A., S. Holtan, I. Donati, B.L. Strand, and G. Skjak-Braek, *Mechanical properties of C-5 epimerized alginates*. Biomacromolecules, 2008. **9**(9): p. 2360-2368.
78. Moe, S.T., K.I. Draget, G. Skjåk-Bræk, and O. Smidsrød, *Alginates*. Food Sci. Technol. (N. Y.), 1995. **67**: p. 245-86.
79. Skjåk-Bræk, G., O. Smidsrød, and B. Larsen, *Tailoring of alginates by enzymatic modification in vitro*. International journal of biological macromolecules, 1986. **8**: p. 330-336.
80. Smidsrød, O. and A. Haug, *Properties of Poly(1,4-hexuronates) in the gel state. II. Comparison of gels of different chemical composition*. Acta Chemica Scandinavica, 1972. **26**: p. 79-88.
81. Sperling, L.H., *Introduction to physical polymer science*. 4 ed. 2006, New Jersey: Wiley & sons. 845.
82. Moe, S.T., K.I. Draget, G. Skjak-Braek, and O. Smidsrød, *Temperature dependence of the elastic modulus of alginate gels*. Carbohydr. Polym., 1992. **19**(4): p. 279-84.
83. Zhang, J., C.R. Daubert, and E.A. Foegeding, *A proposed strain-hardening mechanism for alginate gels*. J. Food Eng., 2006. **80**(1): p. 157-165.
84. Donati, I., Y.A. Mørch, B.L. Strand, G. Skjak-Braek, and S. Paoletti, *Effect of Elongation of Alternating Sequences on Swelling Behavior and Large Deformation Properties of Natural Alginate Gels*. J. Phys. Chem. B, 2009. **113**(39): p. 12916-12922.
85. Dubois, M., K.A. Gilles, J.K. Hamilton, P.A. Rebers, and F. Smith, *Colorimetric method for determination of sugars and related substances*. Anal. Chem., 1956. **28**: p. 350-6.
86. Haug, A. and B. Larsen, *Quantitative determination of the uronic acid composition of alginates*. Acta Chemica Scandinavica, 1962. **16**: p. 1908-1918.
87. Dische, Z., *New color reactions for determination of sugars in polysaccharides*. Methods Biochem Anal, 1955. **2**: p. 313-58.

88. Usov, A.I., *Alginic acids and alginates: analytical methods used for their estimation and characterization of composition and primary structure*. Russ. Chem. Rev., 1999. **68**(11): p. 957-966.
89. Østgaard, K., *Determination of alginate composition by a simple enzymatic assay*. Hydrobiologia, 1993. **260/261**: p. 513-520.
90. Tøndervik, A., G. Klinkenberg, F.L. Aachmann, B.I.G. Svanem, T.E. Ellingsen, S. Valla, . . . H. Sletta, *Novel mannuronan C-5 epimerases suited for tailoring of specific alginate structures obtained by high throughput screening of an epimerase mutant library*. 2012.
91. Gacesa, P., A. Squire, and P.J. Winterburn, *The determination of the uronic acid composition of alginates by anion-exchange liquid chromatography*. Carbohydr. Res., 1983. **118**: p. 1-8.
92. Annison, G., N.W.H. Cheetham, and I. Couperwhite, *Determination of the uronic acid composition of alginates by high-performance liquid chromatography*. J. Chromatogr., 1983. **264**(1): p. 137-43.
93. Honda, S., K. Sudo, K. Kakehi, H. Yuki, and K. Takiura, *Selective microdetermination of unconjugated uronic acids by fluorescence reactions with ethylenediamine sulfate*. Anal. Chim. Acta, 1975. **77**: p. 199-203.
94. Penman, A. and G.R. Sanderson, *Method for the determination of uronic acid sequence in alginates*. Carbohydr. Res., 1972. **25**(2): p. 273-82.
95. Grasdalen, H., B. Larsen, and O. Smidsrød, *<sup>13</sup>C-NMR studies of monomeric composition and sequence in alginate*. Carbohydrate Research, 1981. **89**: p. 179-191.
96. Grasdalen, H., *High-field <sup>1</sup>H-n.m.r. spectroscopy of alginate: Sequential structure and linkage conformations*. Carbohydrate Research, 1983. **118**: p. 255-260.
97. Heyraud, A., C. Gey, C. Leonard, C. Rochas, S. Girond, and B. Kloareg, *NMR spectroscopy analysis of oligoguluronates and oligomannuronates prepared by acid or enzymatic hydrolysis of homopolymeric blocks of alginic acid. Application to the determination of the substrate specificity of Haliotis tuberculata alginate lyase*. Carbohydrate Research, 1996. **289**: p. 11-23.
98. Skjåk-Bræk, G., H. Grasdalen, and B. Larsen, *Monomer sequence and acetylation pattern in some bacterial alginates*. Carbohydrate Research, 1986. **154**: p. 239-250.
99. Sherbrock-Cox, V., N.J. Russell, and P. Gacesa, *The purification and chemical characterization of the alginate present in extracellular material produced by mucoid strains of Pseudomonas aeruginosa*. Carbohydr. Res., 1984. **135**(1): p. 147-54.
100. Horn, S.J., E. Moen, and K. Østgaard, *Direct determination of alginate content in brown algae by near infra-red (NIR) spectroscopy*. Journal of Applied Phycology, 1999. **11**: p. 9-13.
101. Heyraud, A., P. ColinMorel, S. Girond, C. Richard, and B. Kloareg, *HPLC analysis of saturated or unsaturated oligoguluronates and oligomannuronates. Application to the*

- determination of the action pattern of Haliotis tuberculata alginate lyase.* Carbohydrate Research, 1996. **291**: p. 115-126.
102. Heyraud, A., P. Colin-Morel, C. Gey, F. Chavagnat, M. Guinand, and J. Wallach, *An enzymatic method for preparation of homopolymannuronate blocks and strictly alternating sequences of mannuronic and guluronic units.* Carbohydrate Research, 1998. **308**(3-4): p. 417-422.
  103. Campa, C., A. Oust, G. Skjåk-Bræk, B.S. Paulsen, S. Paoletti, B.E. Christensen, and S. Ballance, *Determination of average degree of polymerisation and distribution of oligosaccharides in a partially acid-hydrolysed homopolysaccharide: A comparison of four experimental methods applied to mannuronan.* Journal of Chromatography A, 2004. **1026**(1-2): p. 271-281.
  104. Holtan, S., P. Bruheim, and G. Skjåk-Bræk, *Mode of action and subsite studies of the guluronan block-forming mannuronan C-5 epimerases AlgE1 and AlgE6.* Biochemical Journal, 2006. **395**: p. 319-329.
  105. Krull, L.H. and G.L. Cote, *Determination of gulose and/or guluronic acid by ion chromatography and pulsed amperometric detection.* Carbohydr. Polym., 1991. **17**(3): p. 205-7.
  106. Campa, C., S. Holtan, N. Nilsen, T.M. Bjerkan, B.T. Stokke, and G. Skjåk-Bræk, *Biochemical analysis of the processive mechanism for epimerisation of alginate by mannuronan C-5 epimerase AlgE4.* Biochemical Journal, 2004. **381**(1): p. 155-164.
  107. Stefansson, M., *Assessment of Alginic Acid Molecular Weight and Chemical Composition through Capillary Electrophoresis.* Anal. Chem., 1999. **71**(13): p. 2373-2378.
  108. Zhang, Z., G. Yu, X. Zhao, H. Liu, H. Guan, A.M. Lawson, and W. Chai, *Sequence Analysis of Alginate-Derived Oligosaccharides by Negative-Ion Electrospray Tandem Mass Spectrometry.* J. Am. Soc. Mass Spectrom., 2006. **17**(4): p. 621-630.
  109. Dingsøy, E. and O. Smidsrød, *Light-scattering properties of sodium and magnesium alginate.* The British Polymer Journal, 1977. **9**: p. 56-61.
  110. Strand, K.A., A. Bøe, P.S. Dalberg, T. Sikkeland, and O. Smidsrød, *Dynamic and static light scattering on aqueous solutions of sodium alginate.* Macromolecules, 1982. **15**: p. 570-579.
  111. Horton, J.C., S.E. Harding, J.R. Mitchell, and D.F. Morton-Holmes, *Thermodynamic non-ideality of dilute solutions of sodium alginate studied by sedimentation equilibrium ultracentrifugation.* Food Hydrocolloids, 1991. **5**(1-2): p. 125-7.
  112. Haug, A. and O. Smidsrød, *Determination of Intrinsic Viscosity of Alginates.* Acta Chemica Scandinavica, 1962. **16**(7): p. 1569-&.
  113. Donati, I., A. Gamini, G. Skjåk-Bræk, A. Vetere, C. Campa, A. Coslovi, and S. Paoletti, *Determination of the diadic composition of alginate by means of circular dichroism: a fast and accurate improved method.* Carbohydrate Research, 2003. **338**: p. 1139-1142.

114. Sletmoen, M., K.I. Draget, and B.T. Stokke, *Alginate Oligoguluronates as a Tool for Tailoring Properties of Ca-Alginate Gels*. Macromol. Symp., 2010. **291-292**(Polymer Networks): p. 345-353.
115. Tam, S.K., J. Dusseault, S. Polizu, M. Menard, J.-P. Halle, and L.H. Yahia, *Physicochemical model of alginate-poly-L-lysine microcapsules defined at the micrometric/nanometric scale using ATR-FTIR, XPS, and ToF-SIMS*. Biomaterials, 2005. **26**(34): p. 6950-6961.
116. Tam, S.K., J. Dusseault, S. Polizu, M. Menard, J.-P. Halle, and L.H. Yahia, *Impact of residual contamination on the biofunctional properties of purified alginates used for cell encapsulation*. Biomaterials, 2006. **27**(8): p. 1296-1305.
117. Sikorski, P., F. Mo, G. Skjåk-Bræk, and B.T. Stokke, *Evidence for egg-box-compatible interactions in calcium-alginate gels from fiber X-ray diffraction*. Biomacromolecules, 2007. **8**: p. 2098-2103.
118. Sæther, H.V., H.K. Holme, G. Maurstad, O. Smidsrød, and B.T. Stokke, *Polyelectrolyte complex formation using alginate and chitosan*. Carbohydrate Polymers, 2008. **74**: p. 813-821.
119. Sletmoen, M., G. Skjåk-Bræk, and B.T. Stokke, *Single-molecular pair unbinding studies of mannuronan C-5 epimerase AlgE4 and its polymer substrate*. Biomacromolecules, 2004. **5**: p. 1288-1295.
120. Williams, M.A.K., A. Marshall, R.G. Haverkamp, and K.I. Draget, *Stretching single polysaccharide molecules using AFM: A potential method for the investigation of the intermolecular uronate distribution of alginate?* Food Hydrocolloids, 2007. **22**(1): p. 18-23.
121. Jorgensen, T.E., M. Sletmoen, K.I. Draget, and B.T. Stokke, *Influence of Oligoguluronates on Alginate Gelation, Kinetics, and Polymer Organization*. Biomacromolecules, 2007. **8**(8): p. 2388-2397.
122. Draget, K.I., K. Østgaard, and O. Smidsrød, *Homogeneous alginate gels: a technical approach*. Carbohydr. Polym., 1990. **14**(2): p. 159-78.
123. Martinsen, A., I. Storrø, and G. Skjåk-Bræk, *Alginate as immobilization material: III. Diffusional properties*. Biotechnology and bioengineering, 1992. **39**: p. 186-194.
124. Olderoy, M.O., M.L. Xie, B.L. Strand, E.M. Flaten, P. Sikorski, and J.P. Andreassen, *Growth and Nucleation of Calcium Carbonate Vaterite Crystals in Presence of Alginate*. Crystal Growth & Design, 2009. **9**(12): p. 5176-5183.
125. Strand, B.L., Y.A. Mørch, T. Espevik, and G. Skjåk-Bræk, *Visualization of alginate-poly-L-lysine-alginate microcapsules by confocal laser scanning microscopy*. Biotechnology and bioengineering, 2003. **82**(4): p. 386-394.
126. Thu, B., O. Gåserød, D. Paus, A. Mikkelsen, G. Skjåk-Bræk, R. Toffanin, . . . R. Rizzo, *Inhomogeneous alginate gel spheres: An assessment of the polymer gradients by synchrotron radiation-induced x-ray emission, magnetic resonance microimaging, and mathematical modeling*. Biopolymers, 2000. **53**: p. 60-71.

127. Buchinger, E., *Alginate Epimerases: Segmental Labelling, Structures and Ligand Interactions*, in *Department of Biotechnology, Chemistry and Environmental Engineering*. 2011, Aalborg University: Aalborg. p. 103.
128. Grasdalen, H., B. Larsen, and O. Smidsrød, *C-13-Nmr Studies of Alginate*. *Carbohydrate Research*, 1977. **56**(2): p. C11-C15.
129. Aarstad, O.A., A. Tøndervik, H. Sletta, and G. Skjåk-Bræk, *Alginate Sequencing: An Analysis of Block Distribution in Alginates Using Specific Alginate Degrading Enzymes*. *Biomacromolecules*, 2012. **13**(1): p. 106-116.
130. Iwamoto, M., M. Kurachi, T. Nakashima, D. Kim, K. Yamaguchi, T. Oda, . . . T. Muramatsu, *Structure-activity relationship of alginate oligosaccharides in the induction of cytokine production from RAW264.7 cells*. *FEBS Lett.*, 2005. **579**(20): p. 4423-4429.
131. Lee, Y.C., *Carbohydrate analyses with high-performance anion-exchange chromatography*. *J. Chromatogr., A*, 1996. **720**(1 + 2): p. 137-49.
132. Dionex. *Product manual for CarboPac® MA1, CarboPac® PA1, CarboPac® PA1 and CarboPac® PA100*. 2010 may 2010; Available from: <http://www.dionex.com/en-us/webdocs/4375-Man-031824-08-CarboPac-Combined-May10.pdf>.
133. Dionex. *Analysis of Carbohydrates by High-Performance Anion-Exchange Chromatography with Pulsed Amperometric Detection (HPAE-PAD)*. 2004; Available from: [http://www.dionex.com/en-us/webdocs/5023-TN20\\_LPN032857-04.pdf](http://www.dionex.com/en-us/webdocs/5023-TN20_LPN032857-04.pdf).
134. Kristiansen, K.A., S. Ballance, A. Potthast, and B.E. Christensen, *An evaluation of tritium and fluorescence labelling combined with multi-detector SEC for the detection of carbonyl groups in polysaccharides*. *Carbohydrate Polymers* 2009. **76**: p. 196–205.
135. Bohdanecky, M., *New method for estimating the parameters of the wormlike chain model from the intrinsic viscosity of stiff-chain polymers*. *Macromolecules*, 1983. **16**(9): p. 1483-92.
136. Lin, T.-Y. and W.Z. Hassid, *Pathway of alginic acid synthesis in the marine brown alga, Fucus gardneri*. *J. Biol. Chem.*, 1966. **241**(22): p. 5284-97.
137. Hellebust, J.A. and A. Haug. *Alginic acid synthesis in Laminaria digitata (L.) Lamour*. in *Proc. Int. Seaweed Symp., 6th 1968*. 1969. Maritima 1969: Direction General de Pesca Maritima.
138. Madgwick, J., A. Haug, and B. Larsen, *Polymannuronic acid 5-epimerase from the marine alga Pelvetia canaliculata (L.) Dcne. et Thur*. *Acta Chemica Scandinavica*, 1973. **27**: p. 3592-3594.
139. Rehm, B.H.A. and S. Valla, *Bacterial alginates: biosynthesis and applications*. *Applied microbiology and biotechnology*, 1997. **48**: p. 281-288.
140. Rehm, B., H. Ertesvåg, and S. Valla, *A new Azotobacter vinelandii mannuronan C-5-epimerase gene (algG) is part of an alg gene cluster physically organized in a manner*

- similar to that in *Pseudomonas aeruginosa*. Journal of bacteriology, 1996. **178**: p. 5884-5889.
141. May, T.B. and A.M. Chakrabarty, *Pseudomonas aeruginosa: genes and enzymes of alginate synthesis*. Trends Microbiol, 1994. **2**(5): p. 151-7.
  142. Horan, N.J., T.R. Jarman, and E.A. Dawes, *Effects of carbon source and inorganic phosphate concentration on the production of alginic acid by a mutant of Azotobacter vinelandii and on the enzymes involved in its biosynthesis*. J. Gen. Microbiol., 1981. **127**(1): p. 185-91.
  143. Beale, J.M., Jr. and J.L. Foster, *Carbohydrate fluxes into alginate biosynthesis in Azotobacter vinelandii NCIB 8789: NMR investigations of the triose pools*. Biochemistry, 1996. **35**(14): p. 4492-501.
  144. Maharaj, R., T.B. May, S.K. Wang, and A.M. Chakrabarty, *Sequence of the alg8 and alg44 genes involved in the synthesis of alginate by Pseudomonas aeruginosa*. Gene, 1993. **136**(1-2): p. 267-9.
  145. Shinabarger, D., T.B. May, A. Boyd, M. Ghosh, and A.M. Chakrabarty, *Nucleotide sequence and expression of the Pseudomonas aeruginosa algF gene controlling acetylation of alginate*. Molecular Microbiology, 1993. **9**(5): p. 1027-35.
  146. Franklin, M.J. and D.E. Ohman, *Identification of algF in the alginate biosynthetic gene cluster of Pseudomonas aeruginosa which is required for alginate acetylation*. J. Bacteriol., 1993. **175**(16): p. 5057-65.
  147. Skjåk-Bræk, G., F. Zanetti, and S. Paoletti, *Effect of Acetylation on Some Solution and Gelling Properties of Alginates*. Carbohydrate Research, 1989. **185**(1): p. 131-138.
  148. Skjåk-Bræk, G., B. Larsen, and H. Grasdalen, *The role of O-acetyl groups in the biosynthesis of alginate by Azotobacter vinelandii*. Carbohydrate Research, 1985. **145**: p. 169-174.
  149. Gimmestad, M., H. Sletta, H. Ertesvåg, K. Bakkevig, S. Jain, S. Suh, . . . S. Valla, *The Pseudomonas fluorescens AlgG protein, but not its mannuronan C-5-epimerase activity, is needed for alginate polymer formation*. Journal of bacteriology, 2003. **185**(12): p. 3515-3523.
  150. Jain, S., M.J. Franklin, H. Ertesvåg, S. Valla, and D.E. Ohman, *The dual roles of AlgG in C-5-epimerization and secretion of alginate polymers in Pseudomonas aeruginosa*. Molecular microbiology, 2003. **47**(4): p. 1123-1133.
  151. Bakkevig, K., H. Sletta, M. Gimmestad, R. Aune, H. Ertesvåg, K. Degnes, . . . S. Valla, *Role of the Pseudomonas fluorescens alginate lyase (AlgL) in clearing the periplasm of alginates not exported to the extracellular environment*. Journal of bacteriology, 2005. **187**(24): p. 8375-8384.
  152. Ertesvåg, H., H.K. Hoidal, I.K. Hals, A. Rian, B. Doseth, and S. Valla, *A Family of Modular Type Mannuronan C-5-Epimerase Genes Controls Alginate Structure in Azotobacter-Vinelandii*. Molecular Microbiology, 1995. **16**(4): p. 719-731.

153. Helgerud, T., Gåserud, O., Fjæreide, T., Andersen, P.O., Larsen, C.K, *Food Stabilisers, Thickeners and Gelling Agents*, A. Imeson, Editor. 2009, Wiley-Blackwell: Oxford. p. 50-72.
154. Valla, S., H. Ertesvåg, and G. Skjåk-Bræk, *Genetics and biosynthesis of alginates*. Carbohydrates in Europe, 1996. **14**: p. 14-18.
155. Onsøyen, E., *Commercial applications of alginates*. Carbohydr. Eur., 1996. **14**: p. 26-31.
156. Banning, D., D.Q.M. Craig, I.G. Joliffe, F.C. Hampson, P.F. Field, E.J. Onsoyen, . . . P.W. Dettmar, *Pourable alginate compositions*. 1998, (Reckitt & Colman Products Ltd., UK). Application: WO  
WO. p. 49 pp.
157. Otterlei, M., K. Østgaard, G. Skjåk-Bræk, O. Smidsrød, P. Soonshiong, and T. Espevik, *Induction of Cytokine Production from Human Monocytes Stimulated with Alginate*. Journal of Immunotherapy, 1991. **10**(4): p. 286-291.
158. Espevik, T. and G. Skjåk-Bræk, *Application of alginate gels in biotechnology and biomedicine*. Carbohydrates in Europe, 1996. **14**: p. 19-25.
159. Gombotz, W.R. and S. Wee, *Protein release from alginate matrixes*. Adv. Drug Delivery Rev., 1998. **31**(3): p. 267-285.
160. Shilpa, A., S.S. Agrawal, and A.R. Ray, *Controlled delivery of drugs from alginate matrix*. J. Macromol. Sci., Polym. Rev., 2003. **C43**(2): p. 187-221.
161. Mørch, Y.A., I. Sandvig, O. Olsen, I. Donati, M. Thuen, G. Skjåk-Bræk, . . . C. Brekken, *Mn-alginate gels as a novel system for controlled release of Mn<sup>2+</sup> in manganese-enhanced MRI*. Contrast Media Mol. Imaging, 2012. **7**(2): p. 265-275.
162. Taylor Nordgaard, C. and K.I. Draget, *Oligosaccharides As Modulators of Rheology in Complex Mucous Systems*. Biomacromolecules, 2011. **12**(8): p. 3084-3090.
163. Draget, K.I. and C. Taylor, *Chemical, physical and biological properties of alginates and their biomedical implications*. Food Hydrocolloids, 2010. **25**(2): p. 251-256.
164. Taylor, C., K.I. Draget, and O.A. Smidsrød, *Use of an oligoelectrolyte polyol to treat mucosal hyperviscosity*. 2007, (NTNU Technology Transfer AS, Norway).  
Application: GB  
GB. p. 18pp.
165. Onsoyen, E., R. Myrvold, A. Dessen, and D. Thomas, *Topical compositions containing anti-microbial alginate oligomers*. 2010, (Algipharma IPR AS, Norway).  
Application: WO  
WO. p. 89pp.
166. Onsoyen, E. and R. Myrvold, *Alginate oligomers in combating biofilms*. 2009, (Algipharma Ipr AS, Norway; Dzieglewska, Hanna). Application: WO  
WO. p. 70pp.



167. Smidsrød, O. and G. Skjåk-Bræk, *Alginate as Immobilization Matrix for Cells*. Trends in Biotechnology, 1990. **8**(3): p. 71-78.
168. Yoo, I.-K., G.H. Seong, H.N. Chang, and J.K. Park, *Encapsulation of Lactobacillus casei cells in liquid-core alginate capsules for lactic acid production*. Enzyme Microb. Technol., 1996. **19**(6): p. 428-433.
169. Demirel, G., K.O. Yaykasli, and A. Yasar, *The production of citric acid by using immobilized Aspergillus niger A-9 and investigation of its various effects*. Food Chem., 2004. **89**(3): p. 393-396.
170. Oda, G., H. Samejima, and T. Yamada, *Continuous alcohol fermentation technologies using immobilized yeast cells*. BioTech 83 [Eighty-Three], Proc. Int. Conf. Commer. Appl. Implic. Biotechnol., 1st, 1983: p. 597-611.
171. Draget, K.I., S. Myhre, G. Skjakbrk, and K. Østgaard, *Regeneration, Cultivation and Differentiation of Plant-Protoplasts Immobilized in Ca-Alginate Beads*. Journal of Plant Physiology, 1988. **132**(5): p. 552-556.
172. El-Sayed, A.H.M.M. and H.J. Rehm, *Morphology of Penicillium chrysogenum strains immobilized in calcium alginate beads and used in penicillin fermentation*. Appl. Microbiol. Biotechnol., 1986. **24**(1): p. 89-94.
173. Jarvis, A.P., Jr. and T.A. Grdina, *Production of biologicals [interferon] from microencapsulated living cells*. BioTechniques, 1983. **1**(1): p. 22, 24-7.
174. Bruni, S. and T.M. Chang, *Encapsulated hepatocytes for controlling hyperbilirubinemia in Gunn rats*. Int J Artif Organs, 1991. **14**(4): p. 239-41.
175. Read, T.-A., D.R. Sorensen, R. Mahesparan, P.O. Enger, R. Timpl, B.R. Olsen, . . . R. Bjerkvig, *Local endostatin treatment of gliomas administered by microencapsulated producer cells*. Nat. Biotechnol., 2001. **19**(1): p. 29-34.
176. Augst, A.D., H.J. Kong, and D.J. Mooney, *Alginate hydrogels as biomaterials*. Macromol. Biosci., 2006. **6**(8): p. 623-633.
177. Rowley, J.A. and D.J. Mooney, *Alginate type and RGD density control myoblast phenotype*. J. Biomed. Mater. Res., 2002. **60**(2): p. 217-223.
178. Yang, J., M. Goto, H. Ise, C.-S. Cho, and T. Akaike, *Galactosylated alginate as a scaffold for hepatocytes entrapment*. Biomaterials, 2002. **23**(2): p. 471-9.
179. Valla, S., J.-p. Li, H. Ertesvåg, T. Barbeyron, and U. Lindahl, *Hexuronyl C5-epimerases in alginate and glycosaminoglycan biosynthesis*. Biochimie, 2001. **83**: p. 819-830.
180. Larsen, B. and A. Haug, *Biosynthesis of Alginate .I. Composition and Structure of Alginate Produced by Azotobacter-Vinelandii (Lipman)*. Carbohydrate Research, 1971. **17**(2): p. 287-&.

181. Nyvall, P., E. Corre, C. Boisset, T. Barbeyron, S. Rousvoal, D. Scornet, . . . C. Boyen, *Characterization of mannuronan C-5-epimerase genes from the brown alga Laminaria digitata*. *Plant Physiol.*, 2003. **133**(2): p. 726-735.
182. Franklin, M.J., C.E. Chitnis, P. Gacesa, A. Sonesson, D.C. White, and D.E. Ohman, *Pseudomonas aeruginosa AlgG is a polymer level alginate C5-mannuronan epimerase*. *J. Bacteriol.*, 1994. **176**(7): p. 1821-30.
183. Morea, A., K. Mathee, M.J. Franklin, A. Giacomini, M. O'Regan, and D.E. Ohman, *Characterization of algG encoding C5-epimerase in the alginate biosynthetic gene cluster of Pseudomonas fluorescens*. *Gene*, 2001. **278**(1-2): p. 107-114.
184. Penalzoza-Vazquez, A., S.P. Kidambi, A.M. Chakrabarty, and C.L. Bender, *Characterization of the alginate biosynthetic gene cluster in Pseudomonas syringae pv. syringae*. *J. Bacteriol.*, 1997. **179**(14): p. 4464-4472.
185. Skjåk-Bræk, G. and B. Larsen, *Biosynthesis of alginate: Purification and characterisation of mannuronan C-5-epimerase from Azotobacter vinelandii*. *Carbohydrate Research*, 1985. **139**: p. 273-283.
186. Ertesvag, H., B. Doseth, B. Larsen, G. Skjåk-Bræk, and S. Valla, *Cloning and Expression of an Azotobacter-Vinelandii Mannuronan C-5-Epimerase Gene*. *Journal of Bacteriology*, 1994. **176**(10): p. 2846-2853.
187. Svanem, B.I.G., G. Skjåk-Bræk, H. Ertesvåg, and S. Valla, *Cloning and expression of three new Azotobacter vinelandii genes closely related to a previously described gene family encoding mannuronan C-5-Epimerase*. *Journal of bacteriology*, 1999. **181**: p. 68-77.
188. Bjerkan, T.M., B.E. Lillehov, W.I. Strand, G. Skjåk-Bræk, S. Valla, and H. Ertesvag, *Construction and analyses of hybrid Azotobacter vinelandii mannuronan C-5 epimerases with new epimerization pattern characteristics*. *Biochemical Journal*, 2004. **381**: p. 813-821.
189. Gacesa, P., *Alginate-Modifying Enzymes - a Proposed Unified Mechanism of Action for the Lyases and Epimerases*. *Febs Letters*, 1987. **212**(2): p. 199-202.
190. Rozeboom, H.J., T.M. Bjerkan, K.H. Kalk, H. Ertesvåg, S. Holtan, F.L. Achmann, . . . B.W. Dijkstra, *Structural and mutational characterization of the catalytic A-module of the mannuronan C-5-epimerase AlgE4 from Azotobacter vinelandii*. *The Journal of Biological Chemistry*, 2008. **283**(35): p. 23819-23828.
191. Larsen, B. and H. Grasdalen, *Investigation by NMR spectroscopy of the site of proton exchange catalysed by poly(mannuronic acid) C-5 epimerase*. *Carbohydrate Research*, 1981. **92**: p. 163-167.
192. Skjåk-Bræk, G. and B. Larsen, *A new assay for mannuronan C-5-epimerase activity*. *Carbohydrate Research*, 1982. **103**: p. 133-136.
193. Hagner-Mcwhirter, A., U. Lindahl, and J.p. Li, *Biosynthesis of heparin/heparan sulphate: mechanism of epimerization of glucuronyl C-5*. *Biochemical Journal*, 2000. **347 Pt 1**: p. 69-75.

194. Høidal, H.K., H. Ertesvåg, G. Skjåk-Bræk, B.T. Stokke, and S. Valla, *The recombinant Azotobacter vinelandii mannuronan C-5-Epimerase AlgE4 epimerizes alginate by a nonrandom attack mechanism*. Journal of Biological Chemistry, 1999. **274**: p. 12316-12322.
195. Aachmann, F.L., B.I.G. Svanem, P. Güntert, S.B. Petersen, S. Valla, and R. Wimmer, *NMR structure of the R-module. A parallel  $\beta$ -roll subunit from an Azotobacter vinelandii mannuronan C-5 epimerase*. The Journal of Biological Chemistry, 2006. **281**(11): p. 7350–7356.
196. Li, H., A.D. Robertson, and J.H. Jensen, *Very fast empirical prediction and rationalization of protein pKa values*. Proteins, 2005. **61**(4): p. 704-21.
197. Baker, N.A., D. Sept, S. Joseph, M.J. Holst, and J.A. McCammon, *Electrostatics of nanosystems: application to microtubules and the ribosome*. Proc Natl Acad Sci U S A, 2001. **98**(18): p. 10037-41.
198. DeLano, W.L., *The PyMOL User's Manual*. Vol. 228. 2002, San Carlos, CA, USA: DeLano Scientific. U313-U314.
199. Haug, A. and B. Larsen, *Biosynthesis of Alginate .2. Polymannuronic Acid C-5-Epimerase from Azotobacter-Vinelandii(Lipman)*. Carbohydrate Research, 1971. **17**(2): p. 297-&.
200. Ertesvåg, H. and S. Valla, *The A modules of the Azotobacter vinelandii mannuronan-C-5-epimerase AlgE1 are sufficient for both epimerization and binding of Ca<sup>2+</sup>*. Journal of Bacteriology, 1999. **181**(10): p. 3033-3038.
201. Ertesvåg, H., H.K. Høidal, G. Skjåk-Bræk, and S. Valla, *The Azotobacter vinelandii mannuronan C-5-epimerase AlgE1 consists of two separate catalytic domains*. Journal of Biological Chemistry, 1998. **273**: p. 30927-30932.
202. Ertesvåg, H., H.K. Høidal, H. Schjerven, B.I. Glærum Svanem, and S. Valla, *Mannuronan C-5-Epimerases and their application for in Vitro and in Vivo design of new alginates useful in biotechnology*. Metabolic Engineering, 1999. **1**: p. 262-269.
203. Ramstad, M.V., T.E. Ellingsen, K.D. Josefsen, H.K. Høidal, S. Valla, G. Skjåk-Bræk, and D.W. Levine, *Properties and action pattern of the recombinant mannuronan C-5-epimerase AlgE2*. Enzyme and microbial technology, 1999. **24**(10): p. 636-646.
204. Svanem, B.I.G., W.I. Strand, H. Ertesvåg, G. Skjåk-Bræk, M. Hartmann, T. Barbeyron, and S. Valla, *The catalytic activities of the bifunctional Azotobacter vinelandii mannuronan C-5-epimerase and alginate lyase AlgE7 probably originate from the same active site in the enzyme*. Journal of Biological Chemistry, 2001. **276**(34): p. 31542-31550.
205. Horn, S.J., A. Sørbotten, B. Synstad, P. Sikorski, M. Sørli, K.M. Vårum, and V.G.H. Eijsink, *Endo/exo mechanism and processivity of family 18 chitinases produced by Serratia marcescens*. FEBS Journal, 2006. **273**: p. 491–503.
206. Salmivirta, M., K. Lidholt, and U. Lindahl, *Heparan sulfate: a piece of information*. Faseb J., 1996. **10**(11): p. 1270-1279.

207. Hartmann, M., A.S. Duun, S. Markussen, H. Grasdalen, S. Valla, and G. Skjåk-Bræk, *Time-resolved <sup>1</sup>H and <sup>13</sup>C NMR spectroscopy for detailed analyses of the Azotobacter vinelandii mannuronan C-5 epimerase reaction*. *Biochimica et biophysica acta*, 2002. **1570**: p. 104-112.
208. Strand, B., L., A. Mørch Yrr, R. Syvertsen Kjersti, T. Espevik, and G. Skjåk-Bræk, *Microcapsules made by enzymatically tailored alginate*. *J Biomed Mater Res A*, 2003. **64**(3): p. 540-50.
209. Donati, I., K.I. Draget, M. Borgogna, S. Paoletti, and G. Skjåk-Bræk, *Tailor-made alginate bearing galactose moieties on mannuronic residues: Selective modification achieved by a chemoenzymatic strategy*. *Biomacromolecules*, 2005. **6**: p. 88-98.
210. Kristiansen, K.A., B.C. Schirmer, F.L. Aachmann, G. Skjåk-Bræk, K.I. Draget, and B.E. Christensen, *Novel alginates prepared by independent control of chain stiffness and distribution of G-residues: Structure and gelling properties*. *Carbohydrate Polymers* 2009. **77**: p. 725–735.
211. Crescenzi, V., M. Hartmann, A.E.J. de Nooy, V. Rori, G. Masci, and G. Skjåk-Bræk, *Epimerization of nonnatural uronans with mannuronan C-5-Epimerases to obtain alginatelike polysaccharides*. *Biomacromolecules*, 2000. **1**(3): p. 360-364.
212. Boyen, C., B. Kloreg, M. Polnefuller, and A. Gibor, *Preparation of alginate lyases from marine mollusks for protoplast isolation in brown-algae* *Phycologia*, 1990. **29**(2): p. 173-181.
213. Preiss, J. and G. Ashwell, *Alginic acid metabolism in bacteria. I. Enzymic formation of unsaturated oligosaccharides and 4-deoxy-L-erythro-5-hexoseulose uronic acid*. *J. Biol. Chem.*, 1962. **237**: p. 309-16.
214. Preiss, J. and G. Ashwell, *Alginic acid metabolism in bacteria. II. Enzymic reduction of 4-deoxy-L-erythro-5-hexoseulose uronic acid to 2-keto-3-deoxy-D-gluconic acid*. *J. Biol. Chem.*, 1962. **237**: p. 317-21.
215. Madgwick, J., A. Haug, and B. Larsen, *Alginate lyase in the brown algae Laminaria digitata (Huds.) Lamour*. *Acta Chemica Scandinavica*, 1973. **27**: p. 711-712.
216. Kennedy, L., K. McDowell, and J.W. Sutherland, *Alginases from Azotobacter species*. *J. Gen. Microbiol.*, 1992. **138**(11): p. 2465-71.
217. Dunne, W.M., Jr. and F.L.A. Buckmire, *Partial purification and characterization of a polymannuronic acid depolymerase produced by a mucoid strain of Pseudomonas aeruginosa isolated from a patient with cystic fibrosis*. *Appl. Environ. Microbiol.*, 1985. **50**(3): p. 562-7.
218. Davidson, I.W., C.J. Lawson, and I.W. Sutherland, *An alginate lyase from Azotobacter vinelandii phage*. *J. Gen. Microbiol.*, 1977. **98**(1): p. 223-9.
219. Wong, T.Y., L.A. Preston, and N.L. Schiller, *Alginate lyase: review of major sources and enzyme characteristics, structure-function analysis, biological roles, and applications*. *Annu. Rev. Microbiol.*, 2000. **54**: p. 289-340.

220. Ertesvåg, H., F. Erlien, G. Skjåk-Bræk, B.H.A. Rehm, and S. Valla, *Biochemical properties and substrate specificities of a recombinantly produced Azotobacter vinelandii alginate lyase*. Journal of bacteriology, 1998. **180**: p. 3779-3784.
221. Ertesvåg, H., M. Gimmestad, T.M.B. Heggeset, O. Aarstad, B.I.G. Svanem, and S. Valla, *Characterization of Three New Azotobacter vinelandii Alginate Lyases, One of Which Is Involved in Cyst Germination*. Journal of Bacteriology, 2009. **191**(15): p. 4845-4853.
222. Boyd, A. and A.M. Chakrabarty, *Role of alginate lyase in cell detachment of Pseudomonas aeruginosa*. Appl. Environ. Microbiol., 1994. **60**(7): p. 2355-9.
223. Hisano, T., M. Nishimura, Y. Yonemoto, S. Abe, T. Yamashita, K. Sakaguchi, . . . K. Murata, *Bacterial alginate lyase highly active on acetylated alginates*. J. Ferment. Bioeng., 1993. **75**(5): p. 332-5.
224. Malissard, M., F. Chavagnat, C. Duez, M.-J. Vacheron, M. Guinand, G. Michel, and J.-M. Ghuysen, *Overproduction and properties of the mannuronate alginate lyase AlxMB*. FEMS Microbiol. Lett., 1995. **126**(2): p. 105-12.
225. Chavagnat, F., A. Heyraud, P. Colin-Morel, M. Guinand, and J. Wallach, *Catalytic properties and specificity of a recombinant, overexpressed D-mannuronate lyase*. Carbohydrate Research, 1998. **308**(3-4): p. 409-415.
226. Tøndervik, A., G. Klinkenberg, O.A. Aarstad, F. Drabløs, H. Ertesvåg, T.E. Ellingsen, . . . H. Sletta, *Isolation of mutant alginate lyases with cleavage specificity for diguluronic acid linkages*. Journal of Biological Chemistry, 2010. **285**(46): p. 35284-35292.
227. Brown, B.J. and J.F. Preston, III, *L-Guluronan-specific alginate lyase from a marine bacterium associated with Sargassum*. Carbohydr. Res., 1991. **211**(1): p. 91-102.
228. Nakada, H.I. and P.C. Sweeny, *Alginic acid degradation by eliminases from abalone hepatopancreas*. J. Biol. Chem., 1967. **242**(5): p. 845-52.
229. Boyd, J. and J.R. Turvey, *Studies of alginate-degrading enzymes. Part I. Isolation of a poly- $\alpha$ -L-guluronate lyase from Klebsiella aerogenes*. Carbohydr. Res., 1977. **57**: p. 163-71.
230. Rehm, B.H.A., *Alginate lyase from Pseudomonas aeruginosa CF1/M1 prefers the hexameric oligomannuronate as substrate*. FEMS Microbiol. Lett., 1998. **165**(1): p. 175-180.
231. Shimokawa, T., S. Yoshida, I. Kusakabe, T. Takeuchi, K. Murata, and H. Kobayashi, *Some properties and action mode of (1 $\rightarrow$ 4)- $\alpha$ -L-guluronan lyase from Enterobacter cloacae M-1*. Carbohydr. Res., 1997. **304**(2): p. 125-132.
232. Østgaard, K. and B. Larsen, *Substrate conversion and product inhibition of mannuronate lyase from Haliotis*. Carbohydrate Research, 1993. **246**: p. 229-241.
233. Yonemoto, Y., H. Tanaka, T. Yamashita, N. Kitabatake, Y. Ishida, A. Kimura, and K. Murata, *Promotion of germination and shoot elongation of some plants by alginate*

- oligomers prepared with bacterial alginate lyase*. J. Ferment. Bioeng., 1993. **75**(1): p. 68-70.
234. Akiyama, H., T. Endo, R. Nakakita, K. Murata, Y. Yonemoto, and K. Okayama, *Effect of depolymerized alginates on the growth of bifidobacteria*. Biosci., Biotechnol., Biochem., 1992. **56**(2): p. 355-6.
235. Kloareg, B. and R.S. Quatrano, *Isolation of protoplasts from zygotes of Fucus distichus (L.) Powell (Phaeophyta)*. Plant Sci. (Limerick, Irel.), 1987. **50**(3): p. 189-94.
236. Butler, D.M., K. Østgaard, C. Boyen, L.V. Evans, A. Jensen, and B. Kloareg, *Isolation Conditions for High Yields of Protoplasts from Laminaria-Saccharina and Laminaria-Digitata (Phaeophyceae)*. Journal of Experimental Botany, 1989. **40**(220): p. 1237-1246.
237. Bayer, A.S., S. Park, M.C. Ramos, C.C. Nast, F. Eftekhari, and N.L. Schiller, *Effects of alginase on the natural history and antibiotic therapy of experimental endocarditis caused by mucoid Pseudomonas aeruginosa*. Infect. Immun., 1992. **60**(10): p. 3979-85.
238. Mrsny, R.J., B.A. Lazazzera, A.L. Daugherty, N.L. Schiller, and T.W. Patapoff, *Addition of a bacterial alginate lyase to purulent CF sputum in vitro can result in the disruption of alginate and modification of sputum viscoelasticity*. Pulm. Pharmacol., 1994. **7**(6): p. 357-66.
239. Malissard, M., C. Duez, M. Guinand, M.J. Vacheron, G. Michel, N. Marty, . . . J.M. Ghuysen, *Sequence of a gene encoding a (poly ManA) alginate lyase active on Pseudomonas aeruginosa alginate*. FEMS Microbiol. Lett., 1993. **110**(1): p. 101-6.
240. Kuhn, R., F. Weide, and W. Schollaert, *Oligosaccharide analysis by capillary electrophoresis, MALDI-TOF mass spectrometry and anion exchange chromatography*. Bioforum, 1999. **22**(1-2): p. 29-32.
241. Price, K.N., A. Tuinman, D.C. Baker, C. Chisena, and R.L. Cysyk, *Isolation and characterization by electrospray-ionization mass spectrometry and high-performance anion-exchange chromatography of oligosaccharides derived from hyaluronic acid by hyaluronate lyase digestion: observation of some heretofore unobserved oligosaccharides that contain an odd number of units*. Carbohydr. Res., 1997. **303**(3): p. 303-311.
242. Koch, K., R. Andersson, and P. Aman, *Quantitative analysis of amylopectin unit chains by means of high-performance anion-exchange chromatography with pulsed amperometric detection*. J. Chromatogr., A, 1998. **800**(2): p. 199-206.
243. Guillotin, S.E., J. Van Kampen, P. Boulenguer, H.A. Schols, and A.G.J. Voragen, *Degree of blockiness of amide groups as indicator for difference in physical behavior of amidated pectins*. Biopolymers, 2006. **82**(1): p. 29-37.
244. Østgaard, K., S.H. Knutsen, N. Dyrset, and I.M. Aasen, *Production and characterization of guluronate lyase from Klebsiella pneumoniae for application in seaweed biotechnology*. Enzyme and microbial technology, 1993. **15**: p. 756-763.

245. Rogstad, H., *Rensing og karakterisering av mannuronan C-5 epimeraser i Hansenula polymorpha og mutante epimeraser produsert rekombinant i Escherichia coli*, in *Institutt for bioteknologi*. 2011.
246. Draget, K.I., B. Strand, M. Hartmann, S. Valla, O. Smidsrød, and G. Skjak-Braek, *Ionic and acid gel formation of epimerised alginates; the effect of AlgE4*. *International Journal of Biological Macromolecules*, 2000. **27**(2): p. 117-122.





# Paper I





# Application of high-performance anion-exchange chromatography with pulsed amperometric detection and statistical analysis to study oligosaccharide distributions – a complementary method to investigate the structure and some properties of alginates

Simon Ballance<sup>a,\*</sup>, Synnøve Holtan<sup>a</sup>, Olav Andreas Aarstad<sup>a</sup>, Pawel Sikorski<sup>b</sup>,  
Gudmund Skjåk-Bræk<sup>a</sup>, Bjørn E. Christensen<sup>a</sup>

<sup>a</sup> Norwegian Biopolymer Laboratory (NOBIPOL), Department of Biotechnology, Norwegian University of Science and Technology (NTNU), Sem Sælands vei 6/8, N-7491 Trondheim, Norway

<sup>b</sup> NOBIPOL, Department of Physics, Norwegian University of Science and Technology (NTNU), N-7491 Trondheim, Norway

Received 3 May 2005; received in revised form 13 July 2005; accepted 14 July 2005

Available online 18 August 2005

## Abstract

Alginates comprised of essentially alternating units of mannuronic (M) acid-guluronic (G) acid (MG-alginate), and G-blocks isolated from a seaweed where subjected to partial acid hydrolysis at pH 3.5. The chain-length distribution of oligosaccharides in the hydrolysate were investigated by statistical analysis after their separation with high-performance anion-exchange chromatography and pulsed amperometric detection (HPAEC–PAD). Simulated depolymerisation of the MG-alginate provided an estimate of the ratio between two acid hydrolysis rate constants ( $p = 8.3 \pm 1$ ) and the average distribution of the MM linkages in the original sample of polysaccharide chains. In conclusion, we found HPAEC–PAD together with statistical analysis was a useful method to investigate the fine structure and some properties of binary polysaccharides.

© 2005 Elsevier B.V. All rights reserved.

**Keywords:** Acid hydrolysis; Carbohydrate; Chain-length distribution; Degree of polymerisation

## 1. Introduction

Statistical analysis of the chain-length distribution of oligosaccharides obtained from the partial depolymerisation of polysaccharides can yield information on the mechanism of their formation, and the structure of the polysaccharide they originated from [1]. Our current understanding of the complex three-dimensional structure of amylopectin in starch granules is supported by analysis of the chain-length distribution of its oligosaccharides generated by enzymatic hydrolysis [2]. A similar approach, but using acid rather

than enzymatic hydrolysis, also confirmed that the glycosidic linkages in cellulose were most probably identical [3], and that alginate contained some block sequences comprised of alternating mannuronic (M) and guluronic (G) acid [4]. The conclusions of this latter study were reached by using a combination of gel-filtration chromatography and a kinetic theory to analyse the products of the partial mild acid hydrolysis of a fragment of alginate. Oligosaccharides were fractionated according to their chain-length and the yield of each fraction used in computer simulation. This enabled the statistical determination of the nearest neighbour frequencies in the starting polymer and ultimately a description of its sequential structure [4]. The success of this approach contributed to the understanding that the depolymerisation of natural alginates

\* Corresponding author. Tel.: +47 73598225; fax: +47 73593337.

E-mail address: [simon.ballance@biotech.ntnu.no](mailto:simon.ballance@biotech.ntnu.no) (S. Ballance).

in weakly acidic media was due largely to intramolecular catalysis of glycosidic cleavage by the carboxyl group in the respective aglycone units [5].

In a more recent study [6], we showed that high-performance anion-exchange chromatography (HPAEC) on an analytical column of IonPac AS4A pellicular resin, combined with pulsed amperometric detection, was a useful and sensitive tool for the quantitative chain-length analysis of a partially degraded de-acetylated bacterial (1 → 4)-β-D-mannuronan, referred to as mannuronan hereon (Fig. 1A). Statistical analysis of this distribution confirmed its structure and revealed that hydrolysis of the glycosidic linkage in the polymer chain occurred at random positions. This implied that the process of acid hydrolysis of mannuronan under mildly acidic conditions could be adequately described by one rate constant. It proved to be a useful complementary method to NMR spectroscopy [6].

The advantage of HPAEC using pellicular resins over other methods, including other forms of chromatography (such as that used by Larsen et al. [4]), is its superior ability to achieve baseline separation of defined populations of oligosaccharides from polydisperse preparations. Oligosaccharides, with a chain-length of up to 30–40 monomer units, have previously been routinely separated without extensive optimisation of the chromatographic conditions [7]. Even trace constituents are captured in the analysis. It is therefore not a surprise that numerous other studies have used this technique to assess the chain-length distribution of various preparations of polysaccharide hydrolysates and then used this information to comment on the properties of the original polymer (see review by Zhang and Lee [7]). The most inten-

sively studied of these originate from starch (see review by Wong and Jane [8]).

Despite the potential, to our knowledge there have been few instances where HPAEC with pulsed amperometric detection (PAD) and statistical analysis have been applied to study the chain-length distribution of oligosaccharides originating from glycuronans, especially binary ones, such as most alginates. A major reason for this is often the difficulty in obtaining appropriate oligosaccharide standards of required purity. These are needed firstly to calibrate the molar response of the PAD as a function of chain-length and secondly, in the case of heteropolysaccharides, they are needed to assist in the assignment of peaks in the resulting chromatograms. However, these obstacles are not insurmountable. In an investigation of the distribution of methyl esters in poly-galacturonic acid, a lack of oligosaccharide standards was circumvented by indirectly calculating the PAD response, via UV detection of oligosaccharides tagged with a chromophore at their reducing-end [9]. Other workers have used post-column enzyme reactors to convert eluting oligosaccharides into equivalent amounts of easily quantifiable monomers [10,11].

In this study, we have utilised and extended the previous application of HPAEC–PAD and statistical analysis that investigated the chain-length distribution of oligosaccharides from mannuronan [6]. We now analyse two different alginates whose basic properties have both been prior investigated by NMR. The first is an engineered linear binary heteropolysaccharide with a predominantly alternating [4]-β-D-ManpA-(1 → 4)-α-L-GulpA-(1 →)<sub>n</sub> structure referred to as MG-alginate hereon (Fig. 1B). This alginate was engi-

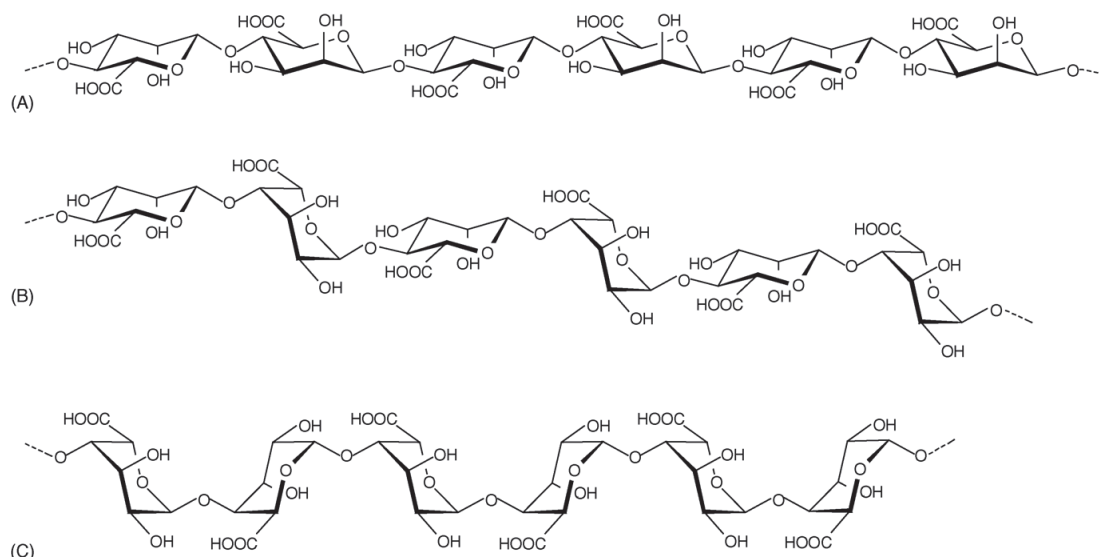


Fig. 1. Conformational representation of segments of mannuronan (A), MG-alginate (B) and G-blocks (C).

neered by in vitro epimerisation of every second M-residue in mannuronan with the recombinant C-5 epimerase AlgE4. Due to mode of action of this enzyme a fully epimerised mannuronan has a molar fraction of guluronic acid ( $F_G$ ) of 0.47. It is thought that blocks of repeating MG units with a number average length  $>20$  [12] are flanked by short  $[4-\beta\text{-D-ManpA-(1}\rightarrow\text{)}]_n$  (M-blocks; Fig. 1A). Therefore, while the majority of the polymer comprises two types of glycosidic linkage,  $\beta\text{-D-ManpA-(1}\rightarrow\text{4)-}\alpha\text{-L-GulpA}$  (MG) and  $\alpha\text{-L-GulpA-(1}\rightarrow\text{4)-}\beta\text{-D-ManpA}$  (GM), it also contains a minor amount of a third linkage of  $\beta\text{-D-ManpA-(1}\rightarrow\text{4)-}\beta\text{-D-ManpA}$  (MM). In solutions with a pH from 2 and 4 these linkages are hydrolysed at very different rates. The GM linkage is hydrolysed the fastest to generate a majority of MG-oligosaccharides with M at their non-reducing end [4,5]. The second glycuronan we study has been extracted from seaweed alginate and comprises predominantly contiguous units of  $[4-\alpha\text{-L-GulpA-(1}\rightarrow\text{)}]_n$  and approximately 4% residual M. We refer hereon to this polymer as G-block seaweed alginate (Fig. 1C).

We now show for both partially acid hydrolysed glycuronans, fractionated by HPAEC and detected by PAD, that it is possible to separate and assign major oligosaccharide fractions. This study demonstrates it is possible to determine the yield of each chain-length fraction via calculation of their respective relative molar response factors ( $\text{MRF}_{\text{rel}}$ ). Statistical analysis of the resulting chain-length distribution can then provide information on its number and weight-average chain-length, the structure of the parent polysaccharide the oligosaccharides originated from, and the process of their formation by acid hydrolysis. In addition, for the MG-alginate, further statistical analysis of chain-length distribution by simulated depolymerisation yields an estimate of the ratio between two acid hydrolysis rate constants. Using the same method we also attempt to provide additional information on the average distribution of the MM linkages in the original polysaccharide chains.

## 2. Materials and methods

### 2.1. Preparation of MG-alginate and isolation of G-block seaweed alginate

MG-alginate was prepared by in vitro epimerisation of mannuronan with AlgE4. It had a number average chain-length ( $\text{DP}_n$ ) of 2400. The synthesis, de-acetylation and epimerisation of the mannuronan to generate the MG-alginate is described elsewhere [13–15]. It had a  $F_G$  of 0.47 and  $F_{GG}$  of 0, as determined by  $^1\text{H}$  and  $^{13}\text{C}$  NMR [15] indicating there were still minor contiguous sequences of M monomers that had not hosted AlgE4. G-blocks were isolated from the stipe alginate of the seaweed *Laminaria hyperborea*. Purification was carried out as described earlier [16,17] to yield a polydisperse preparation with a  $F_G$  of 0.96 ( $F_M$  = remainder) and a  $\text{DP}_n$  of 42 as estimated by  $^1\text{H}$  NMR [6].

### 2.2. Partial acid hydrolysis and preparation of purified oligosaccharides

Five hundred milligrams of MG-alginate or 100 mg of G-blocks was dissolved in water to a concentration of 3.5 and 5 mg/ml, respectively. The pH was then adjusted to 5.6 with 0.1 M HCl, prior to de-oxygenation with nitrogen, followed by incubation at 95 °C for 3.5 h to undergo pre-hydrolysis. The sample was then cooled, pH adjusted to 3.6 with 0.1 M HCl, degassed and hydrolysed as before for a further 3.8 or 12 h for MG-alginate or G-blocks, respectively. After this period the sample was again cooled, neutralised by addition of 0.1 M NaOH, and freeze-dried. These polysaccharide hydrolysates comprised a distribution of oligosaccharides. Hydrolysates of mannuronan were produced in a similar way to that outlined by Campa et al. [6]. These were used as a positive control and for comparison. All hydrolysates were stored in the freezer prior to either direct use, or fractionated according to their chain-length on three columns of preparative grade Superdex 30 (2.6 cm  $\times$  60 cm, serially connected) eluted with 0.1 M  $\text{NH}_4\text{Ac}$  (pH 6.9) to yield oligosaccharide standards (mostly in their  $\text{H}^+$ -form) in a similar manner to that described before [6]. Analysis of these oligosaccharides by  $^1\text{H}$  and  $^{13}\text{C}$  NMR spectroscopy together with electrospray ionisation mass spectrometry (ESI-MS) confirmed their identity and average chain-length to range from 2 to 15 [15].

### 2.3. HPAEC–PAD

A stock solution of 0.01 mg/ml  $\alpha\text{-D-GalpA-(1}\rightarrow\text{4)-D-GalpA}$  was prepared in 1.5 mM NaOH for use as an internal standard. Oligosaccharide standards (0.4–2 mg) were dissolved in the internal standard stock solution to a final concentration of 0.05 mg/ml. Polysaccharide hydrolysates (ca. 1 mg) were dissolved in the internal standard stock solution to a concentration of 1 mg/ml. The chromatography system and conditions used are identical to those described earlier [6]. In this study, however, buffer A comprised 0.1 M NaOH, buffer B contained 1 M NaAc in 0.1 M NaOH and linear gradients of acetate were produced by increasing the concentration of buffer B from 0 to 70% over 80 min. The detection system and pulsed amperometric waveform was identical to that described earlier [6].

Each batch of oligosaccharide standards and polysaccharide hydrolysates, derived from the three different polysaccharide preparations, was analysed in 1 day over a consecutive period of 3 days. Analysis was repeated in three consecutive replicate series. Samples were prepared independently at the start of each day. The buffers were refilled prior to the start of each analysis series from a freshly pre-prepared stock. The gold electrode was not cleaned at any time during the analyses but the combination pH/Ag/AgCl electrode was replaced once. All analysis was completed within a period of 2 months. Integration of peaks in the resulting chromatograms was made with PeakNet software following man-

ual adjustment of the baseline and peak threshold. Integrated areas of multiple peaks observed for each chain-length were summed.

#### 2.4. Determination of relative molar response factors

In order to take into account that each oligosaccharide standard was not pure but contained small amounts of  $\pm$  one monomer residue in chain-length, relative molar response factors ( $MRF_{rel}$ ) were determined for each standard in the chain-length range 2–15 by using linear equations [6]. First a unique relative response factor  $RF(f_x)$  was assigned to each oligosaccharide chain-length by  $f_x = (A_x/A_{i.s.})(m_{i.s.}/m_x)f_{x_{i.s.}}$ , where  $m$  is the sum of moles for each chain-length in the sample;  $A$  is the integrated area of peak(s) from HPAEC–PAD assigned to each chain-length and  $i.s.$  denotes the internal standard. It then goes that the relative molar response factor ( $MRF_{rel}$ ) =  $(A_x/A_{i.s.})(m_{i.s.}/m_x)$ . After determining  $MRF_{rel}$  for each sample in each batch, the mean  $MRF_{rel}$  ( $n=3$ ) for each series was plotted against chain-length.  $MRF_{rel}$  dependence on chain-length was then described by fitting the data firstly to a standard first order logarithmic function, and where applicable, to an equation that gave a good description of each  $MRF_{rel}$  data set. This relationship was used to calculate  $MRF_{rel}$  for oligosaccharides of longer chain-length (>15), as well as for the monomer.

#### 2.5. Statistical analysis of chain-length distribution

Calculated and extrapolated  $MRF_{rel}$  were used to calculate the number and weight chain-length distributions of oligosaccharides in the polysaccharide hydrolysates ( $n=3$ ) together with their corresponding averages as described previously [6]. For comparison, the number-average chain-length ( $DP_n$ ) was also measured with  $^1H$  NMR as described previously [6,15]. Kuhn equations were plotted using the degree of chain scission ( $\alpha$ ) calculated directly from the experimental data points [4,6]. In the case of the MG-alginate the  $\alpha$ -value was weighed to reflect the relative abundance of oligosaccharides in two populations within the chain-length distribution. As an additional test (for G-block oligosaccharides only), the Kuhn equation was also fitted to the experimental data points using a least squares approach.

#### 2.6. Simulation of the depolymerisation of MG-alginates

Depolymerisation of MG-alginates were simulated using custom developed software and a statistical approach (Monte Carlo simulation) similar to what has been described for the enzymatic hydrolysis of chitosans [18]. Acid hydrolysis was simulated as a chemical reaction with an activation barrier dependant on whether the linkage was MG or GM. First an ensemble of  $\sim 10,000$  MG-alginate chains with a  $DP_n$  of 2400 was generated using a most probable distri-

bution with a polydispersity index of 2 [19]. In simulations which take into account the presence of MM linkages in the polymer chain, short M-blocks with a variable length (see below), but complying to a total abundance of 6% of the mass as dictated from a pre-determined  $F_G$  of 0.47, were inserted at random positions. In the simulation process a polymer chain was first selected at random (step A). This was followed by random selection of one linkage within this chain (step B). The selected linkage was hydrolysed with a probability dependent on the sequence of adjacent units (step C). These probabilities were  $p_{GM}$ ,  $p_{MG}$  and  $p_{MM}$  for GM, MG and MM linkages, respectively. The steps A to C were repeated until the required final  $DP_n$  ( $\alpha$ ) was achieved. In the final step of the simulation, the distribution of predicted oligosaccharide fractions was calculated and compared with that obtained from the experimental hydrolysis. The agreement was quantified by a means of an error function ( $S_{err}$ ) defined in Eq. (1), where  $W_i^{obs}$  and  $W_i^{cal}$  are observed and calculated weight fractions of  $i$ th oligosaccharide. Only the chain-length fractions were used for which response factors had been experimentally determined ( $i_{min}=2$ ;  $i_{max}=15$ ).

$$S_{err} = \frac{\sum_{i=i_{min}}^{i_{max}} (W_i^{obs} - W_i^{cal})^2}{\sum_{i=i_{min}}^{i_{max}} (W_i^{obs})^2} \quad (1)$$

Calculations were performed as a function of  $DP_n$  and no rate constant (time dependence) was used. As a consequence, to describe the hydrolysis of MG-alginate under given experimental conditions, it is sufficient to determine the characteristic ratio:  $p = p_{GM}/p_{MG}$  and then the hydrolysis reaction can be described using only one variable. The value of the  $p$ -parameter is determined by minimising the value of  $S_{err}$  [18]. For  $p=1$ , the model predicts a standard Kuhn distribution of the reaction products, as expected for random hydrolysis of a homopolymer with uniform linkages. It is important to note that the value of  $p$  depends on the experimental conditions, and here it is determined only for the hydrolysis reaction described above. For simulations that included extra M-units, the experimentally determined probability of hydrolysing MM linkages ( $p_{MM}$ ) was used. Since it has recently been determined that MM linkages are hydrolysed under the conditions used in this study approximately four times slower than GM linkages [15] we set  $p_{MM} = 0.25p_{GM}$ . In simulations II–IX (Table 1) the polymer chain was constructed by inserting M-blocks with a given length and at random positions to achieve an  $F_G = 0.47$ . The number of M-blocks, and therefore an average distance between them, depends on the block length (Table 1). Each average M- and MG-block length, expressed as the number of monomers in the respective block, were determined in the simulation process.  $F_{MM}$ ,  $F_{MMM}$ ,  $F_{MMMM}$  values were calculated using the average M-block length and assuming a ‘most probable distribution’ of block sizes [20].

Table 1

The difference ( $S_{\text{err}}$ ) between the experimentally determined and simulated (I–IX) weight distribution of chain-lengths in the partial hydrolysis products of an MG-alginate as a function of the average M-block length

Simulation	$F_G$	$F_M$	$F_{MM}$	$F_{MMM}$	$F_{MMMM}$	$F_{M>4}$	<sup>a</sup> Average MG-block length	<sup>a</sup> Average MG-block length	$p$	$S_{\text{err}}$
I	0.5	0.50	0.000	0.000	0.000	0.000	DP <sub>n</sub>	0 <sup>b</sup>	5.7	2.65
II	0.47	0.53	0.060	0.000	0.000	0.000	16	2 <sup>c</sup>	24.5	9.43
III	0.47	0.53	0.005	0.004	0.004	0.047	100	12.8	6.5	1.52
IV	0.47	0.53	0.010	0.008	0.007	0.036	98	7.3	6.9	1.37
V	0.47	0.53	0.017	0.012	0.009	0.021	56	4.5	7.7	1.14
VI	0.47	0.53	0.020	0.013	0.009	0.018	48	4.0	7.4	1.04
<b>VII</b>	<b>0.47</b>	<b>0.53</b>	<b>0.025</b>	<b>0.015</b>	<b>0.008</b>	<b>0.012</b>	<b>38</b>	<b>3.4</b>	<b>8.3</b>	<b>1.01</b>
VIII	0.47	0.53	0.031	0.015	0.007	0.007	32	3.0	8.8	1.12
IX	0.47	0.53	0.036	0.014	0.006	0.004	26	2.7	10.0	1.53

In all simulations, except simulation I which represents a hypothetically pure MG-alginate with an  $F_G$  of 0.5, the molar fraction of guluronic acid ( $F_G$ ) was set at the experimentally determined value of 0.47.  $S_{\text{err}}$  is an error function as defined in Section 2, and  $p$  represents the calculated ratio between the two acid hydrolysis constants  $p_{GM}$  and  $p_{MG}$ .  $F_{MM}$ ,  $F_{MMM}$ ,  $F_{MMMM}$  and  $F_{M>4}$ , respectively, represent the molar fraction of pure mannuronic acid dimers, trimers, tetramers, and oligomers larger than tetramers in the partial hydrolysate of each simulation. Simulation VII (bold type) highlights the simulation parameters that provide the best agreement between observed and predicted chain-length distributions.

<sup>a</sup> Expressed as monomer units.

<sup>b</sup> Result for the hypothetically pure MG-alginate which does not contain M–M linkages.

<sup>c</sup> Polymer in which extra M-units are distributed in mono-disperse M-blocks containing two M-units.

### 3. Results and discussion

#### 3.1. Retention time on the anion-exchange resin as a function of chain-length and sequence

Analysis of oligosaccharide standards and polysaccharide hydrolysates by HPAEC–PAD showed it was possible to obtain a high-resolution separation of oligosaccharides according to chain-length (Fig. 2). This is because retention time increases as the number of negatively charged functional groups concurrently increase [21]. We managed to separate oligosaccharides by their chain-length until they exceeded between 30 and 35 monomer units (Fig. 2A–C).

From examination of Fig. 2D, it is seen that chains of equivalent length but different monomer sequence also have different retention times on the anion-exchange resin. Oligosaccharides of mannuronan are more strongly retained than those of the same chain-length derived from G-blocks. But epimerisation by AlgE4 of every second M-residue in mannuronan results in only a minor decrease in retention time of ensuing oligosaccharides (Fig. 2A). On closer inspection of the MG-oligosaccharides with odd-numbered chain-lengths (Figs. 2D, 3B and D) it is those with the highest number of M which are retained the longest. The physical and chemical factors, other than just monomer sequence, that may explain these differences in retention are complex and not fully understood [7,21]. It is therefore beyond the scope of this article to invoke a detailed discussion on this subject. However, on the basis of monomer sequence, the retention trends described here can assist in the confident assignment of some of the observed chromatographic peaks.

From inspection of the chromatogram of the MG-alginate hydrolysate (Fig. 2B), it is quite evident that oligosaccharides with even-numbered chain-lengths were more abundant than their odd-numbered counterparts. This is because to generate

an even-numbered chain-length two identical linkages must be cleaved. Since the GM linkage is hydrolysed the fastest, the majority of these oligosaccharides would favourably have an M at their non-reducing end and G at their reducing end [5]. Indeed, from examination of the chromatogram obtained after HPAEC–PAD of the <sup>1</sup>H NMR assigned dimer (Fig. 3A), it is safe to assign the major peak to MG (non-reducing residue on the left). The slightly smaller peak, which elutes about a minute later, must therefore arise from GM. This trend is repeated for other larger even-numbered chains (Fig. 3C). For MG-oligosaccharides of equivalent sequence it is those with an M at their reducing end that are retained on the AS4A resin the longest. From the parallel analysis of pure M-oligosaccharides of the same monomer length (not shown), a third minor peak in the chromatogram of the <sup>1</sup>H NMR assigned dimer fraction is firmly assigned as MM (Fig. 3A).

For those oligosaccharides with an odd-number of monomers in their chain (Fig. 3B and D), roughly half should have M at their non-reducing end. This is because to generate an odd numbered oligosaccharide both a GM and an MG linkage must be broken. It is therefore not a surprise that two major peaks of similar size are observed in the chromatogram of the odd-numbered oligosaccharides (Fig. 3B and D). Given what we now know about retention time as a function of sequence we can easily assign these two peaks. Oligosaccharides responsible for the second of the two major peaks must have terminal residues of M and overall comprise one less G residue than M. The opposite is true for the oligosaccharides responsible for the other major peak. These oligosaccharides elute earlier because they have a G residue at each end and overall comprise one less M (Fig. 3B and D).

Assignment of oligosaccharides from G-blocks (Fig. 3 E–H) is even easier as there is only one major peak observed for each standard/chain-length. It is firmly assigned as a pure G-oligosaccharide. Each oligosaccharide standard, both MG-

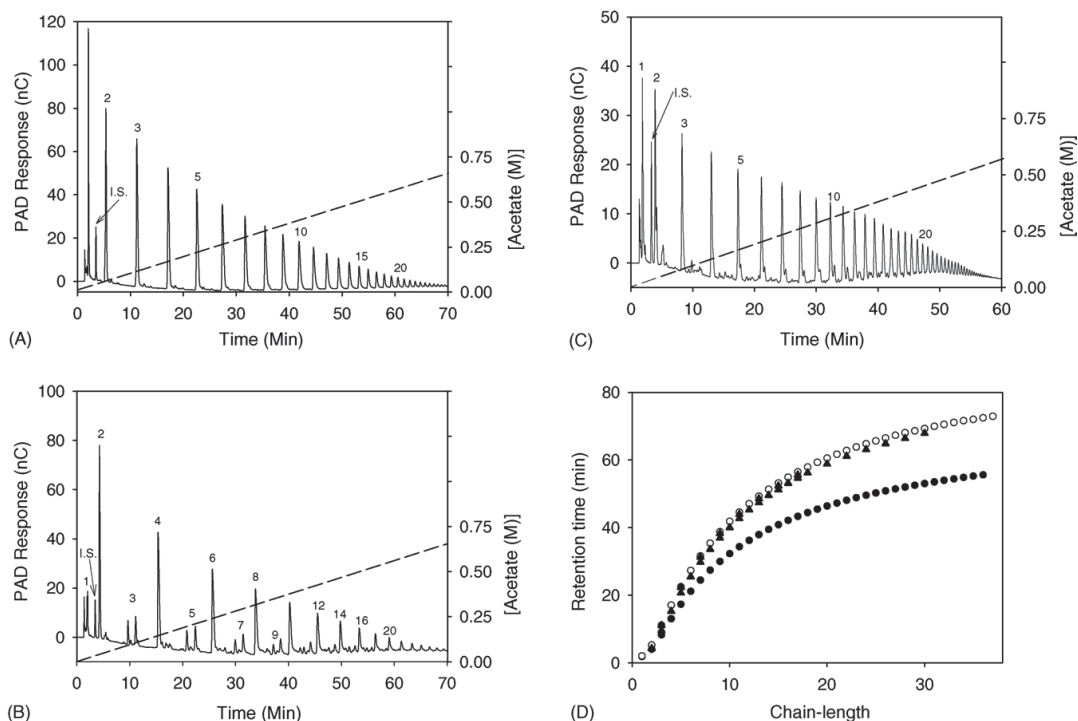


Fig. 2. Typical examples of HPAEC–PAD chromatograms of the oligosaccharide hydrolysis products generated by the partial acid hydrolysis of mannuronan (A), MG-alginate (B) and seaweed alginate G-blocks (C). The abbreviation i.s. denotes the internal standard and the dashed line shows the acetate gradient formed in 0.1 M NaOH at a flow rate of  $1 \text{ ml min}^{-1}$  which was used to elute the IonPac AS4A resin column. Peak labels refer to assigned chain-length. Panel (D) shows the mean ( $n=3$ ) oligosaccharide retention time as a function of chain-length. Open circles (○), filled circles (●) and filled triangles (▲) represent oligosaccharides originating from mannuronan, seaweed alginate G-blocks and MG-alginate, respectively.

and G-, contains a small amount of oligosaccharide  $\pm$  one monomer residue (Fig. 3) together with a host of smaller peaks whose identity is uncertain. The former is a result of the gel-filtration step [6] but the latter may have several origins. Firstly, all the polysaccharides examined were not compositionally pure (see Section 2). It is likely that some of the extra peaks arise from minor oligosaccharide fractions of irregular sequence. Proton NMR assignments of the MG-oligosaccharide standards from gel-filtration confirmed that short chain-length fractions contained some MM sequences. These are more abundant in oligosaccharides with an odd number of residues in their chain [15]. This phenomenon can be explained by the different degradation rates of glycosidic linkages together with the length of M-blocks in the polymer. An interspersed MM dimer sequence within the MG-chain would give irregular odd oligosaccharides with the more rapid degradation of GM than MM and MG linkages. Perhaps this observation explains why, in HPAEC–PAD analysis of these oligosaccharides, more small peaks flank the major peaks in odd-numbered chains (Fig. 3B and D) than in even-numbered ones (Fig. 3A and C). In addition it is also likely that some of these additional peaks in the

oligosaccharide standards (mostly  $\text{H}^+$ -form) arise from their acid-catalysed modification during their formation and storage. After paper chromatography of acid-generated alginate oligosaccharides it was suggested that modification occurred at the reducing end [4]. Whether alkaline  $\beta$ -elimination during HPAEC–PAD analysis also makes a contribution cannot be definitively ruled out, but it seems unlikely (see also [6]). This process should generate monomers but these were not observed to any extent in the chromatograms of purified standards (Fig. 3).

### 3.2. Relative molar response factors

Fig. 4A shows the mean ( $n=3$ )  $\text{MRF}_{\text{rel}}$  for each chain-length obtained from the three glycuronans. Overall they are quite well described by a standard first order logarithmic function  $y = y_0 + a \ln x$ , where  $\text{MRF}_{\text{rel}}$  versus chain-length plotted on a logarithmic axis has a linear relationship ( $R^2 = < 0.96$ ). We observed over the 2-month study period that the PAD response per oligosaccharide batch, even when corrected against the internal standard, decreased with each



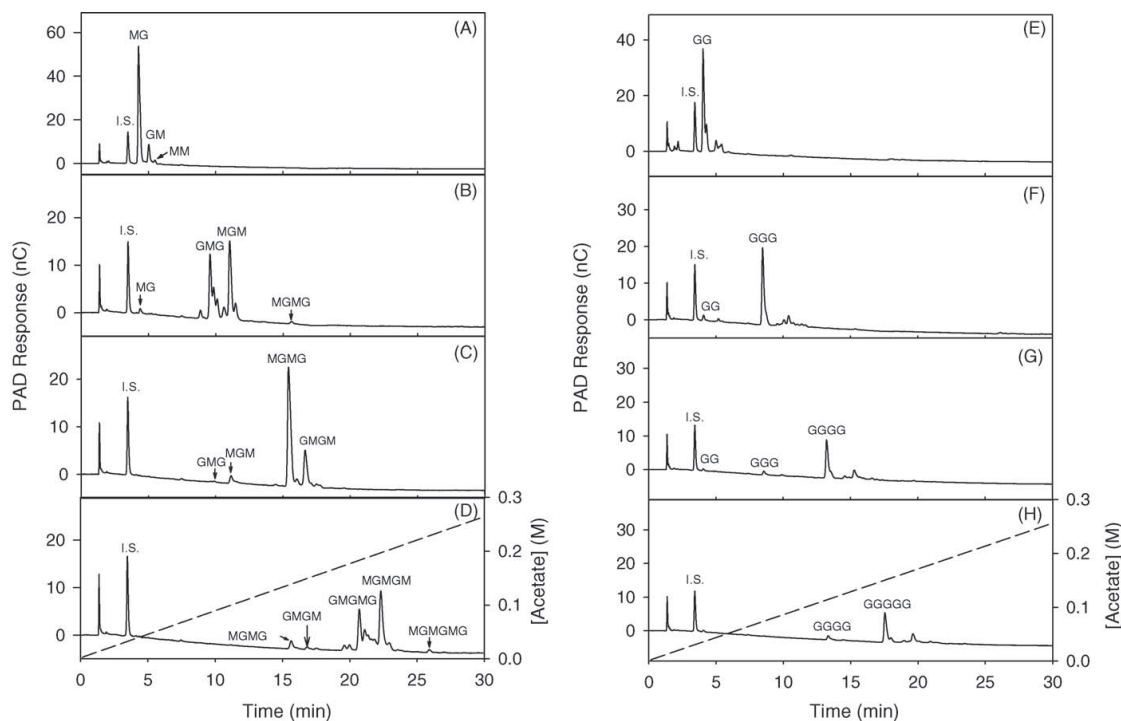


Fig. 3. Typical examples of HPAEC-PAD chromatograms of oligosaccharide standards DP 2–5 originating from MG alginate (A–D) and seaweed alginate G-blocks (E–H). The abbreviation i.s. denotes the internal standard and the dashed line shows the acetate gradient formed in 0.1 M NaOH at a flow rate of  $1 \text{ ml min}^{-1}$  which was used to elute the IonPac AS4A resin column. Other peak labels refer to the assigned identity of oligosaccharides responsible for the peak.

successive replicate series analysed. A gradual decrease in carbohydrate peak areas over time due to working electrode wear/recession is typical when, as in this study, positive electrode cleaning potentials (+0.6 V, 120 ms) are used [22]. However, the overall  $\text{MRF}_{\text{rel}}$  trends were consistent and highly reproducible with G-oligosaccharides having slightly lower response factors than their M and MG counterparts. The gradient ( $a$ ), obtained from a fit of a first order logarithmic function to the calculated  $\text{MRF}_{\text{rel}}$  values for each oligosaccharide batch in each consecutive analysis series shows each of the three successively analysed hydrolysis samples fitted well to a straight line ( $R^2 \leq 0.98$ ; Fig. 4A inset). In addition each line had a similar gradient (Fig. 4A; inset). This serves to validate the mean values ( $n=3$ ) and trends presented in Fig. 4A and B as representative. Our study agrees with the view that as long as a representative internal standard is used when calculating  $\text{MRF}_{\text{rel}}$  then it does not matter whether the gold electrode is partially recessed, fouled, or even sanded and re-polished at an interval during analysis [23]. Why G-oligosaccharides have an overall lower  $\text{MRF}_{\text{rel}}$  value than corresponding M-oligosaccharides is at present unknown. As with the factors that govern the subtle differences in retention times on the anion-exchange resin more than one mechanism

may be responsible. These factors include rates of diffusion, physical shape and chemical composition [24].

With the exception of mannan, which is shown for comparison, it seems the  $\text{MRF}_{\text{rel}}$  for the monomer fraction is significantly underestimated when extrapolated by the first order linear function (Fig. 4A). This has serious adverse consequences when calculating chain-length distributions and averages particularly were  $\text{DP}_n$  is  $<10$ . G-block oligosaccharides, and the extrapolated monomer fractions, were better, but not perfectly described, by a second order logarithmic fit where  $\text{MRF}_{\text{rel}} = y_0 + a(\ln x) + b(\ln x)^2$ ;  $R^2 = 0.96$  (Fig. 4B).  $\text{MRF}_{\text{rel}}$  for MG-oligosaccharides fitted better to a sigmoidal distribution where  $\text{MRF}_{\text{rel}} = a/1 + e^{-(x-x_0)}/b$ ;  $R^2 = 0.97$  (Fig. 4B). Extrapolation of response factors for oligosaccharides with chain-lengths  $>20$  are also prone to some uncertainty [6] and should be taken into consideration when assessing samples with an average  $\text{DP}_n >10$ .

Comparison of calculated values of  $\text{MRF}_{\text{rel}}$  for corresponding M-oligosaccharides (Fig. 4) to those from a previous study [6] show they are about twice the size. The reason for this discrepancy is that the molecular weight of a GalA monomer was erroneously used in the earlier calculations [6] instead of the correct molecular weight of the internal

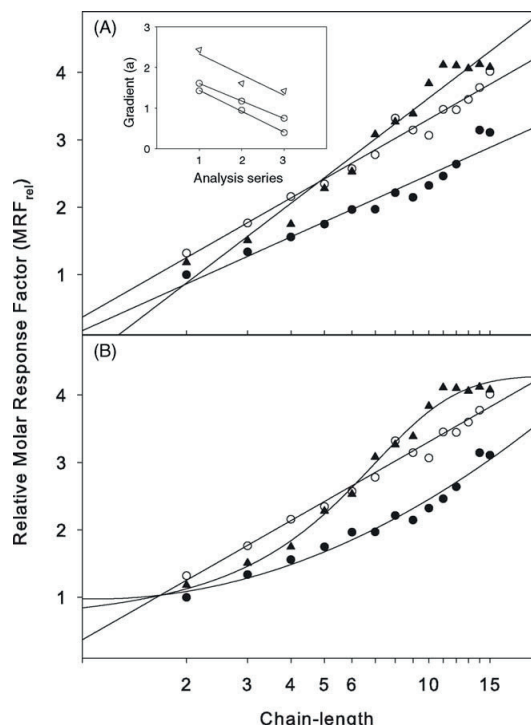


Fig. 4. Mean ( $n=3$ ) relative molar response factors ( $MRF_{rel}$ ) determined for oligosaccharide standards (DP 2–15) originating from mannuronan (open circles,  $\circ$ ), seaweed alginate G-blocks (filled circles,  $\bullet$ ) and MG-alginate (filled triangles,  $\blacktriangle$ ). (A) A first order logarithmic function is fitted to the data. (A) Inset (top left) is a plot of the gradient (a), calculated from the fit of the first order logarithmic function for each oligosaccharide batch in each consecutive analysis series. (B) A second order logarithmic function and a sigmoidal function are fitted to the seaweed alginate G-blocks and MG-alginate  $MRF_{rel}$ , respectively.

GalA dimer standard. However, since the particular molecular weight of the internal standard is only a scaling factor, and scale is only relative, it has no influence on the use of the  $MRF_{rel}$  values in calculating chain-length distributions and associated averages.

### 3.3. Chain-length distributions of partially hydrolysed MG-alginate and G-blocks

The number and weight chain-length distribution is shown in Fig. 5. Two distinct populations of MG-oligosaccharides are evident in their chain-length distribution (Fig. 5A and B). Each population exclusively comprises odd and even-numbered chain-lengths and each is well described by a Kuhn equation (lines in Fig. 5A and B) calculated using the same  $\alpha$ -value (see Section 2). The Kuhn equation also explains the observed number and weight distribution of chains for oligosaccharides generated by the partial acid hydrolysis of G-blocks (Fig. 5C and D). It is therefore assumed that these G-

Table 2

Estimated  $DP_n$  after partial acid hydrolysis of MG-alginate and G-blocks as determined by  $^1H$  NMR and HPAEC–PAD

	HPAEC–PAD		$^1H$ NMR	
	$DP_n$	$DP_w$	$DP_n$	$DP_w$
G-blocks	7.5	13.0	8.1	–
MG-alginate	5.8	10.1	6.5	–

oligosaccharides were generated via the random hydrolysis of glycosidic linkages. For the MG-alginates depolymerisation is more complex. It involves a combination of two hydrolysis processes which are simultaneously operating at different rates. However, glycosidic cleavage in each process is random and it is this that generates the chain-length populations described by the Kuhn equation. A comparison between the  $DP_n$  of the polysaccharide hydrolysates calculated via HPAEC–PAD and  $^1H$  NMR spectroscopy shows reasonable agreement (Table 2).

### 3.4. Simulated depolymerisation of MG-alginate

Fig. 6 shows a comparison between experimentally determined weight fractions of oligosaccharide fractions in the hydrolysate from an MG-alginate with an  $F_G$  of 0.47 and final  $DP_n=5.8$  to that calculated by simulated depolymerisation (simulation I, Table 1) of a hypothetically pure MG-alginate ( $F_G=0.5$ , black bars) to the same final  $DP_n$ . The ratio between GM and MG hydrolysis rates,  $p$  was determined by minimising the difference between observed and predicted weight fractions of oligosaccharides expressed by  $S_{err}$  (Eq. (1)). The best agreement is obtained for  $p=5.7$ , which means that the M–G linkages are hydrolysed 5.7 times slower than GM. However, this calculation does not take into account that the MG-alginate used in the experiment is not pure, and it contains 6% extra M-units distributed in short blocks. To more accurately simulate our polymer, and assess the influence of extra M-units within the polymer chain, a number of additional calculations were carried out. To begin with we simulated a polymer in which all the extra 6% M-linkages were randomly distributed as mono-disperse dimers (simulation II, Table 2). We then repeated the simulations for polymers in which M-blocks have length distribution calculated using average M-block length and assuming a ‘most probable distribution’ of block sizes [20].

There was no satisfactory agreement between simulated and experimentally observed weight fractions of each oligosaccharide fraction when all the M-blocks are mono-disperse dimers (simulation II,  $S_{err}=9.43$ ). This is because, in a polymer with an  $F_G=0.47$ , the average minimum MG-block length is 16 monomer units. More importantly such a polymer would contain a large number of M-blocks at an average interval of one for every eight repeating MG-units. This leads to an almost equal number of odd and even-numbered oligosaccharides being released from the hydrolysis of only one linkage type. Hydrolysis of only the GM linkages can

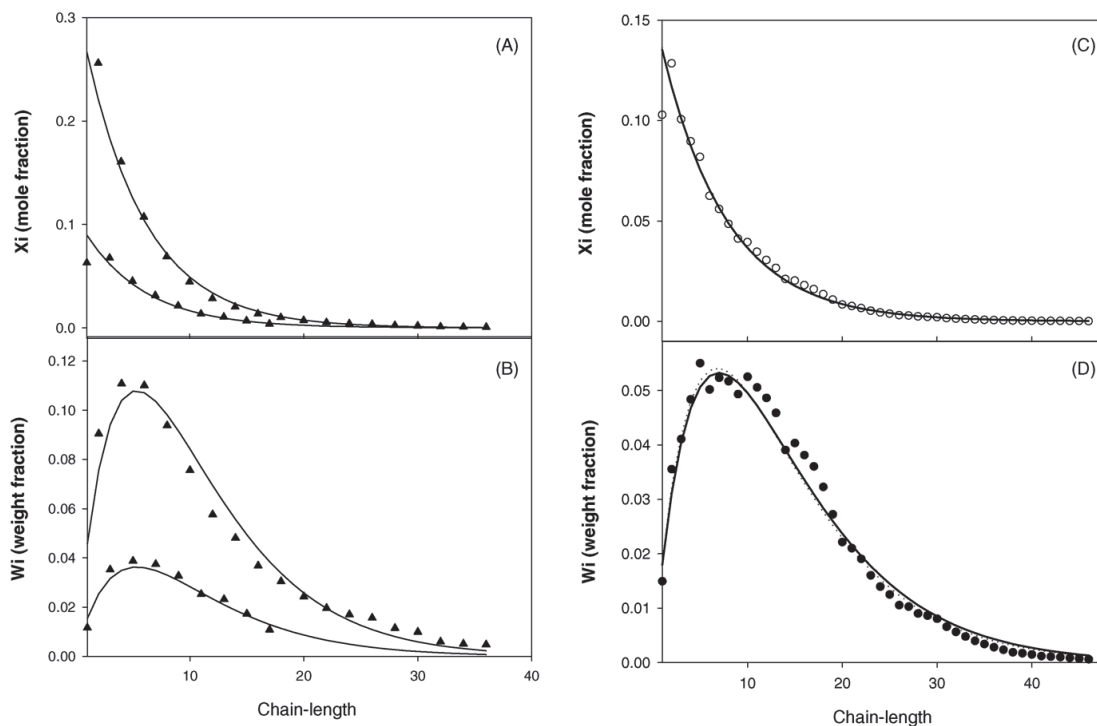


Fig. 5. Number (A and C) and weight (B and D) distribution of oligosaccharides chain-lengths generated by the partial acid hydrolysis of seaweed alginate G-block (filled circles, ●) and MG-alginate (filled triangles, ▲). Kuhn equations for  $DP_n = 7.7$  and  $5.8$  calculated from the raw data for G-block oligosaccharides and MG-alginate oligosaccharides are, respectively, fitted as black lines. In the latter case the fit has been weight adjusted and applied to two populations of even and odd numbered chain-lengths within the chain-length distribution. Small dashes represent the Kuhn equation that best describes the data in terms of a least squares fit.

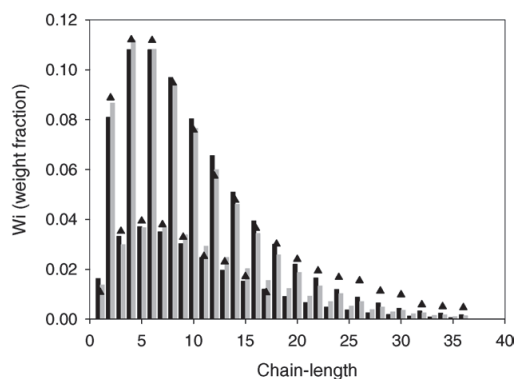


Fig. 6. Weight fraction of MG-oligosaccharide chain-lengths obtained by hydrolysing the starting polymer to an average  $DP_n = 5.8$ . Experimental values (filled triangles, ▲) were obtained using the described HPAEC–PAD method. Filled bars represent the simulated MG-oligosaccharide chain-length fractions assuming the acid depolymerisation of a hypothetically pure MG-alginate ( $F_G = 0.5$ ) and gives a ratio between GM and MG hydrolysis rate as  $p = 5.7$ . Grey bars represent the same simulation but for an MG-alginate ( $F_G = 0.47$ ) with an average M-block length of 3.4 monomer units. The ratio between GM and MG hydrolysis rates was  $p = 8.3$ .

produce both odd and even-numbered chain-lengths. For example: MGMGMMG for a heptamer, and MGMGGMG for a hexamer. For this simulation (Table 1)  $p = 24.5$ . In a parallel study using the same starting MG-alginate ( $F_G = 0.47$ ), similar conditions of partial hydrolysis, and  $^1\text{H}$  NMR to directly determine  $p$ , a value of 10.7 was obtained [15].

A better agreement between the experimental and simulated data is obtained when a hypothetically pure MG-alginate has a poly-disperse distribution of M-blocks inserted into its polymer chain, shown as grey bars in Fig. 6. The  $S_{\text{err}}$  is at a minimum, and 60% lower than what was obtained for a hypothetically pure MG-alginate, when the average M-block length is 3.4 monomer units (simulation VII, Table 1, bold type). For this average length, M-blocks are distributed as 41% dimer, 25% trimer, 13% tetramer and the remainder as pentamers or larger (corresponding  $F_{\text{MM}}$ ,  $F_{\text{MMM}}$ ,  $F_{\text{MMMM}}$  values are shown in Table 1). Furthermore, the average MG-block length of this polymer is around 38 monomer units (Table 1). This value is in good agreement with that previously determined for the same polymer by NMR (see Table 1 in [12]). The calculated ratio between GM and MG hydrolysis rates under the specific condition of our hydrolysis is  $p = 8.3 \pm 1$  (estimated error). This is also in good

agreement with the value measured independently using  $^1\text{H}$  NMR [15].

#### 4. Conclusion

HPAEC–PAD is a useful tool to determine the distribution of oligosaccharides derived from linear binary polysaccharides, such as alginate. Together with other complementary methods, such as NMR, chain-length analysis can reveal physical and structural details of the parent polysaccharides. Confident peak assignments of some major oligosaccharide fractions were made by exploiting mild partial acid hydrolysis as a method of depolymerisation. However, other than on the basis of sequence composition we did not attempt to explain the various chemical and physical factors that governed oligosaccharide retention on the anion-exchange resin.

Because of the presence of several unidentified smaller peaks in the chromatograms integrated peak areas for each chain-length had to be combined in order to calculate the relative molar response factor with some accuracy. A similar approach to circumventing the influence of acid-catalysed modification of alginate oligosaccharides was successfully applied before [4]. Using  $\text{MRF}_{\text{rel}}$  and extrapolation for the monomer and chain-length fraction  $<15$  we calculated chain-length distributions and associated averages which correlated well with complementary measurements made with  $^1\text{H}$  NMR. The chain-length distribution of the MG-alginate hydrolysate contained two populations, one comprising even-numbered and one comprising odd-numbered chain-lengths, both of which were explained by a Kuhn equation. On the other hand, one Kuhn equation explained the entire chain-length distribution observed for the G-blocks. The gross structure of the starting polymers was therefore confirmed. Further statistical simulation of the depolymerisation of alginates compared to the experimentally determined distributions shed further light on the fine structure of the MG-alginate. For the hydrolysis conditions applied it allowed us to give an estimate of  $p=8.3 \pm 1$  for the ratio between the hydrolysis constants of the GM and MG linkage. We tentatively propose this polysaccharide preparation to have an average MG-block length of 19 dimer units separated by regions of MM linkages with an average M-block length of 3.4 monomer units.

One disadvantage of using PAD for detection is the initial time-consuming procedure of having to calibrate the PAD response for the different oligosaccharide sequences and chain-lengths. But once this is done, a calibration standard can be made and stored for future use. If this approach is developed further then it may be possible to investigate the average fine structure of many other types of binary polysaccharide as well as alginate. HPAEC–PAD analysis could especially offer an advantage over current NMR spectroscopy methods, where the characteristic NMR resonance of particular diad and triplet sequences

[25–27] are small and therefore difficult to accurately integrate.

#### Acknowledgements

We thank FMC Biopolymers and Norwegian Research Council under the Centre for Biopolymer Engineering at NOBIPOL, NTNU (Grant No. 145945/130) for financial support. We also thank Kurt Ingar Draget and Anne Sissel Duun for producing the G-block seaweed alginate, Espen Granum for proof reading the manuscript, and various members of NOBIPOL for useful discussions and comments.

#### References

- [1] H.O. Bouveng, B. Lindberg, *Adv. Carbohydr. Chem.* 15 (1960) 53.
- [2] S. Hizukuri, *Carbohydr. Res.* 147 (1986) 342.
- [3] K. Freudenberg, G. Blomquist, *Ber.* B68 (1935) 2070.
- [4] B. Larsen, O. Smidsrød, A. Haug, T. Painter, *Acta Chem. Scand.* 23 (1969) 2375.
- [5] O. Smidsrød, B. Larsen, T. Painter, A. Haug, *Acta Chem. Scand.* 23 (1969) 1573.
- [6] C. Campa, A. Oust, G. Skjåk-Bræk, B.S. Paulsen, S. Paoletti, B.E. Christensen, S. Ballance, *J. Chromatogr. A* 1026 (2004) 271.
- [7] Y. Zhang, Y.C. Lee, in: Z. El Rassi (Ed.), *Carbohydrate Analysis by Modern Chromatography and Electrophoresis* (Journal of Chromatography Library, vol. 66), Elsevier, Amsterdam, 2002, p. 207.
- [8] K.-S. Wong, J.-L. Jane, in: Z. El Rassi (Ed.), *Carbohydrate Analysis by Modern Chromatography and Electrophoresis* (Journal of Chromatography Library, vol. 66), Elsevier, Amsterdam, 2002, p. 403.
- [9] A.J. Mort, F. Qui, N.O. Maness, *Carbohydr. Res.* 247 (1993) 21.
- [10] L.A. Larew, D.C. Johnson, *Anal. Chem.* 60 (1988) 1867.
- [11] J. Emneus, L. Gorton, *Anal. Chem.* 62 (1990) 263.
- [12] C. Campa, S. Holtan, N. Nilsen, T.M. Bjerkan, B.T. Stokke, G. Skjåk-Bræk, *Biochem. J.* 381 (2004) 155.
- [13] H. Ertesvåg, G. Skjåk-Bræk, in: C. Bucke (Ed.), *Methods in Biotechnology*, vol. 10, Humana Press, Totowa, 1999, p. 71.
- [14] M. Gimmetstad, H. Sletta, H. Ertesvåg, K. Bakkevig, S. Jain, S. Suh, G. Skjåk-Bræk, T. Ellingson, D. Ohman, S. Valla, *J. Bacteriol.* 185 (2003) 3515.
- [15] S. Holtan, Q. Zhang, W.I. Strand, G. Skjåk-Bræk., in preparation.
- [16] A. Haug, O. Smidsrød, *Acta Chem. Scand.* 20 (1966) 183.
- [17] A. Haug, B. Larsen, O. Smidsrød, *Acta Chem. Scand.* 21 (1967) 691.
- [18] P. Sikorski, B.T. Stokke, A. Sørbotten, K.M. Vårum, S.J. Horn, V.G.H. Eijssink, *Biopolymers* 77 (2005) 273.
- [19] C. Tanford, *Physical Chemistry of Macromolecules*, Wiley, New York, 1961, p. 710.
- [20] P.J. Flory, *Principles of Polymer Chemistry*, Cornell University Press, New York, 1953, p. 672.
- [21] Y.C. Lee, *Anal. Biochem.* 189 (1990) 151.
- [22] Dionex Corporation, Technical Note 21, 1998, p. 4.
- [23] J.S. Rohrer, J. Thayer, M. Weitzhandler, N. Avdalovic, *Glycobiology* 8 (1998) 35.
- [24] W.R. LaCourse, in: Z. El Rassi (Ed.), *Carbohydrate Analysis by Modern Chromatography and Electrophoresis* (Journal of Chromatography Library, vol. 66), Elsevier, Amsterdam, 2002, p. 905.
- [25] H. Grasdalen, B. Larsen, O. Smidsrød, *Carbohydr. Res.* 56 (1977) C11.
- [26] H. Grasdalen, B. Larsen, O. Smidsrød, *Carbohydr. Res.* 68 (1979) 23.
- [27] H. Grasdalen, *Carbohydr. Res.* 118 (1983) 225.

# Paper II





Contents lists available at ScienceDirect

Carbohydrate Research

journal homepage: [www.elsevier.com/locate/carres](http://www.elsevier.com/locate/carres)

Note

## Preparation of high purity monodisperse oligosaccharides derived from mannuronan by size-exclusion chromatography followed by semi-preparative high-performance anion-exchange chromatography with pulsed amperometric detection

Simon Ballance\*, Olav Andreas Aarstad, Finn Lillelund Aachmann, Gudmund Skjåk-Bræk, Bjørn E. Christensen

NOBIPOL, Department of Biotechnology, Norwegian University of Science and Technology (NTNU), N-7491 Trondheim, Norway

## ARTICLE INFO

## Article history:

Received 10 July 2008

Received in revised form 19 October 2008

Accepted 22 October 2008

Available online 30 October 2008

## Keywords:

Alginate

Uronic acid

Fractionation

Purification

## ABSTRACT

Oligosaccharides of  $[(4)\text{-}\beta\text{-D-ManpA-(}\rightarrow)_n]$  with a degree of polymerisation (DP) of 5, 10 and 15 were generated by partial acid hydrolysis of alginate mannuronan. These were subsequently purified by a combination of size-exclusion chromatography and semi-preparative high-performance anion-exchange chromatography with pulsed amperometric detection. The purity of the isolated oligosaccharides was greater than 96%. With automated operation of the chromatography system, milligram quantities can be generated over a period of a few days. Thus, our methodology now offers some significant advantages over earlier, including our own, protocols focused on uronic acid oligomers, where the final products are either not as pure or more starting material is needed to generate an equivalent yield of product. Removal of ammonium ions in collected fractions after size-exclusion chromatography and prior to freeze-drying was found to be essential to prevent the formation of imines and subsequent Maillard browning products.

© 2008 Elsevier Ltd. All rights reserved.

In earlier work, we had achieved high resolution analytical separations of alginate oligosaccharides on Dionex<sup>™</sup> AS4A pellicular resin with PAD.<sup>1,2</sup> However, during chromatography of  $[(4)\text{-}\beta\text{-D-ManpA-(}\rightarrow)_n]$  oligosaccharides (hereafter referred to as M-oligosaccharides) that were pre-purified by size-exclusion chromatography (SEC) and freeze-dried in ammonium acetate, an unidentified carbohydrate peak was observed in the subsequent chromatogram.<sup>1</sup> The compound responsible for this peak eluted from the anion-exchange column just in front of the mannuronan oligosaccharide (Fig. 7 in<sup>1</sup>).

With these observations in mind, we have now sought to identify and remove this unwanted material because we now assess both SEC and semi-preparative HPAEC-PAD on Ion-Pac AS4A resin eluted with alkali as a method to efficiently prepare high purity, (>96% as assessed by analytical chromatography) essentially monodisperse M-oligosaccharides. The aim is to develop and evaluate the feasibility of a method to produce milligram quantities of M-oligosaccharides in the range of DP 5–15, which could subsequently be used as ultrapure substrates in a range of further experiments. The importance of this research is that it aims to build on,

and make improvements to, similar methodologies, including our own,<sup>1</sup> employed in earlier work.

Treatment of oligosaccharides with AG-50W-X8 cation-exchange resin (H<sup>+</sup>-form) followed by freeze-drying revealed only the presence of essentially monodisperse oligosaccharides as determined by analytical HPAEC-PAD (Fig. 1A). The same result was also obtained if a pooled oligosaccharide SEC fraction in 0.1 M ammonium acetate was injected directly onto analytical HPAEC-PAD (result not shown). It should be noted that oligosaccharides prepared via freeze-drying are in their H<sup>+</sup>-form and may, if analogy is made to mannuronic acid-rich alginate, be unstable if stored at room temperature for long periods.<sup>3</sup> Preferably, they should be stored in the freezer (−18 °C) for a short time as possible or should be converted to their Na<sup>+</sup>-form if stored in the freezer for a longer time.

It would seem that freeze-drying M-oligosaccharides in the presence of ammonia initially generates a reversible equilibrium at the reducing end residue of the oligosaccharide between mannuronic acid (H<sup>+</sup>-form) and 1-deoxy-1-imino-D-mannuronic acid. Further dehydration may then proceed to generate a small quantity of Maillard browning products. It is this incorporation of nitrogen into the reducing end monomer that probably gave rise to a second peak in front of the main oligosaccharide peak in the HPAEC-PAD chromatogram (Fig. 1B). The mechanism is that of

\* Corresponding author at present address: Simon Ballance, NOFIMA Food, Osloveien 1, N-1430, Ås, Norway. Fax: +47 64970333.

E-mail address: [simon.ballance@nofima.no](mailto:simon.ballance@nofima.no) (S. Ballance).

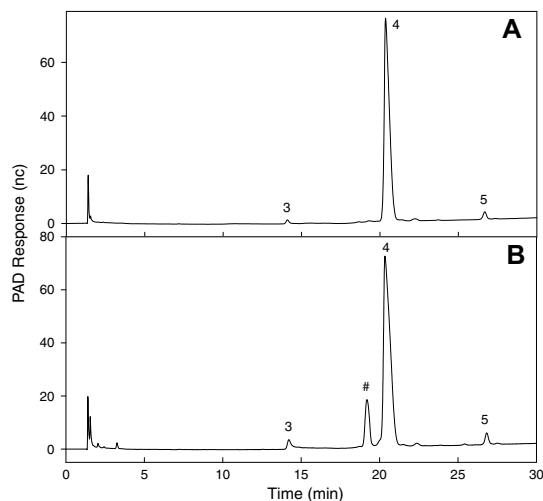


**Figure 1.** Analytical HPAEC-PAD chromatogram of an M-oligosaccharide standard of DP 4 recovered from SEC and (A) freeze-dried or treated with AG-50W-X8 cation-exchange resin prior to freeze-drying (B). Number annotation represents the chain length of oligosaccharides responsible for the peak, while # represents a peak from an oligosaccharide with 1-deoxy-1-imino-mannuronic acid or a Maillard browning product at the reducing end.

initial imine formation driven specifically by removal of water via freeze-drying. Ammonia (nucleophile) is generated upon lyophilisation of ammonium acetate followed by acid catalysis of the car-

boinoline intermediate as the pH drops from 6.9 to a final pH of about 5 with subsequent removal of water.<sup>4</sup> Similar reaction products have been found, where aldoses have been heated under anhydrous conditions in the presence of ammonia and an acid catalyst.<sup>5</sup> Identification of such reaction products in this study was supported by evidence from mass spectroscopy (MS) and NMR.

Analysis by electrospray ionisation quadrupole-time-of-flight (ESI-Q-TOF)-MS of an M-disaccharide sample isolated from SEC and freeze-dried in ammonium acetate detected  $[C_{12}O_{12}H_{19}N-H]^-$  (monoisotopic  $^{12}C/^{14}N$  calculated mass = 368.083) as a measured  $m/z$  of 368.082. This was in addition to the expected main molecular ion<sup>1</sup> of  $[C_{12}O_{13}H_{18}-H]^-$  (monoisotopic  $^{12}C/^{14}N$  calculated mass = 369.067) at  $m/z$  369.067. The relative detected abundance ratio of these two ions was approximately 32:1. In contrast, MS analysis of an M-disaccharide treated with cation-exchange resin, or analysed in ammonium acetate after direct recovery from SEC without freeze-drying, did not detect any molecular ions at around  $m/z$  368, only the main molecular ion at  $m/z$  369 indicating the absence of nitrogen in these carbohydrates.

For  $^1H$  NMR of an M-disaccharide sample isolated from SEC and freeze-dried in ammonium acetate, an aldimine proton was assigned to a doublet peak at 9.62 ppm in the 1D proton spectrum (Fig. 2A). In a  $^{13}C$ -HSQC spectrum (Fig. 2E), this proton was correlated to a carbon atom at 145.56 ppm. These chemical shifts are similar to those of 9.50 ppm for  $^1H$  and 146.70 ppm for  $^{13}C$  predicted by ACD Labs version 5.0 software and are consistent with the literature values.<sup>6</sup> This assignment is also confirmed by the following: (1) in a 2D IP-COSY spectrum, there was a cross-peak from the proton on the imino-carbon to a proton with a chemical shift typical for a sugar moiety at 4.05 ppm (Fig. 2F), however, it was not possible to safely assign the whole spin system due to heavily overlapping sugar signals, (2) no peak was observed in the same

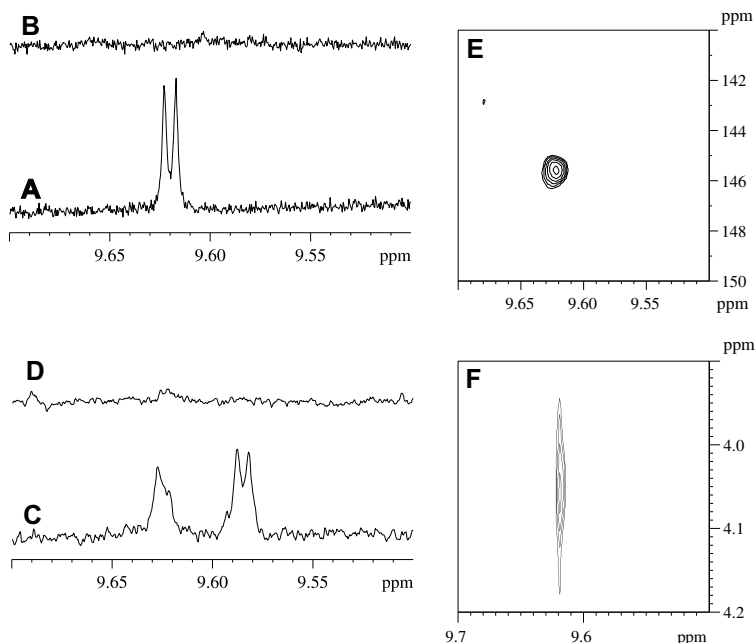


**Figure 2.** NMR spectra of different M- and G-disaccharides in  $DMSO-d_6$  at 298 K. (A) M-Disaccharide recovered from SEC and freeze-dried in ammonium acetate. (B) M-Disaccharide treated with AG-50W-X8 cation-exchange resin prior to freeze-drying. (C) G-Disaccharide recovered from SEC and freeze-dried in ammonium acetate. (D) G-Disaccharide treated with AG-50W-X8 cation-exchange resin prior to freeze-drying. (E)  $^{13}C$ -HSQC spectrum of an M-disaccharide with aldimine proton correlation to the aldimine carbon atom recovered from SEC and freeze-dried in ammonium acetate. (F) A part of a 2D IP-COSY spectrum with the cross-peak from the aldimine proton to the sugar moiety for M-disaccharide recovered from SEC and freeze-dried in ammonium acetate.



spectral region (Fig. 2B) in a corresponding sample treated with the cation-exchange resin. Similar observations were made for a M-trisaccharide (result not shown) and corresponding  $(1\rightarrow4)\text{-}\alpha\text{-L-GalpA-}(\rightarrow)_n$  or G-oligosaccharides (Fig. 2C and D) isolated in a parallel study. It was found that the imino-G oligosaccharide complexes were much less chemically stable than their M counterparts because two doublet peaks in the  $^1\text{H}$  NMR spectrum at 9.58 ppm and 9.63 ppm (Fig. 2C) disappeared after 2 h. Addition of 10%  $\text{D}_2\text{O}$  to the sample did not lead to any change in these two peaks, indicating that both peaks stem from hydrogen atoms attached to a carbon atom. The origin of these two doublet peaks is at present uncertain.

With the methodology in place to limit the formation of imines/Maillard browning contaminants, M-oligosaccharides with a purity of >96% (Table 1, Fig. 3D–F) and a degree of polymerisation of 5, 10 and 15 were recovered from collected fractions after chromatography on a semi-preparative Ion-Pac AS4A column (Fig. 3A–C) eluted with  $\text{NaOH}/\text{NaAc}$ . The detected minor impurities were not identified, but may represent possible degradation/reaction products either before, during or after chromatography. Once an assessment

of purity has been made via analytical chromatography for collected fractions over the target peak on one run from the semi-preparative column, this information can be overlaid onto all successive collections using the Chromeleon software chromatogram overlay function. Even if a small error/mis-judgement is made in collecting/pooling fractions then oligosaccharide purity should be still very good. In all the experiments we have done, the purity of recovered oligosaccharides has never been less than 91% even for oligosaccharides of  $\text{DP} > 15$ . The fact that the chromatogram obtained from the semi-preparative column does not look very nice in terms of peak symmetry and shape (Fig. 3A–C) is because the column is overloaded and the active surface of the PAD is saturated with eluting oligosaccharides. But this is not a problem. Chromatograms of a similar kind have been obtained before.<sup>7</sup> On the negative side, pellicular resin columns typically have a very low loading capacity,<sup>8–10</sup> but this disadvantage can be overcome with automated operation. In this respect, it is possible to collect a few milligrams of highly pure oligosaccharides over the duration of a few days without excessive time demands on personnel (Table 1).

**Table 1**  
Typical purity and yield data for M-oligosaccharides of DP 5, 10 and 15 purified by semi-preparative HPAEC-PAD

Degree of polymerisation	Material injected per run (mg)	Purity of material recovered (%)	Yield per run ( $\mu\text{g}$ )	Purified material recovered as a fraction of total injected	Theoretical yield per day (mg)
5	0.5	99	480	0.96	15.5
10	0.25	97	185	0.74	4.8
15	0.1	96	48	0.48	1.05

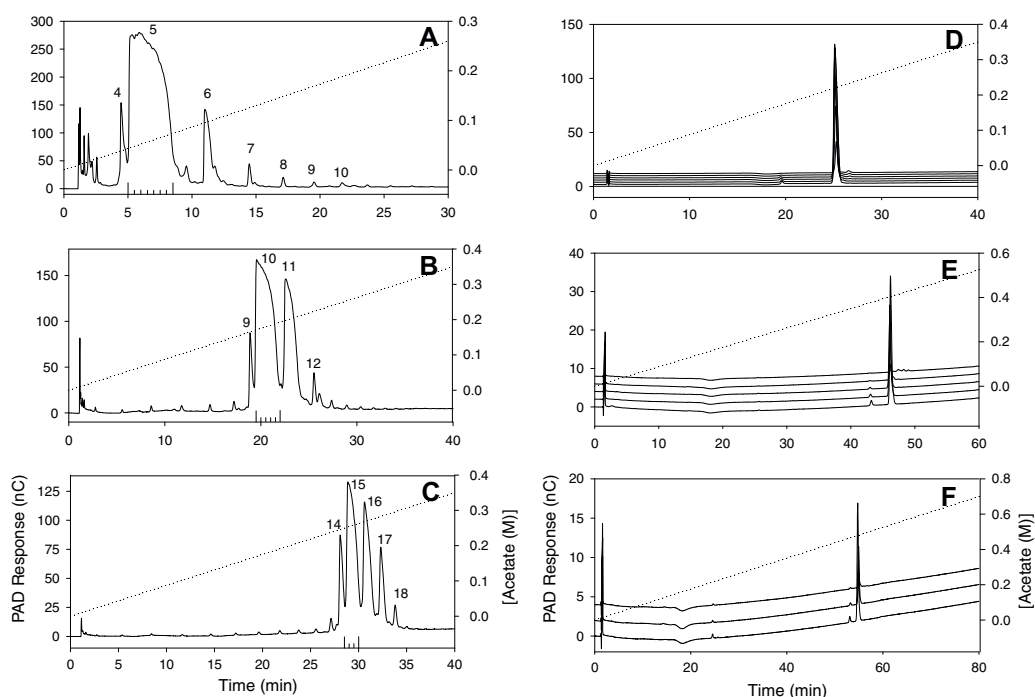


**Figure 3.** Typical semi-preparative HPAEC-PAD chromatograms (A–C) of M-oligosaccharides recovered from SEC and treated with AG-50W-X8 cation-exchange resin. The nominal DP was 5 (A), 10 (B) and 15 (C) from a total injection mass of 0.5, 0.25 and 0.1 mg, respectively. Collected fractions are represented by the bars pointing upwards from the x-axis. Number annotation represents the DP of oligosaccharides responsible for the peak. Analysis by analytical HPAEC-PAD chromatography (D–F) of fractions collected from the semi-preparative HPAEC-PAD chromatography with a nominal DP of 5 (D), 10 (E) and 15 (F). The detector responses of successive analysed fractions are plotted with an off-set of 2 nC. The dotted line is the gradient of acetate.

Overall, our chromatography methodology compares favourably to an earlier study, where oligogalacturonic acids with a DP from 7 to 21 were simultaneously collected after PAD detection from a total of 90 runs (7.5 days continuous run-time) on a preparative (21 × 250 mm) CarboPac PA-1 resin column.<sup>7</sup> Between 0.5 and 6.1 mg of oligosaccharides with a purity of 90+% were obtained from a total injection of 4.5 g start material at 50 mg per injection.<sup>7</sup> In the current study, 100–500 times less material is injected on to the column (Table 1), and this gives a much improved resolution for baseline separation of each oligosaccharide chain length (Fig. 3) leading to the recovery of products with an improved degree of purity (>96%) even if the yield per run is quite low (Table 1). In addition, much less starting material is required, which means an earlier round of oligosaccharide preparation clean-up is not too demanding.

Degradation of collected fractions is minimised because they are neutralised a few seconds after eluting from the column by mixing with acetic acid. No evidence was found of significant alkali degradation or 'peeling' by  $\beta$ -elimination during semi-preparative runs. This is in agreement with earlier observations.<sup>1,10</sup> Although not done in this study, desalting prior to final freeze-drying can be conducted by dialysis against distilled water to give oligosaccharides in their more stable Na<sup>+</sup>-form.

## 1. Experimental

### 1.1. Preparation of milligram amounts of pre-purified oligosaccharides

Oligosaccharides (DP 2–18) were prepared as described earlier by partial acid hydrolysis of mannuronan followed by neutralisation, freeze-drying and finally SEC in 0.1 M ammonium acetate at pH 6.9 on Superdex 30.<sup>1,2</sup> Collected fractions were pooled to yield semi-purified oligosaccharide fractions of 50–100 mL, which were predominantly in their NH<sub>4</sub><sup>+</sup>-form. These were subsequently passed through a 1.6 × 18 cm column of 20–50 mesh AG-50W-X8 cation-exchange resin (BioRad) in its H<sup>+</sup>-form at a flow rate of 3–5 mL/min. This treatment removed and exchanged NH<sub>4</sub><sup>+</sup> for H<sup>+</sup> to generate acetic acid and oligosaccharides in their H<sup>+</sup>-form. The sample was immediately frozen and freeze-dried prior to short-term storage (a maximum of one-two months) at –18 °C. After each round, the cation-exchange resin was regenerated with 10 column volumes of 0.1 M HCl followed by 20 column volumes of water.

### 1.2. Semi-preparative HPAEC-PAD

Oligosaccharides of DP 5, 10 and 15 were dissolved in MQ-water to a concentration of 10 mg/mL. 0.5, 0.25 or 0.1 mg of DP 5, 10 or 15 were injected, respectively, via a 0.1 mL loading loop. The chromatography unit consisted of a Dionex BioLC system (Sunnyvale, CA, USA) coupled to a Dionex AS50 autosampler and a Gilson 204 fraction collector fitted with 40 mL tubes containing 0.25 mL 1 M acetic acid. The LC system was equipped with an IonPac AS4A (9 × 250 mm) anion-exchange column connected to an IonPac AG4A (4 × 50 mm) guard column. Chromatography was performed at room temperature at a calculated optimal flow rate of 5 mL/min. The eluents were held in four 2 l plastic bottles purchased from Dionex<sup>®</sup>, all were connected to the pumps via their own eluent supply tubing. All contained 0.1 M NaOH (eluent A), while the fourth (eluent B) also contained 1 M acetate. Linear gradients of acetate were generated as described in the results. Column effluent was monitored with a pulsed amperometric detector on an Au working electrode and Ag/AgCl reference electrode. The sequence potentials applied to the Au electrode were as for Waveform A.<sup>11</sup> Data acquisition and analysis were performed

on Chromeleon 6.7 software. Fractions of 2.5 mL were collected every 0.5 min over the target peak, the first run of a series of several automated runs were analysed by analytical HPAEC-PAD, and pure fractions of the target pooled. It was possible to collect several sequential runs without replacing the tubes in the fraction collector. All collected fractions had a final pH of 6.5–7.

### 1.3. Analytical-HPAEC-PAD

Quantitative and qualitative analysis was conducted as described before for purity assessment of semi-preparative fractions and pools generated therefrom.<sup>1</sup> Waveform A was applied as the sequence potential to the electrode.

### 1.4. NMR spectroscopy

All homo- and heteronuclear NMR spectra were recorded on a Bruker Avance 600 spectrometer equipped with a 5 mm z-gradient TXI(H/C/N) cryoprobe. The NMR data were processed with the Bruker XWINNMR Ver. 3.6 software, and the spectral analysis was done with CARRA Ver. 1.4.<sup>12</sup> Samples of oligosaccharides (DP 2–3) from SEC chromatography, either treated or untreated with cation-exchange resin, were chosen so as to readily detect the resonances from the reducing-end<sup>1</sup>. They were prepared by dissolving 1.5–4 mg in 500  $\mu$ L 99.9% DMSO-*d*<sub>6</sub> or in 550  $\mu$ L 99.9% DMSO-*d*<sub>6</sub> mixed with 10% of 99.9% D<sub>2</sub>O. Homonuclear 1D, 2D in-phase correlation spectroscopy (IP-COSY) and heteronuclear <sup>13</sup>C single quantum coherence (HSQC) spectra were recorded at 298 K.<sup>13</sup> The residual proton and carbon signal from DMSO-*d*<sub>6</sub> were used for spectra calibration.

### 1.5. Mass spectroscopy

M-Disaccharides 0.5–1 mg/mL, analogous to those analysed by NMR, were dissolved in water or in case of the sample taken directly from SEC in 0.1 M ammonium acetate. 3  $\mu$ L were injected at a flow rate of 0.25 mL/min via an Agilent 1200 HPLC connected to an Agilent 6520 Q-TOF (quadrupole time-of-flight) mass spectrometer with negative mode electrospray ionisation. Automatic calibration of the mass axis was performed with continuous infusion of an Agilent reference mixture through a second nebulizer needle in the ion source. Agilent masshunter workstation software was used for data analysis.

### Acknowledgements

We thank Olav Smidsrød, Svein Valla, the Norwegian Research Council and NTNU for their kind financial support. We also thank Håvard Sletta and Anders Brunsvik for kindly carrying out the mass spectroscopy.

### References

1. Campa, C.; Oust, A.; Skjåk-Bræk, G.; Paulsen, B. S.; Paoletti, S.; Christensen, B. E.; Ballance, S. *J. Chromatogr., Sect. A* **2004**, *1026*, 271–281.
2. Ballance, S.; Holtan, S.; Aarstad, O. A.; Sikorski, P.; Skjåk-Bræk, G.; Christensen, B. E. *J. Chromatogr., Sect. A* **2005**, *1093*, 59–68.
3. Holme, H. K.; Lindmo, K.; Kristiansen, A.; Smidsrød, O. *Carbohydr. Poly.* **2003**, *54*, 431–438.
4. McMurry, J. *Organic Chemistry*; Brookes and Cole: California, 1988. p 1241.
5. Klug, E. D. U.S. Patent 2,197,540, 1940.
6. Lacombe, S.; Pellerin, B.; Guillemin, J. C.; Denis, J. M.; Pfister-Guillouzo, G. *J. Org. Chem.* **1989**, *54*, 5958–5963.
7. Hotchkiss, A. T.; Lecrinier, S. L.; Hicks, K. B. *Carbohydr. Res.* **2001**, *334*, 135–140.
8. Spiro, M. D.; Kates, K. A.; Koller, A. L.; O'Neill, M. A.; Albersheim, P.; Darvill, A. G. *Carbohydr. Res.* **1993**, *247*, 9–20.
9. Zhang, Y.; Lee, Y. C. High-performance Anion-exchange Chromatography of Carbohydrate on Pellicular Resin Columns. In *Carbohydrate Analysis by Modern Chromatography and Electrophoresis*; El Rassi, Z., Ed.; Journal of Chromatography Library, Elsevier: Amsterdam, 2002; pp 207–250. Vol. 66.

10. Hicks, K. B.; Hotchkiss, A. T. Preparative HPLC of Carbohydrates. In *Carbohydrate Analysis by Modern Chromatography and Electrophoresis*; El Rassi, Z., Ed.; Journal of Chromatography Library, Elsevier: Amsterdam, 2002; pp 529–534. Vol. 66.
11. Dionex Corporation, Technical Note 21, 1998, pp 1–4.
12. Keller, R. L. J. *The Computer Aided Resonance Assignment Tutorial*; Catina Verlag: Goldau, Switzerland, 2004. p 73.
13. Xia, Y.; Legge, G.; Jun, K. Y.; Qi, Y.; Lee, H.; Gao, X. *Magn. Reson. Chem.* **2005**, *43*, 372–379.



# Paper III



## Isolation of Mutant Alginate Lyases with Cleavage Specificity for Di-guluronic Acid Linkages<sup>\*[5]</sup>

Received for publication, July 21, 2010, and in revised form, September 1, 2010. Published, JBC Papers in Press, September 7, 2010, DOI 10.1074/jbc.M110.162800

Anne Tøndervik<sup>‡§1</sup>, Geir Klinkenberg<sup>‡</sup>, Olav A. Aarstad<sup>§</sup>, Finn Drabløs<sup>§</sup>, Helga Ertesvåg<sup>§</sup>, Trond E. Ellingsen<sup>‡</sup>, Gudmund Skjåk-Bræk<sup>§</sup>, Svein Valla<sup>§</sup>, and Håvard Sletta<sup>‡</sup>

From the <sup>‡</sup>Department of Biotechnology, SINTEF Materials and Chemistry, N-7465 Trondheim, Norway and the Departments of <sup>§</sup>Biotechnology and <sup>¶</sup>Cancer Research and Molecular Medicine, The Norwegian University of Science and Technology, N-7491 Trondheim, Norway

Alginates are commercially valuable and complex polysaccharides composed of varying amounts and distribution patterns of 1–4-linked  $\beta$ -D-mannuronic acid (M) and  $\alpha$ -L-guluronic acid (G). This structural variability strongly affects polymer physicochemical properties and thereby both commercial applications and biological functions. One promising approach to alginate fine structure elucidation involves the use of alginate lyases, which degrade the polysaccharide by cleaving the glycosidic linkages through a  $\beta$ -elimination reaction. For such studies one would ideally like to have different lyases, each of which cleaves only one of the four possible linkages in alginates: G-G, G-M, M-G, and M-M. So far no lyase specific for only G-G linkages has been described, and here we report the construction of such an enzyme by mutating the gene encoding *Klebsiella pneumoniae* lyase AlyA (a polysaccharide lyase family 7 lyase), which cleaves both G-G and G-M linkages. After error-prone PCR mutagenesis and high throughput screening of ~7000 lyase mutants, enzyme variants with a strongly improved G-G specificity were identified. Furthermore, in the absence of  $\text{Ca}^{2+}$ , one of these lyases (AlyA5) was found to display no detectable activity against G-M linkages. G-G linkages were cleaved with ~10% of the optimal activity under the same conditions. The substitutions conferring altered specificity to the mutant enzymes are located in conserved regions in the polysaccharide lyase family 7 alginate lyases. Structure–function analyses by comparison with the known three-dimensional structure of *Sphingomonas* sp. A1 lyase A1-II' suggests that the improved G-G specificity might be caused by increased affinity for nonproductive binding of the alternating G-M structure.

ranged in blocks of continuous M residues (M-blocks), G residues (G-blocks), or alternating residues (MG-blocks). Alginate is produced by marine brown algae and by bacteria belonging to the genera *Azotobacter* and *Pseudomonas* (1–4). Biosynthesis of alginate involves the initial production of polymannuronate followed by the introduction of G residues catalyzed by mannuronan C-5 epimerases (5–7). *Pseudomonas* alginates differ from those obtained by other sources in lacking G-blocks, and bacterial alginates, as opposed to the seaweed polymers, can be acetylated to various degrees at positions O-2 and/or O-3 on the M residues (8). The material properties of alginates are determined by intrinsic properties like the polymer chain length, acetylation level, and the monomer composition and distribution pattern.

Commercially alginate is harvested from seaweed and has been utilized extensively for a variety of industrial and biotechnological purposes (9–11). In recent years, much attention has been drawn to new and promising applications of alginates in pharmacy and medicine, e.g. in drug or protein delivery, cell encapsulation, tissue regeneration, surgery, and wound management (12–18). With the entry of alginate-based biomaterials into the field of human medicine, the term “tailor-made alginate” has been introduced. This means that one ideally wants to produce and use alginate molecules with defined properties optimally suited for a given application. Hence there is an emerging need for more detailed information concerning the alginate fine structure. Although the total monomer composition and the dyad and triad frequencies can be elucidated by, for example, high resolution NMR spectroscopy (8), there is limited knowledge on the distribution and the absolute length of the various block types.

A promising approach to the challenge of alginate sequence elucidation is the use of lyases to degrade complex alginate molecules followed by analyses on the resulting population of alginate oligomers (19, 20). This concept has become increasingly attractive with the continuous development of chromatographic methods. Ideal lyases in this case are enzymes that cleave only one of the four possible types of linkages (M-M, M-G, G-M, and G-G) in the alginate. For instance, after degradation with an M-M specific lyase, one can obtain information about the amount and length of G-blocks and MG-blocks in the substrate.

Alginate lyases catalyze the degradation of alginate targeting the glycosidic 1  $\rightarrow$  4 O-linkages between monomers by a  $\beta$ -elimination mechanism leaving a 4-deoxy-L-erythro-hex-4-enopyranosyluronic acid (often denoted as  $\Delta$ ) as the nonreduc-

Alginate is a linear polysaccharide widely used in industry and is comprised of 1–4-linked  $\beta$ -D-mannuronic acid (M)<sup>2</sup> and its C-5 epimer  $\alpha$ -L-guluronic acid (G). The monomers are ar-

\* The work was supported by The Research Council of Norway Project 182695-I40 and by FMC Biopolymer and Algipharm AS.

[5] The on-line version of this article (available at <http://www.jbc.org>) contains supplemental Table S1.

<sup>1</sup> To whom correspondence should be addressed: SINTEF Materials and Chemistry, Dept. of Biotechnology, Post Box 4760, N-7465 Trondheim, Norway. Tel.: 47-93498620; Fax: 47-73596995; E-mail: Anne.Tondervik@sintef.no.

<sup>2</sup> The abbreviations used are: M,  $\beta$ -D-mannuronic acid; G,  $\alpha$ -L-guluronic acid; PL-7, polysaccharide lyase family 7; MOPS, 4-morpholinepropanesulfonic acid; HPAEC-PAD, high performance anion exchange chromatography with pulsed amperometric detection.

ing terminal residue (21). Lyases can be isolated from a variety of organisms including algae, marine invertebrates (e.g. mollusks), bacteriophages, and several marine and terrestrial bacterial species (19). The enzymes are generally classified as M- or G-lyases (EC 4.2.2.3 and EC 4.2.2.11) according to their dominating cleaving reaction on M- or G-rich alginates. The majority of lyases characterized at present display activity toward more than one of the four types of linkages.

*Klebsiella pneumoniae* produces an extracellular alginate lyase, AlyA, which according to the primary structure is classified in the polysaccharide lyase family 7 (PL-7) (22, 23). AlyA is endolytic, acting on G-blocks and MG-blocks where G-M linkages are cleaved in the latter substrate (24). The three-dimensional structure for three of the PL-7 lyases have been determined: A1-II' from *Sphingomonas* sp. A1, ALY-1 from *Corynebacterium* sp. ALY-1, and PA1167 from *Pseudomonas aeruginosa* PAO1 (25–27). These structures indicate a common basic framework for PL-7 lyases, which is a  $\beta$ -sandwich fold consisting of two  $\beta$ -sheets (SA and SB) creating a deep active cleft that is covered by two flexible loops (L1 and L2). Despite structural similarities, their substrate preferences differ. A1-II' is reported to have a broad substrate range, acting equally well on G-blocks, M-blocks, and MG-blocks (28). PA1167 has limited activity on G-blocks, acts preferentially on MG-blocks, but also has activity toward M-blocks (27). ALY-1 is reported to be much more active toward a G-rich substrate (81% G) than toward an M-rich (82% M) substrate; however, the activity of ALY-1 toward a specific substrate like MG-blocks has not been reported (29). A1-II, which is another lyase from *Sphingomonas* sp. A1, is reported to have 2.5–5 times higher activity on polyG than on polyMG (27, 28). Furthermore, the lyase from ATCC43367 is reported to cleave only M-M linkages (30).

In the present work we aimed at modifying the specificity of the *K. pneumoniae* AlyA to obtain a lyase with preference for cleaving only G-G linkages, a type of specificity that to our knowledge has not been described. AlyA was chosen as a basis because of its inherent high activity on G-G linkages and our previous experience with expression and purification of this lyase (24). To identify the mutants we used *in vitro*-made alginates with highly defined composition as substrates in a high throughput screening protocol. Mutants with the desired properties were identified, and their enhanced specificity appears to mainly be caused by increased affinity toward nonproductive M-G binding.

## EXPERIMENTAL PROCEDURES

**Bacterial Strains, Growth Conditions, and DNA Manipulations**—*Escherichia coli* strains DH5 $\alpha$  (BRL) and XL10-Gold<sup>®</sup> (Stratagene) were used as general cloning hosts and for establishing the mutant library, respectively. *K. pneumoniae* (formerly *K. aerogenes*, type 25) was used for cloning of the *alyA* gene. Bacteria were routinely grown at 37 °C in L broth (5 g of yeast extract, 10 g of tryptone, and 10 g of NaCl/liter) or on L agar (L broth supplemented with 20 g of agar/liter). For protein expression, the strains were grown in triple strength L broth (15 g of yeast extract, 30 g of tryptone, and 10 g of NaCl/liter). Growth media were supplemented with ampicillin (100  $\mu$ g/ml)

when appropriate. For growth in 96-well plates, a reduced Hi-Ye medium with the following composition was used: Na<sub>2</sub>HPO<sub>4</sub>·2H<sub>2</sub>O, 12.3 g/liter; KH<sub>2</sub>PO<sub>4</sub>, 4.29 g/liter; NH<sub>4</sub>Cl, 0.43 g/liter; NaCl, 0.71 g/liter; glucose, 2.86 g/liter; yeast extract, 2.86 g/liter; citric acid, 1.43 g/liter; MgSO<sub>4</sub>, 1.86 mM; Fe(III)-citrate, 118  $\mu$ M; H<sub>3</sub>BO<sub>3</sub>, 21.0  $\mu$ M; MnCl<sub>2</sub>, 37.6  $\mu$ M; EDTA, 9.86  $\mu$ M; CuCl<sub>2</sub>, 3.86  $\mu$ M; Na<sub>2</sub>MoO<sub>4</sub>, 4.29  $\mu$ M; CoCl<sub>2</sub>, 4.71  $\mu$ M; and zinc acetate, 17.3  $\mu$ M. Cultures were induced for protein expression using an induction solution containing: glycerol (99%), 25.8 g/liter; yeast extract, 24 g/liter; and *m*-toluic acid to a final concentration of 0.5 mM. Standard recombinant DNA protocols were performed as described elsewhere (31). Plasmids were isolated by the Wizard<sup>®</sup> Plus SV minipreps DNA purification system (Promega). Transformation of XL10-Gold<sup>®</sup> ultracompetent cells was performed according to the instructions from the manufacturer and for DH5 $\alpha$  according to the RbCl transformation protocol (New England Biolabs). DNA sequencing was performed using the BigDye<sup>®</sup> Terminator version 1.1 cycle sequencing kit (Applied Biosystems).

**Vector Constructions and Random and Site-directed Mutagenesis**—Primers used for cloning and mutagenesis are given in supplemental Table S1. The *alyA* gene including the signal sequence was PCR-amplified from the genome of *K. pneumoniae* and ligated into pGEM-5Zf (Promega) as an NdeI-NotI fragment yielding pAT74. pAT74 was used as template for random- and site-directed mutagenesis using the GeneMorph<sup>®</sup> II random mutagenesis kit and the QuikChange<sup>®</sup> II site-directed mutagenesis kit from Stratagene, respectively, and introduction of mutations was verified by sequencing. For protein expression, the wild type or mutant lyase genes were ligated into an expression vector containing the regulatory *Pm/xylS* promoter system. The vector utilized was identical to pJBphOx-271d (32) except for the ML1–14 mutation in *Pm* causing increased expression levels (33). As described under “Results,” variants of the eight mutants isolated in the screen were made to decide the contribution of the individual substitutions on the observed phenotype. When possible these constructs were made by subcloning fragments containing the specific mutations into the vector containing wild type *alyA*; otherwise mutations were reconstructed by site-directed mutagenesis.

**Production and Purification of polyMG and polyG**—An alginate with a regular poly-alternating structure, polyMG, with  $F_G = 0.47$  and  $F_{GG} = 0$  was produced by epimerization of manuronan with the recombinantly produced mannuronan C-5 epimerase AlGE4 and characterized by NMR as described previously (34). polyG with  $F_G = 0.94$  and a degree of polymerization of 18.5 was prepared from *Laminaria hyperborea* stipes as described elsewhere (21, 35).

**Measurement of Alginate Lyase Activity**—Alginate lyase activity was determined by monitoring the increase in  $A_{230}$  caused by production of unsaturated uronic acids as the lyase cleaves glycosidic bonds in the polymer chain. Unless otherwise stated, the activity was measured at room temperature in 96-well microtiter plates using a mixture of 240  $\mu$ l of buffer (50 mM Tris-HCl, 0.2 M NaCl, 1 mM CaCl<sub>2</sub>, pH 7.5), 60  $\mu$ l of alginate substrate (4 mg/ml), and 10–20  $\mu$ l of protein extract. One unit of enzyme activity was defined as the amount of enzyme that increased  $A_{230}$  by 1 unit/min. The lyase activity was determined as the



## Alginate Lyases with Enhanced Specificity

initial activity when the increase in  $A_{230}$  was linear. The lyase activity measurements were performed at least in triplicate.

**Robotic Screening of the *alyA* Mutant Library**—The *E. coli* library was plated on LB-agar in 25 × 25-cm Petri dishes (Corning CLS431301) and incubated overnight at 37 °C. The colonies were picked using a Genetix Q-Pix2 robotic colony picker and transferred to 96-well microplates (Greiner M3186) containing 80  $\mu$ l of reduced Hi-Ye medium. The microplates were incubated at 30 °C, 900 rpm (3-mm amplitude) and 80% relative humidity. After 24 h, 40  $\mu$ l of induction solution was added to each well using an Asys Hi-Tech Flexispence microplate dispenser. The microplates were incubated at 37 °C, 900 rpm and 80% relative humidity for 4 h after induction and were frozen at –40 °C prior to analysis. After thawing, the microplates were added 30  $\mu$ l of B-PER II solution (Pierce) per well, shaken for 30 s (900 rpm, 3 mm amplitude), and incubated at room temperature for 1 h. After incubation, the microplates were shaken (850 rpm, 3-mm amplitude) for 10 min and then centrifuged for 30 min at 3500 × *g*. For measurement of alginate lyase activity, 384-well microplates (Corning CLS3675) were filled with 50  $\mu$ l of assay buffer (40 mM MOPS, 20 mM NaCl, 2 mM CaCl<sub>2</sub>, pH 6.8) containing either polyG or polyMG alginate (0.2 mg/ml). Each 384-well plate contained 192 wells filled with polyG and the rest with polyMG. 4  $\mu$ l of cell free extract was then added to two wells in the 384-well assay plate, one with each of the two types of alginate. The wells in the 384-well plate were mixed by pipetting (3 × 25  $\mu$ l), and the absorbance at 230 nm ( $A_{230}$ ) was read in a Molecular Devices SpectraMax 384+ microplate reader shortly after mixing and after 40 and 120 min of incubation at room temperature. The increase in absorption during incubation was calculated for each type of alginate, and  $\Delta A_{230}$  was used for evaluation of the G-G and M-G activity of the enzyme extracts. The tests were performed with parallel cultures in microwell plates (96 parallels) to determine the accuracy of the screening protocols, and the standard deviation was generally below 5% in the enzyme assay. All liquid and microplate handling was performed by a Tecan Genesis RSP 200 robotic liquid handling work station.

**Protein Expression and Purification**—The cultures were grown in 50 ml of 3 × LB medium in 500-ml baffled flasks at 30 °C for 3 h before induction of the *P<sub>m</sub>* promoter with 0.5 mM *m*-toluic acid. Cultivation was continued for an additional 4 h before harvesting the cells by centrifugation. The cells were disrupted by sonication in 20 mM Na<sub>2</sub>HPO<sub>4</sub>, 1 mM CaCl<sub>2</sub> (pH 6.8), and centrifuged for 30 min at 20 000 × *g*. The supernatant was filtered (0.2  $\mu$ m) and applied on a 5-ml HiTrap HP SP column equilibrated with the same buffer as above. The proteins were eluted by a stepwise NaCl gradient (total gradient from 0 to 1 M) in the same buffer and collected in 5-ml fractions. The fractions were tested for alginate lyase activity, and protein content of active fractions was determined by the Bio-Rad microassay procedure. Bovine serum albumin was used as standard. The purity of lyase-containing fractions was analyzed by SDS-PAGE.

**Analysis of Alginate Degradation by High Performance Anion Exchange Chromatography with Pulsed Amperometric Detection (HPAEC-PAD)**—Lyase degradation of polyG and polyMG was performed in 50 mM Tris-HCl, 0.2 M NaCl, 1 mM CaCl<sub>2</sub>, pH 7.5, at room temperature, and the substrate concentration used

was 1 mg/ml. To inactivate the lyases, the samples were boiled for 10 min after the addition of 1% SDS. Analysis of lyase-degraded alginate samples was performed using a Dionex BioLC system (Dionex Corp, Sunnyvale, CA) consisting of an AS50 autosampler, an ED40 Electrochemical Detector with a non-disposable gold working electrode, and a GP50 Gradient Pump. All of the samples (1 mg/ml, 25  $\mu$ l) were injected via a 100- $\mu$ l loading loop. The oligosaccharides were separated at room temperature by gradient elution with 0–700 mM sodium acetate in 100 mM sodium hydroxide over 80 min on a Dionex IonPac AS4A (4 × 250 mm) anion exchange column connected to an IonPac AG4A (4 × 50 mm) guard column. The flow rate was set to 1 ml/min using waveform A for detection. Data acquisition and analysis were performed using Chromeleon 6.7 software (20). Oligomer standards up to hexamer were produced by fractionation of partially lyase-degraded polyG and polyMG on SEC columns as described earlier (36). The fractions were analyzed with <sup>1</sup>H NMR to determine chain length and chemical composition.

**Bioinformatic Analysis of Mutations**—The experimental three-dimensional structures of *Sphingomonas* sp. A1 lyase A1-II' (37) with GGG (Protein Data Bank code 2ZAB) and MMG (Protein Data Bank code 2ZAC) in the substrate binding pocket were downloaded from the Research Collaboratory for Structural Bioinformatics (RCSB) Protein Data Bank (38). The structures were analyzed with ligand-protein contacts (39) and LigPlot (40) and visualized with SwissProtein Data BankViewer (41). Identification and alignment of homologous protein sequences was done with PSI-Blast (42) and ClustalX (43).

## RESULTS

**Construction and Screening of an *alyA* Mutant Library for Identification of Enzymes Exhibiting Increased Specificity toward G-G Linkages**—Initial studies showed that the specific activities of AlyA on polyMG and polyG are 937 and 765 units/mg, respectively (Table 1). Because of the defined nature of the substrates, this is considered to be the activity on G-M and G-G linkages, respectively. The undesired activity against G-M bonds is therefore somewhat higher than against the G-G bonds in the wild type enzyme. A library of mutated *alyA* genes was then constructed by error-prone PCR, and the experimental conditions were adjusted to achieve an average frequency of two to seven nucleotide changes/gene, also verified by sequencing of the lyase gene in 40 randomly selected clones (data not shown). The library (~108,000 primary clones) was established in *E. coli* XL10-Gold® cells. 6720 colonies were randomly picked, transferred to 96-well microtiter plates with growth medium, incubated, and induced by *m*-toluic acid for lyase expression in 96-well plates. Cell-free extract from each culture was prepared and evaluated for enzymatic activity, using polyMG and polyG as substrates. The ratio between the activity against polyMG and polyG for each extract was chosen as the selection criterion in the screen, this value being 1.2 for wild type AlyA. In the primary screen ~100 clones were identified that displayed a maximum polyMG/polyG ratio of 0.3, and after rescreenings of these clones, eight strains displaying the lowest polyMG/polyG activity ratios were chosen for further characterization. The corresponding variant lyases were

TABLE 1

Activity of wild type AlyA, mutants selected in the screen (AlyA1 and AlyA3–8), and constructed mutants on polyG and polyMG

Lyase	Amino acid substitution(s)	Activity		Activity polyMG/ activity polyG
		polyG <sup>a</sup>	polyMG <sup>a</sup>	
		<i>units/mg</i>	<i>units/mg</i>	
AlyA (wild type)		765 ± 50	937 ± 47	1.2
AlyA1	S86L	31 ± 2	9.1 ± 0.4	0.3
AlyA3	S37I	53.8 ± 0.7	4.3 ± 0.1	0.1
AlyA4	V6I, T85A	23.6 ± 0.9	2.16 ± 0.02	0.1
	V6I	858 ± 136	851 ± 71	1.0
	T85A	24.8 ± 0.3	4.41 ± 0.06	0.2
AlyA5	G26E, P39H	246 ± 22	19.5 ± 0.5	0.1
	G26E	692 ± 119	787 ± 19	1.1
	P39H	356 ± 10	37 ± 11	0.1
AlyA6	I51M, T89I, G304V	153 ± 9	13.26 ± 0.07	0.1
	I51M, T89I	227 ± 13	18.8 ± 0.1	0.1
	I51M	731 ± 24	786 ± 43	1.1
	T89I	218 ± 7	31 ± 2	0.1
	G304V	828 ± 26	878 ± 67	1.1
AlyA7	S35R, P39T, A224V	43.2 ± 0.7	3.4 ± 0.6	0.1
	S35R, P39T	32.6 ± 0.6	6.87 ± 0.07	0.2
	S35R	443 ± 10	448 ± 5	1.0
	P39T	216 ± 2	71 ± 1	0.3
AlyA8	A78S, T89I, A217E	187 ± 13	29.8 ± 0.4	0.2
	A78S, T89I	228 ± 15	34.3 ± 0.9	0.2
	A78S	820 ± 35	938 ± 94	1.1
	T89I	218 ± 7	31 ± 2	0.1

<sup>a</sup> A unit is the amount of enzyme required to increase  $A_{230}$  by 1 unit/min. The activity measurements were performed at least in triplicate, and the standard deviations of the means are given. AlyA1 and AlyA3–8 are mutants isolated in the screen. The mutants constructed to analyze the contribution of the separate amino acid substitutions in AlyA1 and AlyA3–8 are listed under each original mutant lyase.

denoted AlyA1–8, and DNA sequence analyses showed that none of them were identical (Table 1). The number of deduced amino acid substitutions was either one (AlyA1–3), two (AlyA4–5), or three (AlyA6–8). AlyA2 differed from AlyA1 only by carrying an additional silent mutation at a site corresponding to Asp<sup>237</sup>. AlyA2 was therefore not included in further studies. Silent mutations were also identified in AlyA3 (Val<sup>151</sup>), AlyA6 (Thr<sup>220</sup>), and AlyA7 (Ile<sup>80</sup> and Tyr<sup>175</sup>). Note also that the T89I substitution was found both in AlyA6 and AlyA8 and that Pro<sup>39</sup> was substituted to both His (AlyA5) and Thr (AlyA7). This observation correlates well with the finding that these two residues are particularly important for substrate specificity (see below).

AlyA1 and AlyA3–8 were partially purified by ion exchange chromatography, and the activity against polyG and polyMG was determined. For some enzymes, the level of activity on both substrates was considerably reduced compared with that of the wild type enzyme, but a strongly increased specificity toward G-G linkages was confirmed (Table 1 and Fig. 1). The activity against polyG was highest for AlyA5 (~32% compared with wild type) and lowest for AlyA4 (~3%). AlyA4 also displayed the lowest activity against polyMG (~0.23%), and AlyA8 displayed the highest (~3%). Based on all of these activity measurements, the enzymes could also be arranged with respect to their specificities against polyG, and these calculations showed that for five of the seven enzymes (AlyA3–7), the ratios between the activities on polyMG and polyG is 0.1, which is ~12-fold less than for the wild type enzyme. For AlyA8 and AlyA1, the ratios were not equally low (0.2 and 0.3, respectively). Because AlyA5 displayed the highest activity against polyG, it appeared to be the best candidate for further applications in analyses of alginate fine structures, and the biochemical properties of this enzyme was therefore studied in further detail.

*HPAEC-PAD Analysis of Oligosaccharide Pools Generated by Degradation of polyG and polyMG Confirmed That AlyA5 Can Be Used to Selectively Degrade G-blocks*—The composition of the oligosaccharide pools after partial degradation of polyG and polyMG with AlyA wild type and AlyA5 was analyzed using HPAEC-PAD. This technique allows for separation of oligomers with a degree of polymerization up to 40. Furthermore, oligomers with an identical degree of polymerization can be separated on the basis of G and M content because elution time increases with increasing M. Likewise, elution time increases with the introduction of unsaturated uronic acids (denoted by  $\Delta$  in Fig. 2), i.e. GGG elutes from the column before  $\Delta$ GG.

By controlling enzyme concentrations and incubation times, polyG was degraded with AlyA and AlyA5 to reach the same level of degradation as measured by  $A_{230}$  in each reaction ( $A_{230} = 2$ ). The chromatograms (Fig. 2, A and B) show that for both enzymes G-oligomers down to dimers can be detected, and the degradation patterns are similar. The peaks marked *Dp4* represent tetramers of different compositions, but the exact composition in each peak could not be identified. The analysis was also repeated under the same reaction conditions, using polyMG as substrate (Fig. 2, C and D). Degradation with AlyA resulted in a pool of oligomers with a degree of polymerization in the entire detection range, whereas for AlyA5 oligomers could not be detected at all. These results therefore confirmed that by keeping the enzyme concentrations at the minimum required for degradation of polyG, AlyA5 can be used to selectively degrade G-blocks into oligomers.

*Activity of AlyA5 against polyMG Can Be Further Reduced by Omitting Ca<sup>2+</sup> from the Incubation Mixture*—For optimal activity, alginate lyases display different requirements for conditions like, for example, ionic strength and the presence of cations (19). Initial studies showed that AlyA activity is optimal on a complex substrate like LF10/60 in a 50 mM Tris buffer at pH 7.5 when supplemented with 0.2 M NaCl and 1 mM Ca<sup>2+</sup>. However, at the enzyme active site level such a substrate can be seen as a composite of many different substrates (G-blocks, M-blocks, and MG-blocks). It therefore seemed possible that the activity requirements are not the same for the different substructures in the substrate. Because of the defined nature of the substrates used here, this hypothesis could be experimentally tested. AlyA activity against polyG was found not to be affected by the concentration of Ca<sup>2+</sup> (0–2 mM). In contrast, AlyA5 activity was stimulated by increasing levels of this cation (Fig. 3A).

Interestingly, the activities of both AlyA and AlyA5 on polyMG are strongly stimulated by Ca<sup>2+</sup>, and in the case of AlyA5 there was no detectable activity in the absence of this cation (Fig. 3B). It could therefore be concluded that by avoiding Ca<sup>2+</sup> in the incubation mixture, AlyA5 becomes completely specific for polyG under the given conditions. This Ca<sup>2+</sup> dependence of AlyA5 does not appear to be a general feature of the variant enzymes, because AlyA1 was found to behave similarly to AlyA in this respect (data not shown).

*Amino Acid Substitutions Responsible for Increased G-G Specificity Are Most Often, but Not Always, Associated with Severe Loss of Total Enzyme Activity*—Because AlyA4–8 all contained more than one deduced amino acid substitution, it

## Alginate Lyases with Enhanced Specificity

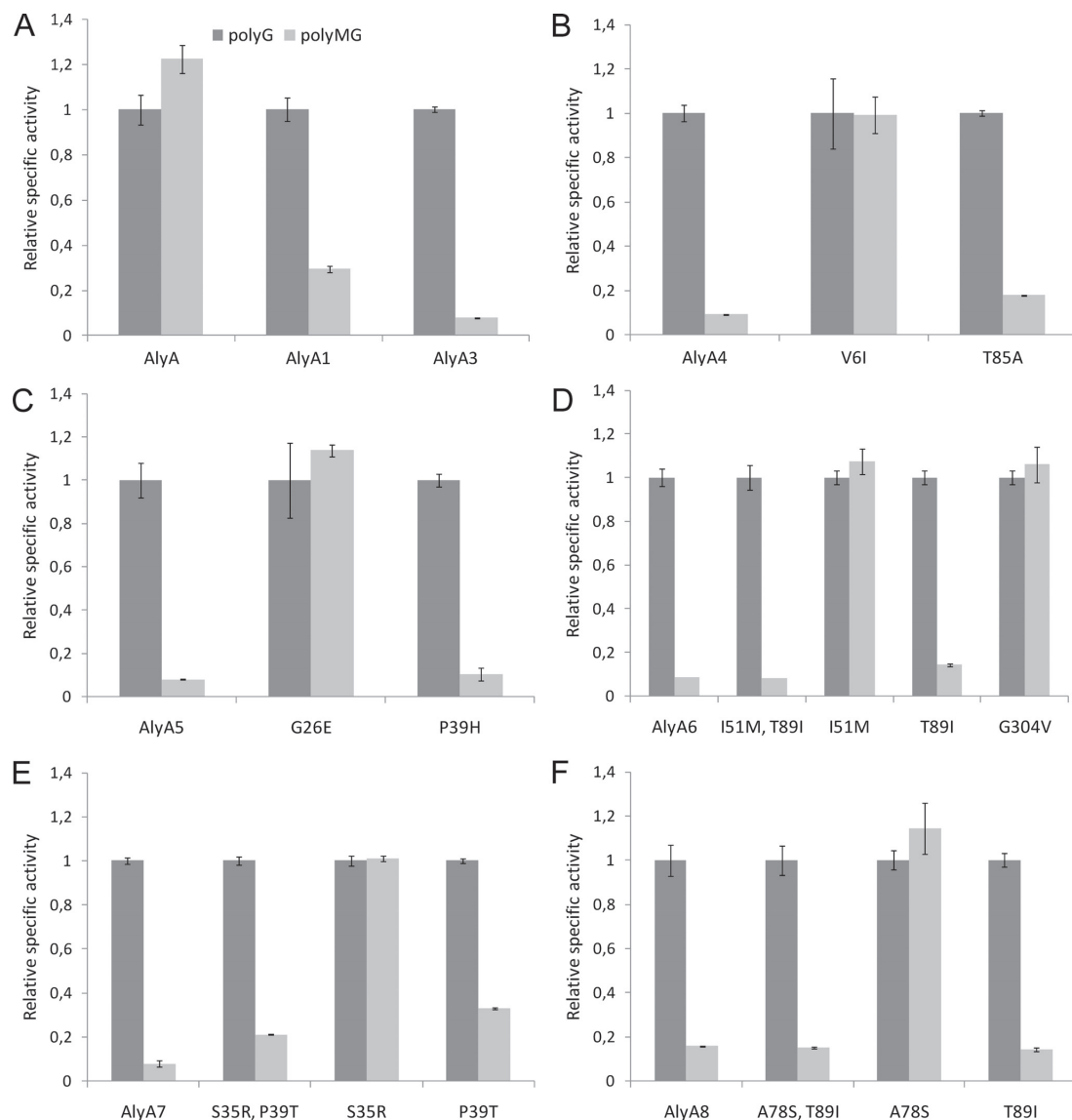


FIGURE 1. Relative specific activity (units/mg) of AlyA wild type (A) and variant enzymes (A–F) against polyG and polyMG. For each lyase, the specific activity against polyG is set to 1. The reaction conditions were 50 mM Tris, pH 7.5, with 0.2 M NaCl and 1 mM CaCl<sub>2</sub>. The absolute values for the specific activities against each substrate are given in Table 1.

appeared possible that some substitutions did not contribute to the observed specificity and possibly also led to reduced total activity against polyG. We therefore constructed a series of new mutants aiming at analyzing the contribution of each separate amino acid substitution. The results showed that none of the single substitution enzymes displayed more preferable properties than the originally isolated variants, relative to the criteria used to identify AlyA5 as the best candidate (Table 1 and Fig. 1). Many of the variants displayed an activity against both polyG and polyMG that was closer to that of the wild type enzyme

(V6I, G26E, I51M, G304V, S35R, and A78S). These substitutions alone therefore did not contribute much to improve the specificity of the enzyme against polyG. In contrast, for AlyA4 and AlyA5, which contained only two substitutions, one of the two substitutions alone (T85A and P39H, respectively) was sufficient to generate most but not all of the improved specificity. AlyA6–8 carry three substitutions each, and T89I and P39T were the best single substitution candidates with respect to the desired specificity. Among these, T89I is the most useful, displaying the lowest activity ratio between polyMG and polyG.

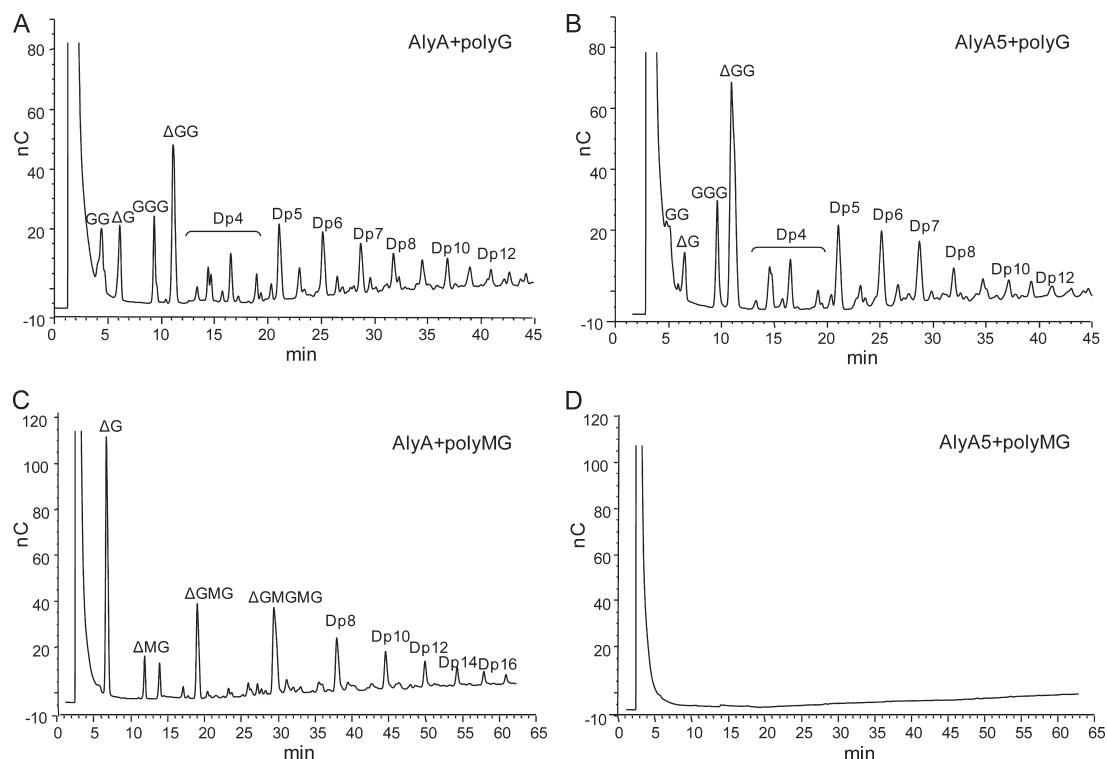


FIGURE 2. HPAEC-PAD analysis of oligosaccharides from degraded samples of polyG and polyMG by AlyA wild type (A and C) and AlyA5 (B and D). Degradation (1 mg/ml substrate) was performed in 50 mM Tris with 0.2 M NaCl and 1 mM  $\text{CaCl}_2$  and was allowed to proceed until  $A_{230} = 2$  in the polyG reaction mixtures; i.e., polyG was degraded to the same extent by the two enzymes. The corresponding polyMG degradation reactions were stopped at the same time points. Lyases were inactivated by boiling with 1% SDS for 10 min before chromatographic analysis.  $\Delta$  denotes the unsaturated uronic acid on the nonreducing end of the alginate molecules resulting from lyase degradation. *Dpn* denotes an oligomer with *n* residues. The early signal present in all chromatograms is the salt peak. The saturated dimer and trimer (GG and GGG) originate from the reducing end of the polyG molecules.

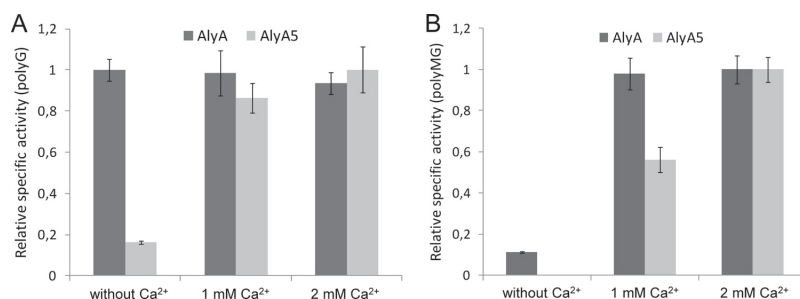


FIGURE 3. Relative specific activity of AlyA (wild type) and AlyA5 against polyG (A) and polyMG (B) with varying concentrations of  $\text{CaCl}_2$  in the reaction buffer. The basis buffer used was 50 mM Tris, 0.2 M NaCl, pH 7.5. For each lyase, the condition giving the highest activity is set to 1. In the absence of  $\text{Ca}^{2+}$ , no activity ( $<1$  unit/mg) of AlyA5 on polyMG could be detected.

Three variants with two substitutions were also made based on the mutations in *alyA6–8*, and among these I51M/T89I is the most interesting in that it retains quite high activity against polyG while it also displays low activity against polyMG.

One major conclusion from all of these data is therefore that the P39H and I51M/T89I variants are the most promising candidates among those constructed, and I51M/T89I is very simi-

lar to AlyA5 both with respect to specificity and activity against polyG. Another interesting observation is that if one considers enhanced specificity only, substitutions S37L, T85A, and S86L also came out as promising, but with the disadvantage that the activity against polyG is quite low. This leads to the conclusion that the substitutions conferring increased G-G specificity are mainly localized to residues Ser<sup>37</sup>, Pro<sup>39</sup>, Thr<sup>85</sup>, and Thr<sup>89</sup> in strand SA2 and flexible loop L1 that are predicted to be present in AlyA (Fig. 4).

It appeared possible that substitutions from different parent variant enzymes might be combined to improve specificity toward G-G linkages further without excessive loss of activity, and the most promising candidate for such an experiment appeared to involve combination of the P39H, I51M, and T89I substitutions. This combination was constructed, but the resulting enzyme turned out to almost completely lack activity

## Alginate Lyases with Enhanced Specificity

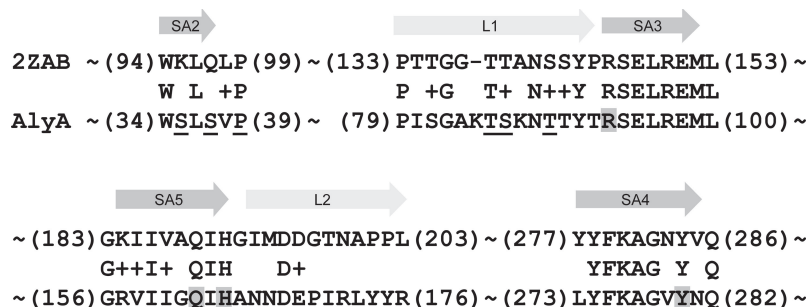


FIGURE 4. Amino acid sequences of strands 2–5 in  $\beta$ -sheet A (SA2–SA5) and flexible loop 1 and 2 (L1 and L2) of AlyA, aligned against lyase A1-II' (Protein Data Bank code 2ZAB) according to PSI-Blast. SA3–5 constitute the most conserved regions in PL7 family lyases. The numbers in parentheses indicate the positions of the amino acid residues in A1-II' and AlyA. The underlined residues were found to be substituted in AlyA mutants isolated in the screen, leading to modified specificity of the resulting lyase. Putative catalytic residues are shaded. Please observe that 2ZAB is the Y284F mutant of A1-II' but that it has been changed back to Tyr<sup>284</sup> in the alignment to highlight the conserved active site.

against both polyG and polyMG, indicating a subtle relation between activity and specificity in AlyA.

*The Properties of AlyA Variants with Substitutions in Conserved Residues Are Consistent with Structural Predictions*—To deduce the molecular mechanisms underlying the properties of the variant lyases described here, we wanted to generate additional support for certain critical assumptions regarding AlyA structure. Iterative PSI-Blast searching with AlyA against the NCBI protein sequence library showed significant similarity to several proteins with known three-dimensional structure; for example, the A1-II' lyase (Protein Data Bank code 2ZAB) was identified by PSI-Blast as having 22% identity and 35% similarity to AlyA over 284 positions, with an *E* value of  $1.0 \times 10^{-42}$ . Sequence alignment with PA1167, ALY-1, and A1-II' indicated that Arg<sup>93</sup>, Gln<sup>162</sup>, His<sup>164</sup>, and Tyr<sup>280</sup> constitute the catalytic residues of AlyA (26). In agreement with this assumption, we found that alanine substitutions in these residues resulted in enzymes with detectable but very low activity against both polyG and polyMG (0.01–1.3% of wt activity; data not shown). We also found that the low activities are not related to reduced expression levels, because SDS-PAGE analyses showed that the enzymes are produced in amounts similar to the wild type enzyme. Thus, the active site is probably organized as predicted. Furthermore, several residues around and in SA3, SA4, and SA5 are conserved among the PL-7 lyases (Fig. 4), and the effect of introducing alanine substitutions by site-specific mutagenesis in some of these residues was also investigated. Most of these variant enzymes (E95A, I160A, Y274A, F275A, and K276A) displayed reduced activity on both polyG and polyMG (0.2–14% of wild type activity; data not shown), whereas the substrate specificity was not significantly changed. In contrast, the Y91A and R97A substitutions resulted in enzymes with increased G-G and M-G specificity, respectively. The total activities were in both cases low: 64 (polyG) and 19 units/mg (polyMG) for Y91A and 24 (polyG) and 104 units/mg (polyMG) for R97A. These data are therefore consistent with the assumption that the main features of our structural predictions are correct, and possi-

ble explanations for the observed changes in substrate specificities have therefore been further elaborated under "Discussion."

## DISCUSSION

To better understand the underlying reasons for the substrate specificities of the variant lyases reported here, we have used sequence alignment between AlyA and A1-II' (Fig. 4) as a basis for an analysis of protein-substrate interactions. The structures of A1-II' complexed with GGG and MMG trimers were analyzed for ligand-protein contacts, and the different interaction types were summarized for selected residues (Table 2). The analysis focused

on mutations in AlyA with significant effect on specificity or activity. Mutations affecting specificity are according to this analysis mainly associated with subsite +2 and to some degree subsite +3 (Arg<sup>97</sup>). Mutations affecting subsite +1, on the other hand, seem to mainly interfere with active site residues, generally leading to reduced activity without significant changes in specificity. However, interactions in Table 2 have to be evaluated with some care. Most mutations will lead to subtle structural changes across the protein, and the effect will be difficult to predict. This is illustrated for example by residues Pro<sup>39</sup> and Thr<sup>85</sup>, where mutations lead to increased specificity even though these residues are not predicted to be in contact with substrate.

During the lyase catalytic reaction, cleavage of the glycosidic linkage occurs between subsites –1 and +1, with the nonreducing end positioned at –1. AlyA seems to cleave G-M linkages in polyMG by accommodating the substrate with G in –1 and +2 and M in +1 and +3. The altered specificity of the isolated mutants can be explained by considering two main types of possible changes introduced by the substitutions. First, the increased G-G specificity could be a result of increased preference for G or reduced preference for M in subsites +1 and +3. However, this should not reduce the activity toward polyG as much as is observed here. A more likely explanation may therefore be an increased preference for M in +2 and possibly in +4. This would lead to nonproductive binding of polyMG and presumably also lower activity toward polyG because of generally weaker interactions in +2. The effects introduced by the identified mutations support the latter hypothesis. In general, reduced polarity will increase the preference for M, which has a greater potential for hydrophobic interactions than G (44). This can be seen in Ser<sup>37</sup> (AlyA3) and Ser<sup>86</sup> (AlyA1), both of which show hydrogen bonding toward +2 (Table 2). Substitution to Ile and Leu, respectively, therefore favors M at +2, *i.e.* nonproductive binding of polyMG. The P39T mutation (AlyA7) seems to exert indirect effects on substrate binding because Pro<sup>39</sup> is not in direct contact with the substrate. Pro<sup>39</sup> terminates  $\beta$ -strand SA2 (Fig. 2), and P39T may lead to elongation of SA2, which in turn will distort the

**TABLE 2**  
Correlations between mutation effects on substrate binding

The table shows specific interactions between residues and substrates (GGG and MMG) in experimental three-dimensional structures (Protein Data Bank codes 2ZAB and 2ZAC, respectively). Interactions are shown for selected residues in these structures corresponding to residues in AlyA where mutations lead to significant changes in specificity and/or activity. The interactions are shown for subsites +1, +2, and +3 in both structures. The position of each residue in the structure is indicated (strands SA2–SA5, loop L1). Interactions were estimated with ligand-protein contacts and include stabilizing interactions (hydrogen bonds (Hb) and hydrophobic contacts (Ph)), destabilizing interactions (hydrophilic-hydrophobic contacts (HH), acceptor-acceptor contacts (AA)), and other nonclassified interactions (O). The contact surface area is shown for each contact type, and the dominating interactions are shown in bold type. Destabilizing interactions are indicated with negative contact surface areas. The comments in the table indicate possible explanations of the observed effects from the mutations.

Position	Mutation	Structure	+1 G	+2 G	+3 G	+1 M	+2 M	+3 G	Comments
<b>Reduced activity</b>									
Arg <sup>93</sup>	Ala	Arg <sup>146</sup> SA3	Hb (17.3) O (15.0)	Hb (1.7) O (13.4)		Hb (13.3) O (5.2)	Hb (1.7) O (7.6)		Active site
Glu <sup>95</sup>	Ala	Glu <sup>148</sup> SA3							H-bonds to Arg <sup>146</sup> and Gln <sup>189</sup>
Ile <sup>160</sup>	Ala	Val <sup>187</sup> SA5							May affect loop with Gln <sup>189</sup> and His <sup>191</sup>
Gln <sup>162</sup>	Ala	Gln <sup>189</sup> SA5	Hb (12.6) AA (-17.8) O (3.1)			Hb (21.0) AA (-18.2) O (4.1)			Active site
His <sup>164</sup>	Ala	His <sup>191</sup> SA5	Hb (16.1) HH (-1.1) O (17.5)	Hb (0.5) O (2.7)		Hb (13.5) O (10.1)	Hb (1.4) O (7.0)		Active site
Tyr <sup>274</sup>	Ala	Tyr <sup>278</sup> SA4		Hb (9.9) O (17.5)	Hb (2.8)		O (21.2)	Hb (2.4) O (0.2)	Stacking interaction with Arg <sup>150</sup> and His <sup>191</sup>
Phe <sup>275</sup>	Ala	Phe <sup>279</sup> SA4							May affect strand with Tyr <sup>278</sup> and Lys <sup>280</sup>
Lys <sup>276</sup>	Ala	Lys <sup>280</sup> SA4	Hb (3.3)	Hb (16.4) O (14.5)			Hb (17.0) O (7.8)		H-bond to Arg <sup>146</sup>
Tyr <sup>280</sup>	Ala	Phe <sup>284</sup> SA4	Ph (8.6) O (17.8)			O (36.2)			Active site (mutated Y284F), stacking interaction with Arg <sup>146</sup>
<b>PolyG preference (with reduced activity)</b>									
Ser <sup>37</sup>	Ile	Gln <sup>97</sup> SA2		Hb (19.6)	Hb (5.4) O (2.5)		Hb (18.9) O (3.2)	Hb (6.7) O (1.6)	Increased preference for M in +2 (nonproductive on polyMG)
Pro <sup>39</sup>	His/Thr	Pro <sup>99</sup>							May affect loop with e.g. Gln <sup>97</sup>
Thr <sup>85</sup>	Ala	Thr <sup>138</sup> L1		Hb (15.8)	Ph (8.5)		Hb (19.8)	Ph (7.2)	May affect loop with e.g. Thr <sup>139</sup>
Ser <sup>86</sup>	Leu	Thr <sup>139</sup> L1		HH (-5.2) O (13.4)	HH (-7.6) O (2.7)		HH (-6.2) O (8.7)	HH (-4.9) O (1.7)	Increased preference for M in +2 (nonproductive on polyMG)
Thr <sup>89</sup>	Ile/Ala	Ser <sup>142</sup> L1	O (4.7)			Hb (0.2) O (6.7) O (0.3)			May affect loop with Thr <sup>139</sup> , for example
Tyr <sup>91</sup>	Ala	Tyr <sup>144</sup> L1							May affect loop with Thr <sup>139</sup> , for example
<b>PolyMG preference (with reduced activity)</b>									
Arg <sup>97</sup>	Ala	Arg <sup>150</sup> SA3		HH (-1.2)	Hb (39.0) HH (-0.2) O (5.8)		Ph (0.2)	Hb (39.9) O (6.2)	Increased preference for M in +3 (productive on polyMG)

$\beta$ -strand and affect hydrogen bonding by Ser<sup>37</sup>. Similar indirect effects can be seen for residues Thr<sup>85</sup> and possibly Thr<sup>89</sup> residing in loop L1. Although these residues show only limited direct interaction with substrates, they can exert an indirect effect on residue Ser<sup>86</sup> by modifying the properties of the loop. Residue Ser<sup>86</sup> resides in L1 and hydrogen bonding to +2 may be lost if the loop conformation is changed. It should be noted that L1 in AlyA contains two serine and four threonine residues, pointing to the importance of potential for polar interactions in this structural element.

In summary, the introduced mutations apparently lead to lyases with reduced ability for interaction with polyMG in a productive manner, *i.e.* the enzymes are rendered less effective toward this substrate. The activity toward polyG is also reduced, however to a lower extent, and the mutant lyases therefore appear as having increased specificity toward G-G linkages.

We found it intriguing that AlyA5 lyase activity is much more Ca<sup>2+</sup>-dependent than its parent enzyme, and none of the close homologues of AlyA with known three-dimensional structure include bound Ca<sup>2+</sup>. In contrast, the more distantly related enzymes  $\beta$ -1,4-glucuronan lyase from the fungus *Trichoderma reesei* (45) and alginate lyase from *Alteromonas* sp. (the structure is published as Protein Data Bank entry 1J1T) both include Ca<sup>2+</sup>. The ions are bound at different positions in these struc-

tures and apparently play mainly structural and stabilizing roles. Thus, it is possible that Ca<sup>2+</sup> serves a similar function in AlyA5. A substitution in Pro<sup>39</sup> may cause significant structural changes in strand SA2 (see above), and Ca<sup>2+</sup> might be essential for stabilizing the affected region after mutation.

The aim of the present work was to isolate mutants of AlyA with increased specificity for G-G linkages. To our knowledge the mutants reported here represent the most G-G-specific alginate lyases known at present. It is also an advantage that AlyA5 or its derivatives can be efficiently produced in *E. coli*, and we are currently aiming at using the mutant enzymes together with other lyases displaying relevant specificities as tools to more efficiently deduce the fine structure of alginates.

## REFERENCES

- Linker, A., and Jones, R. S. (1964) *Nature* **204**, 187–188
- Govan, J. R., Fyfe, J. A., and Jarman, T. R. (1981) *J. Gen. Microbiol.* **125**, 217–220
- Gorin, P., and Spencer, J. (1966) *Can. J. Microbiol.* **44**, 993–998
- Cote, G., and Krull, L. (1988) *Carbohydr. Res.* **181**, 143–152
- Haug, A., and Larsen, B. (1969) *Biochim. Biophys. Acta* **192**, 557–559
- Haug, A., and Larsen, B. (1971) *Carbohydr. Res.* **17**, 297–308
- Ertesvåg, H., Hoidal, H. K., Hals, I. K., Rian, A., Døseth, B., and Valla, S. (1995) *Mol. Microbiol.* **16**, 719–731
- Skjåk-Braek, G., Grasdalen, H., and Larsen, B. (1986) *Carbohydr. Res.* **154**, 239–250
- Remminghorst, U., and Rehm, B. H. (2006) *Biotechnol. Lett.* **28**,

## Alginate Lyases with Enhanced Specificity

- 1701–1712
10. Onsoyoyen, E. (1996) *Carbohydr. Eur.* **14**, 26–31
  11. Skjåk-Braek, G., and Espevik, T. (1996) *Carbohydr. Eur.* **14**, 19–23
  12. Coviello, T., Matricardi, P., Marianecchi, C., and Alhaique, F. (2007) *J. Control. Release* **119**, 5–24
  13. Zimmermann, H., Shirley, S. G., and Zimmermann, U. (2007) *Curr. Diab. Rep.* **7**, 314–320
  14. Hashimoto, T., Suzuki, Y., Suzuki, K., Nakashima, T., Tanihara, M., and Ide, C. (2005) *J. Mater. Sci. Mater. Med.* **16**, 503–509
  15. Smelcerovic, A., Knezevic-Jugovic, Z., and Petronijevic, Z. (2008) *Curr. Pharm. Des.* **14**, 3168–3195
  16. Petruyte, S. (2008) *Dan. Med. Bull.* **55**, 72–77
  17. Boateng, J. S., Matthews, K. H., Stevens, H. N., and Eccleston, G. M. (2008) *J. Pharm. Sci.* **97**, 2892–2923
  18. Thomas, S. (2000) *J. Wound Care* **9**, 56–60
  19. Wong, T. Y., Preston, L. A., and Schiller, N. L. (2000) *Annu. Rev. Microbiol.* **54**, 289–340
  20. Campa, C., Oust, A., Skjåk-Braek, G., Paulsen, B. S., Paoletti, S., Christensen, B. E., and Ballance, S. (2004) *J. Chromatogr. A* **1026**, 271–281
  21. Haug, A., Larsen, B., and Smidsrød, O. (1967) *Acta Chem. Scand.* **21**, 691–704
  22. Boyd, J., and Turvey, J. R. (1977) *Carbohydr. Res.* **57**, 163–171
  23. Baron, A. J., Wong, T. Y., Hicks, S. J., Gacesa, P., Willcock, D., and McPherson, M. J. (1994) *Gene* **143**, 61–66
  24. Haugen, F., Kortner, F., and Larsen, B. (1990) *Carbohydr. Res.* **198**, 101–109
  25. Yamasaki, M., Ogura, K., Hashimoto, W., Mikami, B., and Murata, K. (2005) *J. Mol. Biol.* **352**, 11–21
  26. Osawa, T., Matsubara, Y., Muramatsu, T., Kimura, M., and Kakuta, Y. (2005) *J. Mol. Biol.* **345**, 1111–1118
  27. Yamasaki, M., Moriaki, S., Miyake, O., Hashimoto, W., Murata, K., and Mikami, B. (2004) *J. Biol. Chem.* **279**, 31863–31872
  28. Miyake, O., Ochiai, A., Hashimoto, W., and Murata, K. (2004) *J. Bacteriol.* **186**, 2891–2896
  29. Matsubara, Y., Kawada, R., Iwasaki, K., Oda, T., and Muramatsu, T. (1998) *J. Protein Chem.* **17**, 29–36
  30. Chavagnat, F., Heyraud, A., Colin-Morel, P., Guinand, M., and Wallach, J. (1998) *Carbohydr. Res.* **308**, 409–415
  31. Sambrook, J., and Russel, D. (2001) *Molecular Cloning: A Laboratory Manual*, 3rd Ed., Cold Spring Harbor Laboratory, Cold Spring Harbor, NY
  32. Sletta, H., Tøndervik, A., Hakvåg, S., Aune, T. E., Nedal, A., Aune, R., Evensen, G., Valla, S., Ellingsen, T. E., and Brautaset, T. (2007) *Appl. Environ. Microbiol.* **73**, 906–912
  33. Bakke, I., Berg, L., Aune, T. E., Brautaset, T., Sletta, H., Tøndervik, A., and Valla, S. (2009) *Appl. Environ. Microbiol.* **75**, 2002–2011
  34. Holtan, S., Zhang, Q., Strand, W. I., and Skjåk-Braek, G. (2006) *Biomacromolecules* **7**, 2108–2121
  35. Haug, A., Larsen, B., and Smidsrød, O. (1974) *Carbohydr. Res.* **32**, 217–225
  36. Ballance, S., Holtan, S., Aarstad, O. A., Sikorski, P., Skjåk-Braek, G., and Christensen, B. E. (2005) *J. Chromatogr.* **1093**, 59–68
  37. Ogura, K., Yamasaki, M., Mikami, B., Hashimoto, W., and Murata, K. (2008) *J. Mol. Biol.* **380**, 373–385
  38. Berman, H. M., Westbrook, J., Feng, Z., Gilliland, G., Bhat, T. N., Weissig, H., Shindyalov, I. N., and Bourne, P. E. (2000) *Nucleic Acids Res.* **28**, 235–242
  39. Sobolev, V., Sorokine, A., Prilusky, J., Abola, E. E., and Edelman, M. (1999) *Bioinformatics* **15**, 327–332
  40. Wallace, A. C., Laskowski, R. A., and Thornton, J. M. (1995) *Protein Eng.* **8**, 127–134
  41. Guex, N., and Peitsch, M. C. (1997) *Electrophoresis* **18**, 2714–2723
  42. Altschul, S. F., Madden, T. L., Schäffer, A. A., Zhang, J., Zhang, Z., Miller, W., and Lipman, D. J. (1997) *Nucleic Acids Res.* **25**, 3389–3402
  43. Thompson, J. D., Gibson, T. J., and Higgins, D. G. (2003) *Curr. Prot. Bioinform.* 2.3.1–2.3.22
  44. Chan, C., Burrows, L. L., and Deber, C. M. (2004) *J. Biol. Chem.* **279**, 38749–38754
  45. Konno, N., Ishida, T., Igarashi, K., Fushinobu, S., Habu, N., Samejima, M., and Isogai, A. (2009) *FEBS Lett.* **583**, 1323–1326





# Paper IV



# Alginate Sequencing: An Analysis of Block Distribution in Alginates Using Specific Alginate Degrading Enzymes

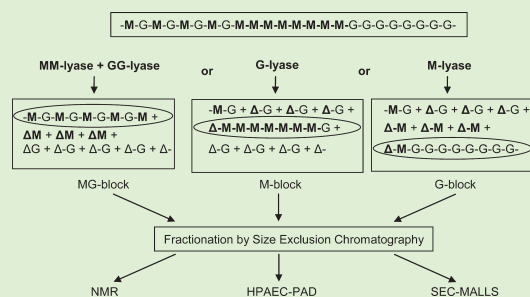
Olav Andreas Aarstad,<sup>\*,†</sup> Anne Tøndervik,<sup>‡</sup> Håvard Sletta,<sup>‡</sup> and Gudmund Skjåk-Bræk<sup>†</sup>

<sup>†</sup>Department of Biotechnology, Norwegian University of Science and Technology, NTNU Sem Sælands vei 6-8, N-7491 Trondheim, Norway

<sup>‡</sup>Department of Biotechnology, SINTEF Materials and Chemistry, N-7465 Trondheim, Norway

## Supporting Information

**ABSTRACT:** Distribution and proportion of  $\beta$ -D-mannuronic and  $\alpha$ -L-guluronic acid in alginates are important for understanding the chemical-physical properties of the polymer. The present state of art methods, which is based on NMR, provides a statistical description of alginates. In this work, a method was developed that also gives information of the distribution of block lengths of each of the three block types (M, G, and MG blocks). This was achieved using a combination of alginate lyases with different substrate specificities, including a novel lyase that specifically cleaves diguluronic acid linkages. Reaction products and isolated fragments of alginates degraded with these lyases were subsequently analyzed with <sup>1</sup>H NMR, HPAEC-PAD, and SEC-MALLS. The method was applied on three seaweed alginates with large differences in sequence parameters ( $F_G = 0.32$  to  $0.67$ ). All samples contained considerable amounts of extremely long G blocks ( $DP > 100$ ). The finding of long M blocks ( $DP \geq 90$ ) suggests that also algal epimerases act by a multiple attack mechanism. Alternating sequences (MG-blocks) were found to be much shorter than the other block types. In connection with method development, an oligomer library comprising both saturated and unsaturated oligomers of various composition and DP 2–15 was made.



## INTRODUCTION

The heterogeneity of polysaccharides with respect to chemical composition and chain length has hampered the development of sequencing strategies analogous to those used for polynucleotides and polypeptides. Nevertheless, structural elucidation and sequencing of polysaccharides is a prerequisite for understanding their physical properties. Moreover, polysaccharides such as heparin and heparin sulfate contain biologically active epitopes that have been attributed to specific sugar sequences.<sup>1</sup> Our hypothesis is that the binary heteropolysaccharides alginate is particularly well-suited for a sequencing approach to achieve a better understanding of not only their functional and biological properties but also their use as a model system for other more complex polysaccharides. Alginate is a collective term for a family of polysaccharides produced by brown algae and bacteria.<sup>2–4</sup> They are linear copolymers of 1→4 linked  $\beta$ -D-mannuronic acid (M) and  $\alpha$ -L-guluronic acid (G) arranged in a blockwise pattern along the chain with homopolymeric regions of M (M blocks) and G (G blocks) interspaced with regions of alternating structure (MG blocks). This nonrandom block structure in alginates is a consequence of a unique biosynthetic pathway where the guluronic acid residues are introduced into a preformed mannuronan polymer by a family of isoenzymes with C-5 epimerase activity;<sup>5–7</sup> for example, the bacterium *Azotobacter*

*vinelandii* encodes seven epimerases named AlgE1–AlgE7.<sup>8–10</sup> These epimerases act processively on the mannuronan chain introducing either GMG or GG blocks of various length<sup>11–15</sup> and are therefore responsible for the plethora of alginate structure.

Alginates form hydrogels with divalent cations such as  $Ca^{2+}$ , and this has been attributed to the ion-binding properties of the G blocks, forming the so-called “egg-box” model<sup>16</sup> that implies that junction zones are formed by two facing helical G sequences: each cross-linking ion (i.e.,  $Ca^{2+}$ ) interacts with two adjacent G residues as well as with two G residues in the opposing chain. Currently, sequence determination of alginates is based on high-resolution <sup>1</sup>H and <sup>13</sup>C NMR spectroscopy.<sup>17–20</sup> This makes it possible to determine the monad frequencies  $F_M$  and  $F_G$ , the four nearest neighboring (diad) frequencies  $F_{GG}$ ,  $F_{MG}$ ,  $F_{GM}$ , and  $F_{MM}$ , and the eight next nearest neighboring (triad) frequencies. Knowledge of these frequencies enables for example the calculation of the average G-block length larger than 1, a value that correlate well with ion-binding and gelling properties.<sup>21–23</sup> Recent studies have, however, shown that G blocks are not the only sequences involved in junction

Received: September 19, 2011

Revised: November 1, 2011

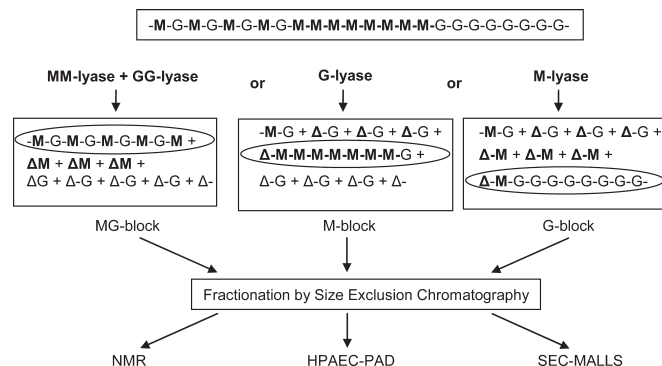


**Figure 1.** Schematic presentation of an approach to fine structure study on alginates.

formation.<sup>24,25</sup> More specifically, the direct involvement of repeating MG units in the formation of both mixed GG/MG and MG/MG junctions was proposed. There is a need for further understanding, particularly of the absolute length and distribution of the various blocks. Moreover, some alginates have immune-stimulating properties, although the detailed molecular structure of the epitopes is still unknown.<sup>26,27</sup> Therefore, a more thorough "sequencing" of alginates would be crucial for designing bioactive materials.

The overall sequencing strategy described in this Article (outlined in Figure 1) involves enzymatic degradation of the polymers into smaller fragments, followed by determination of size, composition, and sequence of the fragments using SEC, NMR, HPAEC-PAD, and SEC-MALLS.

Utilizing alginate lyases with appropriate specificity, the polymer is degraded while the blocks of interest are conserved. Fractionation by SEC, followed by analysis of composition and chain length of the fragments yields information on block distribution.

Guluronic acid, mannuronic acid, and 4-deoxy-L-erythro-hex-4-enepyranosyluronate are abbreviated G, M, and  $\Delta$ .

Enzymes that hydrolyze specific glycosidic linkages are invaluable tools for structural analysis of macromolecules. This is also the case with alginate specific degrading enzymes, of which all presently identified are lyases. These enzymes split alginate by  $\beta$ -elimination, leaving an unchanged saturated uronate on the reducing end and an unsaturated (4-deoxy-L-erythro-hex-4-enepyranosyluronate) residue symbolized with ( $\Delta$ ) at the non-reducing end. Alginate lyases are widely distributed in nature, either in organisms utilizing alginate as carbon source or in bacteriophages. They are all endolyases, and their specificity is commonly directed toward one of the residues in the glycosidic linkage. For example, the lyase from *Klebsiella aerogenes* cleaves G-G and G-M specifically for the guluronate in the glycon position leaving a reducing guluronate end and an unsaturated end originating from either M or G.<sup>28</sup> The lyase from *A. vinelandii* is specific for M in the glycon position cleaving M-M and M-G. Other enzymes are specific for both sugars such as M-M specific lyase from *P. alginovora*.<sup>29</sup> Although the chemical identity of the aglycon is lost by the lyase-catalyzed reaction, the unsaturated end functions as both a chromophore (UV abs. at 230 nm) and a "tag" easily identified by NMR. Combined with MS and NMR, specific lyases have been used successfully in analyses of subsite specificity for the epimerases<sup>14</sup> as well as in analysis of block length and block length distribution in

epimerised alginates.<sup>15</sup> We are currently using enzyme engineering for developing more specific lyases to be used in alginate sequencing. It is important to realize that in an alginate chain population neither the size nor the composition and sequence of each chain will be alike. The scope of this study is therefore to analyze the length and distribution of the three block types in alginate from various sources rather than to search for the end-to-end sequential structure of a single alginate molecule.

## MATERIALS AND METHODS

**Alginates.** Poly-M ( $F_G = 0$ ) was isolated from an *algG* mutant of *Pseudomonas fluorescens*.<sup>30</sup> Purification and deacetylation were done as described elsewhere.<sup>31</sup>

Poly-MG ( $F_G = 0.46$  and  $F_{GG} = 0.00$ ) was prepared from mannuronan epimerized with the mannuronan C-5 epimerase AlgE4. Mannuronan (0.25% w/v) was dissolved in 50 mM MOPS buffer, pH 6.9, with 2.5 mM  $\text{CaCl}_2$  and 10 mM NaCl. A crude enzyme solution of AlgE4 was added to give a mannuronan/enzyme ratio of 200. The solution was incubated at 37 °C with gentle stirring. After 24 h, EDTA was added to a final concentration of 4 mM in order to deplete the solution for  $\text{Ca}^{2+}$  ions and thereby stop the epimerization reaction. The solution was dialyzed against 50 mM NaCl and finally against MQ water until the conductivity was below 4  $\mu\text{S}$  at 4 °C, followed by neutralization with 100 mM NaOH and freeze-drying.

Poly-G ( $F_G = 0.95$ ) with a number-average degree of polymerization,  $\text{DP}_n \approx 20$ , was prepared from *L. hyperborea* according to Haug et al.<sup>32,33</sup>

Acid hydrolysates of Poly-M, Poly-G, and Poly-MG were prepared by a two-step hydrolysis at pH 5.6 and 3.8, as described by Holtan et al.<sup>34</sup>

Sodium alginates from *Macrocystis pyrifera* were purchased from Sigma Chemicals. Sodium alginates from *Durvillea potatorum* and *Laminaria hyperborea* (SF60) were obtained from FMC Biopolymer. Chemical composition, molecular weight ( $M_w$ ), degree of polymerization ( $\text{DP}_n$ ), and polydispersity index (PI) measured with  $^1\text{H}$  NMR and SEC-MALLS are reported in Table S1 in the Supporting Information.

**Lyase Degradation of Alginates.** Partially lyase-degraded Poly-M and Poly-MG were made by the addition of  $(2.2 \text{ and } 2.75) \times 10^{-3}$  U/mg substrate of M-lyase from *Haliotis tuberculata* to a 0.25% solution of substrate in 200 mM  $\text{NH}_4\text{Ac}$ , pH 6.9, with 50 mM NaCl, followed by incubation at 30 °C for 27 and 51 h, respectively. Partially lyase-degraded Poly-G were made in the same manner by incubation of a 2% w/v solution of G blocks in the same solvent with 0.04 U/mg substrate of the G-lyase AlyA from *Klebsiella pneumoniae* for 30 min. The lyase reactions were terminated by heating the solutions at 95 °C for 10 min.

An oligomer library based on an homologous series of  $\Delta G$ ,  $\Delta M$ ,  $\Delta MG$ ,  $M$ ,  $G$ , and  $MG$  oligomers with DP 2–10 was made by fractionation of acid hydrolysates and lysates on SEC columns, as described below. These were later used as standards for NMR and HPAEC-PAD.

*D. potatorum*, *L. hyperborea*, and *M. pyrifera* alginates (1% w/v, 50–100 mg) were degraded by M-lyase, G-lyase, or a combination of MM-lyase and GG-lyase using the same solvent and temperature as above. pH was adjusted to 7.45 to 7.50 by the addition of 0.1 M NaOH prior to addition of lyase. Incubation time and enzyme amounts are given in relevant figures. After termination of the reaction, solutions were freeze-dried.

It is important to avoid Tris buffer during sample preparation because this will cause imine formation and possible Maillard browning. Imines are also formed in the presence of  $NH_4Ac$  but to a lesser extent.<sup>35</sup> After freeze-drying, which promotes the reaction further, the final yield is about 50 and 1–10% for the two buffering agents, respectively (unpublished data). It may be possible to increase the yield if one wants to exploit the intermediate imine functionality for further reactions.

**Epimerases and Lyases.** The mannuronan C-5 epimerase AlgE4 was produced by fermentation of a recombinant strain of *Escherichia coli*.<sup>8,31</sup> The enzyme was partially purified by ion exchange chromatography on Q-sepharose FF and by hydrophobic interaction chromatography on phenyl sepharose (Pharmacia). Specificity and origin of alginate lyases used in this work are shown in Table S2 in Supporting Information. The AlyA, AlyAS, *H. tuberculata*, and AlxM lyases are hereafter referred to as G-, GG-, M-, and MM-lyases, respectively, to emphasize their specificity.

Alginate lyase from *Halobacterium tuberculata* was purified from abalones, as described by Boyen et al.<sup>36</sup> AlyA, AlyAS, and AlxM alginate lyases were produced recombinantly in *E. coli* RV308. The genes encoding AlxM were PCR-amplified from the genome of strain ATCC43367 and cloned into an expression vector as previously described for AlyA and AlyAS.<sup>37</sup> Fermentations at high cell density for recombinant protein production were performed as previously described,<sup>38</sup> and lyases were purified by ion-exchange chromatography on SP-Sephacrose FF (GE Healthcare) after mechanical disruption of the bacterial cells. Purity of the protein fractions was analyzed by SDS-PAGE.

Lyase activity ( $U \equiv \text{Abs} \cdot \text{min}^{-1}$ ) was measured as the increase in absorbance at 230 nm using Poly-M, Poly-MG, and Poly-G as substrates. Lyases (0.01 to 0.08 U/mg substrate) were added to a quartz cuvette with 0.5 mg/mL of substrate in 200 mM  $NH_4Ac$ , pH 6.9, with 50 mM NaCl, and a time progress curve was recorded for 30 min at 22 °C.

**HPAEC-PAD.** The AS4A column used in this study was originally intended for separation of inorganic anions but has been used for separation of alginate oligomers because of its low charge density. Carbowac PA100 or PA200 columns are designed for separation of oligosaccharides but were in this case found to cause unnecessary long retention times or a need for high concentrations of eluent.

Lyase-degraded alginates and acid hydrolysates were analyzed on a Dionex BioLC system (Dionex, Sunnyvale, CA) consisting of an AS50 autosampler, an ED40 electrochemical detector with a nondisposable gold working electrode, and a GP50 gradient pump, as previously described.<sup>37,39</sup> Samples were separated at room temperature on a Dionex IonPac AS4A (4 × 250 mm) anion-exchange column connected to an IonPac AG4A (4 × 50 mm) guard column using a linear gradient of 8.75 mM sodium acetate/min in 100 mM sodium hydroxide. Hydrolysates and homologous series of alginate oligomers were used for peak assignment. Data acquisition and analysis were performed using Chromeleon 6.6 software. Detector response factors previously reported<sup>39,40</sup> were used to calculate the relative amount of identified oligomers.

**Fractionation of Alginates by Size Exclusion Chromatography.** Lyase-degraded alginates and acid hydrolysates (50–150 mg) were fractionated on three Superdex 30 size exclusion columns (2.6 cm × 60 cm, serially connected), as described elsewhere.<sup>15</sup> The detector used was an online refractive index detector (Shimadzu

RID-6A). Collected fractions (4–6 mL) were pooled and freeze-dried three times for removal of  $NH_4Ac$ .

**<sup>1</sup>H NMR Spectroscopy.** Samples (1–5 mg) were dissolved in 600  $\mu\text{L}$  of  $D_2O$ , and the pH<sup>\*</sup> was adjusted to 6.5 to 7 with NaOD. 3-(Trimethylsilyl)-propionic-2,2,3,3-*d*<sub>4</sub> acid sodium salt (TSP) (Aldrich, Milwaukee, WI) in  $D_2O$  (1%, 5  $\mu\text{L}$ ) was added as the internal standard. Triethylenetetraamine-hexaacetate (TTHA) (0.3M, 20  $\mu\text{L}$ ) was routinely added as a calcium chelator. <sup>1</sup>H NMR spectra were recorded on a Bruker DPX 300 or 400 spectrometer at 90 °C. Spectra were obtained using a 30° pulseflip-angle, a spectral width of 4789 Hz, and a 32 K data block size. Peaks were assigned according to previous work.<sup>14,20</sup>

**SEC-MALLS.** Samples (1–5 mg/mL, 100–200  $\mu\text{L}$ , 0.2  $\mu\text{m}$  filtered) were analyzed on a HPLC system consisting of an online degasser, HPLA isocratic pump, autoinjector, precolumn, and Tosoh Biosep TSK 6000, 5000, and 4000 (PWXL) columns serially connected. The outlet was connected to a Dawn Helios II MALLS photometer (Wyatt), followed by a Optilab T-rEX differential refractometer. The mobile phase was 50 mM  $Na_2SO_4$ /10 mM EDTA, pH 6. Data were collected and processed using ASTRA 5.0 and in some instances processed further in an Excel spreadsheet.<sup>41</sup>

## RESULTS AND DISCUSSION

The aim of this study was to elucidate the block structure of complex natural alginates of algal origin by using specific lyases combined with analytical tools. It is therefore crucial to obtain information on the characteristics of the lyases. Specificity, end products, and minimum substrate requirements were therefore studied using fully characterized alginate samples like Poly-M, Poly-MG, Poly-G, and oligomers with well-defined chain length and composition.

**Analysis of Lyase Specificity Toward Poly-M, Poly-MG, and Poly-G.** The use of lyases as a sequencing tool relies on high specificities of the enzymes toward defined glycosidic linkages. The activity of the different lyases utilized in this study toward each of the three pure block structures was analyzed as described in the Materials and Methods and is given in Table S3 in the Supporting Information.

**HPAEC-PAD Analysis of Lyase End Products.** The lyases were incubated with their optimal substrate, and the products after complete degradation were analyzed by HPAEC-PAD.

Poly-M were degraded into dimers and trimers by the M-lyases. The presence of unsaturated monomers in the mixtures cannot be excluded because they would be masked by the void. The G-lyases degraded their G-block substrate into dimers and trimers, but the lysates also contained oligomers with chain-length 4–6. This may be caused by differences in subsites and how the enzymes bind oligomers but is mainly a consequence of the fact that Poly-G contains ~5% M residues, which are not substrates for the G and GG-lyases and results in more complex chromatograms with several compounds for each chain length.

Because the only saturated oligomers originate from the nonreducing end, it can be noted that HPAEC-PAD analyses of completely lyase degraded alginates provide an alternative method to measure the  $DP_n$  of the starting material.

From the ratio between saturated and unsaturated oligomers,  $DP_n$  of the original sample is given by the expression

$$\overline{DP}_n = \frac{2(C_2 + C_{\Delta 2}) + 3(C_3 + C_{\Delta 3}) + 4(C_4 + C_{\Delta 4})}{(C_2 + C_3 + C_4)} \quad (1)$$

where  $C_n$  and  $C_{\Delta n}$  are molar concentrations of saturated and unsaturated  $n$ -mer.

The linear dynamic range of a PAD detector is  $>10^3$ , and the detection limit is in the picomolar region. In principle, this

should be both a more sensitive and a more accurate method than  $^1\text{H}$  NMR, SEC-MALLS, and colorimetric assays such as the Shomogyi–Nelson method. In practice, resolution and possible side reactions during sample preparation, followed by chromatography under alkaline conditions limit the scope. If a sample contains all possible di-, tri-, and tetramers, baseline separation of up to 42 compounds may be required. Columns with higher charge density such as CarboPac PA1 or PA10 may be better suited for this purpose.

**Lyase Activity on Alginate Oligomers of Different Composition.** Unsaturated G-, M-, and MG-oligomers from the oligomer library were incubated with the relevant lyases in order to find the shortest oligomer that could be a substrate for degradation by each lyase. The M- and MM-lyases can degrade an unsaturated tetramer ( $\Delta\text{MMM}$ ), whereas the G- and GG-lyase require a hexamer to support activity. Substrates and products are listed in Table S4 in the Supporting Information.

**Optimization of Specific Degradation Conditions.** The main indication of appropriate conditions for lyase degradation is that the long oligomers of each block type are compositionally pure. Regarding the analysis of MG-block distribution, it is important to avoid significant G-M cleavage and at the same time choose conditions that will degrade all M and G blocks with  $\text{DP} > 6$ . The combination of  $^1\text{H}$  NMR and HPAEC-PAD will in most cases provide enough information about both sequence and amount of shorter oligomers. The degradation conditions are less critical in the analysis of G- and M-block distribution because the cleavage of G-G and M-M bonds by M- and G-lyase, respectively, is very slow.

Optimal conditions for degradation by MM-lyase were found using Poly-MG ( $F_G = 0,46$ ) as a negative control. With the same conditions necessary to degrade all MM sequences with  $\text{DP} > 4$  in our starting materials, Poly-MG was almost intact, as shown in Figure S5 in the Supporting Information. Short MM sequences between long MG blocks are cleaved into dimer and trimer. The weight fraction of these are close to  $F_{\text{MM}}$  in the undegraded sample. An  $^1\text{H}$  NMR spectrum of the remaining void fraction confirms that there are not any detectable MM sequences left. The  $\overline{\text{DP}}_n$  of this fraction was estimated to be  $\sim 75$ . (See Figure S6 in Supporting Information.)

In a similar approach, a time series of Poly-G and Poly-MG incubated with the same amount of GG-lyase from 1 to 48 h was analyzed with HPAEC-PAD. After 24 h, there are only trace amounts of oligomers with  $\text{DP} > 7$  left in the Poly-G lysate, whereas only a small fraction of Poly-MG is degraded. (See Figure S7 in the Supporting Information.) The difference between 24 and 48 h is small for Poly-G, but Poly-MG is significantly degraded after 48 h. It was therefore concluded that 24 h is close to the optimal incubation time.

**Analysis of Block Distribution in Alginates from Brown Seaweed.** The sequencing strategy depicted in Figure 1 was then applied on alginates with varying composition. Commercially available alginates from whole plants of the brown kelps *Durvillea potatorum* and *Macrocystis pyrifera* and from the stipes of *Laminaria hyperborea* (SF60) were chosen as starting materials. These alginates have comparable  $M_w$  yet large differences in composition and sequence (as determined by  $^1\text{H}$  NMR), which makes them very suitable for a first validation of the method. SEC chromatograms of the lyase degraded alginates are shown in Figure 2.

Samples (100 mg) were separated on three Superdex 30 columns serially connected using 0.1 M  $\text{NH}_4\text{Ac}$  as mobile phase

and a flow rate of 0.8 mL/min. All chromatograms were normalized to adjust for differences in injection volumes.

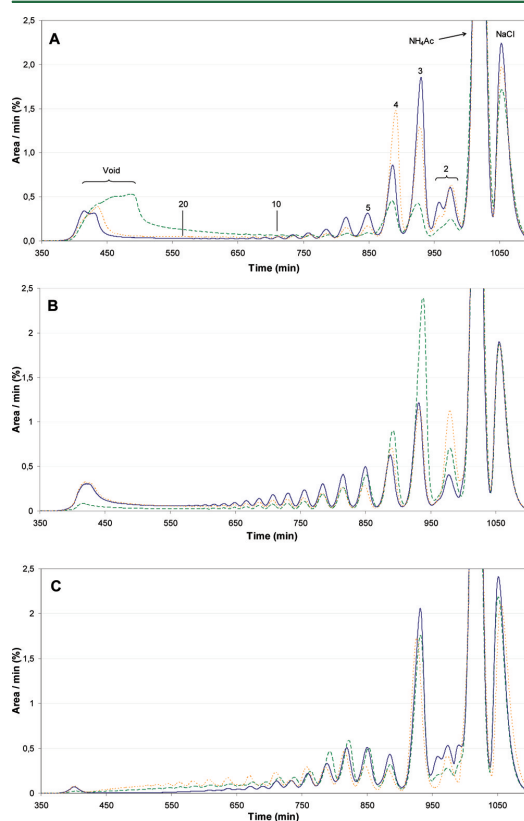


**Figure 2.** SEC chromatograms of *D. Potatorum* (blue —), *M. Pyrifera* (yellow ●●●), and *L. hyperborea* (green —) incubated for 24 h with (A) M-lyase (1.6U), (B) G-lyase (8.5U), and (C) a combination of MM-lyase (2U) and GG-lyase (0.69U).

A common feature of all samples degraded by M- and G-lyases is the bimodal distribution of oligomers. This is most evident for samples degraded by M-lyase (Figure 2A). The dimer fractions in Figure 2A,C consist of two unresolved peaks due to partial separation of  $\Delta\text{G}$  and  $\Delta\text{M}$ . The void fraction contains oligomers with chain lengths starting from  $\sim 35$  and shows various degree of asymmetry. In particular, *L. hyperborea* degraded by M-lyase has a large, asymmetric void peak. The shape of the void fraction should not be interpreted as the distribution of chain lengths  $> 35$  because these oligomers are not separated and there may be additional chromatographic artifacts such as tailing caused by column overload.

Chromatograms of samples degraded by MM- and GG-lyase (Figure 2C) are markedly different from the others because they lack a prominent void peak, suggesting that pure MG-sequences are not as extended as M and G blocks. Because the conditions were the same in our control experiments, it is not likely that this is a result of unwanted degradation of MG blocks. There also seems to be a regular pattern starting from about  $\text{DP}_{10}$ , where even-numbered oligomers are more

abundant than odd-numbered oligomers. This is most apparent for *M. pyrifera* and gives an indication of longer polyalternating blocks in this alginate. The resolution was slightly lower than that for M and G blocks. This may be due to larger flexibility in alternating sequences and is perhaps also an indication of compositional heterogeneity.

During analysis of *M. pyrifera* degraded by MM- and GG-lyase, it was discovered that the high  $M_w$  part of the void remained constant when the concentration of GG-lyase was increased from 2 to 8 times. In addition, a relatively narrow peak appears in the void region of all chromatograms of samples degraded with MM and GG-lyase. It is therefore likely that our samples contain a small fraction of impurities. The protein content in various alginates has been found to be in the range of 0.1 to 1.5% of dry weight.<sup>42</sup> From the chromatograms of samples degraded by MM and GG-lyase, the upper limit of high-molecular-weight compounds other than alginate was estimated to 0.5% for *L. hyperborea* and 1.4% for *D. potatorum* and *M. pyrifera*. Although the contribution is quite small, this part of the void was subtracted from every chromatogram in the calculation of weight distribution.

**Distribution of G-, M-, and MG-Oligomers in Alginates from Brown Seaweed.** Chain-length assignment and calculation of weight fractions of each chain-length were based on SEC chromatograms. To calculate the distribution of oligomers, we made a calibration curve. For each chromatogram, the logarithm of chain length as a function of retention time for oligomers with chain-length 2–16 was plotted. Integration limits for resolved peaks were set manually. The regression line was then extrapolated to estimate chain lengths of the unresolved part of the chromatograms. Assuming that the detector response is independent of composition and chain length and adjusting for baseline drift, the weight fraction is proportional to peak area. The distribution of oligomers in the degraded alginate samples is given in Figure 3A–C, and a discussion of block distribution follows below.

It is important to distinguish between the distribution of blocks and the distribution of oligomers because oligomers, in particular the shorter ones, are compositionally heterogeneous. The composition near the reducing ends are dependent on the degradation pattern of the lyases and will be discussed in connection with NMR analysis of oligomers

Figure 3A shows that all samples contain a considerable amount of G blocks with DP > 20 (15.8, 19.7, and 51.7% in *D. potatorum*, *M. pyrifera*, and SF60, respectively), whereas the fraction of intermediate block lengths (DP 10–20) is relatively low (4.4, 6.5, and 12.6%). The high G-alginate from *L. hyperborea* differs from the others in that there are four to six times more oligomers with chain lengths between 20 and 30 and also, as expected, a much larger void.

As an indirect test of purity and also as an attempt to verify that <sup>1</sup>H NMR is consistent with SEC data, we have calculated the fraction of GG measured from the SEC chromatogram, which equals the fraction of GG measured from <sup>1</sup>H NMR (Table S1 of the Supporting Information).

Assuming no internal M and that the RI signal is proportional to the weight concentration, the starting DP for the sum of G blocks in the chromatograms can be estimated. Because  $\Delta$  always originates from a M unit and some of the G blocks also have M in neighbor to this as well as on the reducing end, the fraction of G blocks is given by the expression

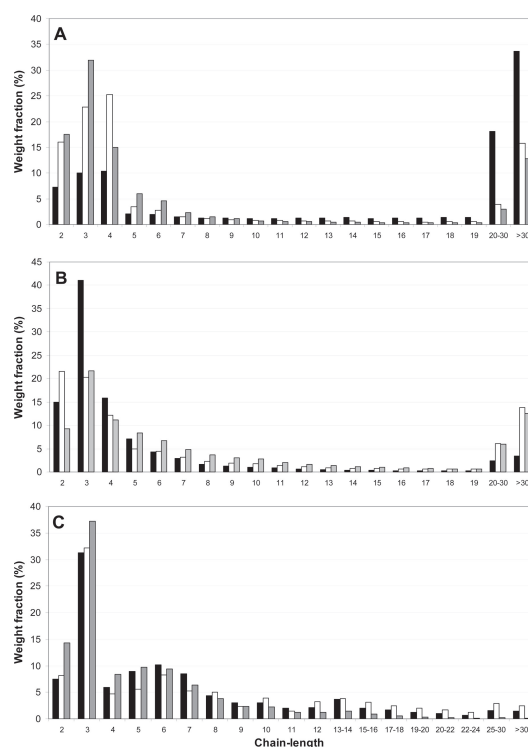


**Figure 3.** Weight distribution of oligomers in alginates from *D. potatorum* (gray square), *M. pyrifera* (white square), and *L. hyperborea* (black square) degraded by (A) M-lyase, (B) G-lyase, and (C) MM-GG-lyase calculated from Figure 2.

$$F_{GG} = \frac{1}{A_{\text{total}}} \sum_{DP=i}^n A_i (1 - 1/i(1 + f_{i\Delta M} + f_{iMred})) \quad (2)$$

where  $F_{GG}$  is the fraction of GG measured from <sup>1</sup>H NMR.  $A_i$  is the area of a G block with chain length  $i$  and  $A_{\text{total}}$  is the total area of the chromatogram.  $f_{i\Delta M} = F_{i\Delta M}/(F_{i\Delta M} + F_{i\Delta G})$  is the fraction of M residues next to the nonreducing end, and  $f_{iMred} = F_{iMred}/(F_{iMred} + F_{iGred})$  is the fraction of M residues on the reducing end.

In addition to void fractions, we have <sup>1</sup>H NMR data from oligomers up to DP6. It was therefore not possible to give an exact value for the contribution from  $f_{i\Delta M}$  and  $f_{iMred}$ . Using  $f_{i\Delta M} + f_{iMred} = 1$ , close to the average for the fractions analyzed by NMR,  $F_{GG}$  corresponds to the sum of DP > 8, 11, and 12 in the chromatograms of *D. potatorum*, *L. hyperborea*, and *M. pyrifera*. Although the low amount of oligomers with DP 6–20 makes the calculation uncertain and  $F_{GG}$  obtained from NMR gives a slightly distorted picture of the actual situation, this indicates that the G blocks contain a small amount of M residues.

The distribution of M blocks in the different alginates (Figure 3B) is in accordance with their respective  $F_{MM}$ . Also here there is a considerable number of long blocks, even for the high-G alginate. Several epimerases from *A. vinelandii* have been found to exhibit a processive mode of action or act by a preferred attack mechanism.<sup>13,15</sup> This seems to apply also for

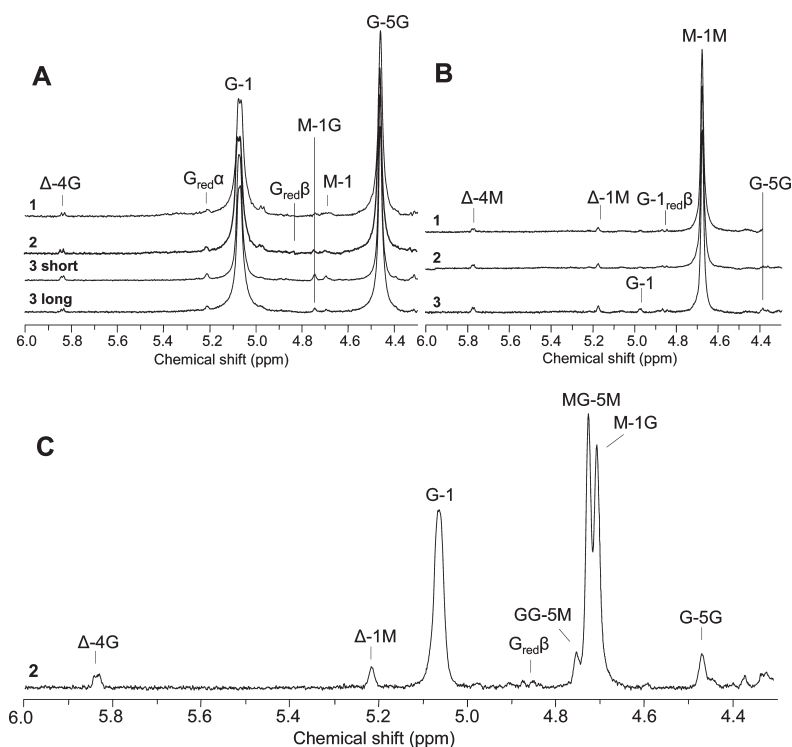


**Figure 4.**  $^1\text{H}$  NMR (400 MHz) spectra of void fractions from SEC separations of *D. potatorum* (1), *M. pyriferia* (2), and *L. hyperborea* (3) degraded by (A) M-lyase, (B) G-lyase, and (C) MM- and GG-lyase. The voids of *L. hyperborea* degraded by M-lyase were collected in two fractions, 3a and 3b, in order of elution.

**Table 1.** SEC-MALLS and  $^1\text{H}$ -NMR Analysis of the Void Fractions in Figure 2<sup>a</sup>

alginate	lyase	block	purity (%)	$M_w$ (KDa)	$M_n$ (KDa)	PI	$\overline{DP}_n^b$	$\overline{DP}_n^c$
<i>D. Pot.</i>	G	M	$\geq 99$	42.6	18.1	2.4	91	94
<i>M. Pyr.</i>	G	M	$\geq 99$	37.3	17.8	2.1	90	96
<i>L. Hyp.</i>	G	M	$\geq 99$		9.5			54
<i>D. Pot.</i>	M	G	$\geq 98$	63.1	32.3	2.0	163	273
<i>M. Pyr.</i>	M	G	$\geq 98$	53.9	26.3	2.1	132	105
<i>L. Hyp. a<sup>d</sup></i>	M	G	$\geq 98$	48.0	23.9	2.0	120	117
<i>L. Hyp. b<sup>d</sup></i>	M	G	$\geq 97$	28.2	12.2	2.3	61	70
<i>M. pyr.</i>	MM+GG	MG	$\geq 93$		6.9			39

<sup>a</sup>Average chain length ( $\overline{DP}_n$ ) and polydispersity index (PI) were calculated from  $M_w$  and  $M_n$  values. <sup>b</sup>SEC-MALLS. <sup>c</sup> $^1\text{H}$  NMR. <sup>d</sup>voids of *L. hyperborea* degraded by M-lyase were collected in two fractions, a and b, in order of elution

algal epimerases. If the epimerases bind randomly to the substrate and dissociates after each reaction, then one would expect that  $N_{M>1} \approx 1/F_G$  and this is clearly not the case here. Using the same approach as for G blocks,  $F_{MM}$  in *D. potatorum*, *L. hyperborea*, and *M. pyriferia* corresponds to the fraction of oligomers with DP > 5, 5, and 6.

Apart from a large fraction of trimer, the distribution of oligomers in samples degraded with MM- and GG-lyase is more uniform than the distributions of M and G blocks (Figure 3C). The combination of slightly lower resolution and a pattern with small odd-numbered and larger even-numbered oligomers made it impossible to find integration limits for each oligomer with DP > 12. Fractions were calculated from DP 13–24 for every pair. Both *M. pyriferia* and to some extent *L. hyperborea* con-

tain a small fraction of long MG blocks, whereas *D. potatorum* is almost devoid of oligomers with DP > 20.  $F_{MGM}$  in *D. potatorum*, *M. pyriferia*, and *L. hyperborea* corresponds to the fraction of oligomers with DP > 9, 12, and 14.

**Structural Analysis of Oligomers in the Void Fractions.** To examine the purity and chain length of the longest oligomers, void fractions in the SEC chromatograms shown in Figure 2 were collected and analyzed by NMR-spectroscopy and SEC-MALLS.  $^1\text{H}$  NMR spectra of the void fractions (Figure 4) confirm that the G and M blocks are compositionally homogeneous (Table 1). The alginates contain a smaller amount of long MG-blocks and only in the case of *M. pyriferia* was enough material for an NMR analysis. *M. pyriferia* has the highest  $F_{MG}$ , so the initial assumption would



be that it is easier to obtain pure MG blocks from this sample. However, when the same conditions sufficient to cleave most G-G sequences in *D. potato* and *L. hyperborea*, were applied to *M. pyrifera*,  $^1\text{H}$  NMR of the void fraction showed that there still was a significant number of G-G sequences left. In another experiment, the amount of GG-lyase was doubled, and  $F_{\text{GG}}$  in the void fraction of this sample (Figure 4C) was  $\sim 7\%$ .

**Extremely Long Homogeneous Sequences Are Present in the Void.**  $\overline{\text{DP}}_n$  of the void fractions were estimated from  $^1\text{H}$  NMR spectra by taking the ratio between internal signals and  $\Delta$ -4 signals from the nonreducing end. Because of the low intensity of the latter, some of the signals were difficult to integrate. SEC-MALLS was therefore used as a comparative method in the cases where enough material was available. Purity and chain lengths of the void fractions are summarized in Table 1.

If the oligomers in the void fraction are not compositionally pure, then this will lead to a considerable overestimation of block length. When residues other than the block type are randomly distributed, the difference between true and observed block length is given by

$$\text{DP}_{\text{observed}} = (1 + F_i/F_{\text{red end}})\text{DP}_{\text{real}} \quad (3)$$

where  $F_i$  is the fraction of M- or G- residues that does not contribute to the block and  $F_{\text{red end}}$  is the fraction of reducing ends.

This is a concern for extremely long sequences and for the least pure MG blocks. However, given GG-lyases have a low activity on short G oligomers, it is likely that much of the remaining GG sequences are located near the ends. The difference between real and observed block length would in this case be much less than if the GG sequences were randomly distributed.

The results obtained from  $^1\text{H}$  NMR and SEC-MALLS are generally in good agreement, except for the G block from *D. potato*, where SEC-MALLS probably gives a more realistic value. The presence of considerable amounts of not only extremely long G blocks but also very long M and MG blocks has not previously been reported and should be considered in structure–function models.

Calculation of average G-block length has previously mainly been based on sequence frequencies obtained from  $^1\text{H}$  NMR, using the expression  $N_{G>1} = (F_G - F_{\text{MGM}})/F_{\text{GGM}}$ . It is important to note that alginates are partially acid hydrolyzed to  $\overline{\text{DP}}_n$  between 20 and 40 prior to NMR analysis to reduce line broadening. Not only is determination of block length affected but also sequence parameters as glycosidic bonds are hydrolyzed with different rates ( $k_{\text{GM}} > k_{\text{MM}} > k_{\text{MG}} > k_{\text{GG}}$ ).<sup>34,43</sup>  $N_{G>1}$  therefore cannot be directly compared with our data.

From Figures 2A and 4A, it is obvious that the average G-block length is greatly underestimated from NMR (Table S1 of the Supporting Information). Although it is not possible to calculate an average G-block length from the SEC chromatograms, Figure 4A shows that most of the G-blocks have a DP > 20. Moreover, HPAEC-PAD and NMR analyses of short oligomers (discussed later) confirm that these do not contain enough GG-sequences so as to skew the number average chain length significantly.  $N_{G>1}$  should therefore be used with care and for comparison only.

**Structural Analysis of Oligomers.** The combination of HPAEC-PAD and NMR spectroscopy can be used to separate and identify short heterogeneous oligomers, as demonstrated below. This provides additional information on the overall

structure of alginate, like possible heterogeneous regions in the transition region between different block types, for example, 1–3 G units by adjacent M units. Short blocks (DP  $\leq 7$ ) may also be detected.

When analyzing the block distribution, one has to take into account that the lyase subsite specificity will affect the apparent block distribution. Because none of the lyases are able to cleave M-G bonds, the actual block length is at least one unit shorter than the oligomer. The cleavage pattern in the sequence immediately before and after a block will also influence on the observed distribution of blocks. This is illustrated in Figure 5.

Substrate	Lyase	Cleavage sites	DP
3 2 1                    a b ↓ ↓ ↓                    ↓ ↓ -G-G-G-M-M-M-M-M-G-G-	G	1a	7
		1b	8
		2a	8
		2b	9
		3a	9
		3b	10
2 1                        a b c ↓ ↓                        ↓ ↓ ↓ -M-M-M-G-G-G-G-G-M-M-	M	1a	7
		1b	8
		1c	9
		2a	8
		2b	9
		2c	10
2 1                        a b ↓ ↓                        ↓ ↓ -M-M-M-G-M-G-M-G-M-M-G-	MM	1a	7
		1b	8
		2a	8
		2b	9
2 1                        a b ↓ ↓                        ↓ ↓ -G-G-G-G-M-G-M-G-M-G-G-	GG	1a	7
		1b	8
		2a	8
		2b	9

**Figure 5.** Influence on the degradation pattern of lyases on observed block length. Arrows indicate different possible cleavage sites. DP denotes the resulting chain length.

**NMR Analysis of the Composition of Oligomers.**  $^1\text{H}$  NMR analysis of short oligomers provides detailed information about composition and can be used to study how the cleavage pattern of the lyases affects observed block length. An example of  $^1\text{H}$  NMR spectra of a dimer separated from *M. pyrifera* degraded by M-lyase and a tetramer separated from *M. pyrifera* degraded by G-lyase is shown in Figure 6.

Particularly useful are the  $\Delta$ 4-G (5.84 ppm) and  $\Delta$ 4-M (5.78 ppm) signals from the nonreducing end and the signal from  $\text{G-}S_{\text{red}}\alpha$  (4.6 ppm) because there are no overlapping signals in these regions. Furthermore, it was noticed that  $\text{G-}S_{\text{red}}\alpha$  shifts slightly depending on the neighbor, thus enabling the calculation of  $\text{M-}G_{\text{red}}/\text{G-}G_{\text{red}}$ . Determination of reducing ends in lysase-degraded samples is complicated by the fact that  $\text{G-}1_{\text{red}}\alpha$  and  $\text{M-}1_{\text{red}}\alpha$  are masked by the  $\Delta$ -1 signal. This can be circumvented if one knows the ratio between  $\alpha$  and  $\beta$  anomers. Heyraud et al. have found  $\text{G}_{\text{red}}\alpha/\text{G}_{\text{red}}\beta$  and  $\text{M}_{\text{red}}\alpha/\text{M}_{\text{red}}\beta$  to be 0.2 and 2.2. Utilizing the  $\text{G-}1_{\text{red}}\beta$ ,  $\text{M-}1_{\text{red}}\beta$ ,  $\text{G-}5_{\text{red}}\alpha$ , and  $\Delta$ -4 signals in dimer fractions of M- and G-lyase degraded samples,

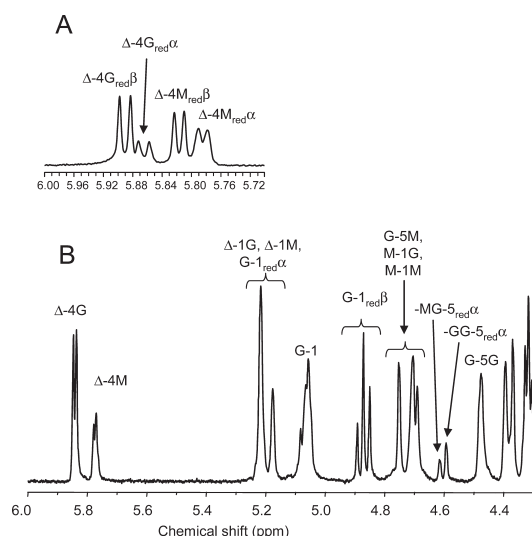


**Figure 6.**  $^1\text{H}$  NMR (400 MHz) spectrum of (A) DP2 separated from *M. pyrifera* degraded by M-lyase and (B) DP4 separated from *M. pyrifera* degraded by G-lyase. The splitting of  $\Delta$ -4 signals in the dimer fraction is assumed to be caused by the anomeric equilibrium.

we get ratios of 0.27 and 1.90 with a deviation of <3% between three measurements. These were later used to calculate  $G_{\text{red}}$  and  $M_{\text{red}}$  for longer oligomers, assuming that influence of chain length on the anomeric ratio is negligible.

Previously, there have been concerns about  $\Delta$ -4 signals being underestimated due to longer relaxation times than their saturated counterparts (unpublished results). Using interscan delay of 1.0 s, this did not seem to be a problem in our case as the total area from the reducing end signals was similar to the area of the  $\Delta$ -4 signals.

Fractions of samples degraded by M-lyase were collected up to DP 4, 5, and 6 for *L. hyperborea*, *M. pyrifera*, and *D. potatorum*. From DP 4, ~90% of the fractions contained G next to the nonreducing end. As in the former case, the composition on the reducing end reflects the sequence and composition of the original samples. Of the odd-numbered fractions, only DP 5 from *M. pyrifera* contains  $G_{\text{red}}$  (19%). The amount of  $G_{\text{red}}$  on even-numbered fractions varies from ~30% in *D. potatorum* to 75% in DP4 from *M. pyrifera*. This is probably due to short alternating oligomers. Although one should be careful in drawing conclusions for longer oligomers, it seems likely that most G blocks are one to three units shorter than the corresponding oligomers.

Fractions of samples degraded by G-lyase were collected up to DP 7. The dimer fraction of samples degraded by G-lyase contains of course only  $\Delta$ G. The amount of G next to the non reducing end decreases in the trimer and tetramer fractions. Somewhat surprisingly,  $\Delta$ -4G signals could not be detected for DP > 4 in *D. potatorum* and *M. Pyrifera*, and DP > 5 for *L. hyperborea*. This indicates that the enzyme cleaves a  $\Delta$ G-M linkage only if all the subsites are filled and that the subsite accommodates five units. Moreover, the binding in +2 and +3 positions is not very selective.

All oligomers contain only G on the reducing ends. The  $M_{\text{red}}/G_{\text{red}}$  ratio probably depends on both the composition of

the starting material as well the lyase specificity because there was no clear correlation between chain length and  $M_{\text{red}}/G_{\text{red}}$  up to DP7.  $G_{\text{red}}$  constitutes ~50% of the reducing ends in fractions from *L. hyperborea* and 30–50% of the reducing ends in fractions from *M. pyrifera* and *D. potatorum*. It is not possible to distinguish between cleavage in positions 1 and 2 in Figure 5 for G-lyase. From the above considerations, it can be assumed the actual block length is one to three units shorter than the oligomers.

Fractions of samples degraded with a combination of MM and GG-lyase were collected up to DP 7. As one could expect, these were more heterogeneous than those obtained from degradation by G and M-lyase, and the analysis of cleavage pattern and blocklength is less clear-cut. In general, there are more G than M next to the nonreducing end, especially in the tetramer fractions, where  $\Delta$ GMG dominates. The fraction of G next to the non reducing end does not vary much from DP 4–7, being ~60% for *D. potatorum* and *M. pyrifera* and 80% for *L. hyperborea*.

There is a striking difference in composition on the reducing end between *L. hyperborea* and the other samples. All fractions of *L. hyperborea*, except the dimer, contain only oligomers with  $G_{\text{red}}$ , whereas  $M_{\text{red}}$  are more abundant in fractions from *D. potatorum* and *M. pyrifera*. An exception is the DP6 fraction of *M. pyrifera* with a large fraction of  $\Delta$ GMGMG. All oligomers except DP 4 from *D. potatorum* and DP 4 and 6 from *M. pyrifera* only have G next to the reducing end. Keeping in mind that also the GG-lyase is unable to cleave  $\Delta$ G4, it is not easy to assess the difference between observed and real block length. It is, however, possible to give an upper estimate based on the NMR spectra from void fractions. The void fraction of *M. pyrifera* has  $DP_n \approx 39$  and  $F_{\text{GG}} \approx 0.07$ . Assuming that there are no internal G-G sequences, this gives an average of 2.7 G next to the ends. The M-1 M signal was not observed in the same void fraction. Because this lyase also degrades  $\Delta$ M4, it is likely that the contribution to the difference between real and observed block length is small. The majority of alternating sequences are probably two to three units shorter than the corresponding oligomers.

**Compositional Heterogeneity of Short Oligomers Is Revealed by HPAEC-PAD.** Data obtained from the  $^1\text{H}$  NMR spectra of collected fractions were compared with HPAEC-PAD chromatograms and standards. This made it possible to identify the most abundant oligomers up to pentamer. Sections of HPAEC-PAD chromatograms with identified peaks are shown in Figure 7. Heyraud et al. have previously separated alginate oligomers on a nucleosil 5  $\mu\text{m}$  SB column.<sup>44</sup> The same elution pattern was observed on a IonPac AS4A column used in our work where four to five unsaturated nonreducing ends and a high fraction of mannuronic acid both cause longer retention times. In addition, the residues at the ends seem to have a larger influence on retention times than a residue inside the chain; for example, MGMG elutes before GMGM.<sup>39</sup>

Even though HPAEC-PAD is a useful technique, it has limitations regarding both identification of peaks and quantification if pure standards are not available. Because the retention time is strongly dependent on sequence, coelution occurs for oligomers with DP > 4. For instance,  $\Delta$ MMM and  $\Delta$ GGG both elute after ~20 min. HPAEC-PAD can therefore not be used to identify and quantify every fragment in a complex degradation mixture but can be viewed more as a fingerprint of each alginate.



significant fraction of extremely long homogeneous G-blocks, causing the distribution of G blocks to differ markedly from second-order Markov statistics.<sup>22</sup> The same alginates also contain a fraction of very long nonepimerised regions, whereas MG blocks were considerably shorter, although the length of the latter is probably somewhat underestimated due to the lower specificity of the GG-lyase compared with that of the other lyases used in this work.

The minimum size for G blocks needed to form stable junctions with Ca<sup>2+</sup> ions has been estimated to be between 8 and 20 units.<sup>23,45</sup> Therefore, the finding of extremely long G blocks in seaweed alginates is intriguing. Stokke et al. have developed a model to predict some of the gelling properties of alginates using a step function, LG<sub>min</sub>, representing the minimum level of G blocks being able to form a junction and the assumption that each G block can form only one junction. The criterion for gel formation is that the functionality, i.e., the number of junctions per molecule, is larger than two. Extremely long G blocks introduce the possibility of more than one junction zone, something that perhaps needs to be incorporated into the model.

It is not yet clear if the longest G blocks have a specific role in alginate gels. Because the binding of Ca<sup>2+</sup> between G blocks is a cooperative process, the formation of junctions between long G blocks is thermodynamically favored. Furthermore, the initiation of this zipper process is faster when there is no need for complete overlap between two G blocks to form a stable junction. Perhaps an alginate gel could be viewed upon as a composite material, where almost fully epimerised molecules form dimers that act as reinforcement bars.

Hydrogels from *M. pyrifera* display the highest degree of syneresis of the alginates investigated. Although a quantitative model is still lacking, the finding of comparatively long MG blocks in *M. pyrifera* confirms that these play an important role in syneresis and large deformation properties of alginate.<sup>25</sup> It is important to have in mind that except for *L. hyperborea* alginate was extracted from whole plants. Because the composition may depend on both age and type of tissue, the wide variation in the observed block length could reflect compositional heterogeneity between different populations of alginate molecules.

The task of studying structure–function relationships would become much simpler if the composition is as homogeneous as possible. Poly-M epimerized to various extents, using different mannuronan-C-5 epimerases, is therefore currently being investigated in our laboratory.

## ■ ASSOCIATED CONTENT

### ■ Supporting Information

Molecular weight ( $M_w$ ) and sequence parameters in alginates used in this study (S1); source and specificity of alginate lyases used in this study (S2); relative activity towards poly-M, poly-MG, and poly-G for the lyases in S2 (S3); reaction products of unsaturated alginate oligomers incubated with alginate lyases (S4); SEC chromatogram of PolyMG incubated with MM-lyase (S5); NMR spectra of (A) void fraction collected from ii) and Poly-MG ( $F_G = 0.46$ ) (S6); and HPAEC-PAD chromatograms of Poly-G and Poly-MG incubated with GG-lyase (S7). This material is available free of charge via the Internet at <http://pubs.acs.org>.

## ■ AUTHOR INFORMATION

### Corresponding Author

\*Tel: (+47)73593317. E-mail: [olava@nt.ntnu.no](mailto:olava@nt.ntnu.no).

## ■ ACKNOWLEDGMENTS

This work has been supported by The Research Council of Norway, project 182695-I40. We thank Wenche Strand for technical assistance and valuable discussions regarding the interpretation of <sup>1</sup>H NMR spectra. Kåre Kristiansen and Ann Sissel Ulset are thanked for help with SEC-MALLS analysis.

## ■ ABBREVIATIONS

DP, degree of polymerization; SEC, size exclusion chromatography; NMR, nuclear magnetic resonance; MALLS, multi-angle laser light scattering; HPAEC-PAD, high-performance anion exchange chromatography with pulsed amperometric detection

## ■ REFERENCES

- (1) Casu, B.; Lindahl, U. In *Advances in Carbohydrate Chemistry and Biochemistry*, Horton, D., Ed.; Academic Press: New York, 2001; pp 159–206.
- (2) Painter, T. J. *Algal Polysaccharides*. In *The Polysaccharides*; Aspinall, G. O., Ed.; Academic Press: New York, 1983; pp 195–285.
- (3) Gorin, P. A. J.; Spencer, J. F. T. *Can. J. Chem.* **1966**, *44*, 993–998.
- (4) Linker, A.; Jones, R. S. *J. Biol. Chem.* **1966**, *241*, 3845–3851.
- (5) Larsen, B.; Haug, A. *Carbohydr. Res.* **1971**, *17*, 287–296.
- (6) Larsen, B.; Haug, A. *Carbohydr. Res.* **1971**, *17*, 297–308.
- (7) Larsen, B.; Haug, A. *Carbohydr. Res.* **1971**, *20*, 225–232.
- (8) Ertesvåg, H.; Doseth, B.; Larsen, B.; Skjåk-Bræk, G.; Valla, S. *J. Bacteriol.* **1994**, *176*, 2846–2853.
- (9) Ertesvåg, H.; Hoidal, H. K.; Hals, I. K.; Rian, A.; Doseth, B.; Valla, S. *Mol. Microbiol.* **1995**, *16*, 719–731.
- (10) Svanem, B. I. G.; Skjåk-Bræk, G.; Ertesvåg, H.; Valla, S. *J. Bacteriol.* **1999**, *181*, 68–77.
- (11) Hoidal, H. K.; Ertesvåg, H.; Skjåk-Bræk, G.; Stokke, B. T.; Valla, S. *J. Biol. Chem.* **1999**, *274*, 12316–12322.
- (12) Hartmann, M.; Duun, A. S.; Markussen, S.; Grasdalen, H.; Valla, S.; Skjåk-Bræk, G. *Biochim. Biophys. Acta* **2002**, *1570*, 104–112.
- (13) Hartmann, M.; Holm, O. B.; Johansen, G. A. B.; Skjåk-Bræk, G.; Stokke, B. T. *Biopolymers* **2002**, *63*, 77–88.
- (14) Campa, C.; Holtan, S.; Nilsen, N.; Bjerkan, T. M.; Stokke, B. T.; Skjåk-Bræk, G. *Biochem. J.* **2004**, *381*, 155–164.
- (15) Holtan, S.; Bruheim, P.; Skjåk-Bræk, G. *Biochem. J.* **2006**, *395*, 319–329.
- (16) Grant, T. G.; Morris, E. R.; Rees, D. A.; Smith, P. J.C.; Thom, D. *FEBS Lett.* **1973**, *32*, 195–198.
- (17) Penman, A.; Sanderson, G. R. *Carbohydr. Res.* **1972**, *25*, 273–82.
- (18) Grasdalen, H.; Larsen, B.; Smidsrød, O. *Carbohydr. Res.* **1977**, *56*, C11–C15.
- (19) Grasdalen, H.; Larsen, B.; Smidsrød, O. *Carbohydr. Res.* **1979**, *68*, 23–31.
- (20) Grasdalen, H. *Carbohydr. Res.* **1983**, *118*, 255.
- (21) Martinsen, A.; Skjåk-Bræk, G.; Smidsrød, O. *Biotechnol. Bioeng.* **1987**, *33*, 79–89.
- (22) Stokke, B. T.; Smidsrød, O.; Bruheim, P.; Skjåk-Bræk, G. *Macromolecules* **1991**, *24*, 4637–4645.
- (23) Stokke, B. T.; Smidsrød, O.; Zanetti, F.; Strand, W.; Skjåk-Bræk, G. *Carbohydr. Polym.* **1993**, *21*, 39–46.
- (24) Donati, I.; Holtan, S.; Mørch, Y. A.; Borgogna, M.; Dentini, M.; Skjåk-Bræk, G. *Biomacromolecules* **2005**, *6*, 1031–1040.
- (25) Donati, I.; Mørch, Y. A.; Strand, B. L.; Skjåk-Bræk, G.; Paoletti, S. *J. Phys. Chem. B* **2009**, *113*, 12916–12922.
- (26) Otterlei, M.; Østgaard, K.; Skjåk-Bræk, G.; Smidsrød, O.; Soon-Shiong, P.; Espevik, T. *J. Immunother.* **1991**, *10*, 286–291.
- (27) Skjåk-Bræk, G.; Flo, T.; Halaas, Ø.; Espevik, T. Immune Stimulating Properties of Di-Equatorially  $\beta(1-4)$  Linked Poly-Uronides. In *Bioactive Carbohydrate Polymers*; Paulsen, B. S., Ed.; Kluwer Academic Publishers: Boston, 2000; pp 85–93.
- (28) Boyd, J.; Turvey, J. R. *Carbohydr. Res.* **1978**, *66*, 187–94.

- (29) Chavagnat, F.; Duez, C.; Guin, M.; Potin, P.; Barbeyron, T. *Biochem. J.* **1996**, *319*, 575–83.
- (30) Gimmestad, M.; Sletta, H.; Ertesvag, H.; Bakkevig, K.; Jain, S.; Suh, S.; Skjåk-Bræk, G.; Ellingsen, T. E.; Ohman, D. E.; Valla, S. *J. Bacteriol.* **2003**, *185*, 3515–3523.
- (31) Ertesvåg, H.; Skjåk-Bræk, G. Modification of Alginate Using Mannuronan C-5-Epimerases. In *Methods in Biotechnology*; Bucke, C., Ed.; Humana Press: Totowa, NJ, 1999; Vol. 10, pp 71–78.
- (32) Haug, A.; Larsen, B.; Smidsrød, O. *Acta Chem. Scand.* **1966**, *20*, 183–190.
- (33) Haug, A.; Larsen, B.; Smidsrød, O. *Acta Chem. Scand.* **1967**, *21*, 691–704.
- (34) Holtan, S.; Zhang, Q.; Strand, W. I.; Skjåk-Bræk, G. *Biomacromolecules* **2006**, *7*, 2108–2121.
- (35) Ballance, S.; Aarstad, O. A.; Aachmann, F.; Skjåk-Bræk, G.; Christensen, B. E. C. *Carbohydr. Res.* **2009**, *344*, 255–259.
- (36) Boyen, C.; Kloareg, B.; Polnefuller, M.; Gibor, A. *Phycologia* **1990**, *29*, 173–181.
- (37) Tøndervik, A.; Klinkenberg, G.; Aarstad, O. A.; Drablos, F.; Ertesvag, H.; Ellingsen, T. E.; Skjak-Braek, G.; Valla, S.; Sletta, H. *J. Biol. Chem.* **2010**, *285*, 35284–35292.
- (38) Sletta, H.; Nedal, A.; Aune, T. E. V.; Hellebust, H.; Hakvag, S.; Aune, R.; Ellingsen, T. E.; Valla, S.; Brautaset, T. *Appl. Environ. Microbiol.* **2004**, *70*, 7033–9.
- (39) Ballance, S.; Holtan, S.; Aarstad, O.; Sikorski, P.; Skjåk-Bræk, G.; Christensen, B. E. *J. Chromatogr. A* **2005**, *1093*, 59–68.
- (40) Campa, C.; Oust, A.; Skjåk-Bræk, G.; Paulsen, B. S.; Paoletti, S.; Christensen, B. E.; Ballance, S. *J. Chromatogr. A* **2004**, *1026*, 271–281.
- (41) Vold, I. M. N.; Kristiansen, K. A.; Christensen, B. E. *Biomacromolecules* **2006**, *7*, 2136–2146.
- (42) Skjåk-Bræk, G.; Murano, E.; Paoletti, S. *Biotechnol. Bioeng.* **1989**, *33*, 90–94.
- (43) Smidsrød, O.; Larsen, B.; Painter, T.; Haug, A. *Acta Chem. Scand.* **1969**, *23*, 1573–1580.
- (44) Heyraud, A.; Colin-Morel, P.; Girond, S.; Richard, C.; Kloareg, B. *Carbohydr. Res.* **1996**, *291*, 115–126.
- (45) Kohn, R.; Larsen, B. *Acta Chem. Scand.* **1972**, *26*, 2455–2468.

## Supporting Information

### S1. Molecular weight ( $M_w$ ) and sequence parameters<sup>a</sup> in alginates used in this study

	$M_w$	DPn	PI	$F_G$	$F_M$	$F_{GG}$	$F_{GM}$	$F_{MM}$	$F_{MGM}$	$F_{GGG}$	$N_{G>1}$
<i>D. potatorum</i>	$1.63 \times 10^5$	$4.7 \times 10^2$	1.76	0.32	0.68	0.20	0.12	0.56	0.07	0.16	6
<i>M. pyrifer</i>	$1.77 \times 10^5$	$4.6 \times 10^2$	1.94	0.41	0.59	0.21	0.20	0.40	0.18	0.17	5
<i>L. hyperborea</i>	$2.00 \times 10^5$	$4.5 \times 10^2$	2.23	0.67	0.33	0.56	0.11	0.23	0.08	0.52	13
Poly-M	$1.21 \times 10^5$	$2.3 \times 10^2$	2.71	-	1.0	-	-	1.0	-	-	-
Poly-MG	$9.59 \times 10^4$	$2.3 \times 10^2$	2.14	0.46	0.54	-	0.46	0.1	-	-	-
Poly-G	$3.07 \times 10^3$	18.5*	-	0.95	0.05	0.86	0.02	0.03	0.01	0.84	-

\* calculated from <sup>1</sup>H-NMR

<sup>a</sup>  $F_G$  and  $F_M$  denotes the fraction of guluronic and mannuronic acid. Fractions of different di- and trimers are indicated with two and three letters.

### S2 Source and specificity of alginate lyases used in this study

Lyase	Specificity	Source	Abbreviation
AlyA	G-G / G-M	<i>K. pneumoniae</i>	G-lyase
AlyA5	G-G	Mutant of AlyA	GG-lyase
<i>H. tuberculata</i> lyase	M-M / G-M	<i>H. tuberculata</i>	M-lyase
AlxM	M-M	<i>Photobacterium sp.</i> (ATCC 43367)	MM-lyase

**S3.** Relative activity towards poly-M, poly-MG and poly-G for the lyases in Table 2.

	Poly-M	poly-MG	Poly-G
M-lyase	1	0.181	0.073
MM-lyase	1	0.041	0.012
G-lyase	0.005	0.50	1
GG-lyase	0.0046	0.0090	1

Relative activity was calculated from slopes in the initial linear region of the curves. The activity towards the optimal substrate is assigned the value 1.

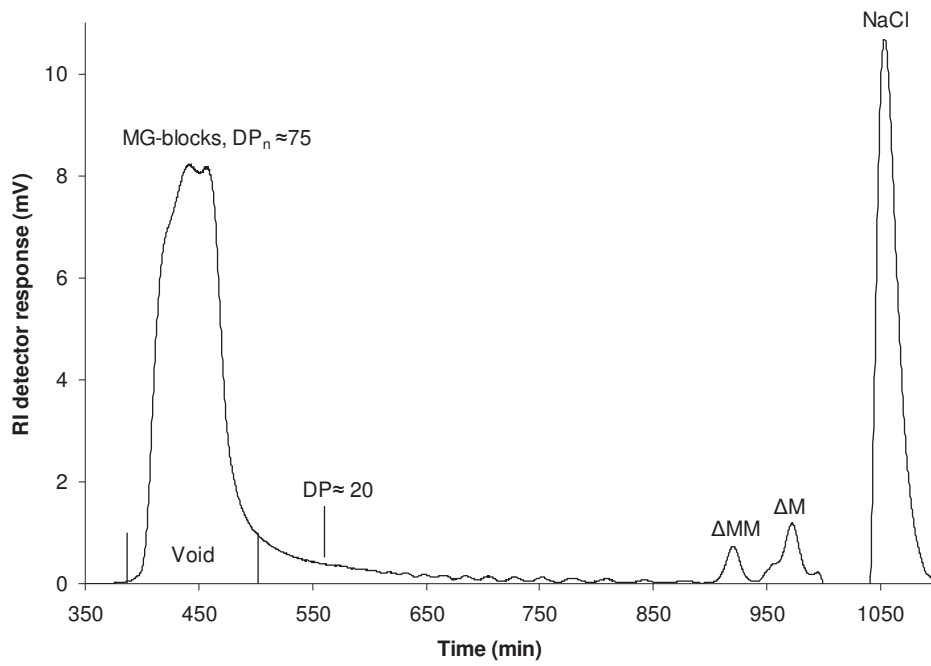
**S4. Reaction products of unsaturated alginate oligomers incubated with alginate lyases**

Lyase	Substrate	Major product	Minor products	
M	$\Delta$ MM	$\Delta$ MM	$\Delta^* + \Delta$ M	
	$\Delta$ MMM	$\Delta$ MM + $\Delta^*$	$\Delta$ M + $\Delta$ M	
	$\Delta$ MMMM	$\Delta$ MM + $\Delta$ M	-	
	$\Delta$ MMMMM	$\Delta$ MM + $\Delta$ MM	$\Delta$ M + $\Delta$ MMM	
	$\Delta$ GMG	-	-	
	$\Delta$ GMGMG	$\Delta$ GMG + $\Delta$ G	-	
	$\Delta$ GMGMGMG	$\Delta$ GMG + $\Delta$ GMG	$\Delta$ G + $\Delta$ G + $\Delta$ GMG	
	MM	$\Delta$ MM	$\Delta$ MM	$\Delta^* + \Delta$ M
		$\Delta$ MMM	$\Delta$ MM + $\Delta^*$	$\Delta$ M + $\Delta$ M
$\Delta$ MMMM		$\Delta$ MM + $\Delta$ M	-	
$\Delta$ MMMMM		$\Delta$ MM + $\Delta$ MM	$\Delta$ M + $\Delta$ MMM	
$\Delta$ GMG		-	-	
$\Delta$ GMGMG		-	-	
$\Delta$ GMGMGMG		-	-	
G		$\Delta$ GGG	-	-
		$\Delta$ GGGG	-	$\Delta$ G + $\Delta$ GG
	$\Delta$ GGGGG	$\Delta$ GG + $\Delta$ GG	$\Delta$ G + $\Delta$ GGG	
	$\Delta$ GGGGGG	$\Delta$ GG + $\Delta$ GGG	$\Delta$ G + $\Delta$ GGGG	
	$\Delta$ GMG	-	-	
	$\Delta$ GMGMG	$\Delta$ GMG + $\Delta$ G	-	
	$\Delta$ GMGMGMG	$\Delta$ GMG + $\Delta$ GMG	$\Delta$ G + $\Delta$ G + $\Delta$ GMG	
	GG	$\Delta$ GGG	-	-
		$\Delta$ GGGG	-	$\Delta$ G + $\Delta$ GG
$\Delta$ GGGGG		$\Delta$ GG + $\Delta$ GG	$\Delta$ G + $\Delta$ GGG	
$\Delta$ GGGGGG		$\Delta$ GG + $\Delta$ GGG	$\Delta$ G + $\Delta$ GGGG	
$\Delta$ GMG		-	-	
$\Delta$ GMGMG		-	$\Delta$ GM + $\Delta$ G 1)	
$\Delta$ GMGMGMG		-	$\Delta$ G + $\Delta$ G + $\Delta$ GMG 1)	

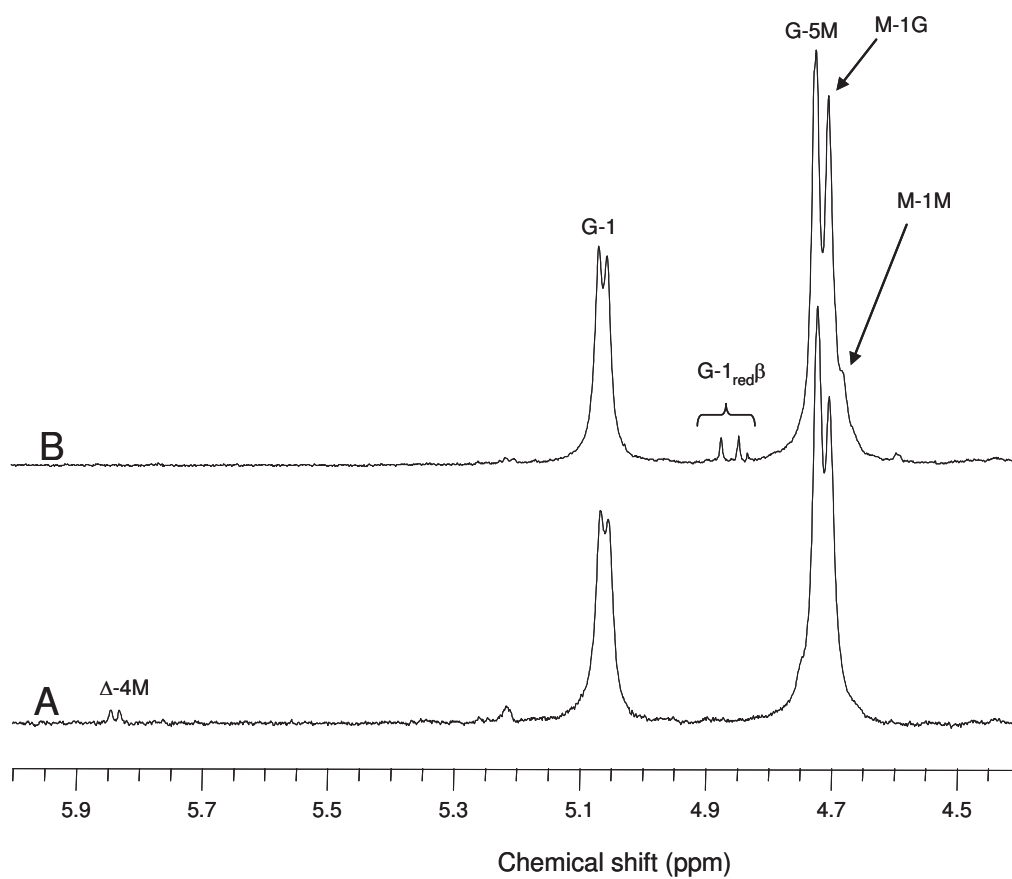
1) Appears only after extensive incubation with a large amount of enzyme. Oligomers were incubated for 24-120 hours with alginate-lyase (0.1-0.5U/mg substrate).

\* 4-deoxy-L-erythro-hex-4-enopyranosyluronate( $\Delta$ ) monomer may rearrange to 4-deoxy-L-erythro-5-hexoseulose.

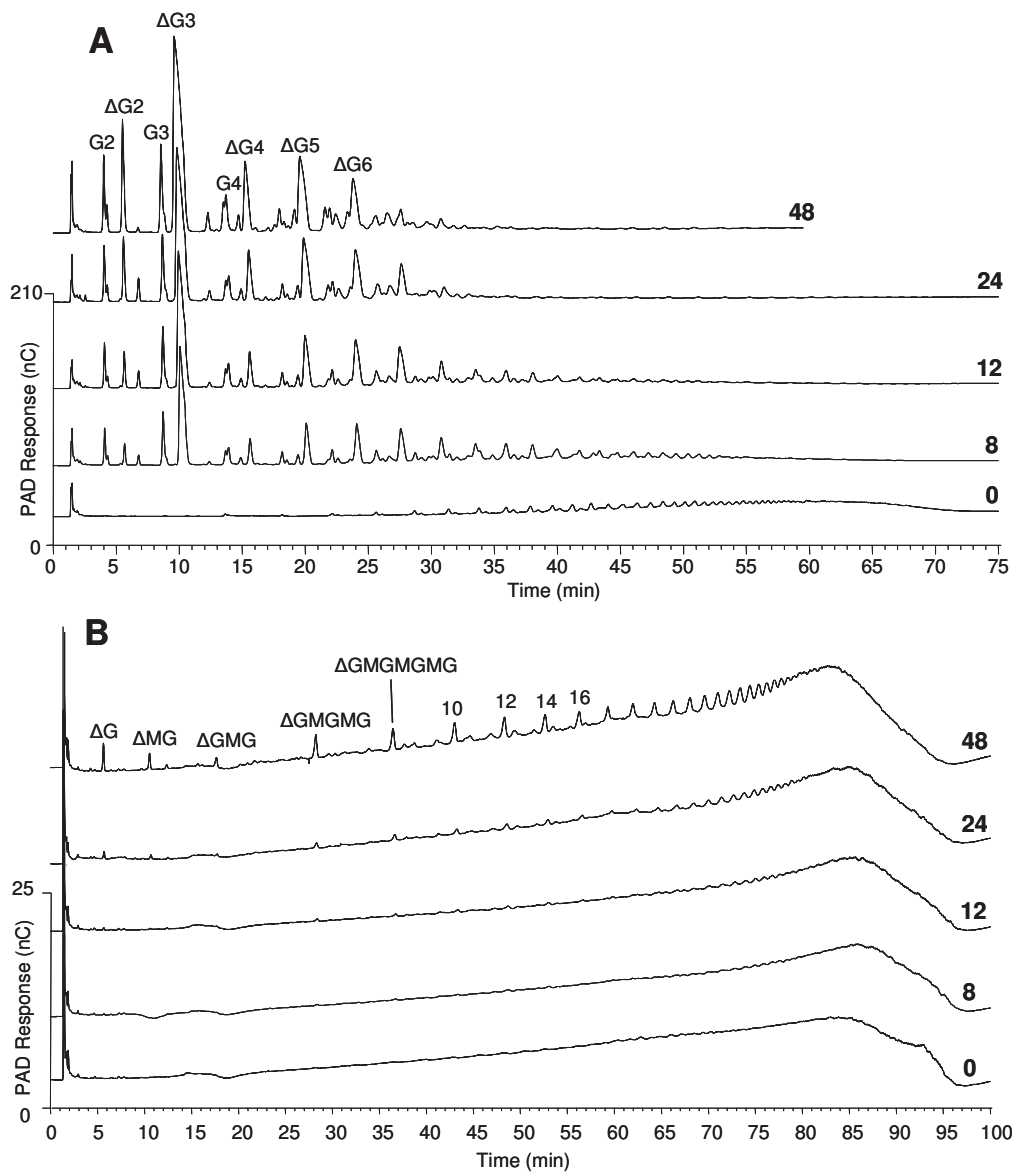




**S5.** SEC chromatogram of PolyMG (50mg) incubated with 0.98U MM-lyase for 24 hours, eluted with 0.1M NH<sub>4</sub>Ac at 0.8ml/min on Superdex 30 columns.



**S6.** Overlaid NMR spectra of (A) void fraction collected from the SEC chromatogram in Fig. S5 and (B) Poly-MG ( $F_G=0.46$ ) partially acid hydrolysed to  $\overline{DP}_n \approx 30$ .



**S7.** Overlaid HPAEC-PAD chromatograms of **(A)** Poly-G (1mg/ml) and **(B)** Poly-MG (1mg/ml) incubated with GG- lyase (0,0069U/mg substrate) at 30°C for 0-48 hours. Samples were separated on a Dionex IonPac AS4A column with a linear gradient of 8.75 mM sodium acetate/min in 100 mM sodium hydroxide at a flow rate of 1ml/min.



# Paper V

Is not included due to copyright



